ANA RITA DAS NEVES LAGARTO BENTO

PhD Thesis

Improving neurite outgrowth in 3D hydrogel matrices by mimicking cell receptor-ECM interactions occurring in neurogenic niches: an engineering approach to develop more efficient neural stem cell hydrogel carriers

Dissertação submetida à Faculdade de Engenharia da Universidade do Porto
para obtenção do grau de Doutor em Engenharia Biomédica

U.PORTO
FEUP FACULDADE DE ENGENHARIA
UNIVERSIDADE DO PORTO

2018

This project was supervised by:

Isabel Freitas de Amaral, PhD (supervisor)
i3S – Instituto de Investigação e Inovação em Saúde, Universidade do Porto
INEB – Instituto de Engenharia Biomédica, Universidade do Porto
FEUP – Faculdade de Engenharia, Universidade do Porto

Ana Paula Pêgo, PhD (co-supervisor)
i3S – Instituto de Investigação e Inovação em Saúde, Universidade do Porto
INEB – Instituto de Engenharia Biomédica, Universidade do Porto
FEUP – Faculdade de Engenharia, Universidade do Porto
ICBAS – Instituto de Ciências Biomédicas Abel Salazar, Universidade do Porto

This work was performed at:

i3S – Instituto de Investigação e Inovação em Saúde, Universidade do Porto
INEB – Instituto de Engenharia Biomédica, Universidade do Porto, Portugal

This work was financially supported by:

By National Funds through FCT – Fundação para a Ciência e a Tecnologia (PTDC/SAU-BMA/118869/2010); projects NORTE-01-0145-FEDER-000008 and NORTE-01-0145-FEDER-000012, supported by Norte Portugal Regional Operational Programme (NORTE 2020), under the PORTUGAL 2020 Partnership Agreement, through the European Regional Development Fund (ERDF) and FEDER – Fundo Europeu de Desenvolvimento Regional funds through the COMPETE 2020 – Operacional Programme for Competitiveness and Internationalisation (POCI), Portugal 2020, and by Portuguese funds through FCT/MCTES in the framework of the project "Institute for Research and Innovation in Health Sciences" (POCI-01-0145-FEDER-007274). Ana Rita Bento was supported by FCT (PhD grant – SFRH/BD/86200/2012).

No coração, talvez, ou diga antes:
Uma ferida rasgada de navalha,
Por onde vai a vida, tão mal gasta.
Na total consciência nos retalha.
O desejar, o querer, o não bastar,
Enganada procura da razão
Que o acaso de sermos justifique,
Eis o que dói, talvez no coração.

José Saramago, em "Os Poemas Possíveis"

Agradecimentos

Esta dissertação é um conjunto de muito trabalho, esforço, luta, paciência, amor, amizade, lágrimas, nervos, alegrias, risos e gargalhadas, insónias, suspiros e vitórias. Aliás, tudo o que fizemos, o que "descobrimos", é um resultado não só da minha dedicação, mas também da dedicação de todas as pessoas envolvidas directamente neste trabalho, particularmente da minha orientadora Isabel Amaral e da minha co-orientadora Ana Paula Pêgo. Admiro-vos muito e foi um prazer contribuir para a ciência em Portugal, com a qualidade e rigor características do nBTT, no i3S. Em especial o meu maior agradecimento à Isabel por ser a Professora que mais me ensinou até hoje, com quem aprendi a fazer coisas de que nem sabia ser capaz! Um agradecimento também muito especial à Ana Paula que sempre teve as palavras certas no momento necessário. Agradeço a todos os que colaboraram neste trabalho, em especial à Maria José Oliveira, uma pessoa fantástica com quem tive o prazer de trabalhar. Agradeço ao Professor Fernando Jorge Monteiro, uma pessoa excepcional e amável que sempre me ajudou em tudo! Agradeço também a todos os investigadores e profissionais do i3S, em especial do INEB, que sempre me ajudaram!

Esta dissertação envolve também directamente todos os que me são mais próximos, aqueles que me inspiram a lutar diariamente contra todos os obstáculos e contrariedades. Essas pessoas, seres magníficos, que enchem a minha vida de luz e de amor, são o meu pilar, a minha família, mãe Clara e irmã Margarida, sem vocês nada disto teria significado. O meu outro pilar, Armando, que traz vida e cor aos meus dias. Também a dedicação dos meus amigos foi um factor indispensável à realização deste trabalho. Vocês inspiraram-me muito. Os meus amigos que tão bem me conhecem e que limpam as minhas lágrimas (porque também as há), mas que sabem rir e dizer as parvoíces certas na hora certa! Os meus amigos fantásticos que fiz durante este doutoramento, pessoas inteligentes, amáveis, são autênticos guerreiros… Os meus colegas do INEB/i3S que se tornaram pessoas indispensáveis durante este caminho de luta. Agradeço imensamente todos os minutos, todas as horas e até dias que dedicaram a ajudar-me! Vocês são amigos que levo no coração para a vida toda.

Agradeço simplesmente a todas as pessoas que me ajudaram, os que partilharam o seu tempo comigo, os que me ajudaram a ver a verdade (e lutar por ela), os que me inspiraram, e claro, a todos os que tornaram este caminho um sucesso, uma vitória de todos nós!

Em obediência ao disposto no Decreto-Lei 388/70, Artigo 8º, parágrafo 2, declaro:

1) Relativamente ao trabalho apresentado no Capítulo II desta dissertação efectuei o planeamento e execução do trabalho experimental, análise e interpretação dos respectivos resultados, e redigi o manuscrito que resultou na seguinte publicação:

Bento A.R., Quelhas P., Oliveira M.J., Pêgo A.P., Amaral I.F. (2017). *Three-dimensional culture of single embryonic stem-derived neural/stem progenitor cells in fibrin hydrogels: neuronal network formation and matrix remodeling.* Journal of Tissue Engineering and Regenerative Medicine 11(12):3494–3507. DOI: 10.1002/term.2262.

2) Relativamente ao trabalho apresentado no Capítulo III desta dissertação efectuei o planeamento e a execução do trabalho experimental, assim como a análise e interpretação dos respectivos resultados:

- Quantificação da adesão celular de ES-NSPCs a ligandos da integrina α6β1 previamente adsorvidos a superfícies 2D na presença de anticorpos funcionais.
- Imobilização de ligandos para a integrina α6β1 em hidrogéis de fibrina e caracterização dos géis funcionalizados em termos de propriedades viscoelásticas.
- Cultura de neurosferas de ES-NSPCs sobre géis de fibrina funcionalizados e quantificação da migração radial na presença de anticorpos funcionais.
- Estudos de diferenciação neuronal de ES-NSPCs dissociadas em géis de fibrina funcionalizados.
- Avaliação da resposta biológica a géis de fibrina funcionalizados num modelo animal (rato) de lesão de espinal medula em termos de impacto da regeneração axonal e na recuperação da função locomotora.

Ainda no âmbito deste trabalho redigi o manuscrito que resultou na seguinte publicação:

Silva J.*, Bento A.R.*, Barros D., Laundos T.L., Sousa S.R., Quelhas P., Sousa M.M., Pêgo A.P., Amaral I.F. (2017). *Fibrin functionalization with synthetic adhesive ligands interacting with α6β1 integrin receptor enhance neurite outgrowth of embryonic stem cell-derived neural stem/progenitors*, Acta Biomaterialia 59:243–256. DOI: 10.1016/j.actbio.2017.07.013. *Ambos os autores contribuíram igualmente para este trabalho.

A reprodução destas publicações foi feita com autorização das respectivas editoras.

Table of Contents

Publications and Awards

Publications

Silva J.*, Bento A.R.*, Barros D., Laundos T.L., Sousa S.R., Quelhas P., Sousa M.M., Pêgo A.P., Amaral I.F. (2017). Fibrin functionalization with synthetic adhesive ligands interacting with α6β1 integrin receptor enhance neurite outgrowth of embryonic stem cell-derived neural stem/progenitors, Acta Biomaterialia 59: 243–256. DOI: 10.1016/j.actbio.2017.07.013.
*Both authors contributed equally.

Bento A.R., Quelhas P., Oliveira M.J., Pêgo A.P., Amaral I.F. (2017). Three-dimensional culture of single embryonic stem-derived neural/stem progenitor cells in fibrin hydrogels: neuronal network formation and matrix remodeling. Journal of tissue engineering and regenerative medicine 11(12): 3494–3507. DOI: 10.1002/term.2262.

Bento A.R., Monteiro C., Oliveira M.J., Pêgo A.P., Amaral I. (2014). *In vitro* cell behavior of dissociated embryonic stem-derived neural stem cells in fibrin hydrogels. Conference Abstract: Journal of Tissue Engineering and Regenerative Medicine, Vol 8 (supplement 1).

Awards

Best poster "Cell-matrix constructs based on embryonic stem cell-derived neural stem/progenitor cells embedded in fibrin hydrogels for central nervous system regeneration" - 4º Encontro de Doutorandos da Faculdade de Medicina da Universidade do Porto, December 2014.

Scientific Communications

Bento A.R., Silva J., Barros D., Laundos T.L., Sousa S.R., Quelhas P., Sousa M.M., Pêgo A.P., Amaral I.F. (2017). Functionalization of fibrin hydrogels with α6β1 integrin-binding adhesive peptides for delivery of pluripotent stem cell-derived neural stem/progenitors. 6th Advanced Summer School - Interrogations at the Biointerface Research/Clinical Interface at the Spine". 19–22 June, Porto, Portugal.

Bento A.R., Silva J., Barros D., Laundos T.L., Sousa S.R., Quelhas P., Sousa M.M., Pêgo A.P., Amaral I.F. (2016). HYD1-conjugated fibrin hydrogels promote cell migration of embryonic stem-derived neural/stem progenitor cells *in vitro* and are permissive to axonal regeneration *in vivo.* 5th Symposium in Applied Bioimaging, 26–28 October, Porto, Portugal.

Bento A.R., Quelhas P., Oliveira M.J., Pêgo A.P., Amaral I.F. (2016). Three-dimensional culture of single embryonic stem-derived neural/stem progenitor cells in fibrin hydrogels: neuronal network formation and matrix remodeling. International Society for Stem Cell Research Annual Meeting, 22–25 June, San Francisco, CA USA.

Bento A.R., Monteiro C., Oliveira M.J., Pêgo A.P., Amaral I.F. (2014). *In vitro* cell behavior of dissociated embryonic stem-derived neural stem cells in fibrin hydrogels. Meeting of the Tissue Engineering and Regenerative Medicine International Society (TERMIS-EU). 10–13 June, Genova, Italy.

Bento A.R., Monteiro C., Oliveira M.J., Pêgo A.P., Amaral I.F. (2014). Cell-matrix constructs based on embryonic stem cell-derived neural stem/progenitor cells embedded in fibrin hydrogels for central nervous system regeneration. 4º Encontro de Doutorandos da Faculdade de Medicina da Universidade do Porto, 9 April, Porto, Portugal.

Bento A.R., Pêgo A.P., Amaral I.F. (2013). Optimization of cell culture parameters for the 3D culture of single embryonic stem cell-derived neural stem cells in fibrin. 13th Meeting of the Portuguese Society for Neurosciences. 30 May–1 June, Luso, Portugal.

Bento A.R., Pêgo A.P., Amaral I.F. (2013). Optimization of cell culture parameters for the 3D culture of single embryonic stem cell-derived neural stem cells in fibrin. 3rd Advanced Summer School - Interrogations at the Biointerface "Inflammation/Repair Interface". 25–28 June, Porto, Portugal.

Abbreviations List

2D/3D	Two-dimensional/ Three-dimensional
AD	Alzheimer’s disease
APC	Allophycocyanin
ANOVA	Analysis of variance
ALS	Amyotrophic lateral sclerosis
BBB	Basso, Beattie and Bresnahan
BDNF	Brain-derived neurotrophic factor
bFGF	Basic fibroblast growth factor
BM	Basement membrane
BSA	Bovine serum albumin
BrdU	5-Bromo-2’-deoxyuridine
cAMP	Cyclic adenosine 3’,5’-monophosphate
CLSM	Confocal laser scanning microscope
cpm	Counts per minute
CNS	Central nervous system
DAPI	4’,6-Diamidino-2-phenylindole
DMEM	Dulbecco's modified eagle’s medium
DNA	Deoxyribonucleic acid
DRG	Dorsal root ganglia
EB	Embryoid body
ECM	Extracellular matrix
EDTA	Ethylenediaminetetraacetic acid
EGF	Epidermal growth factor
ESC	Embryonic stem cell
FACS	Fluorescence-activated cell sorting
Fb	Fibrin
FBS	Fetal bovine serum
FDA	Food and drug administration
FN	Fibronectin

G’	Storage modulus
G’’	Loss modulus
GABA	Gamma aminobutyric acid
GAD67	Glutamic acid decarboxylase 67
GAP43	Growth associated protein 43
GAPDH	Glyceraldehyde-3-phosphate dehydrogenase
GFAP	Glial fibrillary acidic protein
GFP	Green fluorescent protein
GMEM	Glasgow’s minimum essential medium
GSK-3	Glycogen synthase kinase 3
GTPases	Rho family guanosine-5-triphosphatases
hES-NSC	Human embryonic stem-derived neural stem cell
Iba1	Ionized calcium binding adaptor molecule 1
IgG/G1/M	Immunoglobulin G/G1/M
iPSC	Induced pluripotent stem cell
LN	Laminin
LG	Laminin G-like domain
LIF	Leukemia inhibitory factor
mES-NSPC	Murine embryonic stem-derived neural stem/progenitor cell
MNP	Motor neuron progenitor cell
MMP	Matrix metalloproteinase
MSC	Mesenchymal stem cell
MT1-MMP	Membrane type 1 metalloprotease
NCAM	Neural cell adhesion molecule
NF200	Neurofilament 200
NGF	Nerve growth factor
NPC	Neural precursor cell
NSC	Neural stem cell
NSPC	Neural stem/progenitor cell
NT3	Neurotrophin-3

PBS	Phosphate buffer saline
PD	Parkinson’s disease
PDL	Poly-D-lysine
PE	Phycoerythrin
PEG	Poly(ethylene glycol)
PFA	Paraformaldehyde
PI	Propidium iodide
PNS	Peripheral nervous system
PSC	Pluripotent stem cell
OEC	Olfactory ensheathing cell
OPC	Oligodendrocyte progenitor cell
rpm	Revolutions per minute
RGD	Arginine-Glycine-Aspartic acid sequence
RT	Room temperature
SCI	Spinal cord injury
SD	Standard deviation
SSEA-1	Stage specific embryonic antigen 1
TBI	Traumatic brain injury
TBS	Tris-buffered saline
TCPS	Tissue culture polystyrene
TH	Tyrosine hydroxylase
VEGF	Vascular endothelial growth factor
v/v	Volume per volume percent
w/v	Weight per volume percent

Abstract

Central nervous system (CNS) damage often leads to devastating consequences due to the inability of severed axons to regenerate beyond the lesion site. Patients with CNS diseases frequently suffer from permanent dysfunction or paralysis, and current treatments do not constitute a cure. Transplantation of neural stem cells (NSCs) offers the possibility of replacing lost neurons and supporting cells after CNS injury. Moreover, through the release of neurotrophins and growth factors, transplanted NSCs can provide neuroprotection while promoting the regrowth of disrupted axons. Preclinical studies reveal functional benefits of NSC transplantation, and the attempts made to translate NSC therapies into a clinical setting indicate no safety concern. Still, NSCs delivered into the damaged CNS show poor cell survival and migration, and limited differentiation along the neuronal lineage. To overcome this, biodegradable hydrogels are being explored for *in situ* delivery of NSCs. Besides allowing a homogenous NSC distribution at the site of injury, hydrogels can contribute to sequester neurite-promoting factors, providing a supportive niche for cell survival, differentiation and axonal regeneration.

Herein, we proposed to develop an engineering approach to increase the ability of hydrogel matrices to sustain NSC neurite outgrowth and migration by mimicking cell receptor-extracellular matrix (ECM) interactions occurring in neurogenic niches. Specifically, we hypothesized if the tethering of cell adhesive sequences engaging integrin α6β1 or syndecans could enhance hydrogels capacity to support NSC neurite outgrowth, ultimately contributing to the integration of transplanted NSCs. Fibrin gel was selected to test this hypothesis, due to the absence of integrin α6β1 binding domains in its structure along with tunable properties and innate bioactivity.

Firstly, we established a fibrin-based three-dimensional (3D) culture system able to sustain the survival, proliferation, outgrowth, and neuronal differentiation of neural stem/progenitor cells (NSPCs) derived from murine embryonic stem (ES) cells seeded as single cells. In this system, ES-NSPCs were found to remodel fibrin through matrix metalloproteinase secretion and ECM deposition. Importantly, these fibrin hydrogels, with stiffness comparable to that of the human brain, also supported cell viability, neuronal differentiation and ECM deposition of human ES-derived NSCs. Using the developed fibrin platform, we subsequently assessed the response of ES-NSPCs to immobilized cell adhesive motifs interacting with integrin α6β1, a laminin receptor highly expressed by NSCs in neurogenic niches which mediates laminin-dependent

NSC migration. Six α6β1 integrin ligands were tested for their ability to support integrin α6β1-mediated ES-NSPC adhesion. Due to their better performance, peptides T1, HYD1, and A5G81 were selected for covalent immobilization into fibrin. We report that the grafting of HYD1 or T1 to fibrin promotes radial outgrowth from ES-NSPC neurospheres (up to 2.4-fold increase *vs* unmodified fibrin) by interacting with integrins α6β1 and α3β1. Cell outgrowth exhibited a biphasic response to peptide concentration with maximum enhancement being attained at input peptide concentrations of 20 or 40 μM. Fibrin functionalization was also effective in promoting neurite extension of dissociated ES-NSPCs. Subsequently, we assessed the ability of HYD1-functionalized to sustain axonal regeneration. HYD1-functionalized gels were found to provide a permissive environment for axonal regeneration, leading up to a 2.0-fold increase in neurite extension from rat dorsal root ganglia explants, as compared to unmodified fibrin, and to improve functional recovery in spinal cord injured rats (complete transection model). Envisaging the translation of the developed hydrogels into the clinic, we assessed if the tethering of HYD1 or T1 integrin α6β1-binding ligands could also promote the outgrowth of human ES-NSCs. In line with our previous results, fibrin functionalization with HYD1 was effective in enhancing cell outgrowth of hES-NSCs when incorporated at 20 μM, although leading to a smaller increase when compared to that obtained with mES-NSPCs. Furthermore, to improve fibrin bioactivity towards hES-NSCs, we explored the immobilization of a syndecan-binding peptide with neurite outgrowth promoting activity, namely the AG73 peptide sequence from laminin α1 chain, alone or in combination with HYD1. Similarly to HYD1- and T1-functionalized gels, the tethering of AG73 to fibrin induced a biphasic effect on hES-NSC outgrowth, with maximum enhancement being attained at an input peptide concentration of 60 μM. Based on the effect elicited by HYD1 and AG73 when incorporated alone into fibrin, future studies should address if the combined conjugation of 60 μM of AG73 with 20 μM of HYD1 induces an additive or synergistic effect increase on hES-NSC outward migration, when compared to that exerted by single peptides.

Overall, this thesis significantly impacts the development of engineered hydrogels for use as 3D platforms for *in vitro* culture of human pluripotent stem-derived NSCs and to assist NSC transplantation to treat the damaged CNS. Furthermore, the developed fibrin platform can also be useful for pharmacological screening in a 3D microenvironment which better mimics the *in vivo* conditions. Summing up, our results open new avenues in the design of more efficient hydrogel matrices for application in NSC-based regenerative approaches for the treatment of traumatic or neurodegenerative diseases.

Resumo

As lesões no sistema nervoso central (SNC) traduzem-se geralmente em consequências devastadoras devido à incapacidade dos neurónios de regenerar os axónios lesionados e de restabelecer as ligações perdidas. Os pacientes com doenças do SNC sofrem frequentemente de disfunção ou paralisia permanente e actualmente os tratamentos disponíveis não possibilitam a sua cura. O transplante de células estaminais neurais (CENs) veio possibilitar a reposição de neurónios e células da glia danificados por lesões no SNC. Por outro lado, através da libertação de neurotrofinas e de factores de crescimento, as CENs podem contribuir para a neuroprotecção e para o crescimento dos axónios lesados. Os estudos pré-clínicos demonstram que o transplante de CENs leva a melhorias funcionais e os ensaios clínicos realizados revelam tratar-se de um procedimento seguro. Apesar disso, a administração local de CENs está associada a uma baixa viabilidade celular, bem como a uma capacidade reduzida de migração celular e diferenciação neuronal. De forma a aumentar a eficácia do transplante de CENs, o desenvolvimento de hidrogéis biodegradáveis está a ser investigado. Além de permitirem uma distribuição celular homogénea no local da lesão, os hidrogéis podem contribuir para reter moléculas indutoras do crescimento de neurites, estabelecendo um ambiente mais permissivo à sobrevivência celular, diferenciação neuronal e regeneração axonal.

Este estudo teve como objectivo o desenvolvimento de uma estratégia de engenharia para promover a extensão de neurites e a migração de CENs em hidrogéis, inspirada nas interacções célula-matriz extracelular que ocorrem nos nichos neurogénicos. Especificamente, a hipótese deste trabalho consistiu em avaliar se a funcionalização de hidrogéis com sequências adesivas que interagem com a integrina α6β1 ou com sindecanos contribui para o aumento da sua capacidade de suster a extensão de neurites de CENs, proporcionando deste modo a integração das CENs após transplante. De forma a testar esta hipótese, seleccionámos o gel de fibrina, por este não apresentar domínios de ligação à integrina α6β1 na sua estrutura, e também devido às suas propriedades viscoelásticas ajustáveis e bioactividade inata.

Em primeiro lugar, estabelecemos um sistema tridimensional (3D) baseado em gel de fibrina capaz de sustentar a viabilidade, proliferação e diferenciação neuronal de células estaminais/progenitoras neurais (CEPNs) derivadas de células estaminais embrionárias de ratinho, cultivadas no gel como células dissociadas. Neste sistema, as CEPNs conseguiram remodelar o gel de fibrina através da secreção de

metaloproteinases da matriz e deposição de matriz extracelular. Estes hidrogéis de fibrina, com rigidez comparável à do cérebro humano, demonstraram ser capazes de suportar também a viabilidade, diferenciação neuronal e a deposição de matriz extracelular de CENs derivadas de células estaminais embrionárias humanas. A plataforma de fibrina que desenvolvemos foi posteriormente utilizada para explorar a resposta das CEPNs a sequências peptídicas de adesão celular que reconhecem a integrina α6β1. Este receptor celular é reconhecido pela laminina e amplamente expresso pelas CEPNs nos nichos neurogénicos, tenho um papel fundamental na migração das CEPNs induzida por laminina. Neste sentido, avaliámos seis ligandos da integrina α6β1 em termos de capacidade de suportarem a adesão de CEPNs através deste receptor. Os péptidos com melhor desempenho, nomeadamente os péptidos T1, HYD1 e A5G81, foram seguidamente imobilizados em fibrina. Relatamos que a modificação do gel com os péptidos T1 ou HYD1 confere propriedades adesivas que levam a um aumento da extensão radial de neurites de neurosferas de CEPNs (até 2.4 vezes comparativamente ao gel não modificado) através da sua interacção com as integrinas α6β1 e α3β1. A extensão de neurites revelou uma resposta bifásica relativamente à concentração inicial de péptido, tendo-se atingindo os valores máximos para as concentrações de 20 ou 40 μM. A funcionalização da fibrina também promoveu o aumento da extensão de neurites em CEPNs dissociadas. De seguida, avaliámos a capacidade dos géis de fibrina funcionalizados com HYD1 de promover a regeneração axonal. Estes géis mostraram ser capazes de proporcionar um ambiente permissivo para a regeneração axonal, levando a um aumento da extensão de neurites de explantes de gânglios da raiz dorsal de rato (até 2 vezes superior, quando comparado com o gel não modificado), e ainda a uma melhoria na recuperação da função locomotora após lesão da medula espinhal em rato (modelo de transecção completa). Tendo em vista a translação dos hidrogéis funcionalizados desenvolvidos para a clínica, fomos avaliar se a incorporação dos péptidos HYD1 ou T1, também poderia promover a extensão de neurites de CENs derivadas de células estaminais embrionárias humanas. Tal como era expectável, a funcionalização da fibrina com o péptido HYD1 (20 μM de concentração inicial no gel) levou ao aumento da extensão de neurites de CENs humanas, embora o aumento registado tenha sido inferior ao obtido com as CEPNs de ratinho. Além disso, para melhorar a bioactividade da fibrina relativamente às CENs, explorámos a imobilização do péptido AG73, sozinho ou em combinação com o péptido HYD1. O péptido AG73 é um ligando para os receptores celulares sindecanos, derivado do domínio globular da cadeia α1 da laminina, capaz de promover a extensão de neurites. De forma semelhante aos géis funcionalizados com os péptidos HYD1 ou T1, a modificação de hidrogéis de fibrina com o péptido

AG73 originou uma resposta bifásica do crescimento de neurites das CENs, registando-se o aumento máximo para a concentração de 60 μM. Com base no efeito induzido pela imobilização dos péptidos HYD1 e AG73 em separado nos géis de fibrina, futuramente será importante investigar se a incorporação de 60 μM de AG73 em combinação com 20 μM de HYD1 leva a um aumento aditivo ou sinergístico da migração de CENs, comparativamente ao induzido pela incorporação destes péptidos em separado.

No seu conjunto, esta tese veio contribuir significativamente para o desenvolvimento de hidrogéis funcionalizados para utilização como plataformas 3D de cultura de CENs derivadas de células estaminais pluripotentes humanas ou ainda como veículos para transplante de CEPNs no tratamento de lesões do SNC. Por outro lado, o sistema baseado em hidrogéis de fibrina que desenvolvemos pode também ser útil para a triagem de novos fármacos num microambiente 3D que mimetiza melhor o ambiente *in vivo*. Em resumo, os nossos resultados contribuem para o avanço de terapias regenerativas baseadas no transplante de CENs assistido por matrizes de hidrogéis, para o tratamento de doenças traumáticas ou degenerativas do SNC.

Thesis Outline

This thesis has been organized into five chapters.

Chapter I provides the reader with background information necessary to contextualize and justify the research study proposed. It starts by emphasizing the need of developing efficient regenerative approaches to treat CNS lesions caused by physical trauma or neurodegenerative diseases. An overview of the main stem cell-based therapies currently being explored to treat CNS disorders is then provided, focusing on the transplantation of NSCs and its potential benefits. **Chapter I** also highlights the requisite of developing engineered hydrogel matrices to improve the therapeutic efficacy of NSPC transplantation into the injured CNS. The key parameters that need to be addressed while designing hydrogel matrices for NSC delivery are subsequently presented, particularly underlining the incorporation of cell adhesive motifs mimicking these found in neurogenic niches. Due to the abundance of laminin in NSC niches, insight is given into the main cell surface receptors involved in laminin-NSC interactions, including the laminin receptor integrin α6β1 known to mediate NSC migration and neurite extension. Finally, an overview of fibrin hydrogel physical and biological properties is presented. **Chapter I** also includes the main hypothesis and specific objectives of this thesis.

The subsequent chapters address the experimental work developed:

Chapters II focuses on the establishment of the 3D culture of single neural/stem progenitor cells derived from mouse or human ESCs within fibrin hydrogels, underlining the capacity for neuronal network formation and matrix remodeling.

Chapter III addresses the preparation and characterization of fibrin hydrogels functionalized with synthetic adhesive ligands interacting with α6β1 integrin receptor. Particular emphasis is given to the impact of the type and amount of immobilized ligands on ES-NSPC neurite outgrowth. Moreover, the ability of functionalized fibrin to support axonal regeneration after implantation into the damaged CNS is also described.

Chapter IV reports the performance of the functionalized fibrin hydrogels in terms of ability to promote neurite outgrowth of human ES-NSCs, foreseeing the potential translation of the developed gels to the clinic. This study also explores the tethering of a syndecan-binding peptide with neurite outgrowth promoting activity, alone or in combination with α6β1 integrin-binding ligands.

Finally, **Chapter V** provides the concluding remarks, with an overall analysis of the previous chapters, as well as future perspectives.

CHAPTER I

General Introduction and Motivation

Central nervous system diseases

Central nervous system (CNS) damage often leads to devastating consequences due to the inability of severed axons to regenerate beyond the lesion site. This damage can be induced by physical trauma, in spinal cord or traumatic brain injury (SCI; TBI), or by chronic neural degeneration, in the case of neurodegenerative diseases, such as Parkinson's (PD) and Alzheimer's disease (AD), and Amyotrophic Lateral Sclerosis (ALS). Patients with these diseases frequently suffer from permanent dysfunction or paralysis, and involuntarily place a heavy burden on the health care system for many years. In Europe, SCI and TBI incidence per year was estimated to be 16 cases per million [1] and 287.2 cases per 100 000 inhabitants [2], respectively.

In acute cases, for example, in response to ischemic stroke or SCI, different types of neurons and glial cells, including oligodendrocytes, die within a restricted area over a short time period. In chronic cases, there is either a selective loss of a specific cell population, such as dopaminergic neurons in PD and motor neurons in ALS, or a widespread degeneration of many types of neurons, as occurs in AD, over a period of several years [3]. Moreover, neurons that survive to the injury but have their axons damaged, show a reduced or no regeneration capacity, as a result of the growth inhibitory environment established upon injury. When a severe trauma is inflicted to the CNS, a physical and chemical barrier to axonal regeneration is created, which disables patients from recovering. After initial mechanical trauma, neural and vascular structures are disrupted and immune cells infiltrate the lesion site. The recruitment of inflammatory cells and reactive astrocytes over time leads to the formation of a glial scar, often accompanied by a fluid-filled cyst. In parallel, the release of inhibitor molecules associated with myelin, fibrotic tissue or glial scar contribute to the failure of axonal regrowth [4].

Current treatments of these CNS diseases rely on surgical procedures to stabilize affected vertebrae, physical therapy, pharmacological intervention and functional electrical stimulation [5, 6]. Despite alleviating symptoms of the disease or injury, these treatments do not constitute a cure [7]. To date, no proven therapy exists that can efficiently promote the regrowth and restoration of damaged central nerve cells, and also that can stimulate the genesis of new neurons. Furthermore, no current therapeutic modality has demonstrated a positive effect in neurologic outcome, emphasizing the need for continuous research in the pathophysiology and treatment of CNS disorders [8].

Neuroprotective and regenerative approaches currently under investigation

Efforts to treat traumatic CNS injuries have been made both by developing neuroprotective strategies, envisaging the minimization of cell death and axonal degeneration after injury, and by promoting plasticity and axonal growth [9]. In this sense, the delivery of neurotrophic factors and antagonists of neurite outgrowth inhibitors have been investigated to both limit degeneration and promote regeneration [10]. Current strategies also include the transplantation of stem cells, and also the administration of chemokines and growth factors within the lesioned area [11, 12].

Biomaterial-based matrices in the form of hydrogels, sponges, nanofiber scaffolds, and single and multi-channeled guidance tubes, are also being explored to provide an adhesive and mechanical support for axonal regeneration [13]. In order to repair and reconstruct the damaged CNS, these scaffold biomaterials are often combined with bioactive molecules and/or growth factors, or used as vehicles for stem cell delivery providing a permissive microenvironment for stem cell survival and integration into the host tissue [14].

Recently, the *in vivo* reprogramming of reactive glial cells into functional neurons has emerged as a challenging strategy to repair the damaged CNS. This approach uses endogenous cells to regenerate target cells for tissue repair, and is typically accomplished through the use of viral injections that ectopically express transcription factors in a particular cell type that is to be reprogrammed into another target cell type. The *in vivo* reprogramming avoids the complications of cell culture conditions, present in the *in vitro* reprogramming, and the immunorejection associated with cell transplantation [15].

The stimulation of endogenous neural progenitors present in the adult CNS might also be a strategy to improve neurological function after injury [16-18]. In fact, during embryonic development, NSCs derived from the neuroepithelium of the neural tube give rise to radial glial cells, that then retrocede at later developmental stages. In the adult CNS, late descendants of these embryonic NSCs reside in the subventricular zone of the lateral ventricle and the subgranular zone of the dentate gyrus of the hippocampus [19-21]. Neurogenesis in other adult CNS regions is generally believed to be very limited under normal physiological conditions but could be induced after injury [22]. Specifically, in pathological conditions such as stroke and traumatic brain injury, NSCs have been shown to proliferate and differentiate into neurons, able to migrate

into the lesion site [23, 24]. In the spinal cord, ependymal cells lining the central canal have been proven to retain the capacity to differentiate into neurons and glia cells *in vitro*, and are defined as NSCs [25]. However, despite increasing their proliferation after SCI, most of these endogenous progenitors fail to differentiate into neurons, in contrast to NSCs in the brain [26], partially due to the inflammatory microenvironment established upon injury. As a matter of fact, the majority of these cells generate astrocytes that participate in the formation of the glial scar, in which they contribute to contain the lesion and to neuroprotection, by secreting neuroprotective molecules [27, 28]. Since the endogenous process of cell replacement in the adult human CNS is far from being sufficient to repair the damage caused after an injury, the neuronal circuitry remains disrupted and functional neurological outcome is not achieved. Therefore, several therapeutic strategies are being explored based on the modulation of endogenous NSC responses to CNS injury, namely by promoting the recruitment of endogenous neural progenitors to the injury and directing their differentiation into neurons or oligodendrocytes [29].

Cell-based therapies for the treatment of CNS injuries

Advances in regenerative medicine have raised hope in the treatment of CNS injuries and diseases via the delivery of different cell types (Figure 1). These comprise (i) embryonic stem cells (ESCs) or induced pluripotent stem cells (iPSCs) differentiated towards the neural lineage, including NSCs, committed neural progenitors such as oligodendrocyte progenitor cells (OPCs) and neuronal-restricted progenitors, as well as differentiated neuronal cell types such as motor and dopaminergic neurons; (ii) NSCs isolated from human fetal CNS tissue; (iii) NSCs directly converted from adult somatic cells (iNSCs); (iv) mesenchymal stem cells (MSCs) derived from the bone marrow or the umbilical cord; (v) olfactory ensheathing cells (OECs); and (vi) differentiated cell types such as Schwann cells and activated macrophages [30].

The selection of appropriate cell type(s) is a crucial factor that determines the therapeutic effectiveness of the cell transplantation approach. Thus, preclinical experiments should cautiously evaluate the survival of transplanted cells in the host and the efficacy of the grafts in terms of their ability to restore function of specific types of damaged or lost cells. Stem cells are typically expanded *in vitro* to achieve the desired amount of defined cells and should be properly characterized prior to transplantation, namely *in vitro* in terms of their capability to self-renew and to give rise

to a differentiated progeny [31], and *in vivo* considering the possibility of teratoma formation.

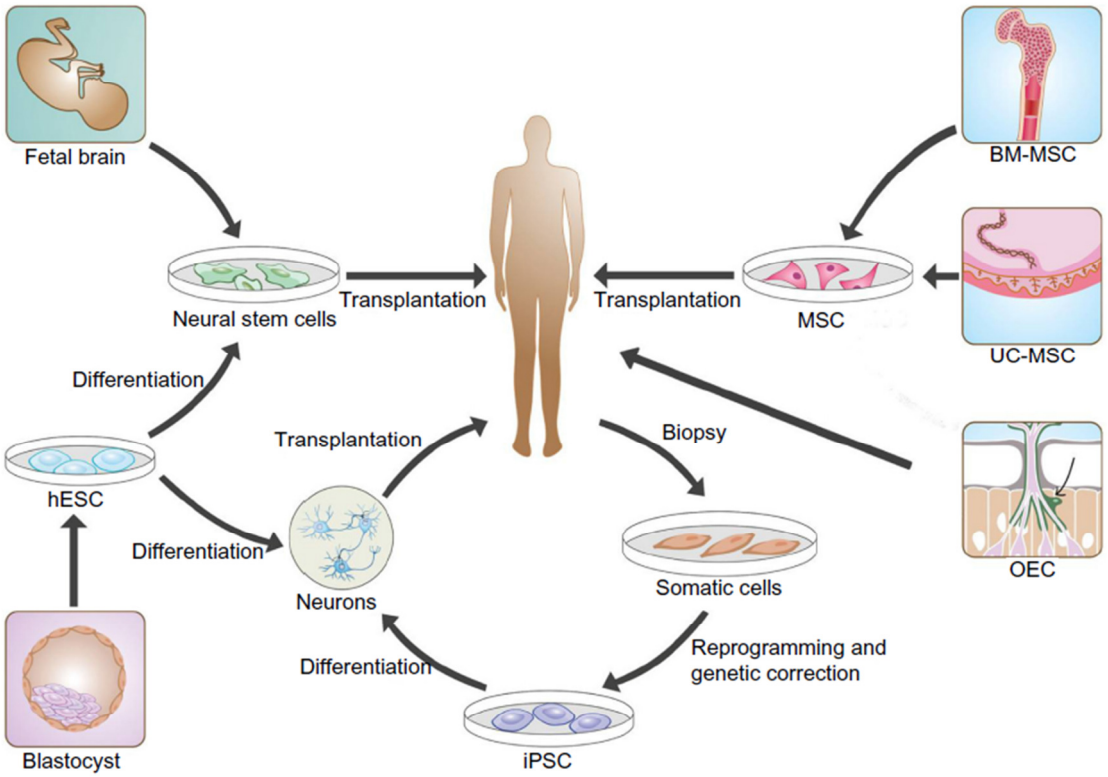

Figure 1. Different cell sources for transplantation to treat CNS disorders: hESC (human embryonic stem cells) isolated from the inner cell mass of a blastocyst; neural stem cells from brains of 3–4-month-old fetuses; BM-MSC (bone marrow-derived mesenchymal stem cells) from adult bone-marrow; UC-MSC (umbilical cord mesenchymal stem cells) from umbilical cord of the newborn; OEC (olfactory ensheathing cells) isolated from adult or fetal olfactory bulb tissue; and iPSC (induced pluripotent stem cells) derived from the reprogrammed somatic cells. Image adapted from Han *et al.* [32], Copyright® 2014, with permission from Dove Medical Press Ltd.

Mesenchymal stem cells (MSCs) can be isolated from several adult tissues, including bone marrow, dental tissue, adipose tissue and Wharton's jelly of the umbilical cord of the newborn [33, 34]. As all stem cells, MSCs retain the capacity of self-renewal, being easy to isolate and expand for autologous application [35]. The transplantation of MSCs was proved to counteract the inflammatory response, by releasing trophic and immunomodulatory molecules [36]. Several clinical trials already approved the safety and efficacy of autologous transplantation of bone marrow-derived mesenchymal cells (BM-MSCs) to treat ALS, stroke [37] and, in particular to treat chronic SCI, resulting in the improvement of neurological function [38-40]. In combination with collagen scaffolds, transplantation of human umbilical cord-derived MSCs led to autonomic neural function recovery in complete chronic SCI patients who underwent physical

rehabilitation [41]. Recently, a phase I study was initiated to evaluate the safety and feasibility of the intrathecal injection of autologous culture-expanded adipose tissue derived-MSCs in patients with severe traumatic SCI (ClinicalTrials.gov ID#: NCT03308565). Despite such evidence regarding clinical trials, when transplanted into the CNS, a high number of MSCs is required and low cell survival rate is observed. Recent studies have shown that the great potential of using MSCs for the treatment of CNS disorders resides in their ability to modulate the function of host tissues, through the expression and release of a broad range of molecules (neurotrophins and cytokines) and microvesicles, rather than their capacity to differentiate into neuronal or glial cells [42-44]. Importantly, preclinical *in vitro* [43, 45-47] and *in vivo* [48] studies have demonstrated that the molecules secreted from different human MSC populations, namely bone marrow, adipose tissue and human umbilical cord perivascular are able to: promote neuronal survival and axonal outgrowth, increase levels of neurogenesis and angiogenesis; inhibit apoptosis and scarring, modulate immune response, and to improve functional outcomes in different models of CNS injury and disease, such as brain ischemia, SCI, Parkinson's and Alzheimer's disease [49]. Thus, the administration of MSC secretome into the lesion site can be used as an alternative to the grafting of stem cells to treat CNS injuries, such as SCI, or even in combination with cell transplantation to improve its effectiveness.

Olfactory ensheathing cells (OECs) are the glial cells that ensheath olfactory axons, within both the PNS and CNS portions of the primary olfactory pathway [50]. In adult mammals, including humans, olfactory mucosa is regenerated and repaired throughout life to maintain the integrity of the sense of smell [51]. After an olfactory nerve injury, OECs are known to facilitate the generation of new olfactory receptor neurons and sustain a channel for their axons to grow along while projecting to their olfactory bulb targets [52, 53]. Due to their unique regenerative potential and autologous origin, the transplantation of OECs derived from the olfactory mucosa or from the olfactory bulb has been successfully tested in preclinical experiments and clinical trials to treat CNS injuries, including stroke and SCI [54-56]. OECs were proved to exert neuroprotective and immunomodulatory effects that create a supportive environment for neuronal survival and axonal regeneration after complete transection SCI *in vivo* [57-59]. A phase I clinical trial demonstrated that autologous OEC transplantation is safe, with no adverse outcomes recorded for three years following transplantation in human paraplegia [60]. Moreover, in 2013, Tabakow *et al.* conducted a phase I clinical trial that demonstrated neurological improvements after OEC transplantation into SCI patients [61]. Currently, the safety and efficacy of transplanting OECs for the treatment

of stroke is also being evaluated in a phase I clinical trial (ClinicalTrials.gov ID#: NCT01327768).

Oligodendrocytes are important glial cells that form the myelin sheaths of the CNS which insulate axons and enable fast propagation of action potentials (saltatory conduction) [62], while providing axons with metabolic support [63, 64]. Oligodendrocyte progenitor cells (OPCs) have been generated from human pluripotent stem cells to be used in cell-based therapies for neurological disorders, including SCI [65-69] and multiple sclerosis [70]. Preclinical studies have shown that transplanted human ES-derived OPCs (hES-OPCs) retain the ability to maturate into oligodendrocytes [66, 69], enhance axonal remyelination and promote functional recovery after SCI [65-68]. The first ES-derived therapy for spinal cord injury was reported by Geron Corporation (GRNOPC1), comprising OPCs originally differentiated from the H7 hESC line [69], which led to the development of a cell therapy product AST-OPC1 (Asterias Biotherapeutics Inc.). Subsequently, AST-OPC1 has been produced from the H1 hESC line for all preclinical testing and clinical development [67]. In 2010, a phase I clinical trial for patients with sensorimotor complete thoracic SCI was initiated using transplantation of hES-OPCs (AST-OPC1; ClinicalTrials.gov ID#: NCT01217008). In parallel, preclinical experiments exploring the efficacy and safety of AST-OPC1 administration into the cervical spinal cord were conducted, which supported initiation of a phase I/IIa dose escalation clinical trial testing AST-OPC1 in patients with cervical SCI (ongoing trial; ClinicalTrials.gov ID#: NCT02302157) [67].

Derivation of motor neuron progenitor cells (MNPs) from hES cells has been also carried out for use in cell replacement therapies, and in particular to treat diseases of motor neuron loss. Transplantation of hES-derived MNPs led to functional improvement in animal models of SCI [71, 72], and to a significant enhancement of the number of spared endogenous neurons in animal models of amyotrophic lateral sclerosis (ALS) and spinal muscle atrophy [73].

Neural stem cells (NSCs) have a unique role in the regeneration of the CNS. Notably, the development of the CNS is initiated early in development by the induction of NSCs or NSC-like precursor cells; this developmental stage is called neural induction. The fact that the entire CNS is generated from the NSCs that arise from this initial induction provides the rationale for utilizing NSCs to recapitulate CNS development in regenerating the damaged CNS [74]. Indeed, the transplantation of NSCs for the treatment of CNS diseases fulfills the essential components of the CNS regeneration. Through the release of soluble factors, including neurotrophic factors, growth factors

and cytokines, transplanted NSCs can protect existing neural cells against damage *in situ* [75], also able to promote the regrowth of disrupted neuronal axons *in vivo* [76]. Furthermore, as multipotent cells, NSCs possess the ability to differentiate into neurons, astrocytes and oligodendrocytes, to further replace lost neural cells (Figure 2). Finally, transplanted neural stem/progenitor cells (NSPCs) have been reported to contribute to functional recovery in experimental models of various CNS diseases, inclusively in long-term periods [75, 77, 78], as described in detail below.

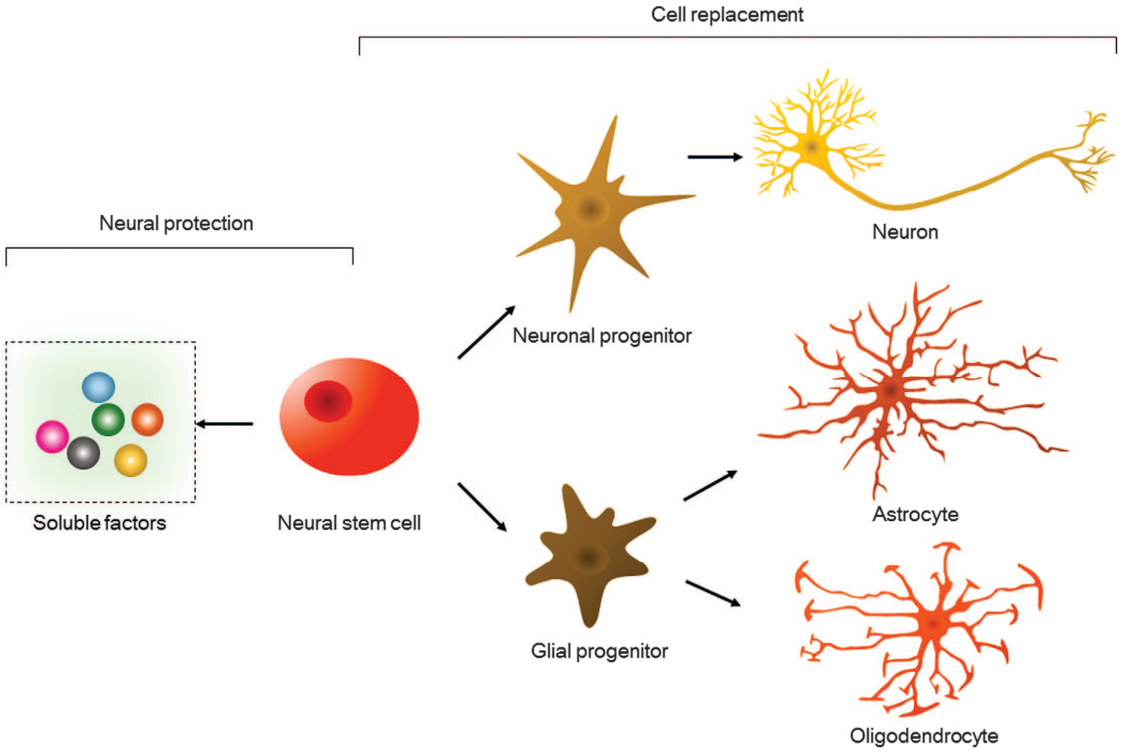

Figure 2. The therapeutic potential of NSCs. Either by neuroprotection or by replacing lost neurons and glial cells, the transplantation of NSCs aims to regenerate the damaged CNS, allowing the reestablishment of a relay neuronal circuitry and restoration of the neurological function. Image reproduced from Tang *et al.* [75], Copyright© 2017, Creative Commons license.

Transplantation of NSCs

Neural stem cells (NSCs) are the fundamental ancestor cells of the CNS (brain, spinal cord, and retina), defined by their ability to self-renew and produce all three major CNS cell types: neurons, astrocytes, and oligodendrocytes. Similarly to MSCs, NSCs have exceptional immunomodulatory properties [79], also playing a crucial neuroprotective role during the CNS regeneration. Neural stem cells can be expanded substantially, proliferating to produce cell lines that can differentiate into functional neurons after *in vivo* transplantation, demonstrating tremendous promise for cell replacement and

regenerative therapies for CNS diseases. As well, human NSCs derived from pluripotent cells or isolated from CNS tissue can be used as undifferentiated cells, relying on the host signals to stimulate their proliferation and differentiation, or their lineage descendants can be utilized, such as neuronal restricted progenitors [80]. In order to successfully repair the injured or diseased CNS it is essential to determine which cellular phenotype is the most appropriate for treating any given condition [81]. Cell source is the first issue that must be addressed to enable the clinical application of NSCs since the cell dose required for adequate transplantation is very high. Specifically, NSCs can be directly isolated from primary CNS tissues, derived from pluripotent stem cells or directly converted from adult somatic cells (Figure 3).

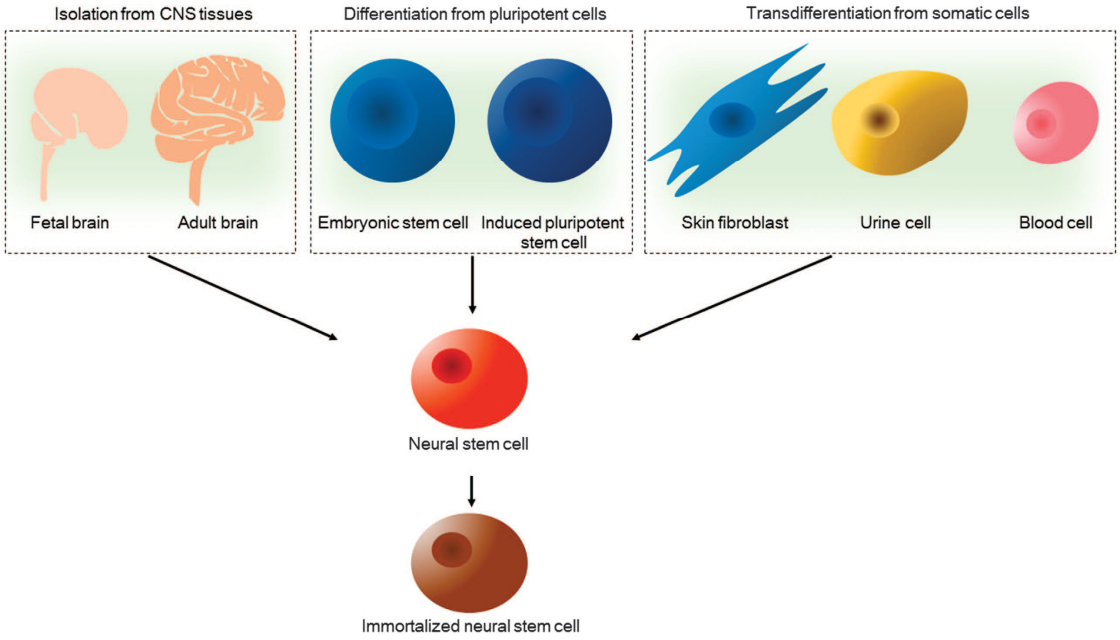

Figure 3. Sources of NSCs. Using recent technical advances, NSCs can be derived via three diverse methods: direct isolation from primary CNS tissues, including fetal brain, adult brain and spinal cord tissue; differentiation from pluripotent stem cells, such as embryonic stem cells and induced pluripotent stem cells; or transdifferentiation from adult somatic cells, such as skin fibroblasts, urine cells and blood cells, which are easily harvested in the clinic. NSCs generated from the above sources can be further immortalized via genetic modification. Image reproduced from Tang *et al.* [75], Copyright© 2017, Creative Commons license.

Transplantation of CNS neural progenitor cells or pluripotent stem (PS)-derived NSCs is being explored in preclinical models of neurodegenerative diseases, including amyotrophic lateral sclerosis [82, 83], Parkinson's disease [84-86], Alzheimer's disease [87, 88], and Huntington's disease [89, 90]; spinal cord injury [78, 91-94]; stroke [95-97]; traumatic brain injury [98, 99]; epilepsy [100]; cerebral palsy [101, 102]; neonatal hypoxic-ischemic encephalopathy [103, 104]; and retinal degenerative diseases [105].

Promising results have led to the initiation of clinical trials using transplantation of NSCs, and some have already been completed [75, 106]. Moreover, recent studies pointed out the need of evaluating the preclinical safety and efficacy of NSC-based therapies in long-term periods [75].

The grafting of exogenous CNS-resident neural progenitor cells may seem attractive to treat the injured CNS since they lack ethical concerns. In fact, NSC primary cell lines generated from human fetal CNS tissue, typically around 8–18 weeks of gestation, are the subject of a number of clinical studies. Transplantation of human fetal spinal cord-derived NSCs was shown to improve neurological function in animal models of SCI [92, 107], ischemic stroke [108] and motor neuron disease [82]. Preclinical studies also revealed benefic effects of transplanting human fetal brain-derived NSCs into the injured CNS [87, 109]. However, their use has been associated to mismatched results and variable data [81]. Indeed, a recent preclinical study has revealed that transplantation of CNS-derived NSCs is not sufficient to achieve a functional neurological outcome after cervical SCI [110]. Additionally, transplanted CNS-derived NSCs also failed to differentiate and did not improve cognitive function in a transgenic model of AD [88].

Embryonic stem cells (ESCs), due to their pluripotency and unlimited capacity for self-renewal, have been explored to generate stable and expandable NSCs [111, 112]. In order to plan their use in cell replacement therapies, protocols have been established to efficiently and reproducibly specify ES cells into pure populations of NSCs [113, 114]. In comparison to CNS-derived NSCs, ES-derived NSCs retain a higher proliferative capacity and neuronal differentiation efficiency [112], which can be of interest to counteract the high levels of cell death occurring following transplantation. Preclinical models of SCI have demonstrated the ability of transplanted human ES-derived NSCs to extend axons over long distances and form synapses with host neurons leading to functional improvement, when embedded in a fibrin matrix containing a cocktail of growth factors [78, 92]. In addition, transplantation of hES-NSC into the injured brain resulted in increased survival of hippocampal neurons and cognitive recovery [115], also allowing functional recovery after stroke [116, 117].

Transplantation of NSCs derived from induced pluripotent stem cells (iPSCs) into the injured CNS has also contributed to functional recovery in several preclinical models [118-121]. Nevertheless, to be taken forward to clinical trials, potential safety issues have to be considered. Despite presenting similarities with ES cells, such as the capacity of self-renewal and generation of multipotent stem cells [122, 123], the

methods used in the artificial induction of cellular pluripotency from somatic cells can lead to genetic, epigenetic and functional abnormalities that can reduce the quality of the iPSC cultures [124]. For this reason, good iPSC clones need to be selected prior to using these cells in molecular and biomedical applications, which is *per se* a demanding and expensive task [124].

Alternatively, direct lineage conversion (transdifferentiation) of somatic cells ensures a fast and straightforward generation of induced NSCs (iNSCs) providing interesting alternatives to the iPSC technology, in particular for the treatment of neurodegenerative diseases [123, 125, 126]. Human fibroblasts were directly converted into expandable multipotent iNSCs by ectopic expression of a single transcription factor, which were able to self-renew and differentiate into astrocytes, oligodendrocytes and functional neurons [123, 126]. However, preclinical studies are required to demonstrate the capacity of human iNSCs to reestablish neuronal circuitry and improve function after transplantation into the injured CNS.

Human NSC transplantation for CNS repair: safety and efficacy in clinical trials

Clinical trials are basically well defined experiments on humans. In general, phase I trials are small studies to assess safety and feasibility, with the main goal of determining the maximum tolerated dose and dose-limiting toxicities. In parallel, correlative studies are usually performed to enlarge the knowledge gained from conducting the trial [37]. Phase II trials include efficacy testing in a small group of well defined, treated and control patients [127]. The focus of phase II studies comprises clinical outcomes that can be measured and result in a benefit for the patient, namely to assess response rate (for example, defined as shrinkage of tumor in brain cancer studies or improvement in neurologic function in patients with amyotrophic lateral sclerosis), time to disease progression and overall survival [37]. Phase III trials are large multi-center studies to test the efficacy and safety of the treatment in a large number of patients as a fundamental step to introduce the drug or procedure to clinical practice. Phase II and phase III trials are always controlled and usually double-blinded to reduce biases introduced by knowledge of the treatment by patients or their clinicians [127].

Several clinical trials have been evaluating the safety and efficacy of transplanting NSPCs either isolated from fetal CNS tissue or derived from hESCs or from autologous

MSCs. In 2011, StemCells Inc. initiated a first phase I/II clinical trial (12 patients) to assess the safety and preliminary efficacy of transplanting human fetal brain-derived NSCs for the treatment of chronic thoracic SCI (HuCNS-SCs; StemCells Inc.; ClinicalTrials.gov ID#NCT01321333). Data from this clinical trial has demonstrated patients improvement in multiple sensory modalities with no safety concerns thus far [128]. Subsequently, StemCells Inc. conducted a phase II clinical trial to assess the efficacy of intramedullary transplantation of HuCNS-SC in cervical SCI (StemCells Inc.; ClinicalTrials.gov ID#NCT02163876). Controversial results prompted StemCells Inc. to terminate this study in 2016, citing a lack of significant improvements and the lack of a trend for improvements over time [110]. Precisely, recent investigations described that HuCNS-SCs failed to improve neurological function in a SCI experimental model [110]. Currently, Neuralstem Inc. is conducting a phase I clinical trial to evaluate the safety of transplanting fetal spinal cord-derived NSCs for the treatment of chronic SCI (Neuralstem Inc.; ongoing trial, ClinicalTrials.gov ID#NCT01772810).

An underway phase I/II clinical trial is evaluating the safety and efficacy of transplanting hES-derived NPCs to treat patients suffering from Parkinson's disease (ClinicalTrials.gov ID#NCT03119636). In spite of the transplantation of iPSC-derived NPCs has led to functional recovery in rodent and non-human primate models of SCI [118, 119, 129], clinical trials have not been initiated yet. In the meanwhile, the evaluation of clinical grade iPSC-derived NPCs has been performed by Okano's group, which is now looking forward to initiate clinical testing in SCI patients [121].

Due to their inherent tumor-tropic properties, the use of NSCs has been explored for targeted delivery of anti-cancer agents to tumor cells. This strategy reduces toxicity to healthy tissues, potentially diminishing undesirable side effects [130]. Envisaging a multimodal approach, the effectiveness of transplanting NSCs loaded with an oncolytic virus was assessed in combination with the standard of care for glioblastoma treatment, namely radiation and chemotherapy [131]. Results from these preclinical studies led to the initiation of a phase I clinical trial to evaluate the safety and efficacy of injecting oncolytic virus-loaded NSCs in combination with standard radiation and chemotherapy for patients with newly diagnosed malignant glioma (ongoing trial, ClinicalTrials.gov ID#NCT03072134) [132].

Table I – Clinical trials using transplantation of neural stem/progenitor cells

Condition	***Transplanted cells***	***Status/outcome results***	***Phase***	***Location***	***Start year***	***Reference****
ALS	Fetal spinal cord-derived NSCs (Neuralstem Inc.)	Safe with unilateral and bilateral intraspinal lumbar or cervical microinjection.	Phase I	United States	2011	NCT01348451 [133-135]
		Safe with intraspinal lumbar and cervical injection at high doses, including sequential procedures.	Phase II	United States	2012	NCT01730716 [136]
	Fetal brain-derived NSCs	Safe with unilateral and bilateral intraspinal lumbar injection; improved tibialis anterior (final follow-up: 7 months).	Phase I	Italy	2012	NCT01640067 [137]
	CNS10-NPC-GDNF	Recruiting.	Phase I	United States	2016	NCT02943850
PD	Parthenogenetic stem cell-derived NSCs	Recruiting.	Phase I	Australia	2015	NCT02452723 [138]
	ES-derived NPCs	Recruiting.	Phase I	China	2017	NCT03119636
	Fetal brain-derived NSCs	Enrolling by invitation.	Phase II/III	China	2017	NCT03128450
MS	Autologous MSCs-derived NPCs	Safe with intrathecal injection; neurological function improvement (final follow-up: 7.4 years).	Phase I	United States	2013	NCT01933802 [139]
		Recruiting.	Phase II	United States	2017	NCT03355365
PMD	Fetal brain-derived NSCs (StemCells Inc., HuCNS-SCs)	Safe with bilateral intracerebral injections into frontal white matter (2 per hemisphere); immunosuppression: 9 months.	Phase I	United States	2009	NCT01005004 [140]
		Completed, no study results.	Phase I	United States	2011	NCT01391637

Batten's Disease (NCL)	Fetal brain-derived NSCs (StemCells Inc., HuCNS-SCs)	Safe with no serious adverse events; immunossupression: 12 months.	Phase I	United Stated	2006	NCT00337636 [141]
		Withdrawn.	Phase I	United Stated	2010	NCT01238315
SCI	Fetal brain-derived NSPCs	Safe, well-tolerated, resulting in a modest neurological function improvement (final follow-up: 12 months).	Phase I/II	Korea	2005	[142]
	Fetal brain-derived NSCs (StemCells Inc., HuCNS-SCs)	Safe with intraspinal injections into superior and inferior margins of thoracic SCI; immunosuppression: 9 months; improvement in overall mean functional outcomes measures (final follow-up: 12 months).	Phase I/II	Canada, Switzerland	2011	NCT01321333 [128]
	Fetal spinal cord-derived NSCs (Neuralstem Inc.)	Recruiting.	Phase I	United States	2013	NCT01772810
	Autologous MSCs-derived NSCs	Active, not recruiting.	Phase I/II	Russia	2014	NCT02326662
	Fetal brain-derived NSCs (StemCells Inc., HuCNS-SCs)	Terminated, no study results.	Phase II	United States, Canada	2014	NCT02163876 [143]
	NSCs combined with a scaffold	Recruiting.	Phase I/II	China	2016	NCT02688049
Stroke	CTX0E03 NSCs (ReNeuron)	Safe with MRI-guided single intracerebral injection into putamen adjacent to infarct area (up to 20 million cells); improved neurological function with no adverse events; no immunosuppression (final follow-up: 2 years).	Phase I	United Kingdom	2010	NCT01151124 [144]
		Overall improvement, including in arm function (final follow-up: 12 months).	Phase II	United Kingdom	2014	NCT02117635

Lower limb ischemia	CTX0E03 NSCs	Active, not recruiting.	Phase I	United Kingdom	2013	NCT01916369
CP	Fetal brain-derived NPCs	Safe with injection in the lateral ventricle, improvement of functional development and no delayed complications (final follow-up: 12 months).	NA	China	2005	[145]
	Fetal brain-derived NSCs	Injection in the lateral ventricle, improvement with varying degrees and no severe adverse reactions (final follow-up: 3 months).	NA	China	2005	[146]
	Autologous MSC-derived NSCs	Safe, optimal improvement in motor function (final follow-up: 6 months).	NA	China	2010	[147]
	NSCs	Active, not recruiting.	NA	China	2016	NCT03005249
AMD	Fetal brain-derived NSCs (StemCells, Inc; HuCNS-SCs)	Completed, no study results.	Phase I/II	United States	2012	NCT01632527
HIE	NPCs with paracrine factors from MSCs	Recruiting.	NA	China	2016	NCT02854579
Glioma	NSCs expressing *E. Coli CD*	Completed, no study results.	Phase I	United States	2010	NCT01172964
		Active, not recruiting.	Phase I	United States	2013	NCT02015819
	NSCs expressing Carboxylesterase	Recruiting.	Phase I	United States	2014	NCT02192359
	NSCs loaded with oncolytic adenovirus	Recruiting.	Phase I	United States	2017	NCT03072134 [132]
GBM	NPCs	Active, not recruiting.	Phase II	United States	2011	NCT01478854

Abbreviations: ALS, amyotrophic lateral sclerosis; AMD, aged macular degeneration; CNS10-NPC-GDNF, human neural progenitor cells secreting glial cell line-derived neurotrophic factor; *E. Coli CD*, cytosine deaminase; CNS, central nervous system; CP, cerebral palsy; CTX0E03, immortalized human neural stem cell line; ESC, embryonic stem cell; GBM, glioblastoma; HIE, neonatal hypoxic-ischemic encephalopathy; HuCNS-SCs, expanded neural stem cell product derived from FACS-purified fetal neural stem cells; MS, multiple sclerosis; MSCs, mesenchymal stem cells; MRI, magnetic resonance imaging; NCL, neuronal ceroid lipofuscinosis; NPCs, neural progenitor cells; NSCs, neural stem cells; NSPCs, neural stem/progenitor cells; PD, Parkinson's disease; PMD, Pelizaeus-Merzbacher disease; SCI, spinal cord injury. (*) ClinicalTrials.gov ID#.

Current limitations of NSC-based therapies

During the past decade, significant advancement has been made towards the clinical implementation of cell-based therapeutics. However, current cell-based approaches have presented limited success, with numerous studies showing fewer than 5% of injected cells persisting at the site of injection within days of transplantation [148]. Despite increasing attention given to clinical trial design, insufficient importance has been set to the establishment of standards for therapeutic routines, including tools and protocols used to deliver cells. A typical cell-based approach procedure is based in three stages: (1) *in vitro* preparation of cellular suspensions; (2) injection route; and (3) retention of the delivered cells post-injection [149]. For efficient injectable cell transplantation, accurate characterization of cellular health post-injection and the development of standardized administration protocols are required (Fig. 4).

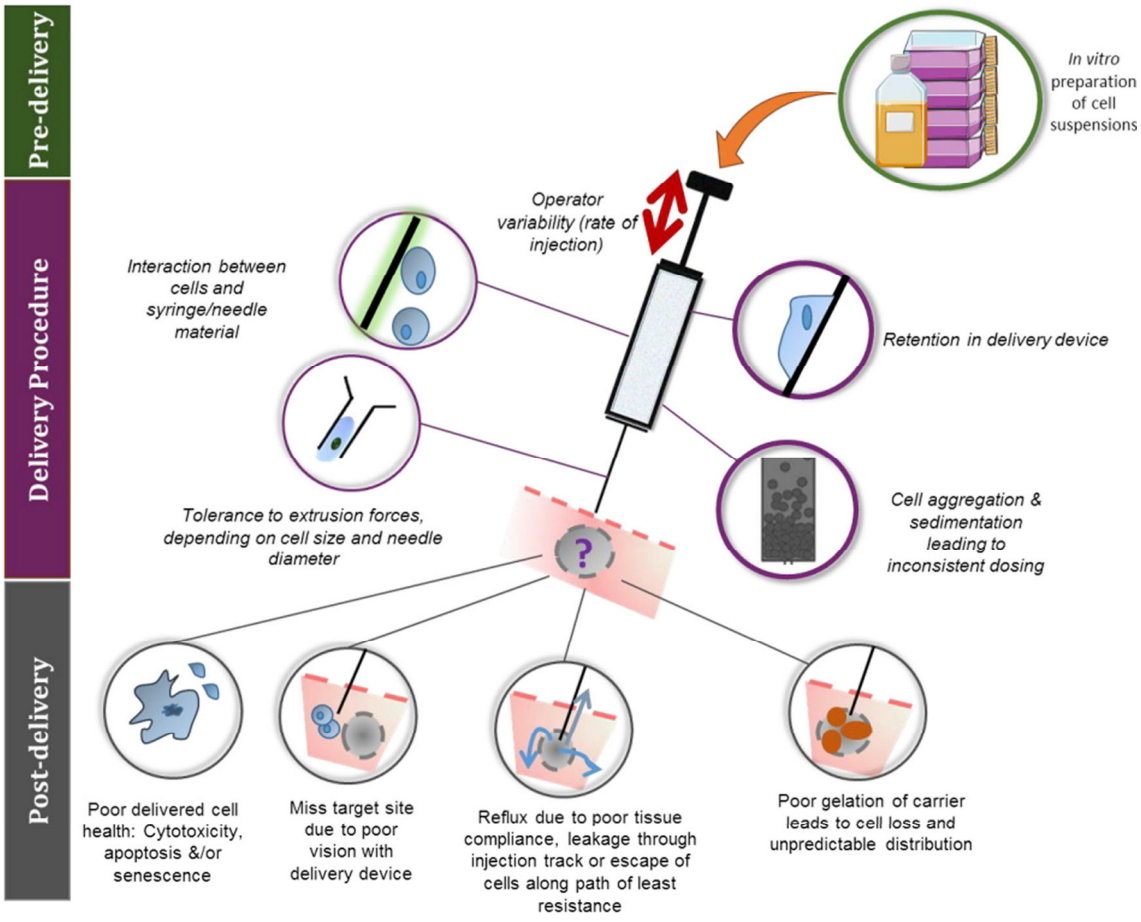

Figure 4. Common problems using injectable cell delivery and possible cell fates. Three stages constitute a typical cell-therapy protocol: *in vitro* preparation (pre-delivery), injection (delivery) and subsequent retention (post-delivery) of injected cells. Image reproduced with permission from Amer *et al.* [148] (Common Creative license).

Purity of NSCs should be primarily addressed *in vitro*, namely through genetic selection using cell sorting, to avoid formation of teratomas, tumors, or expansive ectopic structures that might result from residual undifferentiated cells or other progenitor cells present in the transplanted population [150, 151].

Furthermore, the cell dose/density must be precisely controlled, since it influences the NSC engraftment, integration and functional outcome [152, 153]. In addition, several clinical issues should be carefully addressed including cell suspension vehicle (parenteral or isotonic saline solutions *vs.* biomaterial-assisted cell delivery); spatial and temporal administration protocol (single injection *vs.* multiple and lower volume injections, single dose *vs.* continuous or sequential administration of cells over time); therapeutic window for administration (during the acute or the chronic phase of disease); and route of administration, namely local (intraparenchymal), into the cerebrospinal fluid (intracerebroventricular or intrathecal), or systemic (intravenous or

intra-arterial) [35, 75, 148]. Likewise, growing attention is given to the development of safe and reliable devices to inject NSCs in the human brain or spinal cord. In fact, conventional needle-based and catheter-based cell transplantation tools present considerable failures that may affect clinical translation [154, 155]. Such cell-delivery systems should allow ease loading and use, reproducibility of delivery, possibility of sterilization, freedom from leachable and/or extractable contaminants, and also ensure no visual obstruction through a surgical microscope in high accuracy applications [148].

Despite their functional benefits, exogenously-delivered NSCs into the damaged CNS show poor cell survival and migration, and limited differentiation along the neuronal lineage [10, 156, 157]. Therefore, to achieve long-term functional integration of transplanted NSCs into the host CNS, several issues need to be addressed, namely donor cell migration capacity and axonal outgrowth ability [158]. Additional studies may also be required to better understand the underlying mechanisms of NSC therapy. Variable clinical outcomes observed in two trials for PD [159, 160] have been partially attributed to a failure to properly distribute cells to the target site [161]. Moreover, saline-based suspension vehicles have been found to affect the viability of cells pre-delivery and their survival upon implantation [149]. In this sense, biomaterial-based carriers are required to accomplish an efficient delivery of NSCs, namely by combining single NSCs or aggregates of NSCs (neurospheres) with biodegradable hydrogels. Besides allowing a homogenous NSC distribution at the site of injury, hydrogels contribute to sequester neurite-promoting factors, creating a more favorable microenvironment for cell survival and regeneration [162].

Hydrogels for delivery of neural stem/progenitor cells

Hydrogels are a class of materials that present a three-dimensional (3D) network structure made of hydrophilic polymers cross-linked via chemical bonds or physical interactions, capable of retaining a high amount of water (over 90%). Hydrogels are also highly permeable materials allowing exchange of ions, oxygen, low molecular-weight nutrients and metabolites, providing a permissive microenvironment for cell survival and growth. These properties, together with the relatively mild conditions required for hydrogel processing and functionalization makes them appealing for use as support matrices for cell transplantation, and in 3D platforms for cell culture [163]. Additionally, hydrogel scaffolds can be designed to be used as systems for the localized delivery of drugs or growth factors [164-166], allowing their use in combinatorial therapeutic strategies.

Biophysical properties of the hydrogels are known to modulate NSC behavior [167, 168]. To be used in tissue engineering, hydrogels mechanical properties should match those of native tissue to resist *in vivo* forces and to maintain structural integrity. The overall mesh size, porosity (pore size) and stiffness of hydrogel scaffolds can be adjusted by varying the polymer size and concentration of the monomer/macromer/polymer, as well as the initiator and cross-linker concentrations [169]. In order to increase their functionality and performance, polymeric scaffolds can be chemically modified (e.g. with cell adhesion ligands) through their available functional groups, such as hydroxyl, ester, and carbonyl groups [170].

Injectable polymeric solutions capable of forming a cross-linked 3D network *in situ* upon physical or chemical stimuli hydrogels present several advantages for biomedical applications, namely the capacity of the hydrogel to adapt to the defect shape. Furthermore, the use of *in situ* forming hydrogels allows practice of minimally invasive surgical procedures for implantation (resulting in a faster recovery, smaller scar size and less pain for patients), also able of easy and effective encapsulation of cells and/or drugs [171]. These features make *in situ* forming hydrogels ideal to function as a vehicle for NSC encapsulation and transplantation into complex CNS injury sites as spinal cord and brain [172-174]. Still, hydrogels should create a permissive microenvironment for transplanted NSPC survival, migration and axonal outgrowth, namely by mimicking the biophysical and biochemical properties of the ECM in NSC niches [175-177]. In this sense, the design of hydrogels to deliver NSPC into the damaged CNS should address issues as mechanical strength, microstructure, degradation, and cell-adhesive properties [178] (Figure 5).

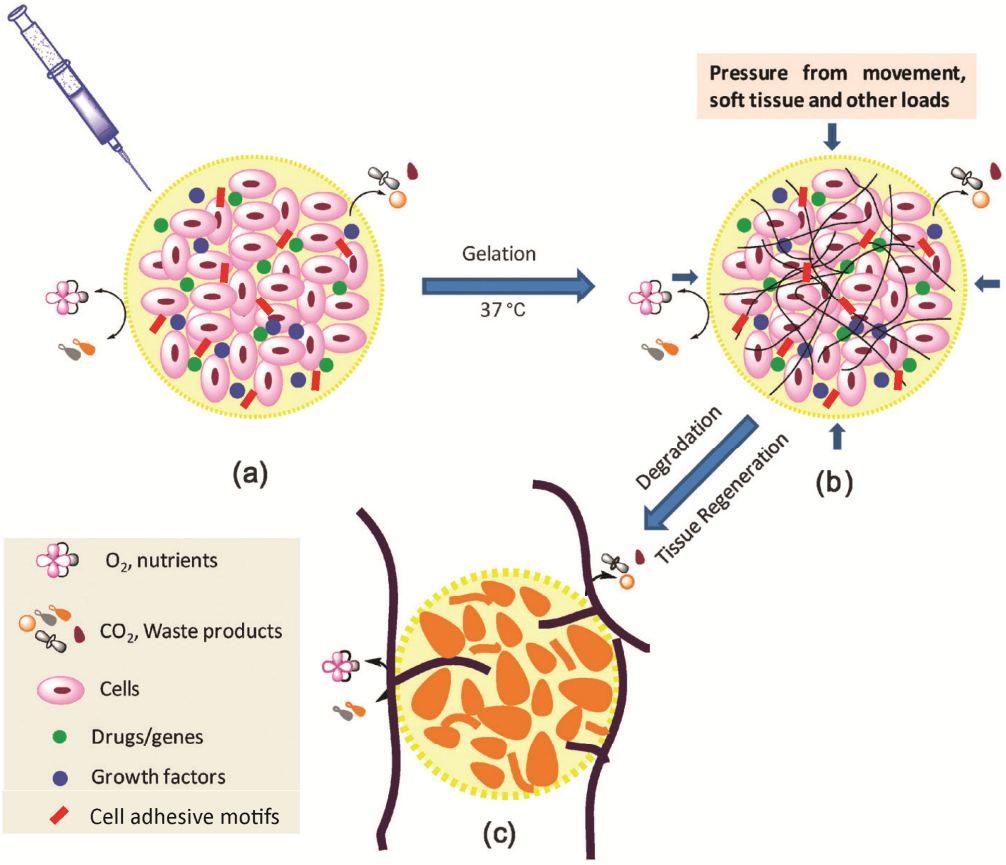

Figure 5. Design of injectable *in situ* forming hydrogels for neural stem/progenitor cell (NSPC) delivery. (a) The polymerizing solution encapsulating NSPCs, which could contain drugs/genes and/or growth factors and/or cell adhesive motifs, should be injected into the damaged tissue. **(b)** Upon physical stimuli (pH, temperature or ionic concentration) or chemical reactions (for example, enzyme catalysis), the injected solution should polymerize *in situ*, forming a hydrogel that can fill the injury cavity and effectively deliver cells. Together, the hydrogel should have: structural and mechanical properties closely matching those of the target tissue mechanical properties that can support the internal/external pressure created by neighboring soft tissue invasion and movements; permeability allowing the continuous exchange of gases/ions and nutrients/metabolites in, out, and within the hydrogel, and tissue-specific biophysical cues for cell-adhesion or ECM/growth factor binding. **(c)** The hydrogel should have a degradation rate adjusted to tissue remodeling (via cell-triggered proteolytic degradation). Image adapted from Li *et al.* [179], Copyright© 2012, with permission from The Royal Society of Chemistry.

Several studies have explored both the use of naturally-derived and synthetic polymers to assist NSPC transplantation into the injured CNS [174, 180-182]. Naturally-derived polymers (e.g. collagen, fibrin or hyaluronic acid) have been extensively explored due to their innate bioactive properties and biocompatibility. Still, synthetic polymers have additional advantages such as low risk of immunogenicity, and tunability which allows a more precise control of bulk properties and degradation rates [183]. The combination of natural and synthetic polymers has been also explored to develop NSPC vehicles [184, 185].

Biophysical and biochemical cues present in the NSC niche

The NSC niche is the *in vivo* specialized microenvironment where NSCs both reside and receive stimuli that determine their fate. In the adult brain, the subventricular zone (SVZ) niche is constituted by support cells, such as endothelial cells and astrocytes, which are found in close proximity to NSCs; and by a specialized basal lamina that extends from perivascular cells at the blood vessels to contact all cell types [186, 187].

At the NSC niche, a wide range of biophysical and biochemical signals dictate cell behavior, including growth factors released by cells; cell-to-cell (at adherens and gap junctions), and cell-extracellular matrix (ECM) contact-mediating signaling [188]. The cellular microenvironment is defined by cells and their ECM, namely in terms of chemical, structural and mechanical properties. Biophysical signals present in the NSC niche include biochemical factors that are spatiotemporally modulated, mechanical cues, and electrostatic cues [189]. To sustain neuronal differentiation, neurite outgrowth, and cell infiltration, hydrogels strength and stiffness should ideally match those of native CNS tissues [190]. In fact, neurons prefer to grow on substrates with lower storage moduli (0.1–1.0 kPa), compared to relatively stiffer surfaces preferred by astrocytes and oligodendrocytes; meanwhile the elastic properties ideal for neurite branching and extension are even more restricted (Fig. 6) [167, 191-197]. These studies highlighted the importance of adjusting the mechanical properties of the hydrogel to direct neural cell lineage, proliferation, and growth. Moreover, the hydrogel compressive modulus can be tuned as a function of degradation and loss of cross-links, enabling hydrogels to degrade on the same time scale during which the encapsulated cells produce their own ECM, allowing tissue repair [198-200].

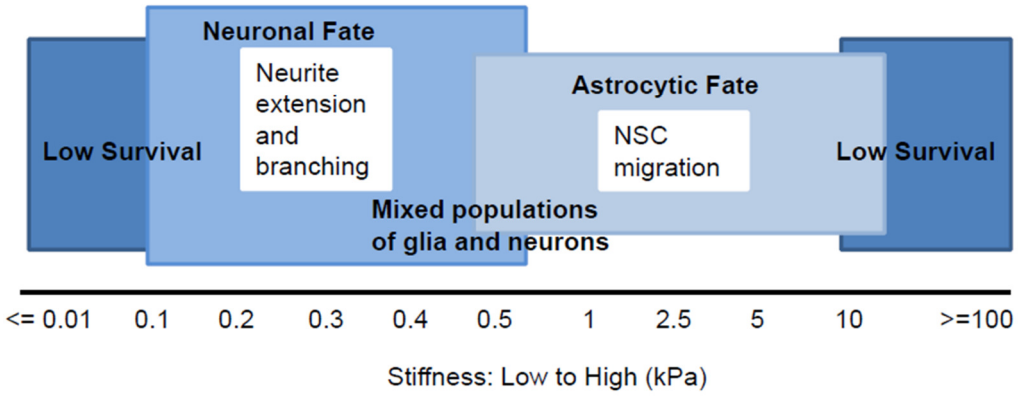

Figure 6. Survival and fate of neural stem cells as a function of biomaterial stiffness. Imaged adapted from Aurand *et al.* [175], Copyright© 2012, with permission from Elsevier.

The ECM is secreted by both support cells, including glial cells, and NSCs. This complex network is enriched in glycoproteins, such as laminin, collagen, tenascin and fibronectin; and glycosaminoglycans (GAGs), such as heparin or heparan sulfate (HS), chondroitin sulfate (CS) and hyaluronic acid. Proteoglycans are composed of at least one glycosaminoglycan (GAG) side chain covalently bound to a core protein [201]. While providing physical support for cells, the ECM harbors specific repertoires of soluble and immobilized factors that regulate tissue morphogenesis, differentiation and homeostasis [202].

Laminins (LNs) are large heterotrimeric glycoproteins that essentially constitute basement membranes (basal laminae), specialized extracellular matrices found in intimate contact with individual cells and cell layers, including at the NSC niche [203]. Presently, at least 16 mammalian LN isoforms have been reported, each with distinct spatiotemporal expression patterns, different domain locations for specific interactions with several molecules that represent different functions [204, 205]. Laminins are constituted by the assembly of three disulfide-linked polypeptides, the α, β and γ chains (Figure 7) [206, 207]. The laminin G domain-like (LG) modules of LN α chains mediate the interactions with cell surface receptors, including integrins, syndecans and α-dystroglycan, regulating multiple cellular activities and signaling pathways, including cell migration, differentiation, tissue remodeling and neurite outgrowth [203, 205, 207, 208].

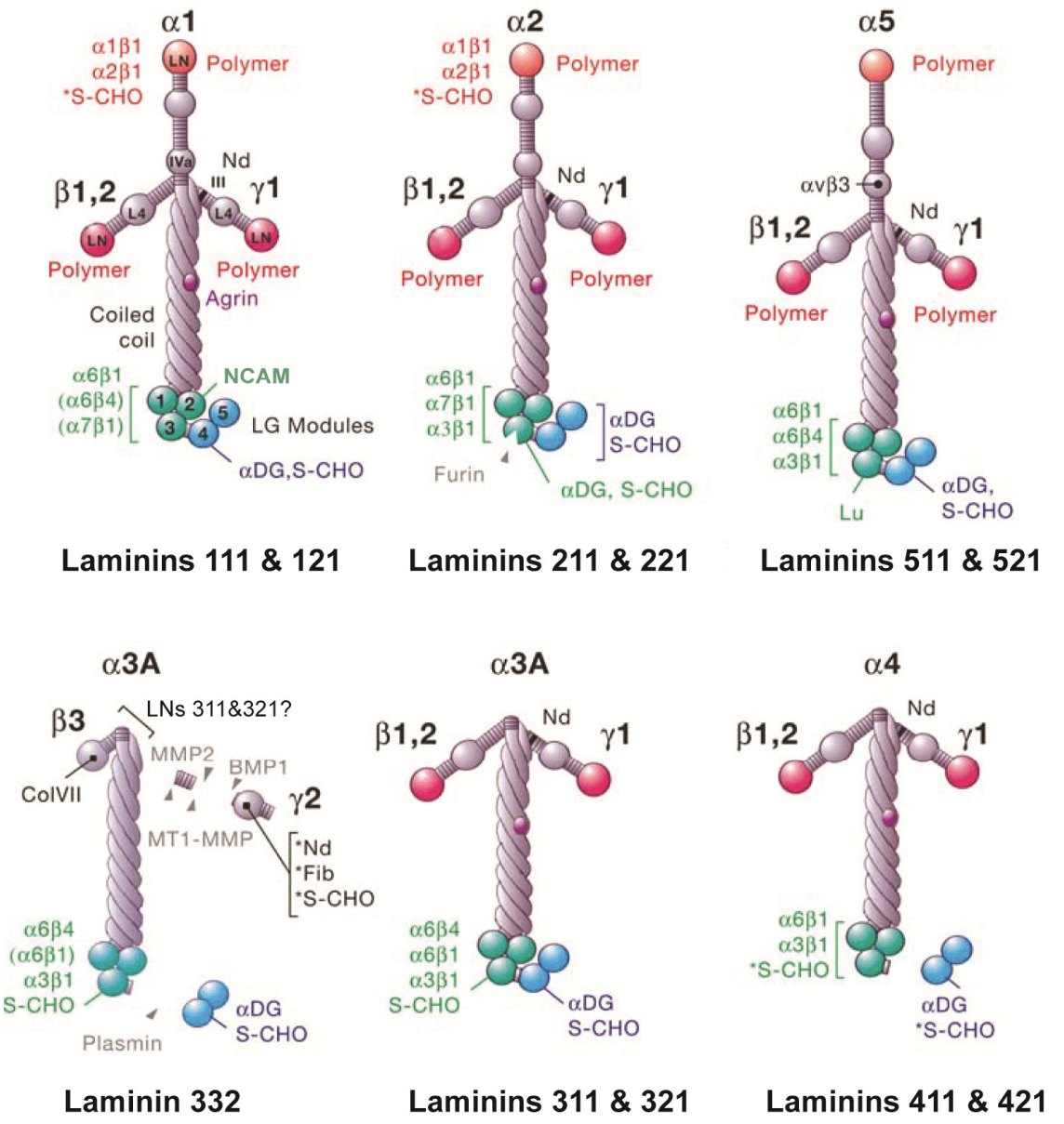

Figure 7. Schematics show domain locations for specific interactions of different laminin isoforms. These include domain locations of architectural scaffolding [polymerization and laminin-binding to other glycoproteins like nidogen (Nd), agrin, other laminins, and fibulins (Fib)]; cell surface anchorage through sulfated carbohydrates (S-CHO), heparin, sulfatides and related molecules; NCAM; and receptor interactions mediated by integrins, such as α6β1 and α3β1, and α-dystroglycan (α-DG). Laminin LG domains are represented in green (LG1–3) and blue (LG4–5). Lower affinity interactions are indicated with asterisks. Proteinases (furin, MT1-MMP, MMP2, BMP1, plasmin), which cause dissociation of distal domains in the case of laminin 332 (but not laminin 211) to alter functional activities, are shown. BMP1, bone morphogenic protein-1. NCAM, neural cell adhesion molecule. MMP, matrix metalloproteinase. MTP1-MMP, membrane type 1-matrix metalloproteinase. Image adapted from Miner and Yurchenco [205], Copyright© 2004, with permission of Annual Reviews.

Laminin 511 (α5β1γ1) is the most common form found in the basement membrane (BM) of the early embryo and most adult tissues [205, 209, 210]. In the CNS, α5-laminins play key roles during neural tube formation, which also were proved to sustain hESCs pluripotency *in vitro*. LN 511 is known to be is the principal component of the BM at the hippocampus that serves as a niche for NSCs in humans. LN 511 is most highly expressed in the neuronal cell layers of the hippocampus, protecting attached neurons from apoptosis caused by excess of excitotoxins [211]. Moreover, laminins are the main constituents of the blood-brain barrier that protects the CNS from the blood circulation and immune system, a part of which is a double BM surrounded by blood vessels. The intrinsic BM of the blood-brain barrier is highly enriched in LN 411 and LN 511 produced by vascular endothelial cells. The external BM contains α1- and α2-laminins, secreted by astrocyte endfeet [210]. Also, α2-laminins are needed for oligodendrocyte maturation and CNS nerve myelination [212].

Integrins are laminin receptors that control both cell-to-ECM and cell-to-cell interactions at the NSC niche. These transmembrane glycoprotein receptors are involved in NSC migration, proliferation and differentiation, as well as BM assembly [213, 214]. On the cytoplasmic face of the plasma membrane, integrins control the assembly of cytoskeletal polymers and signaling complexes, while on the extracellular face, integrins engage either with ECM macromolecules, namely laminin, collagen, fibrinogen and fibronectin, or co-receptors on adjacent cell surfaces, such as syndecans [215]. Integrin receptors are composed of a heterodimer of α and β subunits. There are 18 different α subunits and 8 β subunits that form a limited number of possible combinations. To date, at least 24 unique integrin complexes have been identified, each with its own binding specificity for different subsets of ligands (Figure 8).

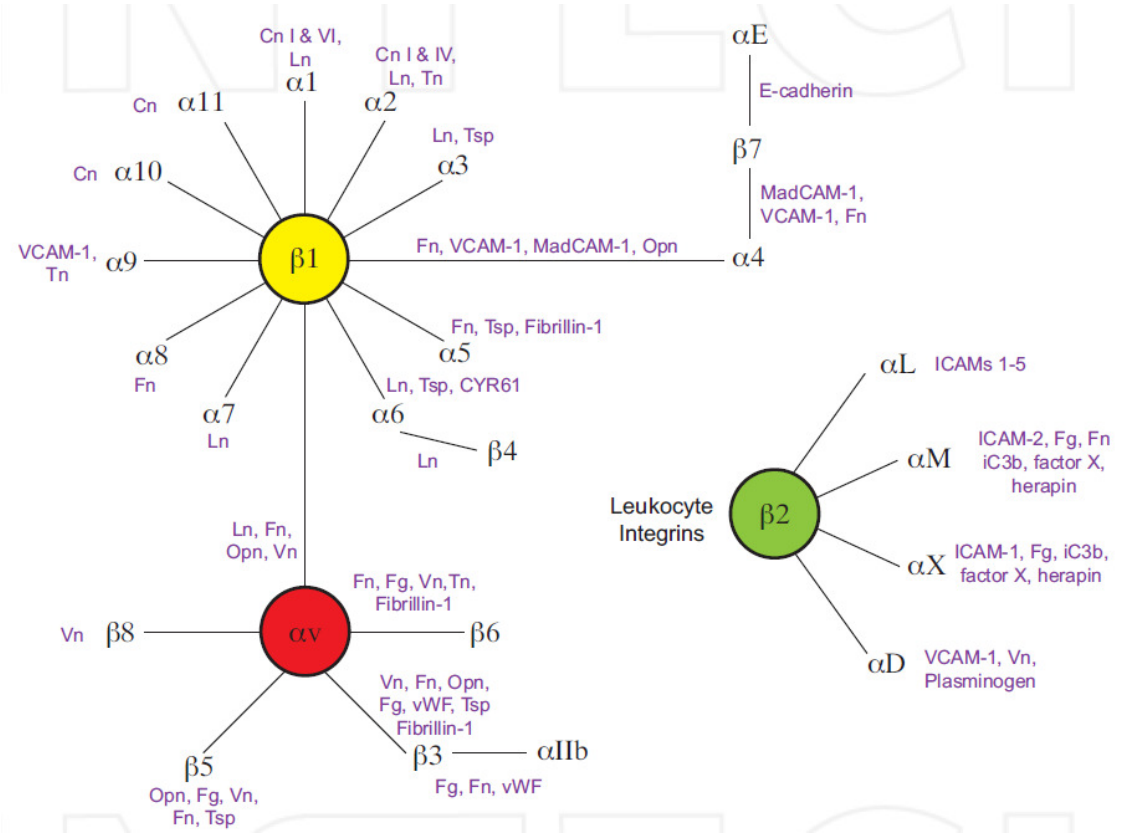

Figure 8. Integrin heterodimers and their ligands. Integrin heterodimers are represented by an α and a β subunit connected by a black line. The ligands for each heterodimer are written in purple. Cn, collagen. CYR61, cysteine-rich angiogenic inducer 61. Fn, fibronectin. Fg, fibrinogen. ICAM, intercellular adhesion molecule. iC3b, by-product of the classical pathway of complement activation. Ln, laminin. MadCAM-1, mucosal vascular cell adhesion molecule 1. Opn, osteopontin. Tn, tenascin. Tsp, thrombospondin. VCAM, vascular cell adhesion molecule. vWF, von Willebrand factor. Image adapted from Young *et al.* [216], Copyright© 2013, Creative Commons Attribution 3.0 license.

All five αv integrins, two β1 integrins (α5β1, α8β1) and αIIbβ3 share the ability to recognize ligands containing the RGD (arginine-glycine-aspartic acid) motif, found in several ECM molecules, which has been identified as a minimum cell recognition sequence mediating adhesion of many cell types, including neurons [217-219]. However, at the cell surface, integrins can exist in a range of conformations that affect their affinity for ligand. Changes in conformation can be regulated by intracellular signaling events such as the binding of cytosolic proteins to integrin tails leading to integrin clustering, focal adhesion formation and further interaction of cytoskeletal proteins [216]. Importantly, the activation state of integrins is tightly regulated by divalent cation occupancy of the ligand-binding domains. These divalent cations, such as Mn^{2+}, Mg^{2+} and Ca^{2+} elicit conformational changes in integrins structure that activate ligand binding and signaling at the cell surface, also allowing a proper control of the intracellular integrin signaling [220, 221] (Figure 9).

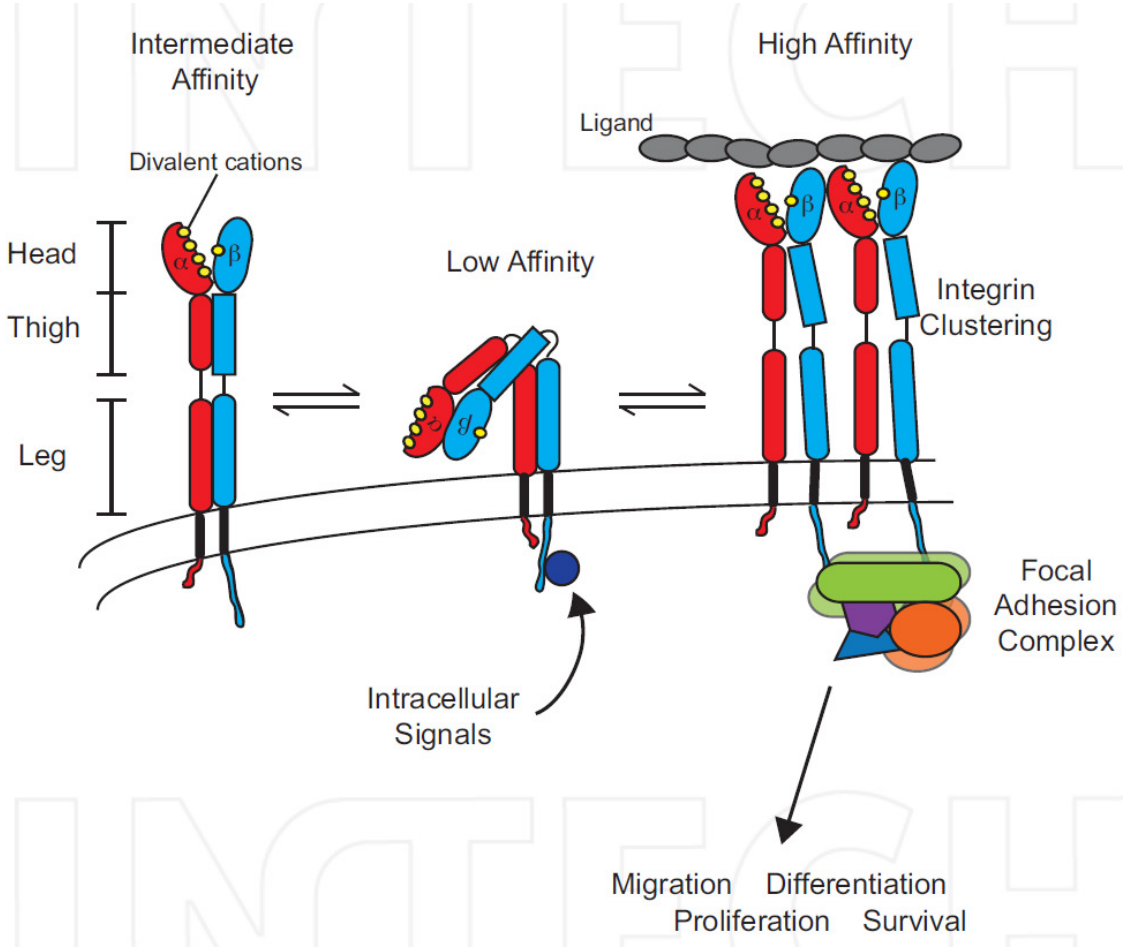

Figure 9. Integrin structure and activation. Integrins are composed of a large extracellular domain and short intracellular tails (with the exception of the β4 tail). The extracellular domain comprises a head region and a stalk region, which includes the "thigh" and "leg" areas of the integrin. Ligand binding occurs at the head region and requires the presence of divalent cations such as manganese, magnesium, and calcium Image reproduced from Young *et al.* [216], Copyright© 2013, Creative Commons Attribution 3.0 license.

Within the CNS, integrins play distinct roles in neural development, synaptogenesis, inflammation and CNS angiogenesis [222]. Integrins are ubiquitously distributed in the CNS, and at least 14 integrin subunit combinations have been reported: α1β1, α2β1, α3β1, α4β1, α5β1, α6β1, α7β1, α8β1, α9β1, αvβ1, αvβ3, αvβ6, αvβ8 and α6β4 [223]. Neural stem/progenitor cells highly express β1 and α6 integrin subunits, and also express at their surface α3, α5, α7 and αv integrin subunits [224-226]. At the NSC niche, β1 integrin-mediated signaling controls NSC survival, maintenance, proliferation, migration and differentiation [227, 228]. Also, integrins α3β1, α6β1 and α5β1 are known to modulate neuronal migration [229-232]. In specific, integrin α6β1 is a key mediator of NSPC migration *in vitro* [227, 233], as well as along the adult mouse rostral migratory stream *in vivo* [230]. Moreover, integrin α6β1 has been shown to direct laminin-dependent outward migration of human ES-NSPCs [234]. Integrin α6β1 binds to LN 511, reported to be a potent adhesive substrate for neuronal cells [235], namely

supporting the attachment and network formation of hPS-derived neurons [236]. The binding site for integrin α6β1 in LN 511 is located in the LG1 module of the globular domain of LN α chain, and requires the tandem assortment of LG1–3 modules and the glutamic acid residue within the C-terminal region of LN γ chain for active conformation and full binding activity [237-239] (Figure 7). Being the principal laminin receptor in the CNS, integrin α6β1 also binds to other relevant laminin isoforms such as LN 111 (highly expressed during embryogenesis) and LN 332 (specific for epithelial cell adhesion) [240].

Also important are the αv integrins which act as key regulators of neuronal migration during the development of the cerebral cortex, and of vasculogenesis and angiogenesis in the brain, being essential for proper cerebral blood vessel development [229, 241].

Besides integrins, syndecans are also important cell adhesion receptors present at the NSC niche. Syndecans are transmembrane proteoglycans that play critical regulatory roles in many biological processes, including wound healing, inflammation, neural patterning, and angiogenesis. There are four members of the syndecan family in mammals, three of which (syndecans-1 to -3) have a restricted tissue distribution, and the fourth of which (syndecan-4) is expressed ubiquitously [242]. Syndecans are composed of large heparan sulfate and/or chondroitin sulfate chains covalently attached to the extracellular domain and short cytoplasmic tails that interact with a variety of molecules, such as growth factors and ECM proteins, such as laminin and fibronectin (Figure 10) [243]. Extracellular domain shedding is reported to play a key role in regulating syndecan-ligand interactions and intracellular signaling, including cooperation with integrin receptors to control cell adhesion [242].

At the cytoplasmic surface, heparan sulfate chains of syndecans bind to the LG4–5 region of LN α chains [244, 245]. Given that LG modules in the globular domains of LN α chains are capable of binding to syndecan and integrin α6β1, it is likely that both receptors could associate to act synergistically to modulate cell function. In fact, recent investigations show that the cross-talk between integrins and syndecans is complex and can be regulated by innumerous mechanisms that are not yet fully understood [242].

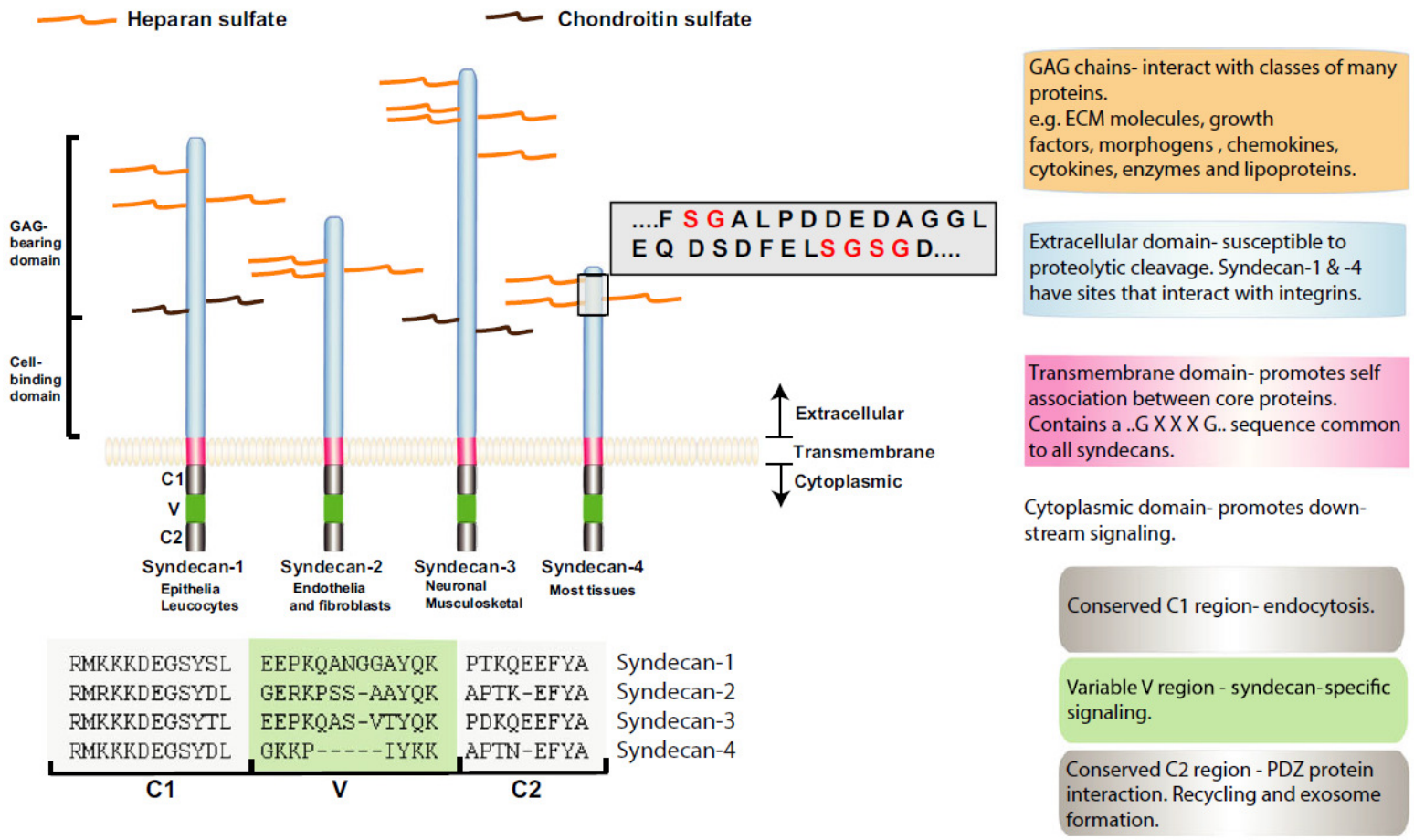

Figure 10. Schematic of the mammalian syndecans, illustrating structure and interactions. ECM, extracellular matrix. GAG, glycosaminoglycan. PDZ, acronym combining the first letters of the first three proteins in which these domains were identified: post-synaptic density 95 (PSD-95), *Drosophila* discs large (Ddl1), and zonula occludens-1 (ZO-1). Image reproduced from Couchman *et al.* [246], Copyright© 2014, with permission from John Wiley & Sons.

Several investigations address the key role of the syndecan family in the biology and function of NSCs. Syndecan-1 is required for mouse neural precursor cells maintenance and proliferation [247], and also contributes to the regulation of LN 332 deposition [248]. Syndecan-1 was also reported to regulate axonal regeneration, possibly by promoting growth cone stability and migration, and guiding axons to their pre-injury targets [249]. Syndecan-2 regulates the maturation of dendritic spines in neurons [250], small protrusions that receive synapses, allowing functional contact between the axon terminal of a neuron with a target cell [251]. Syndecan-3 is known to mediate neuronal migration and neurite outgrowth through the binding of its heparan sulfate chains to heparin binding growth-associated molecule and other growth factors [252-254]. Oikari and colleagues recently reported that syndecan-1, -2 and -3 presented high expression in basal human NSCs derived from the H9 embryonic stem cells, with extended culture upregulating syndecan-2 and -3 expression [255]. They also observed syndecan-4 expression upregulation following neuronal differentiation of hES-SCs [255], which is in accordance to previous studies showing that syndecan-4 modulates neural induction [256]. Syndecan-4 was also found to localize to focal adhesions [257], which in turn regulate axon growth/guidance, and control cell migration and adhesion to the local substrate [251].

Biomimetic cell adhesive motifs

The use of hydrogels that mimic both the cell adhesive and mechanical properties of the CNS has been explored to increase the efficiency of NSC transplantation [14, 258]. The tethering of binding sites for cell adhesion receptors to a hydrogel is fundamental for cell anchorage to the surrounding matrix, as well as to enhance NSC migration and neurite outgrowth after delivery into the injured CNS [261]. Cell migration is a process requiring a sustained balance between adhesion and tractile forces governed by a signaling axis involving integrin-ligand interactions, small GTPase RhoA (Ras homolog family member A) signaling, and actomyosin contractility forces, ultimately dependent on matrix properties, soluble factors and proteolytic activity [259, 260]. Hydrogels chemically modified with peptide sequences such as laminin-derived IKVAV [174], or with ECM proteins like collagen I, fibronectin and laminin [262] have been used to deliver NSCs into the injured CNS. Also, the use of cell adhesive motifs to functionalize hydrogels can improve cell adhesion potential, enhancing cell survival, proliferation and migration [263, 264]. The RGD (arginine-glycine-aspartic acid) sequence, for example, found in fibronectin, collagen, fibrinogen and laminin (in laminin the RGD sequence is a cryptic domain, only available after proteolytic cleavage), has been identified as a

minimum cell recognition sequence mediating adhesion of many cell types, including neurons [217, 218].

Several studies report the use of full length proteins to modify hydrogels for application in stem cell-based CNS regenerative therapies. Most of them integrate ECM-derived proteins into the hydrogel structure, such as laminin, fibronectin and collagen [226, 262, 265-267]. Still, the incorporation of smaller peptides containing the domain of interest of the native ECM protein has brought some advantages to the field [261]. Proteins are folded chains, where every unit is a single amino acid and the order of these units determines the protein's tertiary structure through molecular geometry and intramolecular chemical interactions. On the other hand, peptides are shorter chains of up to around 50 amino acids. This gives them a simpler and more predictable structure that makes them easier to manipulate and reproduce synthetically [268]. The use of small synthetic bioadhesive peptides allows the achievement of higher densities of cell-adhesion domains and, consequently, higher biological activity, even if the peptides lack multiple binding domains of native ECM molecule [261]. Short peptides have the ability to emulate certain properties of the full-length protein that they are derived from [269]. In this way, small peptides provide an extensive range of biophysical cues that can be used to recreate biological processes such as enabling naturally occurring enzyme-mediated degradation [270], specific binding of biomolecules such as growth factors, or directing cell adhesion, migration, proliferation and differentiation [271, 272]. Moreover, because they are shorter, peptides are less immunogenic comparing to proteins constituting an interesting therapeutic approach.

A number of cell adhesive sequences have been explored to confer bioactivity to hydrogel vehicles designed for NSC transplantation or *in vitro* culture, aiming to replicate the *in vivo* NSC niche. Sequences specific to neural adhesion and neurite outgrowth are found primarily in the ECM molecule laminin, including YIGSR and IKVAV, RNIAEIIKDI and RYVVLPR. YIGSR, found in LN β1 chain [273], and IKVAV, found near the globular region of LN α1 chain [274], bind the 67 and 110 kDa cell surface receptors, respectively, also known to be recognized by the β1-integrin receptor subunit [275-277], which is highly expressed by NSPCs. Indeed, the incorporation of YIGSR and IKVAV sequences in hydrogels has been largely explored to enhance neurite outgrowth and/or NSPC migration [278, 279]. Other ECM-derived sequences have been explored, namely the RKRLQVQLSIRT sequence (AG73 peptide) from the LG4 module of LN α1 chain, which was shown to interact with syndecan-1 and -4 [280, 281]. The modification of natural hydrogel matrices with the

AG73 peptide was reported to promote neurite outgrowth, namely on alginate- [282] or collagen-based [283] matrices.

In addition to laminin-derived peptides, the incorporation of RGDS domain sequence derived from fibronectin into hydrogels has been successfully used to promote NPC adhesion and neurite outgrowth [284-286]. Besides, the modification of fibrin hydrogels with a bioactive sequence present in collagen type I and fibril forming collagens (DGEA) was shown to enhance neurite outgrowth from chicken dorsal root ganglia [287].

Of note, some studies report that the combination of laminin-derived peptides can have additive or even synergistic effects when compared to the use of individual peptides [278]. In specific, the incorporation of an equimolar mixture of RGD, IKVAV, YIGSR and RNIAEIIKDI peptides into fibrin matrices synergistically improved neurite outgrowth from dorsal root ganglia [288]. Similarly, the incorporation of a mixture of IKVAV and YIGSR (1:1 w/w) in dextran hydrogels led to a higher increase in neurite extension when compared to that elicited by RGDS alone [289].

A list of cell adhesive motifs to incorporate within 3D hydrogel matrices for CNS-targeted therapies, including bioactive sequences of natural and non-natural origin, is provided in Table II.

Table II – Cell adhesive sequences explored to engineering hydrogel matrices for application in the CNS, and correspondent biological effect.

Adhesive ligands derived from the ECM				
Sequence	***Derived from***	***Cell surface receptor***	***Hydrogel backbone***	***Biological effect***
IKVAV	Mouse LN α1 chain	110 kDa LN binding protein [274] and integrin α3β1 [290, 291]	Fibrin	Neurite outgrowth (DRGs) [292]
			SAP amphiphile	Neurite outgrowth and neuronal differentiation of NPCs [293]
			RADA16-based SAP	NSPC survival and neurite outgrowth [174]
			PEG	Neurite outgrowth (PC12 neuronal cells) [294]
			Alginate	NPC migration and neurite outgrowth [295]
			Hyaluronic acid	iPS-NPC survival [296]
Cyclic IKVAV	Mouse LN α1 chain	Integrins α3β1 and α7β1 [297]	PEG	hNSC adhesion, migration and neuronal differentiation [298]
YIGSR	Mouse LN α1 chain	67 kDa non-integrin protein receptor [299] and integrin α4β1 [276]	Agarose	Neurite outgrowth (DRGs) [292, 300]
			Fibrin	
			Alginate	Neurite extension (PC12 neuronal cells) [301]
			PEG-based	NPC survival [302]
RNIAEIIKDI	Mouse LN γ1 chain	Integrin α2β1 [303]	Fibrin	Neurite outgrowth (DRGs) [288]
PPFLMLLKGSTR (G3P)	LG3 module of LN 332 α chain	Integrin α3β1	Collagen	NSC adhesion and survival [304]
RKRLQVQLSIRT (AG73)	LG4 module of mouse LN α1 chain	Syndecan-1 and -4 [280, 281].	Alginate	Neurite outgrowth (PC12 neuronal cells) [282, 283]
			Collagen	

RGD	Fibronectin, LN*, collagen and fibrinogen	Integrins α5β1 and αvβ3 [305]	Fibrin	Neurite outgrowth (DRGs) [288]
RGDS	Fibronectin	Integrins α5β1, αvβ1, αvβ3, αvβ5, αvβ6 and α8β1 [305, 306]	Agarose	Neurite outgrowth (dissociated DRG cells) [284]
			PEG	Neurite extension (PC12 neuronal cells) [294]
				hES-NPC adhesion and neuronal differentiation [285]
			Hyaluronic acid	Neurite outgrowth (hNPCs) [286]
CGGNGEPRGD TYRAY [bsp-RGD(15)]	Rat bone sialoprotein	N.D.	Interpenetrating synthetic polymer network	NSC adhesion [307]
DGEA	Collagen type I	Integrin α2β1 [308]	Fibrin	Neurite outgrowth (DRGs) [287]
Other natural-derived cell adhesive ligands				
Sequence	***Derived from***	***Cell surface receptor***	***Hydrogel backbone***	***Biological effect***
HAV	EC1 domain of N-cadherin	Cadherins [309-311]	Fibrin	Neurite outgrowth (DRGs) [288]
HAVDIGGGC (HAVDI)			PEG-based	hiPS-NSC survival and neural differentiation [312]
Non-natural cell adhesive ligands				
Sequence	***Derived from***	***Cell surface receptor***	***Hydrogel backbone***	***Biological effect***
SKPPGTSS (BMHP1)	Phage display peptide library	N.D.	RADA16-based SAP	NSC adhesion and neurite outgrowth [313, 314]
PFSSTKT (BMHP2)				

Abbreviations: BMHP, bone marrow homing peptide; DRG, dorsal root ganglia; hES-NPC, human embryonic stem-derived neural progenitor cell; iPS-NPCs, induced pluripotent stem-derived neural progenitor cells; LN, laminin; N.D., not described; NSC, neural stem cell; NSPC, neural stem/progenitor cell; PEG, poly(ethylene glycol); SAP, self-assembling peptide. (*) cryptic domain in laminin α1 chain.

Fibrin for NSPC delivery

To develop a vehicle to efficiently deliver neural stem/progenitor cells (NSPCs), the selection of a suitable polymer should be the first step, carefully based on its biophysical and biochemical properties. Fibrin is one of the most abundant and well characterized polymers in nature, and still it continues to reveal fascinating features of self-assembly and soft elasticity [315]. Fibrin is a Food and Drug Administration (FDA)-approved biocompatible material which exhibits minimal inflammation and foreign body reaction and is readily absorbed during the normal wound healing process [316]. In clinical practice, fibrin is commonly used as a hemostatic agent, in skin substitutes and wound healing, as well as in drug delivery systems [315-317]. In neurosurgery, fibrin sealant patches are used to seal the dura mater, and to prevent post-operative cerebrospinal fluid leakage [318].

Fibrin precursor solutions can be injected into an injury site for *in situ* polymerization, which allows it to fill gaps with complex shape, such as cavities at spinal cord injury sites. Moreover, fibrin gels are easy to handle and can be delivered using minimally invasive surgical procedures, which results in a faster recovery, smaller scar size and less pain for patients [315]. Fibrin degradation, termed fibrinolysis, is mediated by cleavage at specific sites by the serine protease plasmin, an enzyme present in the blood [319, 320], and by matrix metalloproteinases [321]. Due to its mechanical properties, and susceptibility to proteolytic degradation, fibrin is able to constitute a provisional matrix for cells normally residing in soft tissues, such as the CNS, providing both mechanical and biological support that may enhance tissue regeneration [315, 322].

Fibrin-based products can be prepared from homologous human plasma, as a source of fibrinogen, or from autologous human plasma. Fibrin clots are formed at the final key step of the blood coagulation cascade. Fibrin polymerization is initiated by the thrombin cleavage of fibrinopeptides A and B from the *N*-termini of the Aα- and Bβ-chains of fibrinogen to produce fibrin monomer (Figures 11 and 12) [323, 324]. The fibrin monomers self-assemble yielding protofibrils which then aggregate into fibers. The elongation and the thickening of fibrin fibers are accompanied by branching, which enables the formation of a 3D network [324]. Fibrin clots are then cross-linked by the coagulation factor XIIIa, generated from its precursor factor XIII by thrombin in the presence of calcium ions (Ca^{2+}) and fibrin(ogen), which makes the clot more stiff and less susceptible to proteolytic degradation.

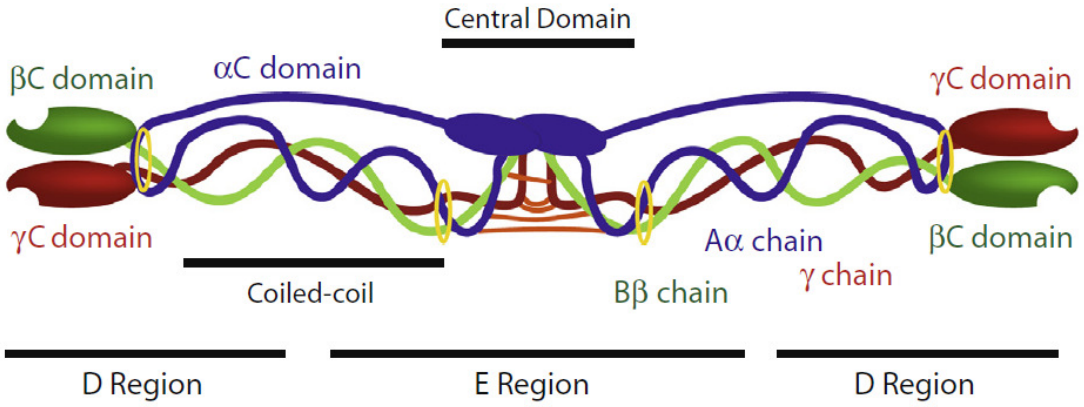

Figure 11. Fibrinogen structure. Fibrinogen, the circulating inactive precursor of fibrin monomers, is a 340 kDa dimeric glycoprotein, with each dimer being composed of three distinct chains, designated as the Aα (in blue), Bβ (in green) and γ chains (in red). Interchain disulfide bridges (in orange) connect the six polypeptide chains in the central domain and disulfide rings (in yellow) stabilize the coiled-coil regions. Image reproduced from Brown and Barker [324], Copyright© 2013, with permission from Elsevier.

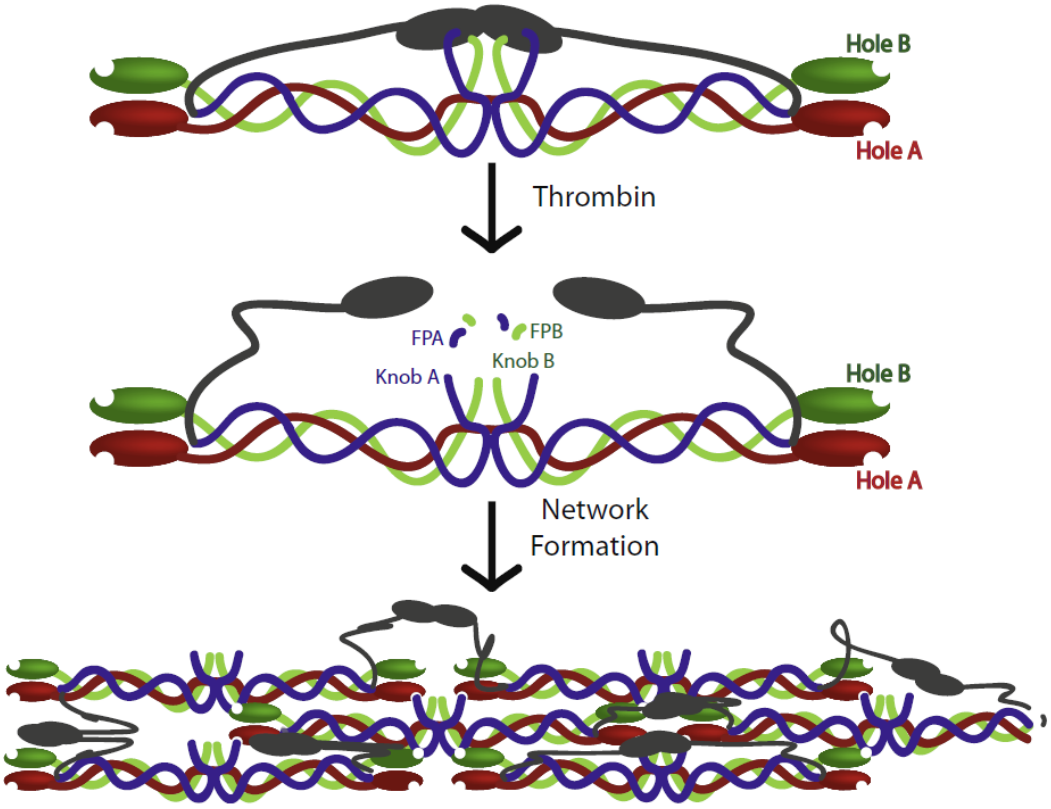

Figure 12. Fibrin polymerization. α chains are shown in blue, β chains are shown in green and γ chains are shown in red. αC domains are shown in gray. Upon conversion of fibrinogen into fibrin, fibrinogen αC-domains containing the RGD recognition motif form ordered αC polymers. FPA, fibrinogen peptide A. FPB, fibrinogen peptide B. Image reproduced from Brown and Barker [324], Copyright© 2013, with permission from Elsevier.

In order to modulate NSPC behavior and neurite outgrowth, fibrin structure and viscoelastic properties can be controlled by tuning the kinetic parameters. For instance, increasing fibrinogen usually result in a stiffer, less malleable clot with a longer degradation time [324]. Increasing thrombin concentration accelerates the gelation time, which creates a gel with more tightly-packed thin fibers, whereas reducing the thrombin concentration results in a gel with thicker fibers, fewer branch fibers and a higher porosity [325, 326]. Moreover, increasing the concentration of factor XIIa also contributes to a denser structure with increased clot stiffness [327]. Worth mentioning, fibrin matrix stiffness is also modulated by extrinsic cellular activity. When cells are cultured inside fibrin the degradation process is often accelerated, and fibrin clot structure is altered, due to cell-secreted fibrin-digesting enzymes (i.e., plasmin and matrix metalloproteinase pathways) and their associated activators [328].

Fibrin contains numerous binding sites for important molecules that direct NSC behavior, such as heparin and fibronectin. Heparin-binding domains are positioned at the *N*-terminus of Bβ chain of fibrinogen, and the binding site to fibronectin locates at the αC terminus (Fig. 11). Importantly, fibrin(ogen) binds growth factors like platelet-derived growth factor (PDGF), fibroblast growth factor (FGF), transforming growth factor-β (TGF-β), neurotrophin-3 (NT3) and brain-derived neurotrophic factor (BDNF) through its heparin-binding domain [329]. All of the referred growth factors are involved in promoting tissue repair, and NT3 and BDNF are key players in NSC survival, proliferation, migration and neuronal differentiation [330]. Furthermore, fibrin(ogen) contains binding sequences for integrins αvβ3, αvβ5, αvβ6, αMβ2, αxβ2 and αIIbβ3 that allow direct cell anchorage to fibrin [331]. These integrin-binding sequences include two RGD motifs located in the Aα chain in the coiled-coil region (Aα 95–97) and in the carboxyl terminus (Aα 572–574) [332]. Specifically, the binding of integrin αvβ3 to the Aα572–574 RGD motif of fibrinogen is known to promote endothelial cell adhesion, migration and proliferation during angiogenesis [333-335]. Fibrin is also known to promote neurite extension, likely via integrin αvβ3 [336, 337]. Indeed, since neural progenitors express integrin αvβ3 in the embryonic neocortex, particularly involved in sustaining NPC proliferation [338], this cell receptor might also participate in the modulation of embryonic stem (ES)-derived NSPC behavior within fibrin matrices *(discussed in Chapter IV).* As well, given that integrin αvβ1 is expressed by NSPCs [222], also identified as a receptor for fibrinogen [339], this integrin could also participate in the modulation of ES-NSPC interactions with fibrinogen and fibrin.

Fibrin sealants have been initially used as scaffold materials in an experimental of spinal cord injury (SCI), leading to similar outcome when compared to equine collagen [322]. The results from this study demonstrated that the implantation of fibrin sealants in the spinal cord is safe and contributes to a significant improvement of functional recovery after SCI. Since then, fibrin gels have been explored in therapies to treat the damaged CNS, usually resulting in improved function recovery [92, 172, 173]. Using an *in vivo* model of subacute SCI, pre-polymerized fibrin hydrogels implanted into the lesion site increased neurite sprouting and delayed astrocyte accumulation in the lesioned areas [340]. The use of fibrin hydrogel to deliver pluripotent stem-derived NSCs into the injured spinal cord was initially explored by Shelly E. Sakiyama-Elbert [173, 341, 342] and, more recently, by Mark H. Tuszynski [78, 92, 94, 343]. Most of these studies used fibrin hydrogel in combination with growth factors to enhance graft survival following transplantation. For instance, in a recent study by Paul Lu and colleagues, the transplantation of human H9 ES-derived NSCs within a fibrin hydrogel containing a cocktail of growth factors led to functional recovery in a rat model of SCI (hemisection). Interestingly, axons emerging early from NSC grafts were observed in very high numbers, persisting after 18 months post-grafting [78].

Despite the presence of two pairs of endogenous RGD sequences in fibrin that provide adhesiveness cues for neurite outgrowth [344, 345], fibrin functionalization with ECM-derived peptides or recombinant ECM protein domains has been explored to endow it with bioactive cues absent in its native structure. Engineered growth factors or recombinant ECM fragments can be non-covalently bound to fibrin by fusing the recombinant protein to a fibrin-binding domain [346]. For a more effective incorporation of biomolecules into fibrin the cross-linking action of the transglutaminase factor XIIIa can be used. In this approach, the factor XIIIa enzymatic substrate sequence of α2-plasmin inhibitor, Asn-Gln-Glu-Gln-Val-Ser-Pro-Leu (NQEQVSPL), is fused to bioactive peptides or recombinant proteins, allowing these to be covalently incorporated into fibrin during factor XIIIa-induced cross-linking [287, 288]. This cross-linking approach was used to immobilize different RGD-containing cell adhesive sequences in fibrin and enhance neurite outgrowth in 3D hydrogels. Of note, neurite outgrowth from DRG explants in fibrin containing variable amounts of RGD peptides were shown to depend on the adhesion site density and affinity [292].

Motivation

The studies presented in this thesis aimed at developing an engineering approach to increase the ability of 3D hydrogel matrices to sustain neurite outgrowth and migration of neural stem cells, by mimicking cell receptor-ECM interactions occurring in neurogenic niches. This strategy is expected to enhance the efficacy of NSPC-based regenerative therapies to treat CNS disorders and injuries. To pursue this objective, we hypothesized that the functionalization of hydrogel matrices with cell adhesive sequences interacting with α6β1 integrin or syndecans could enhance their ability to support NSC migration and neurite outgrowth, and ultimately contribute to the integration of transplanted cells into the damaged CNS and neuronal relay formation. Fibrin gel was selected to test this hypothesis, due to the absence of α6β1 integrin binding domains in its structure, along with its tunable properties and innate bioactivity. Specific objectives included:

- To assess the ability of fibrin hydrogels to support the culture of NSPCs derived from murine ESCs (ES-NSPCs), when seeded as single cell suspension.
- To determine the range of fibrinogen concentrations leading to the maximum NSPC viability, migration, proliferation, neuronal differentiation and ECM remodeling.
- To validate the 3D platform developed for the culture of human ES-derived NSCs (hES-NSCs), in terms of ability to support cell viability, neuronal differentiation and ECM remodeling.
- To select among six different integrin α6β1 ligands adsorbed to 2D surfaces these capable of supporting integrin α6β1-mediated ES-NSPC adhesion, and of sustaining ES-NSPC viability, migration, and neuronal differentiation.
- To prepare and characterize fibrin gels functionalized with integrin α6β1 ligands concerning the peptide binding efficiency, microstructure, and viscoelastic properties.
- To evaluate the effect of immobilized integrin α6β1 ligands on cell outward migration from ES-NSPC neurospheres seeded on functionalized fibrin gels.
- To examine the impact of immobilized integrin α6β1 ligands on neurite extension, cell viability, total cell number, and neuronal differentiation of ES-NSPCs embedded as single cells within fibrin hydrogels.
- To assess the effect of functionalized fibrin hydrogels on neurite extension from primary neurons, using an *ex vivo* model of axonal growth.

- To evaluate the effect of fibrin functionalization with integrin α6β1 ligands on axonal regeneration and locomotor function after implantation in an experimental model of spinal cord injury.
- To evaluate if fibrin functionalization with the selected integrin α6β1 ligands could also be effective in promoting the outgrowth of hES-NSCs.
- To explore fibrin functionalization with syndecan-binding peptides, alone, or in combination with integrin α6β1-binding peptides, and to detect if the combination of the two types of ligands has an additive or a synergistic effect on hES-NSC neurite outgrowth in fibrin hydrogels.

References

[1] B.B. Lee, R.A. Cripps, M. Fitzharris, P.C. Wing, The global map for traumatic spinal cord injury epidemiology: update 2011, global incidence rate, Spinal cord 52 (2013) 110.

[2] M. Majdan, D. Plancikova, A. Brazinova, M. Rusnak, D. Nieboer, V. Feigin, A. Maas, Epidemiology of traumatic brain injuries in Europe: a cross-sectional analysis, The Lancet Public Health 1(2) (2016) e76-e83.

[3] O. Lindvall, Z. Kokaia, Stem cells in human neurodegenerative disorders--time for clinical translation?, The Journal of clinical investigation 120(1) (2010) 29-40.

[4] G. Yiu, Z. He, Glial inhibition of CNS axon regeneration, Nature reviews. Neuroscience 7(8) (2006) 617-27.

[5] C.H. Ho, R.J. Triolo, A.L. Elias, K.L. Kilgore, A.F. DiMarco, K. Bogie, A.H. Vette, M. Audu, R. Kobetic, S.R. Chang, K.M. Chan, S. Dukelow, D.J. Bourbeau, S.W. Brose, K.J. Gustafson, Z. Kiss, V.K. Mushahwar, Functional Electrical Stimulation and Spinal Cord Injury, Physical medicine and rehabilitation clinics of North America 25(3) (2014) 631-ix.

[6] I. Vismara, S. Papa, F. Rossi, G. Forloni, P. Veglianese, Current Options for Cell Therapy in Spinal Cord Injury, Trends Mol Med 23(9) (2017) 831-849.

[7] J.T.S. Pettikiriarachchi, C.L. Parish, M.S. Shoichet, J.S. Forsythe, D.R. Nisbet, Biomaterials for Brain Tissue Engineering, Australian Journal of Chemistry 63(8) (2010) 1143.

[8] J.P. de Rivero Vaccari, W.D. Dietrich, R.W. Keane, Therapeutics targeting the inflammasome after central nervous system injury, Transl Res 167(1) (2016) 35-45.

[9] M. Oudega, E.J. Bradbury, M.S. Ramer, Chapter 38 - Combination therapies, in: J. Verhaagen, J.W. McDonald (Eds.), Handbook of Clinical Neurology, Elsevier2012, pp. 617-636.

[10] S. Thuret, L.D. Moon, F.H. Gage, Therapeutic interventions after spinal cord injury, Nature reviews. Neuroscience 7(8) (2006) 628-43.

[11] G. Gincberg, H. Arien-Zakay, P. Lazarovici, P.I. Lelkes, Neural stem cells: therapeutic potential for neurodegenerative diseases, British medical bulletin 104 (2012) 7-19.

[12] R.C. Trueman, A. Klein, H.S. Lindgren, M.J. Lelos, S.B. Dunnett, Repair of the CNS using endogenous and transplanted neural stem cells, Current topics in behavioral neurosciences 15 (2013) 357-98.

[13] M. Wang, P. Zhai, X. Chen, D.J. Schreyer, X. Sun, F. Cui, Bioengineered scaffolds for spinal cord repair, Tissue engineering. Part B, Reviews 17(3) (2011) 177-94.

[14] H. Kim, M.J. Cooke, M.S. Shoichet, Creating permissive microenvironments for stem cell transplantation into the central nervous system, Trends Biotechnol 30(1) (2012) 55-63.
[15] H. Li, G. Chen, In Vivo Reprogramming for CNS Repair: Regenerating Neurons from Endogenous Glial Cells, Neuron 91(4) (2016) 728-738.
[16] F.J. Obermair, A. Schroter, M. Thallmair, Endogenous neural progenitor cells as therapeutic target after spinal cord injury, Physiology (Bethesda) 23 (2008) 296-304.
[17] T. Walker, J. Huang, K. Young, Neural Stem and Progenitor Cells in Nervous System Function and Therapy, Stem Cells Int 2016 (2016) 1890568.
[18] R. Zhang, Z. Zhang, M. Chopp, Function of neural stem cells in ischemic brain repair processes, Journal of cerebral blood flow and metabolism : official journal of the International Society of Cerebral Blood Flow and Metabolism 36(12) (2016) 2034-2043.
[19] N. Sanai, A.D. Tramontin, A. Quinones-Hinojosa, N.M. Barbaro, N. Gupta, S. Kunwar, M.T. Lawton, M.W. McDermott, A.T. Parsa, J. Manuel-Garcia Verdugo, M.S. Berger, A. Alvarez-Buylla, Unique astrocyte ribbon in adult human brain contains neural stem cells but lacks chain migration, Nature 427(6976) (2004) 740-4.
[20] G.l. Ming, H. Song, Adult Neurogenesis in the Mammalian Brain: Significant Answers and Significant Questions, Neuron 70(4) 687-702.
[21] Allison M. Bond, G.-l. Ming, H. Song, Adult Mammalian Neural Stem Cells and Neurogenesis: Five Decades Later, Cell Stem Cell 17(4) (2015) 385-395.
[22] E. Gould, How widespread is adult neurogenesis in mammals?, Nature reviews. Neuroscience 8(6) (2007) 481-8.
[23] R. Zhang, Z. Zhang, L. Wang, Y. Wang, A. Gousev, L. Zhang, K.L. Ho, C. Morshead, M. Chopp, Activated neural stem cells contribute to stroke-induced neurogenesis and neuroblast migration toward the infarct boundary in adult rats, Journal of cerebral blood flow and metabolism : official journal of the International Society of Cerebral Blood Flow and Metabolism 24(4) (2004) 441-8.
[24] R.M. Richardson, D. Sun, M.R. Bullock, Neurogenesis after traumatic brain injury, Neurosurgery clinics of North America 18(1) (2007) 169-81, xi.
[25] H. Sabelstrom, M. Stenudd, J. Frisen, Neural stem cells in the adult spinal cord, Experimental neurology 260 (2014) 44-9.
[26] J. Namiki, C.H. Tator, Cell proliferation and nestin expression in the ependyma of the adult rat spinal cord after injury, Journal of neuropathology and experimental neurology 58(5) (1999) 489-98.
[27] C.A. Gregoire, B.L. Goldenstein, E.M. Floriddia, F. Barnabe-Heider, K.J. Fernandes, Endogenous neural stem cell responses to stroke and spinal cord injury, Glia 63(8) (2015) 1469-82.

[28] M.A. Anderson, J.E. Burda, Y.L. Ren, Y. Ao, T.M. O'Shea, R. Kawaguchi, G. Coppola, B.S. Khakh, T.J. Deming, M.V. Sofroniew, Astrocyte scar formation aids central nervous system axon regeneration, Nature 532(7598) (2016) 195-200.
[29] L. Ottoboni, A. Merlini, G. Martino, Neural Stem Cell Plasticity: Advantages in Therapy for the Injured Central Nervous System, Frontiers in Cell and Developmental Biology 5 (2017) 52.
[30] X.M. Xu, S.M. Onifer, Transplantation-mediated strategies to promote axonal regeneration following spinal cord injury, Respiratory physiology & neurobiology 169(2) (2009) 171-82.
[31] H. Lin, Cell biology of stem cells: an enigma of asymmetry and self-renewal, The Journal of cell biology 180(2) (2008) 257-60.
[32] W.W. Fabin Han, Chao Chen, Research progress in animal models and stem cell therapy for Alzheimer's disease., Journal of Neurorestoratology 3 (2015) 11-22.
[33] P. Bianco, "Mesenchymal" stem cells, Annual review of cell and developmental biology 30 (2014) 677-704.
[34] C. Nombela-Arrieta, J. Ritz, L.E. Silberstein, The elusive nature and function of mesenchymal stem cells, Nature reviews. Molecular cell biology 12(2) (2011) 126-31.
[35] A.P. Pêgo, S. Kubinova, D. Cizkova, I. Vanicky, F.M. Mar, M.M. Sousa, E. Sykova, Regenerative medicine for the treatment of spinal cord injury: more than just promises?, Journal of cellular and molecular medicine 16(11) (2012) 2564-82.
[36] A. Uccelli, A. Laroni, M.S. Freedman, Mesenchymal stem cells for the treatment of multiple sclerosis and other neurological diseases, Lancet Neurol 10(7) (2011) 649-56.
[37] K. Aboody, A. Capela, N. Niazi, Jeffrey H. Stern, S. Temple, Translating Stem Cell Studies to the Clinic for CNS Repair: Current State of the Art and the Need for a Rosetta Stone, Neuron 70(4) (2011) 597-613.
[38] G. Dai, X. Liu, Z. Zhang, Z. Yang, Y. Dai, R. Xu, Transplantation of autologous bone marrow mesenchymal stem cells in the treatment of complete and chronic cervical spinal cord injury, Brain research 1533 (2013) 73-9.
[39] W.A. El-Kheir, H. Gabr, M.R. Awad, O. Ghannam, Y. Barakat, H.A. Farghali, Z.M. El Maadawi, I. Ewes, H.E. Sabaawy, Autologous bone marrow-derived cell therapy combined with physical therapy induces functional improvement in chronic spinal cord injury patients, Cell transplantation 23(6) (2014) 729-45.
[40] M.V. Mendonca, T.F. Larocca, B.S. de Freitas Souza, C.F. Villarreal, L.F. Silva, A.C. Matos, M.A. Novaes, C.M. Bahia, A.C. de Oliveira Melo Martinez, C.M. Kaneto, S.B. Furtado, G.P. Sampaio, M.B. Soares, R.R. dos Santos, Safety and neurological assessments after autologous transplantation of bone marrow mesenchymal stem cells

in subjects with chronic spinal cord injury, Stem cell research & therapy 5(6) (2014) 126.

[41] Y. Zhao, F. Tang, Z. Xiao, G. Han, N. Wang, N. Yin, B. Chen, X. Jiang, C. Yun, W. Han, C. Zhao, S. Cheng, S. Zhang, J. Dai, Clinical Study of NeuroRegen Scaffold Combined With Human Mesenchymal Stem Cells for the Repair of Chronic Complete Spinal Cord Injury, Cell transplantation 26(5) (2017) 891-900.

[42] L. Crigler, R.C. Robey, A. Asawachaicharn, D. Gaupp, D.G. Phinney, Human mesenchymal stem cell subpopulations express a variety of neuro-regulatory molecules and promote neuronal cell survival and neuritogenesis, Experimental neurology 198(1) (2006) 54-64.

[43] N. Nakano, Y. Nakai, T.B. Seo, Y. Yamada, T. Ohno, A. Yamanaka, Y. Nagai, M. Fukushima, Y. Suzuki, T. Nakatani, C. Ide, Characterization of conditioned medium of cultured bone marrow stromal cells, Neuroscience letters 483(1) (2010) 57-61.

[44] V.B. Konala, M.K. Mamidi, R. Bhonde, A.K. Das, R. Pochampally, R. Pal, The current landscape of the mesenchymal stromal cell secretome: A new paradigm for cell-free regeneration, Cytotherapy 18(1) (2016) 13-24.

[45] J.P. DeLany, Z.E. Floyd, S. Zvonic, A. Smith, A. Gravois, E. Reiners, X. Wu, G. Kilroy, M. Lefevre, J.M. Gimble, Proteomic analysis of primary cultures of human adipose-derived stem cells: modulation by Adipogenesis, Mol Cell Proteomics 4(6) (2005) 731-40.

[46] S. Zvonic, M. Lefevre, G. Kilroy, Z.E. Floyd, J.P. DeLany, I. Kheterpal, A. Gravois, R. Dow, A. White, X. Wu, J.M. Gimble, Secretome of primary cultures of human adipose-derived stem cells: modulation of serpins by adipogenesis, Mol Cell Proteomics 6(1) (2007) 18-28.

[47] Y. Egashira, S. Sugitani, Y. Suzuki, K. Mishiro, K. Tsuruma, M. Shimazawa, S. Yoshimura, T. Iwama, H. Hara, The conditioned medium of murine and human adipose-derived stem cells exerts neuroprotective effects against experimental stroke model, Brain research 1461 (2012) 87-95.

[48] Y.C. Lin, T.L. Ko, Y.H. Shih, M.Y. Lin, T.W. Fu, H.S. Hsiao, J.Y. Hsu, Y.S. Fu, Human umbilical mesenchymal stem cells promote recovery after ischemic stroke, Stroke 42(7) (2011) 2045-53.

[49] A.O. Pires, B. Mendes-Pinheiro, F.G. Teixeira, S.I. Anjo, S. Ribeiro-Samy, E.D. Gomes, S.C. Serra, N.A. Silva, B. Manadas, N. Sousa, A.J. Salgado, Unveiling the Differences of Secretome of Human Bone Marrow Mesenchymal Stem Cells, Adipose Tissue-Derived Stem Cells, and Human Umbilical Cord Perivascular Cells: A Proteomic Analysis, Stem cells and development 25(14) (2016) 1073-83.

[50] R. Doucette, Olfactory ensheathing cells: potential for glial cell transplantation into areas of CNS injury, Histology and histopathology 10(2) (1995) 503-7.
[51] A. Mackay-Sim, J.A. St John, Olfactory ensheathing cells from the nose: clinical application in human spinal cord injuries, Experimental neurology 229(1) (2011) 174-80.
[52] A.C. Lipson, J. Widenfalk, E. Lindqvist, T. Ebendal, L. Olson, Neurotrophic properties of olfactory ensheathing glia, Experimental neurology 180(2) (2003) 167-71.
[53] Y. Li, P.M. Field, G. Raisman, Olfactory ensheathing cells and olfactory nerve fibroblasts maintain continuous open channels for regrowth of olfactory nerve fibres, Glia 52(3) (2005) 245-51.
[54] R. Watzlawick, J. Rind, E.S. Sena, B. Brommer, T. Zhang, M.A. Kopp, U. Dirnagl, M.R. Macleod, D.W. Howells, J.M. Schwab, Olfactory Ensheathing Cell Transplantation in Experimental Spinal Cord Injury: Effect size and Reporting Bias of 62 Experimental Treatments: A Systematic Review and Meta-Analysis, PLoS biology 14(5) (2016) e1002468.
[55] W.C. Shyu, D.D. Liu, S.Z. Lin, W.W. Li, C.Y. Su, Y.C. Chang, H.J. Wang, H.W. Wang, C.H. Tsai, H. Li, Implantation of olfactory ensheathing cells promotes neuroplasticity in murine models of stroke, The Journal of clinical investigation 118(7) (2008) 2482-95.
[56] X. Shi, Y. Kang, Q. Hu, C. Chen, L. Yang, K. Wang, L. Chen, H. Huang, C. Zhou, A long-term observation of olfactory ensheathing cells transplantation to repair white matter and functional recovery in a focal ischemia model in rat, Brain research 1317 (2010) 257-267.
[57] J. Lu, F. Feron, A. Mackay-Sim, P.M. Waite, Olfactory ensheathing cells promote locomotor recovery after delayed transplantation into transected spinal cord, Brain : a journal of neurology 125(Pt 1) (2002) 14-21.
[58] C.A. Gorrie, I. Hayward, N. Cameron, G. Kailainathan, N. Nandapalan, R. Sutharsan, J. Wang, A. Mackay-Sim, P.M. Waite, Effects of human OEC-derived cell transplants in rodent spinal cord contusion injury, Brain research 1337 (2010) 8-20.
[59] R.R. Khankan, K.G. Griffis, J.R. Haggerty-Skeans, H. Zhong, R.R. Roy, V.R. Edgerton, P.E. Phelps, Olfactory Ensheathing Cell Transplantation after a Complete Spinal Cord Transection Mediates Neuroprotective and Immunomodulatory Mechanisms to Facilitate Regeneration, The Journal of neuroscience : the official journal of the Society for Neuroscience 36(23) (2016) 6269-86.
[60] A. Mackay-Sim, F. Feron, J. Cochrane, L. Bassingthwaighte, C. Bayliss, W. Davies, P. Fronek, C. Gray, G. Kerr, P. Licina, A. Nowitzke, C. Perry, P.A. Silburn, S. Urquhart, T. Geraghty, Autologous olfactory ensheathing cell transplantation in human

paraplegia: a 3-year clinical trial, Brain : a journal of neurology 131(Pt 9) (2008) 2376-86.

[61] P. Tabakow, W. Jarmundowicz, B. Czapiga, W. Fortuna, R. Miedzybrodzki, M. Czyz, J. Huber, D. Szarek, S. Okurowski, P. Szewczyk, A. Gorski, G. Raisman, Transplantation of autologous olfactory ensheathing cells in complete human spinal cord injury, Cell transplantation 22(9) (2013) 1591-612.

[62] D.L. Sherman, P.J. Brophy, Mechanisms of axon ensheathment and myelin growth, Nature reviews. Neuroscience 6(9) (2005) 683-90.

[63] Y. Lee, B.M. Morrison, Y. Li, S. Lengacher, M.H. Farah, P.N. Hoffman, Y. Liu, A. Tsingalia, L. Jin, P.W. Zhang, L. Pellerin, P.J. Magistretti, J.D. Rothstein, Oligodendroglia metabolically support axons and contribute to neurodegeneration, Nature 487(7408) (2012) 443-8.

[64] U. Funfschilling, L.M. Supplie, D. Mahad, S. Boretius, A.S. Saab, J. Edgar, B.G. Brinkmann, C.M. Kassmann, I.D. Tzvetanova, W. Mobius, F. Diaz, D. Meijer, U. Suter, B. Hamprecht, M.W. Sereda, C.T. Moraes, J. Frahm, S. Goebbels, K.A. Nave, Glycolytic oligodendrocytes maintain myelin and long-term axonal integrity, Nature 485(7399) (2012) 517-21.

[65] H.S. Keirstead, G. Nistor, G. Bernal, M. Totoiu, F. Cloutier, K. Sharp, O. Steward, Human embryonic stem cell-derived oligodendrocyte progenitor cell transplants remyelinate and restore locomotion after spinal cord injury, The Journal of neuroscience : the official journal of the Society for Neuroscience 25(19) (2005) 4694-705.

[66] C.A. Priest, N.C. Manley, J. Denham, E.D. Wirth, 3rd, J.S. Lebkowski, Preclinical safety of human embryonic stem cell-derived oligodendrocyte progenitors supporting clinical trials in spinal cord injury, Regen Med 10(8) (2015) 939-58.

[67] N.C. Manley, C.A. Priest, J. Denham, E.D. Wirth, 3rd, J.S. Lebkowski, Human Embryonic Stem Cell-Derived Oligodendrocyte Progenitor Cells: Preclinical Efficacy and Safety in Cervical Spinal Cord Injury, Stem Cells Transl Med 6(10) (2017) 1917-1929.

[68] J. Yang, L.L. Xiong, Y.C. Wang, X. He, L. Jiang, S.J. Fu, X.F. Han, J. Liu, T.H. Wang, Oligodendrocyte precursor cell transplantation promotes functional recovery following contusive spinal cord injury in rats and is associated with altered microRNA expression, Mol Med Rep 17(1) (2018) 771-782.

[69] G.I. Nistor, M.O. Totoiu, N. Haque, M.K. Carpenter, H.S. Keirstead, Human embryonic stem cells differentiate into oligodendrocytes in high purity and myelinate after spinal cord transplantation, Glia 49(3) (2005) 385-96.

[70] P. Douvaras, J. Wang, M. Zimmer, S. Hanchuk, Melanie A. O'Bara, S. Sadiq, Fraser J. Sim, J. Goldman, V. Fossati, Efficient Generation of Myelinating Oligodendrocytes from Primary Progressive Multiple Sclerosis Patients by Induced Pluripotent Stem Cells, Stem Cell Reports 3(2) (2014) 250-259.

[71] S. Erceg, M. Ronaghi, M. Oria, M.G. Rosello, M.A. Arago, M.G. Lopez, I. Radojevic, V. Moreno-Manzano, F.J. Rodriguez-Jimenez, S.S. Bhattacharya, J. Cordoba, M. Stojkovic, Transplanted oligodendrocytes and motoneuron progenitors generated from human embryonic stem cells promote locomotor recovery after spinal cord transection, Stem Cells 28(9) (2010) 1541-9.

[72] S.L. Rossi, G. Nistor, T. Wyatt, H.Z. Yin, A.J. Poole, J.H. Weiss, M.J. Gardener, S. Dijkstra, D.F. Fischer, H.S. Keirstead, Histological and functional benefit following transplantation of motor neuron progenitors to the injured rat spinal cord, PloS one 5(7) (2010) e11852.

[73] T.J. Wyatt, S.L. Rossi, M.M. Siegenthaler, J. Frame, R. Robles, G. Nistor, H.S. Keirstead, Human motor neuron progenitor transplantation leads to endogenous neuronal sparing in 3 models of motor neuron loss, Stem Cells Int 2011 (2011) 207230.

[74] H. Okano, Neural stem cells and strategies for the regeneration of the central nervous system, Proc Jpn Acad Ser B Phys Biol Sci 86(4) (2010) 438-50.

[75] Y. Tang, P. Yu, L. Cheng, Current progress in the derivation and therapeutic application of neural stem cells, Cell Death Dis 8(10) (2017) e3108.

[76] P. Lu, L.L. Jones, E.Y. Snyder, M.H. Tuszynski, Neural stem cells constitutively secrete neurotrophic factors and promote extensive host axonal growth after spinal cord injury, Experimental neurology 181(2) (2003) 115-29.

[77] K. Reekmans, J. Praet, J. Daans, V. Reumers, P. Pauwels, A. Van der Linden, Z.N. Berneman, P. Ponsaerts, Current challenges for the advancement of neural stem cell biology and transplantation research, Stem cell reviews 8(1) (2012) 262-78.

[78] P. Lu, S. Ceto, Y. Wang, L. Graham, D. Wu, H. Kumamaru, E. Staufenberg, M.H. Tuszynski, Prolonged human neural stem cell maturation supports recovery in injured rodent CNS, J Clin Invest (2017).

[79] L. Ottoboni, D. De Feo, A. Merlini, G. Martino, Commonalities in immune modulation between mesenchymal stem cells (MSCs) and neural stem/precursor cells (NPCs), Immunology letters 168(2) (2015) 228-39.

[80] K. Aboody, A. Capela, N. Niazi, Jeffrey H. Stern, S. Temple, Translating Stem Cell Studies to the Clinic for CNS Repair: Current State of the Art and the Need for a Rosetta Stone, Neuron 70(4) 597-613.

[81] S. Temple, L. Studer, Lessons Learned from Pioneering Neural Stem Cell Studies, Stem Cell Reports 8(2) (2017) 191-193.

[82] L. Xu, J. Yan, D. Chen, A.M. Welsh, T. Hazel, K. Johe, G. Hatfield, V.E. Koliatsos, Human neural stem cell grafts ameliorate motor neuron disease in SOD-1 transgenic rats, Transplantation 82(7) (2006) 865-75.

[83] M. Nizzardo, C. Simone, F. Rizzo, M. Ruggieri, S. Salani, G. Riboldi, I. Faravelli, C. Zanetta, N. Bresolin, G.P. Comi, S. Corti, Minimally invasive transplantation of iPSC-derived ALDHhiSSCloVLA4+ neural stem cells effectively improves the phenotype of an amyotrophic lateral sclerosis model, Human molecular genetics 23(2) (2014) 342-54.

[84] T. Yasuhara, N. Matsukawa, K. Hara, G. Yu, L. Xu, M. Maki, S.U. Kim, C.V. Borlongan, Transplantation of human neural stem cells exerts neuroprotection in a rat model of Parkinson's disease, The Journal of neuroscience : the official journal of the Society for Neuroscience 26(48) (2006) 12497-511.

[85] F.X. Zuo, X.J. Bao, X.C. Sun, J. Wu, Q.R. Bai, G. Chen, X.Y. Li, Q.Y. Zhou, Y.F. Yang, Q. Shen, R.Z. Wang, Transplantation of Human Neural Stem Cells in a Parkinsonian Model Exerts Neuroprotection via Regulation of the Host Microenvironment, Int J Mol Sci 16(11) (2015) 26473-92.

[86] R. Gonzalez, I. Garitaonandia, M. Poustovoitov, T. Abramihina, C. McEntire, B. Culp, J. Attwood, A. Noskov, T. Christiansen-Weber, M. Khater, S. Mora-Castilla, C. To, A. Crain, G. Sherman, A. Semechkin, L.C. Laurent, J.D. Elsworth, J. Sladek, E.Y. Snyder, D.E. Redmond, Jr., R.A. Kern, Neural Stem Cells Derived from Human Parthenogenetic Stem Cells Engraft and Promote Recovery in a Nonhuman Primate Model of Parkinson's Disease, Cell transplantation 25(11) (2016) 1945-1966.

[87] X. Li, H. Zhu, X. Sun, F. Zuo, J. Lei, Z. Wang, X. Bao, R. Wang, Human Neural Stem Cell Transplantation Rescues Cognitive Defects in APP/PS1 Model of Alzheimer's Disease by Enhancing Neuronal Connectivity and Metabolic Activity, Front Aging Neurosci 8 (2016) 282.

[88] S.E. Marsh, S.T. Yeung, M. Torres, L. Lau, J.L. Davis, E.S. Monuki, W.W. Poon, M. Blurton-Jones, HuCNS-SC Human NSCs Fail to Differentiate, Form Ectopic Clusters, and Provide No Cognitive Benefits in a Transgenic Model of Alzheimer's Disease, Stem cell reports 8(2) (2017) 235-248.

[89] V. Johann, J. Schiefer, C. Sass, J. Mey, G. Brook, A. Kruttgen, C. Schlangen, C. Bernreuther, M. Schachner, M. Dihne, C.M. Kosinski, Time of transplantation and cell preparation determine neural stem cell survival in a mouse model of Huntington's disease, Experimental brain research. Experimentelle Hirnforschung. Experimentation cerebrale 177(4) (2007) 458-70.

[90] C.R. Yang, R.K. Yu, Intracerebral transplantation of neural stem cells combined with trehalose ingestion alleviates pathology in a mouse model of Huntington's disease, Journal of neuroscience research 87(1) (2009) 26-33.
[91] O. Tsuji, K. Miura, Y. Okada, K. Fujiyoshi, M. Mukaino, N. Nagoshi, K. Kitamura, G. Kumagai, M. Nishino, S. Tomisato, H. Higashi, T. Nagai, H. Katoh, K. Kohda, Y. Matsuzaki, M. Yuzaki, E. Ikeda, Y. Toyama, M. Nakamura, S. Yamanaka, H. Okano, Therapeutic potential of appropriately evaluated safe-induced pluripotent stem cells for spinal cord injury, Proceedings of the National Academy of Sciences of the United States of America 107(28) (2010) 12704-9.
[92] P. Lu, Y. Wang, L. Graham, K. McHale, M. Gao, D. Wu, J. Brock, A. Blesch, E.S. Rosenzweig, L.A. Havton, B. Zheng, J.M. Conner, M. Marsala, M.H. Tuszynski, Long-distance growth and connectivity of neural stem cells after severe spinal cord injury, Cell 150(6) (2012) 1264-73.
[93] S.N. Nemati, R. Jabbari, M. Hajinasrollah, N. Zare Mehrjerdi, H. Azizi, K. Hemmesi, R. Moghiminasr, Z. Azhdari, A. Talebi, S. Mohitmafi, A. Vosough Taqi Dizaj, G. Sharifi, H. Baharvand, O. Rezaee, S. Kiani, Transplantation of adult monkey neural stem cells into a contusion spinal cord injury model in rhesus macaque monkeys, Cell journal 16(2) (2014) 117-130.
[94] P. Lu, G. Woodruff, Y. Wang, L. Graham, M. Hunt, D. Wu, E. Boehle, R. Ahmad, G. Poplawski, J. Brock, L.S. Goldstein, M.H. Tuszynski, Long-distance axonal growth from human induced pluripotent stem cells after spinal cord injury, Neuron 83(4) (2014) 789-96.
[95] H.J. Lee, K.S. Kim, E.J. Kim, H.B. Choi, K.H. Lee, I.H. Park, Y. Ko, S.W. Jeong, S.U. Kim, Brain transplantation of immortalized human neural stem cells promotes functional recovery in mouse intracerebral hemorrhage stroke model, Stem Cells 25(5) (2007) 1204-12.
[96] P. Stroemer, S. Patel, A. Hope, C. Oliveira, K. Pollock, J. Sinden, The neural stem cell line CTX0E03 promotes behavioral recovery and endogenous neurogenesis after experimental stroke in a dose-dependent fashion, Neurorehabil Neural Repair 23(9) (2009) 895-909.
[97] J. Li, Y. Tang, Y. Wang, R. Tang, W. Jiang, G.Y. Yang, W.Q. Gao, Neurovascular recovery via co-transplanted neural and vascular progenitors leads to improved functional restoration after ischemic stroke in rats, Stem cell reports 3(1) (2014) 101-14.
[98] P.N. Koutsoudaki, F. Papastefanaki, A. Stamatakis, G. Kouroupi, E. Xingi, F. Stylianopoulou, R. Matsas, Neural stem/progenitor cells differentiate into

oligodendrocytes, reduce inflammation, and ameliorate learning deficits after transplantation in a mouse model of traumatic brain injury, Glia 64(5) (2016) 763-79.
[99] H. Duan, X. Li, C. Wang, P. Hao, W. Song, M. Li, W. Zhao, Y. Gao, Z. Yang, Functional hyaluronate collagen scaffolds induce NSCs differentiation into functional neurons in repairing the traumatic brain injury, Acta Biomater 45 (2016) 182-195.
[100] B. Waldau, B. Hattiangady, R. Kuruba, A.K. Shetty, Medial ganglionic eminence-derived neural stem cell grafts ease spontaneous seizures and restore GDNF expression in a rat model of chronic temporal lobe epilepsy, Stem Cells 28(7) (2010) 1153-64.
[101] X.R. Zheng, S.S. Zhang, F. Yin, J.L. Tang, Y.J. Yang, X. Wang, L. Zhong, Neuroprotection of VEGF-expression neural stem cells in neonatal cerebral palsy rats, Behav Brain Res 230(1) (2012) 108-15.
[102] J. Tan, X. Zheng, S. Zhang, Y. Yang, X. Wang, X. Yu, L. Zhong, Response of the sensorimotor cortex of cerebral palsy rats receiving transplantation of vascular endothelial growth factor 165-transfected neural stem cells, Neural Regen Res 9(19) (2014) 1763-9.
[103] L. Wang, F. Jiang, Q. Li, X. He, J. Ma, Mild hypothermia combined with neural stem cell transplantation for hypoxic-ischemic encephalopathy: neuroprotective effects of combined therapy, Neural Regen Res 9(19) (2014) 1745-52.
[104] Y.B. Li, Y. Wang, J.P. Tang, D. Chen, S.L. Wang, Neuroprotective effects of ginsenoside Rg1-induced neural stem cell transplantation on hypoxic-ischemic encephalopathy, Neural Regen Res 10(5) (2015) 753-9.
[105] M.K. Jones, B. Lu, M. Saghizadeh, S. Wang, Gene expression changes in the retina following subretinal injection of human neural progenitor cells into a rodent model for retinal degeneration, Molecular vision 22 (2016) 472-90.
[106] A. Trounson, C. McDonald, Stem Cell Therapies in Clinical Trials: Progress and Challenges, Cell Stem Cell 17(1) 11-22.
[107] S. van Gorp, M. Leerink, O. Kakinohana, O. Platoshyn, C. Santucci, J. Galik, E.A. Joosten, M. Hruska-Plochan, D. Goldberg, S. Marsala, K. Johe, J.D. Ciacci, M. Marsala, Amelioration of motor/sensory dysfunction and spasticity in a rat model of acute lumbar spinal cord injury by human neural stem cell transplantation, Stem cell research & therapy 4(3) (2013) 57.
[108] N. Tajiri, D.M. Quach, Y. Kaneko, S. Wu, D. Lee, T. Lam, K.L. Hayama, T.G. Hazel, K. Johe, M.C. Wu, C.V. Borlongan, Behavioral and Histopathological Assessment of Adult Ischemic Rat Brains after Intracerebral Transplantation of NSI-566RSC Cell Lines, PloS one 9(3) (2014) e91408.

[109] D.L. Salazar, N. Uchida, F.P. Hamers, B.J. Cummings, A.J. Anderson, Human neural stem cells differentiate and promote locomotor recovery in an early chronic spinal cord injury NOD-scid mouse model, PloS one 5(8) (2010) e12272.
[110] A.J. Anderson, K.M. Piltti, M.J. Hooshmand, R.A. Nishi, B.J. Cummings, Preclinical Efficacy Failure of Human CNS-Derived Stem Cells for Use in the Pathway Study of Cervical Spinal Cord Injury, Stem cell reports 8(2) (2017) 249-263.
[111] J.W. McDonald, D. Becker, T.F. Holekamp, M. Howard, S. Liu, A. Lu, J. Lu, M.M. Platik, Y. Qu, T. Stewart, S. Vadivelu, Repair of the injured spinal cord and the potential of embryonic stem cell transplantation, Journal of neurotrauma 21(4) (2004) 383-93.
[112] E. Colombo, S.G. Giannelli, R. Galli, E. Tagliafico, C. Foroni, E. Tenedini, S. Ferrari, S. Ferrari, G. Corte, A. Vescovi, G. Cossu, V. Broccoli, Embryonic stem-derived versus somatic neural stem cells: a comparative analysis of their developmental potential and molecular phenotype, Stem Cells 24(4) (2006) 825-34.
[113] T. Incitti, A. Messina, Y. Bozzi, S. Casarosa, Sorting of Sox1-GFP Mouse Embryonic Stem Cells Enhances Neuronal Identity Acquisition upon Factor-Free Monolayer Differentiation, BioResearch open access 3(3) (2014) 127-35.
[114] Q.L. Ying, M. Stavridis, D. Griffiths, M. Li, A. Smith, Conversion of embryonic stem cells into neuroectodermal precursors in adherent monoculture, Nature biotechnology 21(2) (2003) 183-6.
[115] D.L. Haus, L. Lopez-Velazquez, E.M. Gold, K.M. Cunningham, H. Perez, A.J. Anderson, B.J. Cummings, Transplantation of human neural stem cells restores cognition in an immunodeficient rodent model of traumatic brain injury, Experimental neurology 281 (2016) 1-16.
[116] M.M. Daadi, A.L. Maag, G.K. Steinberg, Adherent self-renewable human embryonic stem cell-derived neural stem cell line: functional engraftment in experimental stroke model, PloS one 3(2) (2008) e1644.
[117] A.U. Hicks, R.S. Lappalainen, S. Narkilahti, R. Suuronen, D. Corbett, J. Sivenius, O. Hovatta, J. Jolkkonen, Transplantation of human embryonic stem cell-derived neural precursor cells and enriched environment after cortical stroke in rats: cell survival and functional recovery, The European journal of neuroscience 29(3) (2009) 562-74.
[118] S. Nori, Y. Okada, A. Yasuda, O. Tsuji, Y. Takahashi, Y. Kobayashi, K. Fujiyoshi, M. Koike, Y. Uchiyama, E. Ikeda, Y. Toyama, S. Yamanaka, M. Nakamura, H. Okano, Grafted human-induced pluripotent stem-cell-derived neurospheres promote motor functional recovery after spinal cord injury in mice, Proceedings of the National Academy of Sciences of the United States of America 108(40) (2011) 16825-30.
[119] Y. Kobayashi, Y. Okada, G. Itakura, H. Iwai, S. Nishimura, A. Yasuda, S. Nori, K. Hikishima, T. Konomi, K. Fujiyoshi, O. Tsuji, Y. Toyama, S. Yamanaka, M. Nakamura,

H. Okano, Pre-evaluated safe human iPSC-derived neural stem cells promote functional recovery after spinal cord injury in common marmoset without tumorigenicity, PloS one 7(12) (2012) e52787.

[120] T. Yuan, W. Liao, N.H. Feng, Y.L. Lou, X. Niu, A.J. Zhang, Y. Wang, Z.F. Deng, Human induced pluripotent stem cell-derived neural stem cells survive, migrate, differentiate, and improve neurologic function in a rat model of middle cerebral artery occlusion, Stem cell research & therapy 4(3) (2013) 73-73.

[121] N. Nagoshi, H. Okano, Applications of induced pluripotent stem cell technologies in spinal cord injury, Journal of neurochemistry 141(6) (2017) 848-860.

[122] K. Takahashi, S. Yamanaka, Induction of pluripotent stem cells from mouse embryonic and adult fibroblast cultures by defined factors, Cell 126(4) (2006) 663-76.

[123] Karen L. Ring, Leslie M. Tong, Maureen E. Balestra, R. Javier, Y. Andrews-Zwilling, G. Li, D. Walker, William R. Zhang, Anatol C. Kreitzer, Y. Huang, Direct Reprogramming of Mouse and Human Fibroblasts into Multipotent Neural Stem Cells with a Single Factor, Cell Stem Cell 11(1) (2012) 100-109.

[124] N. Tapia, Hans R. Schöler, Molecular Obstacles to Clinical Translation of iPSCs, Cell Stem Cell 19(3) 298-309.

[125] L. Wang, L. Wang, W. Huang, H. Su, Y. Xue, Z. Su, B. Liao, H. Wang, X. Bao, D. Qin, J. He, W. Wu, K.F. So, G. Pan, D. Pei, Generation of integration-free neural progenitor cells from cells in human urine, Nature methods 10(1) (2013) 84-9.

[126] E. Shahbazi, S. Moradi, S. Nemati, L. Satarian, M. Basiri, H. Gourabi, N. Zare Mehrjardi, P. Gunther, A. Lampert, K. Handler, F.F. Hatay, D. Schmidt, M. Molcanyi, J. Hescheler, J.L. Schultze, T. Saric, H. Baharvand, Conversion of Human Fibroblasts to Stably Self-Renewing Neural Stem Cells with a Single Zinc-Finger Transcription Factor, Stem cell reports 6(4) (2016) 539-551.

[127] A. Mackay-Sim, J.A. St John, Olfactory ensheathing cells from the nose: Clinical application in human spinal cord injuries, Experimental neurology 229(1) (2011) 174-180.

[128] A.C.S. Curtis, M. Fehlings, S. Huhn. Phase I/II clinical trial of HuCNS-SC cells in chronic thoracic spinal cord injury—interim analysis. 2014. http://www.stem-art.com/Library/ClinicalTrials/Phase%20I%20i%20II%20clinical%20trial%20of%20HuCNS-SCs%20in%20chronic%20%20thoracic%20spinal%20cord%20injury.pdf. Acessed October, 2017.

[129] H. Iwai, H. Shimada, S. Nishimura, Y. Kobayashi, G. Itakura, K. Hori, K. Hikishima, H. Ebise, N. Negishi, S. Shibata, S. Habu, Y. Toyama, M. Nakamura, H. Okano, Allogeneic Neural Stem/Progenitor Cells Derived From Embryonic Stem Cells

Promote Functional Recovery After Transplantation Into Injured Spinal Cord of Nonhuman Primates, Stem Cells Translational Medicine 4(7) (2015) 708-719.
[130] K.S. Aboody, J. Najbauer, M.K. Danks, Stem and progenitor cell-mediated tumor selective gene therapy, Gene therapy 15(10) (2008) 739-52.
[131] A.L. Tobias, B. Thaci, B. Auffinger, E. Rincón, I.V. Balyasnikova, C.K. Kim, Y. Han, L. Zhang, K.S. Aboody, A.U. Ahmed, M.S. Lesniak, The Timing of Neural Stem Cell-Based Virotherapy Is Critical for Optimal Therapeutic Efficacy When Applied With Radiation and Chemotherapy for the Treatment of Glioblastoma, Stem Cells Translational Medicine 2(9) (2013) 655-666.
[132] A.U. Ahmed, B. Thaci, A.L. Tobias, B. Auffinger, L. Zhang, Y. Cheng, C.K. Kim, C. Yunis, Y. Han, N.G. Alexiades, X. Fan, K.S. Aboody, M.S. Lesniak, A preclinical evaluation of neural stem cell-based cell carrier for targeted antiglioma oncolytic virotherapy, Journal of the National Cancer Institute 105(13) (2013) 968-77.
[133] J. Riley, T. Federici, M. Polak, C. Kelly, J. Glass, B. Raore, J. Taub, V. Kesner, E.L. Feldman, N.M. Boulis, Intraspinal stem cell transplantation in amyotrophic lateral sclerosis: a phase I safety trial, technical note, and lumbar safety outcomes, Neurosurgery 71(2) (2012) 405-16; discussion 416.
[134] E.L. Feldman, N.M. Boulis, J. Hur, K. Johe, S.B. Rutkove, T. Federici, M. Polak, J. Bordeau, S.A. Sakowski, J.D. Glass, Intraspinal Neural Stem Cell Transplantation in Amyotrophic Lateral Sclerosis: Phase 1 Trial Outcomes, Annals of Neurology 75(3) (2014) 363-373.
[135] J.D. Glass, N.M. Boulis, K. Johe, S.B. Rutkove, T. Federici, M. Polak, C. Kelly, E.L. Feldman, Lumbar Intraspinal Injection of Neural Stem Cells in Patients with Amyotrophic Lateral Sclerosis: Results of a Phase I Trial in 12 Patients, Stem cells (Dayton, Ohio) 30(6) (2012) 1144-1151.
[136] J.D. Glass, V.S. Hertzberg, N.M. Boulis, J. Riley, T. Federici, M. Polak, J. Bordeau, C. Fournier, K. Johe, T. Hazel, M. Cudkowicz, N. Atassi, L.F. Borges, S.B. Rutkove, J. Duell, P.G. Patil, S.A. Goutman, E.L. Feldman, Transplantation of spinal cord-derived neural stem cells for ALS: Analysis of phase 1 and 2 trials, Neurology 87(4) (2016) 392-400.
[137] L. Mazzini, M. Gelati, D.C. Profico, G. Sgaravizzi, M. Projetti Pensi, G. Muzi, C. Ricciolini, L. Rota Nodari, S. Carletti, C. Giorgi, C. Spera, F. Domenico, E. Bersano, F. Petruzzelli, C. Cisari, A. Maglione, M.F. Sarnelli, A. Stecco, G. Querin, S. Masiero, R. Cantello, D. Ferrari, C. Zalfa, E. Binda, A. Visioli, D. Trombetta, A. Novelli, B. Torres, L. Bernardini, A. Carriero, P. Prandi, S. Servo, A. Cerino, V. Cima, A. Gaiani, N. Nasuelli, M. Massara, J. Glass, G. Sorarù, N.M. Boulis, A.L. Vescovi, Human neural stem cell

transplantation in ALS: initial results from a phase I trial, Journal of Translational Medicine 13 (2015) 17.
[138] I. Garitaonandia, R. Gonzalez, T. Christiansen-Weber, T. Abramihina, M. Poustovoitov, A. Noskov, G. Sherman, A. Semechkin, E. Snyder, R. Kern, Neural Stem Cell Tumorigenicity and Biodistribution Assessment for Phase I Clinical Trial in Parkinson's Disease, Sci Rep 6 (2016) 34478.
[139] V.K. Harris, T. Vyshkina, S.A. Sadiq, Clinical safety of intrathecal administration of mesenchymal stromal cell-derived neural progenitors in multiple sclerosis, Cytotherapy 18(12) (2016) 1476-1482.
[140] N. Gupta, R.G. Henry, J. Strober, S.-M. Kang, D.A. Lim, M. Bucci, E. Caverzasi, L. Gaetano, M.L. Mandelli, T. Ryan, R. Perry, J. Farrell, R.J. Jeremy, M. Ulman, S.L. Huhn, A.J. Barkovich, D.H. Rowitch, Neural Stem Cell Engraftment and Myelination in the Human Brain, Science translational medicine 4(155) (2012) 155ra137-155ra137.
[141] N.R. Selden, A. Al-Uzri, S.L. Huhn, T.K. Koch, D.M. Sikora, M.D. Nguyen-Driver, D.J. Guillaume, J.L. Koh, S.H. Gultekin, J.C. Anderson, H. Vogel, T.L. Sutcliffe, Y. Jacobs, R.D. Steiner, Central nervous system stem cell transplantation for children with neuronal ceroid lipofuscinosis, Journal of neurosurgery. Pediatrics 11(6) (2013) 643-52.
[142] J.C. Shin, K.N. Kim, J. Yoo, I.S. Kim, S. Yun, H. Lee, K. Jung, K. Hwang, M. Kim, I.S. Lee, J.E. Shin, K.I. Park, Clinical Trial of Human Fetal Brain-Derived Neural Stem/Progenitor Cell Transplantation in Patients with Traumatic Cervical Spinal Cord Injury, Neural Plast 2015 (2015) 630932.
[143] G.M. Ghobrial, K.D. Anderson, M. Dididze, J. Martinez-Barrizonte, G.H. Sunn, K.L. Gant, A.D. Levi, Human Neural Stem Cell Transplantation in Chronic Cervical Spinal Cord Injury: Functional Outcomes at 12 Months in a Phase II Clinical Trial, Neurosurgery 64(CN_suppl_1) (2017) 87-91.
[144] D. Kalladka, J. Sinden, K. Pollock, C. Haig, J. McLean, W. Smith, A. McConnachie, C. Santosh, P.M. Bath, L. Dunn, K.W. Muir, Human neural stem cells in patients with chronic ischaemic stroke (PISCES): a phase 1, first-in-man study, Lancet 388(10046) (2016) 787-96.
[145] Z. Luan, W. Liu, S. Qu, K. Du, S. He, Z. Wang, Y. Yang, C. Wang, X. Gong, Effects of neural progenitor cell transplantation in children with severe cerebral palsy, Cell transplantation 21 Suppl 1 (2012) S91-8.
[146] S. He, Z. Luan, S. Qu, X. Qiu, D. Xin, W. Jia, Y. Shen, Z. Yu, T. Xu, Ultrasound guided neural stem cell transplantation through the lateral ventricle for treatment of cerebral palsy in children, Neural Regeneration Research 7(32) (2012) 2529-2535.

[147] G. Chen, Y. Wang, Z. Xu, F. Fang, R. Xu, Y. Wang, X. Hu, L. Fan, H. Liu, Neural stem cell-like cells derived from autologous bone mesenchymal stem cells for the treatment of patients with cerebral palsy, J Transl Med 11 (2013) 21.
[148] M.H. Amer, F. Rose, K.M. Shakesheff, M. Modo, L.J. White, Translational considerations in injectable cell-based therapeutics for neurological applications: concepts, progress and challenges, NPJ Regen Med 2(1) (2017) 23.
[149] T. Rossetti, F. Nicholls, M. Modo, Intracerebral Cell Implantation: Preparation and Characterization of Cell Suspensions, Cell transplantation 25(4) (2016) 645-64.
[150] S. Chung, B.S. Shin, E. Hedlund, J. Pruszak, A. Ferree, U.J. Kang, O. Isacson, K.S. Kim, Genetic selection of sox1-GFP-expressing neural precursors removes residual tumorigenic pluripotent stem cells and attenuates tumor formation after transplantation, Journal of neurochemistry 97(5) (2006) 1467-80.
[151] J. Pruszak, K.-C. Sonntag, M.H. Aung, R. Sanchez-Pernaute, O. Isacson, Markers and Methods for Cell Sorting of Human Embryonic Stem Cell-Derived Neural Cell Populations, Stem cells (Dayton, Ohio) 25(9) (2007) 2257-2268.
[152] K.M. Piltti, G.M. Funes, S.N. Avakian, A.A. Salibian, K.I. Huang, K. Carta, N. Kamei, L.A. Flanagan, E.S. Monuki, N. Uchida, B.J. Cummings, A.J. Anderson, Increasing Human Neural Stem Cell Transplantation Dose Alters Oligodendroglial and Neuronal Differentiation after Spinal Cord Injury, Stem Cell Reports 8(6) (2017) 1534-1548.
[153] V. Darsalia, S.J. Allison, C. Cusulin, E. Monni, D. Kuzdas, T. Kallur, O. Lindvall, Z. Kokaia, Cell number and timing of transplantation determine survival of human neural stem cell grafts in stroke-damaged rat brain, Journal of Cerebral Blood Flow & Metabolism 31(1) (2011) 235-242.
[154] I. Mendez, M. Hong, S. Smith, A. Dagher, J. Desrosiers, Neural transplantation cannula and microinjector system: experimental and clinical experience. Technical note, J Neurosurg 92(3) (2000) 493-9.
[155] C.R. Bjarkam, A.N. Glud, L. Margolin, K. Reinhart, R. Franklin, D. Deding, K.S. Ettrup, L.M. Fitting, M.S. Nielsen, J.C. Sorensen, M.G. Cunningham, Safety and function of a new clinical intracerebral microinjection instrument for stem cells and therapeutics examined in the Gottingen minipig, Stereotactic and functional neurosurgery 88(1) (2010) 56-63.
[156] S. Kelly, T.M. Bliss, A.K. Shah, G.H. Sun, M. Ma, W.C. Foo, J. Masel, M.A. Yenari, I.L. Weissman, N. Uchida, T. Palmer, G.K. Steinberg, Transplanted human fetal neural stem cells survive, migrate, and differentiate in ischemic rat cerebral cortex, Proceedings of the National Academy of Sciences of the United States of America 101(32) (2004) 11839-44.

[157] K.N. Corps, T.L. Roth, D.B. McGavern, Inflammation and neuroprotection in traumatic brain injury, JAMA Neurol 72(3) (2015) 355-62.
[158] J.A. Steinbeck, L. Studer, Moving stem cells to the clinic: potential and limitations for brain repair, Neuron 86(1) (2015) 187-206.
[159] C.W. Olanow, C.G. Goetz, J.H. Kordower, A.J. Stoessl, V. Sossi, M.F. Brin, K.M. Shannon, G.M. Nauert, D.P. Perl, J. Godbold, T.B. Freeman, A double-blind controlled trial of bilateral fetal nigral transplantation in Parkinson's disease, Annals of neurology 54(3) (2003) 403-14.
[160] C.W. Olanow, T. Freeman, J. Kordower, Transplantation of embryonic dopamine neurons for severe Parkinson's disease, The New England journal of medicine 345(2) (2001) 146; author reply 147.
[161] O. Lindvall, A. Bjorklund, Cell therapy in Parkinson's disease, NeuroRx : the journal of the American Society for Experimental NeuroTherapeutics 1(4) (2004) 382-93.
[162] S. Han, K. Yang, Y. Shin, J.S. Lee, R.D. Kamm, S. Chung, S.W. Cho, Three-dimensional extracellular matrix-mediated neural stem cell differentiation in a microfluidic device, Lab on a chip 12(13) (2012) 2305-8.
[163] K.Y. Lee, D.J. Mooney, Hydrogels for tissue engineering, Chem Rev 101(7) (2001) 1869-79.
[164] S.M. Willerth, T.E. Faxel, D.I. Gottlieb, S.E. Sakiyama-Elbert, The effects of soluble growth factors on embryonic stem cell differentiation inside of fibrin scaffolds, Stem Cells 25(9) (2007) 2235-44.
[165] S.M. Willerth, P.J. Johnson, D.J. Maxwell, S.R. Parsons, M.E. Doukas, S.E. Sakiyama-Elbert, Rationally designed peptides for controlled release of nerve growth factor from fibrin matrices, Journal of biomedical materials research. Part A 80(1) (2007) 13-23.
[166] M.D. Wood, S.E. Sakiyama-Elbert, Release rate controls biological activity of nerve growth factor released from fibrin matrices containing affinity-based delivery systems, Journal of biomedical materials research. Part A 84(2) (2008) 300-12.
[167] A. Banerjee, M. Arha, S. Choudhary, R.S. Ashton, S.R. Bhatia, D.V. Schaffer, R.S. Kane, The influence of hydrogel modulus on the proliferation and differentiation of encapsulated neural stem cells, Biomaterials 30(27) (2009) 4695-9.
[168] N.D. Leipzig, M.S. Shoichet, The effect of substrate stiffness on adult neural stem cell behavior, Biomaterials 30(36) (2009) 6867-78.
[169] D. Macaya, M. Spector, Injectable hydrogel materials for spinal cord regeneration: a review, Biomed Mater 7(1) (2012) 012001.

[170] A.S. Hoffman, Hydrogels for biomedical applications, Advanced drug delivery reviews 64(Supplement) (2012) 18-23.
[171] Y.L. Li, J. Rodrigues, H. Tomas, Injectable and biodegradable hydrogels: gelation, biodegradation and biomedical applications, Chemical Society reviews 41(6) (2012) 2193-2221.
[172] S.M. Willerth, S.E. Sakiyama-Elbert, Cell therapy for spinal cord regeneration, Advanced drug delivery reviews 60(2) (2008) 263-76.
[173] P.J. Johnson, A. Tatara, D.A. McCreedy, A. Shiu, S.E. Sakiyama-Elbert, Tissue-engineered fibrin scaffolds containing neural progenitors enhance functional recovery in a subacute model of SCI, Soft matter 6(20) (2010) 5127-5137.
[174] T.Y. Cheng, M.H. Chen, W.H. Chang, M.Y. Huang, T.W. Wang, Neural stem cells encapsulated in a functionalized self-assembling peptide hydrogel for brain tissue engineering, Biomaterials 34(8) (2013) 2005-16.
[175] E.R. Aurand, K.J. Lampe, K.B. Bjugstad, Defining and designing polymers and hydrogels for neural tissue engineering, Neuroscience research 72(3) (2012) 199-213.
[176] J.Z. Gasiorowski, C.J. Murphy, P.F. Nealey, Biophysical cues and cell behavior: the big impact of little things, Annual review of biomedical engineering 15(1) (2013) 155-76.
[177] A. Conway, D.V. Schaffer, Biophysical regulation of stem cell behavior within the niche, Stem cell research & therapy 3(6) (2012) 50.
[178] A.M. Jonker, D.W.P.M. Lowik, J.C.M. van Hest, Peptide- and Protein-Based Hydrogels, Chem Mater 24(5) (2012) 759-773.
[179] Y. Li, J. Rodrigues, H. Tomas, Injectable and biodegradable hydrogels: gelation, biodegradation and biomedical applications, Chemical Society reviews 41(6) (2012) 2193-221.
[180] M. Uemura, M.M. Refaat, M. Shinoyama, H. Hayashi, N. Hashimoto, J. Takahashi, Matrigel supports survival and neuronal differentiation of grafted embryonic stem cell-derived neural precursor cells, Journal of neuroscience research 88(3) (2010) 542-51.
[181] J. Lam, W.E. Lowry, S.T. Carmichael, T. Segura, Delivery of iPS-NPCs to the Stroke Cavity within a Hyaluronic Acid Matrix Promotes the Differentiation of Transplanted Cells, Advanced Functional Materials 24(44) (2014) 7053-7062.
[182] P. Moshayedi, L.R. Nih, I.L. Llorente, A.R. Berg, J. Cinkornpumin, W.E. Lowry, T. Segura, S.T. Carmichael, Systematic optimization of an engineered hydrogel allows for selective control of human neural stem cell survival and differentiation after transplantation in the stroke brain, Biomaterials 105 (2016) 145-55.

[183] Z.Z. Khaing, R.C. Thomas, S.A. Geissler, C.E. Schmidt, Advanced biomaterials for repairing the nervous system: what can hydrogels do for the brain?, Materials Today 17(7) (2014) 332-340.
[184] T.C. Lim, W.S. Toh, L.S. Wang, M. Kurisawa, M. Spector, The effect of injectable gelatin-hydroxyphenylpropionic acid hydrogel matrices on the proliferation, migration, differentiation and oxidative stress resistance of adult neural stem cells, Biomaterials 33(12) (2012) 3446-55.
[185] T. Fuhrmann, P. Anandakumaran, S. Payne, M. Pakulska, B.V. Varga, A. Nagy, C. Tator, M.S. Shoichet, Combined delivery of chondroitinase ABC and human induced pluripotent stem cell-derived neuroepithelial cells promote tissue repair in an animal model of spinal cord injury, Biomed Mater (2017).
[186] A. Alvarez-Buylla, D.A. Lim, For the Long Run, Neuron 41(5) 683-686.
[187] P.A. Riquelme, E. Drapeau, F. Doetsch, Brain micro-ecologies: neural stem cell niches in the adult mammalian brain, Philosophical transactions of the Royal Society of London. Series B, Biological sciences 363(1489) (2008) 123-37.
[188] J.D. Lathia, B. Patton, D.M. Eckley, T. Magnus, M.R. Mughal, T. Sasaki, M.A. Caldwell, M.S. Rao, M.P. Mattson, C. ffrench-Constant, Patterns of laminins and integrins in the embryonic ventricular zone of the CNS, The Journal of comparative neurology 505(6) (2007) 630-43.
[189] A. Conway, D.V. Schaffer, Biophysical regulation of stem cell behavior within the niche, Stem cell research & therapy 3(6) (2012) 50-50.
[190] K.S. Straley, C.W. Foo, S.C. Heilshorn, Biomaterial design strategies for the treatment of spinal cord injuries, Journal of neurotrauma 27(1) (2010) 1-19.
[191] A.J. Engler, S. Sen, H.L. Sweeney, D.E. Discher, Matrix elasticity directs stem cell lineage specification, Cell 126(4) (2006) 677-89.
[192] P.C. Georges, W.J. Miller, D.F. Meaney, E.S. Sawyer, P.A. Janmey, Matrices with compliance comparable to that of brain tissue select neuronal over glial growth in mixed cortical cultures, Biophysical journal 90(8) (2006) 3012-8.
[193] K. Saha, A.J. Keung, E.F. Irwin, Y. Li, L. Little, D.V. Schaffer, K.E. Healy, Substrate modulus directs neural stem cell behavior, Biophysical journal 95(9) (2008) 4426-38.
[194] S.R. Hynes, M.F. Rauch, J.P. Bertram, E.B. Lavik, A library of tunable poly(ethylene glycol)/poly(L-lysine) hydrogels to investigate the material cues that influence neural stem cell differentiation, Journal of biomedical materials research. Part A 89(2) (2009) 499-509.
[195] L.A. Flanagan, Y.E. Ju, B. Marg, M. Osterfield, P.A. Janmey, Neurite branching on deformable substrates, Neuroreport 13(18) (2002) 2411-5.

[196] S.K. Seidlits, Z.Z. Khaing, R.R. Petersen, J.D. Nickels, J.E. Vanscoy, J.B. Shear, C.E. Schmidt, The effects of hyaluronic acid hydrogels with tunable mechanical properties on neural progenitor cell differentiation, Biomaterials 31(14) (2010) 3930-40.
[197] K. Brannvall, K. Bergman, U. Wallenquist, S. Svahn, T. Bowden, J. Hilborn, K. Forsberg-Nilsson, Enhanced neuronal differentiation in a three-dimensional collagen-hyaluronan matrix, Journal of neuroscience research 85(10) (2007) 2138-46.
[198] A.T. Metters, K.S. Anseth, C.N. Bowman, Fundamental studies of a novel, biodegradable PEG-b-PLA hydrogel, Polymer 41(11) (2000) 3993-4004.
[199] K.S. Anseth, A.T. Metters, S.J. Bryant, P.J. Martens, J.H. Elisseeff, C.N. Bowman, In situ forming degradable networks and their application in tissue engineering and drug delivery, Journal of controlled release : official journal of the Controlled Release Society 78(1-3) (2002) 199-209.
[200] A.M. Hawkins, T.A. Milbrandt, D.A. Puleo, J.Z. Hilt, Synthesis and analysis of degradation, mechanical and toxicity properties of poly(β-amino ester) degradable hydrogels, Acta Biomaterialia 7(5) (2011) 1956-1964.
[201] D.R. Zimmermann, M.T. Dours-Zimmermann, Extracellular matrix of the central nervous system: from neglect to challenge, Histochemistry and cell biology 130(4) (2008) 635-53.
[202] C. Frantz, K.M. Stewart, V.M. Weaver, The extracellular matrix at a glance, Journal of Cell Science 123(24) (2010) 4195-4200.
[203] H. Colognato, P.D. Yurchenco, Form and function: the laminin family of heterotrimers, Developmental dynamics : an official publication of the American Association of Anatomists 218(2) (2000) 213-34.
[204] N. Pouliot, N. Kusuma, Laminin-511: A multi-functional adhesion protein regulating cell migration, tumor invasion and metastasis, Cell Adhesion & Migration 7(1) (2013) 142-149.
[205] J.H. Miner, P.D. Yurchenco, Laminin functions in tissue morphogenesis, Annual review of cell and developmental biology 20 (2004) 255-84.
[206] M. Aumailley, The laminin family, Cell adhesion & migration 7(1) (2013) 48-55.
[207] V. Kostourou, V. Papalazarou, Non-collagenous ECM proteins in blood vessel morphogenesis and cancer, Biochimica et biophysica acta 1840(8) (2014) 2403-13.
[208] J.D. Hood, D.A. Cheresh, Role of integrins in cell invasion and migration, Nat Rev Cancer 2(2) (2002) 91-100.
[209] J.H. Miner, R.M. Lewis, J.R. Sanes, Molecular Cloning of a Novel Laminin Chain, α5, and Widespread Expression in Adult Mouse Tissues, Journal of Biological Chemistry 270(48) (1995) 28523-28526.

[210] A. Domogatskaya, S. Rodin, K. Tryggvason, Functional diversity of laminins, Annual review of cell and developmental biology 28 (2012) 523-53.
[211] J.A. Indyk, Z.L. Chen, S.E. Tsirka, S. Strickland, Laminin chain expression suggests that laminin-10 is a major isoform in the mouse hippocampus and is degraded by the tissue plasminogen activator/plasmin protease cascade during excitotoxic injury, Neuroscience 116(2) (2003) 359-71.
[212] S.J. Chun, M.N. Rasband, R.L. Sidman, A.A. Habib, T. Vartanian, Integrin-linked kinase is required for laminin-2-induced oligodendrocyte cell spreading and CNS myelination, The Journal of cell biology 163(2) (2003) 397-408.
[213] A.M. Belkin, M.A. Stepp, Integrins as receptors for laminins, Microsc Res Techniq 51(3) (2000) 280-301.
[214] A.B.J. Prowse, F. Chong, P.P. Gray, T.P. Munro, Stem cell integrins: Implications for *ex-vivo* culture and cellular therapies, Stem Cell Res 6(1) (2011) 1-12.
[215] M.R. Morgan, M.J. Humphries, M.D. Bass, Synergistic control of cell adhesion by integrins and syndecans, Nature reviews. Molecular cell biology 8(12) (2007) 957-69.
[216] Shanique A. Young, Ryon Graf and Dwayne G. Stupack (2013). Neuroblastoma Integrins, Neuroblastoma, Prof. Hiroyuki Shimada (Ed.), InTech, DOI: 10.5772/55991. Available from: https://www.intechopen.com/books/neuroblastoma/neuroblastoma-integrins.
[217] M. Singh, C. Berkland, M.S. Detamore, Strategies and applications for incorporating physical and chemical signal gradients in tissue engineering, Tissue engineering. Part B, Reviews 14(4) (2008) 341-66.
[218] U. Hersel, C. Dahmen, H. Kessler, RGD modified polymers: biomaterials for stimulated cell adhesion and beyond, Biomaterials 24(24) (2003) 4385-415.
[219] J.D. Humphries, A. Byron, M.J. Humphries, Integrin ligands at a glance, Journal of Cell Science 119(19) (2006) 3901-3903.
[220] B.H. Luo, C.V. Carman, T.A. Springer, Structural basis of integrin regulation and signaling, Annual Review of Immunology 2007, pp. 619-647.
[221] K. Zhang, J. Chen, The regulation of integrin function by divalent cations, Cell adhesion & migration 6(1) (2012) 20-29.
[222] R. Milner, I.L. Campbell, The integrin family of cell adhesion molecules has multiple functions within the CNS, Journal of Neuroscience Research 69(3) (2002) 286-291.
[223] X. Wu, D.S. Reddy, Integrins as receptor targets for neurological disorders, Pharmacol Ther 134(1) (2012) 68-81.

[224] L.A. Flanagan, L.M. Rebaza, S. Derzic, P.H. Schwartz, E.S. Monuki, Regulation of human neural precursor cells by laminin and integrins, Journal of neuroscience research 83(5) (2006) 845-56.
[225] P.E. Hall, J.D. Lathia, N.G. Miller, M.A. Caldwell, C. ffrench-Constant, Integrins are markers of human neural stem cells, Stem Cells 24(9) (2006) 2078-84.
[226] J. Arulmoli, H.J. Wright, D.T.T. Phan, U. Sheth, R.A. Que, G.A. Botten, M. Keating, E.L. Botvinick, M.M. Pathak, T.I. Zarembinski, D.S. Yanni, O.V. Razorenova, C.C.W. Hughes, L.A. Flanagan, Combination scaffolds of salmon fibrin, hyaluronic acid, and laminin for human neural stem cell and vascular tissue engineering, Acta Biomater 43 (2016) 122-138.
[227] M.C. Tate, A.J. Garcia, B.G. Keselowsky, M.A. Schumm, D.R. Archer, M.C. LaPlaca, Specific β(1) integrins mediate adhesion, migration, and differentiation of neural progenitors derived from the embryonic striatum, Molecular and Cellular Neuroscience 27(1) (2004) 22-31.
[228] L.S. Campos, β1 integrins and neural stem cells: making sense of the extracellular environment, Bioessays 27(7) (2005) 698-707.
[229] E.S. Anton, J.A. Kreidberg, P. Rakic, Distinct functions of α3 and αv integrin receptors in neuronal migration and laminar organization of the cerebral cortex, Neuron 22(2) (1999) 277-89.
[230] J.G. Emsley, T. Hagg, α6β1 integrin directs migration of neuronal precursors in adult mouse forebrain, Experimental neurology 183(2) (2003) 273-85.
[231] R.S. Schmid, S. Shelton, A. Stanco, Y. Yokota, J.A. Kreidberg, E.S. Anton, α3β1 integrin modulates neuronal migration and placement during early stages of cerebral cortical development, Development 131(24) (2004) 6023-6031.
[232] G. Marchetti, S. Escuin, A. Van Der Flier, A. De Arcangelis, R.O. Hynes, E. Georges-Labouesse, Integrin α5β1 is necessary for regulation of radial migration of cortical neurons during mouse brain development, The European journal of neuroscience 31(3) (2010) 399-409.
[233] T.S. Jacques, J.B. Relvas, S. Nishimura, R. Pytela, G.M. Edwards, C.H. Streuli, C. ffrench-Constant, Neural precursor cell chain migration and division are regulated through different β1 integrins, Development 125(16) (1998) 3167-77.
[234] W. Ma, T. Tavakoli, E. Derby, Y. Serebryakova, M.S. Rao, M.P. Mattson, Cell-extracellular matrix interactions regulate neural differentiation of human embryonic stem cells, Bmc Dev Biol 8 (2008) 90.
[235] E. Fusaoka-Nishioka, C. Shimono, Y. Taniguchi, A. Togawa, A. Yamada, E. Inoue, H. Onodera, K. Sekiguchi, T. Imai, Differential effects of laminin isoforms on

axon and dendrite development in hippocampal neurons, Neuroscience research 71(4) (2011) 421-426.

[236] A. Hyysalo, M. Ristola, M.E.L. Mäkinen, S. Häyrynen, M. Nykter, S. Narkilahti, Laminin α5 substrates promote survival, network formation and functional development of human pluripotent stem cell-derived neurons *in vitro*, Stem Cell Research 24(Supplement C) (2017) 118-127.

[237] H. Ido, K. Harada, Y. Yagi, K. Sekiguchi, Probing the integrin-binding site within the globular domain of laminin-511 with the function-blocking monoclonal antibody 4C7, Matrix Biology 25(2) (2006) 112-117.

[238] H. Ido, A. Nakamura, R. Kobayashi, S. Ito, S. Li, S. Futaki, K. Sekiguchi, The requirement of the glutamic acid residue at the third position from the carboxyl termini of the laminin γ chains in integrin binding by laminins, Journal of Biological Chemistry 282(15) (2007) 11144-11154.

[239] R. Timpl, D. Tisi, J.F. Talts, Z. Andac, T. Sasaki, E. Hohenester, Structure and function of laminin LG modules, Matrix biology : journal of the International Society for Matrix Biology 19(4) (2000) 309-17.

[240] R. Nishiuchi, J. Takagi, M. Hayashi, H. Ido, Y. Yagi, N. Sanzen, T. Tsuji, M. Yamada, K. Sekiguchi, Ligand-binding specificities of laminin-binding integrins: A comprehensive survey of laminin-integrin interactions using recombinant α3β1, α6β1, α7β1 and α6β4 integrins, Matrix Biology 25(3) (2006) 189-197.

[241] J.H. McCarty, A. Lacy-Hulbert, A. Charest, R.T. Bronson, D. Crowley, D. Housman, J. Savill, J. Roes, R.O. Hynes, Selective ablation of αv integrins in the central nervous system leads to cerebral hemorrhage, seizures, axonal degeneration and premature death, Development 132(1) (2005) 165-76.

[242] M.R. Morgan, M.J. Humphries, M.D. Bass, Synergistic control of cell adhesion by integrins and syndecans, Nature reviews. Molecular cell biology 8(12) (2007) 957-969.

[243] M.D. Bass, M.R. Morgan, M.J. Humphries, Syndecans Shed Their Reputation as Inert Molecules, Science signaling 2(64) (2009) pe18.

[244] O. Okamoto, S. Bachy, U. Odenthal, J. Bernaud, D. Rigal, H. Lortat-Jacob, N. Smyth, P. Rousselle, Normal human keratinocytes bind to the α3 LG4/5 domain of unprocessed laminin-5 through the receptor syndecan-1, The Journal of biological chemistry 278(45) (2003) 44168-77.

[245] A. Utani, M. Nomizu, H. Matsuura, K. Kato, T. Kobayashi, U. Takeda, S. Aota, P.K. Nielsen, H. Shinkai, A unique sequence of the laminin α3 G domain binds to heparin and promotes cell adhesion through syndecan-2 and -4, The Journal of biological chemistry 276(31) (2001) 28779-88.

[246] J.R. Couchman, S. Gopal, H.C. Lim, S. Nørgaard, H.A.B. Multhaupt, Syndecans: from peripheral coreceptors to mainstream regulators of cell behaviour, International Journal of Experimental Pathology 96(1) (2015) 1-10.
[247] Q. Wang, L. Yang, C. Alexander, S. Temple, The niche factor syndecan-1 regulates the maintenance and proliferation of neural progenitor cells during mammalian cortical development, PloS one 7(8) (2012) e42883.
[248] M.A. Stepp, Y. Liu, S. Pal-Ghosh, R.A. Jurjus, G. Tadvalkar, A. Sekaran, K. Losicco, L. Jiang, M. Larsen, L. Li, S.H. Yuspa, Reduced migration, altered matrix and enhanced TGF-β1 signaling are signatures of mouse keratinocytes lacking Sdc1, Journal of cell science 120(Pt 16) (2007) 2851-63.
[249] T.J. Edwards, M. Hammarlund, Syndecan promotes axon regeneration by stabilizing growth cone migration, Cell Rep 8(1) (2014) 272-83.
[250] I.M. Ethell, Y. Yamaguchi, Cell surface heparan sulfate proteoglycan syndecan-2 induces the maturation of dendritic spines in rat hippocampal neurons, The Journal of cell biology 144(3) (1999) 575-86.
[251] H. Togashi, T. Sakisaka, Y. Takai, Cell adhesion molecules in the central nervous system, Cell adhesion & migration 3(1) (2009) 29-35.
[252] E. Raulo, M.A. Chernousov, D.J. Carey, R. Nolo, H. Rauvala, Isolation of a neuronal cell surface receptor of heparin binding growth-associated molecule (HB-GAM). Identification as N-syndecan (syndecan-3), The Journal of biological chemistry 269(17) (1994) 12999-3004.
[253] A. Hienola, S. Tumova, E. Kulesskiy, H. Rauvala, N-syndecan deficiency impairs neural migration in brain, The Journal of cell biology 174(4) (2006) 569-80.
[254] T. Kinnunen, M. Kaksonen, J. Saarinen, N. Kalkkinen, H.B. Peng, H. Rauvala, Cortactin-Src kinase signaling pathway is involved in N-syndecan-dependent neurite outgrowth, The Journal of biological chemistry 273(17) (1998) 10702-8.
[255] L.E. Oikari, R.K. Okolicsanyi, A. Qin, C. Yu, L.R. Griffiths, L.M. Haupt, Cell surface heparan sulfate proteoglycans as novel markers of human neural stem cell fate determination, Stem Cell Res 16(1) (2016) 92-104.
[256] S. Kuriyama, R. Mayor, A role for Syndecan-4 in neural induction involving ERK- and PKC-dependent pathways, Development 136(4) (2009) 575-84.
[257] A. Woods, J.R. Couchman, Syndecan 4 heparan sulfate proteoglycan is a selectively enriched and widespread focal adhesion component, Molecular biology of the cell 5(2) (1994) 183-92.
[258] M.J. Cooke, K. Vulic, M.S. Shoichet, Design of biomaterials to enhance stem cell survival when transplanted into the damaged central nervous system, Soft matter 6(20) (2010) 4988.

[259] M.H. Zaman, L.M. Trapani, A.L. Sieminski, D. MacKellar, H. Gong, R.D. Kamm, A. Wells, D.A. Lauffenburger, P. Matsudaira, Migration of tumor cells in 3D matrices is governed by matrix stiffness along with cell-matrix adhesion and proteolysis, Proceedings of the National Academy of Sciences 103(29) (2006) 10889-10894.
[260] R.J. Petrie, K.M. Yamada, At the leading edge of three-dimensional cell migration, Journal of cell science 125(24) (2012) 5917-5926.
[261] K.J. Lampe, S.C. Heilshorn, Building stem cell niches from the molecule up through engineered peptide materials, Neuroscience letters 519(2) (2012) 138-46.
[262] C.C. Tate, D.A. Shear, M.C. Tate, D.R. Archer, D.G. Stein, M.C. LaPlaca, Laminin and fibronectin scaffolds enhance neural stem cell transplantation into the injured brain, Journal of tissue engineering and regenerative medicine 3(3) (2009) 208-17.
[263] S.S. Rao, J.O. Winter, Adhesion molecule-modified biomaterials for neural tissue engineering, Frontiers in neuroengineering 2 (2009) 6.
[264] X. Li, X. Liu, B. Josey, C.J. Chou, Y. Tan, N. Zhang, X. Wen, Short laminin peptide for improved neural stem cell growth, Stem Cells Transl Med 3(5) (2014) 662-70.
[265] S.E. Stabenfeldt, A.J. García, M.C. LaPlaca, Thermoreversible laminin-functionalized hydrogel for neural tissue engineering, Journal of Biomedical Materials Research Part A 77A(4) (2006) 718-725.
[266] D.K. Cullen, M.C. Lessing, M.C. LaPlaca, Collagen-dependent neurite outgrowth and response to dynamic deformation in three-dimensional neuronal cultures, Annals of biomedical engineering 35(5) (2007) 835-46.
[267] J. Zhong, A. Chan, L. Morad, H.I. Kornblum, G. Fan, S.T. Carmichael, Hydrogel matrix to support stem cell survival after brain transplantation in stroke, Neurorehabil Neural Repair 24(7) (2010) 636-44.
[268] K.H. Smith, E. Tejeda-Montes, M. Poch, A. Mata, Integrating top-down and self-assembly in the fabrication of peptide and protein-based biomedical materials, Chem Soc Rev 40(9) (2011) 4563-4577.
[269] M.D. Pierschbacher, E. Ruoslahti, Cell attachment activity of fibronectin can be duplicated by small synthetic fragments of the molecule, Nature 309(5963) (1984) 30-3.
[270] H.W. Jun, V. Yuwono, S.E. Paramonov, J.D. Hartgerink, Enzyme-Mediated Degradation of Peptide-Amphiphile Nanofiber Networks, Adv Mater 17(21) (2005) 2612-2617.
[271] R. Derda, S. Musah, B.P. Orner, J.R. Klim, L. Li, L.L. Kiessling, High-throughput discovery of synthetic surfaces that support proliferation of pluripotent cells, Journal of the American Chemical Society 132(4) (2010) 1289-95.

[272] D. Stroumpoulis, H. Zhang, L. Rubalcava, J. Gliem, M. Tirrell, Cell adhesion and growth to Peptide-patterned supported lipid membranes, Langmuir : the ACS journal of surfaces and colloids 23(7) (2007) 3849-56.
[273] J. Graf, R.C. Ogle, F.A. Robey, M. Sasaki, G.R. Martin, Y. Yamada, H.K. Kleinman, A pentapeptide from the laminin B1 chain mediates cell adhesion and binds the 67,000 laminin receptor, Biochemistry 26(22) (1987) 6896-900.
[274] H.K. Kleinman, B.S. Weeks, F.B. Cannon, T.M. Sweeney, G.C. Sephel, B. Clement, M. Zain, M.O. Olson, M. Jucker, B.A. Burrous, Identification of a 110-kDa nonintegrin cell surface laminin-binding protein which recognizes an A chain neurite-promoting peptide, Arch Biochem Biophys 290(2) (1991) 320-5.
[275] D.E. Hall, L.F. Reichardt, E. Crowley, B. Holley, H. Moezzi, A. Sonnenberg, C.H. Damsky, The α1β1 and α6β1 integrin heterodimers mediate cell attachment to distinct sites on laminin, The Journal of Cell Biology 110(6) (1990) 2175-2184.
[276] T. Maeda, K. Titani, K. Sekiguchi, Cell-adhesive activity and receptor-binding specificity of the laminin-derived YIGSR sequence grafted onto Staphylococcal protein A, Journal of biochemistry 115(2) (1994) 182-9.
[277] L. Pan, H.A. North, V. Sahni, S.J. Jeong, T.L. McGuire, E.J. Berns, S.I. Stupp, J.A. Kessler, β1-Integrin and Integrin Linked Kinase Regulate Astrocytic Differentiation of Neural Stem Cells, PloS one 9(8) (2014) e104335.
[278] Y.W. Tong, M.S. Shoichet, Enhancing the neuronal interaction on fluoropolymer surfaces with mixed peptides or spacer group linkers, Biomaterials 22(10) (2001) 1029-34.
[279] T.T. Yu, M.S. Shoichet, Guided cell adhesion and outgrowth in peptide-modified channels for neural tissue engineering, Biomaterials 26(13) (2005) 1507-14.
[280] M.P. Hoffman, M. Nomizu, E. Roque, S. Lee, D.W. Jung, Y. Yamada, H.K. Kleinman, Laminin-1 and laminin-2 G-domain synthetic peptides bind syndecan-1 and are involved in acinar formation of a human submandibular gland cell line, The Journal of biological chemistry 273(44) (1998) 28633-41.
[281] M. Mochizuki, D. Philp, K. Hozumi, N. Suzuki, Y. Yamada, H.K. Kleinman, M. Nomizu, Angiogenic activity of syndecan-binding laminin peptide AG73 (RKRLQVQLSIRT), Arch Biochem Biophys 459(2) (2007) 249-55.
[282] Y. Yamada, K. Hozumi, F. Katagiri, Y. Kikkawa, M. Nomizu, Biological activity of laminin peptide-conjugated alginate and chitosan matrices, Biopolymers 94(6) (2010) 711-20.
[283] Y. Yamada, F. Katagiri, K. Hozumi, Y. Kikkawa, M. Nomizu, Cell behavior on protein matrices containing laminin α1 peptide AG73, Biomaterials 32(19) (2011) 4327-35.

[284] Y. Luo, M.S. Shoichet, A photolabile hydrogel for guided three-dimensional cell growth and migration, Nature materials 3(4) (2004) 249-53.
[285] M.P. Schwartz, Z. Hou, N.E. Propson, J. Zhang, C.J. Engstrom, V. Santos Costa, P. Jiang, B.K. Nguyen, J.M. Bolin, W. Daly, Y. Wang, R. Stewart, C.D. Page, W.L. Murphy, J.A. Thomson, Human pluripotent stem cell-derived neural constructs for predicting neural toxicity, Proceedings of the National Academy of Sciences of the United States of America 112(40) (2015) 12516-21.
[286] D. Tarus, L. Hamard, F. Caraguel, D. Wion, A. Szarpak-Jankowska, B. van der Sanden, R. Auzely-Velty, Design of Hyaluronic Acid Hydrogels to Promote Neurite Outgrowth in Three Dimensions, ACS Appl Mater Interfaces 8(38) (2016) 25051-9.
[287] J.C. Schense, J.A. Hubbell, Cross-linking exogenous bifunctional peptides into fibrin gels with factor XIIIa, Bioconjugate chemistry 10(1) (1999) 75-81.
[288] J.C. Schense, J. Bloch, P. Aebischer, J.A. Hubbell, Enzymatic incorporation of bioactive peptides into fibrin matrices enhances neurite extension, Nature biotechnology 18(4) (2000) 415-9.
[289] S.G. Lévesque, M.S. Shoichet, Synthesis of cell-adhesive dextran hydrogels and macroporous scaffolds, Biomaterials 27(30) (2006) 5277-5285.
[290] E. Agius, Y. Sagot, A.M. Duprat, P. Cochard, Antibodies directed against the β1-integrin subunit and peptides containing the IKVAV sequence of laminin perturb neurite outgrowth of peripheral neurons on immature spinal cord substrata, Neuroscience 71(3) (1996) 773-86.
[291] I. Caniggia, J. Liu, R. Han, J. Wang, A.K. Tanswell, G. Laurie, M. Post, Identification of receptors binding fibronectin and laminin on fetal rat lung cells, American Journal of Physiology-Lung Cellular and Molecular Physiology 270(3) (1996) L459-L468.
[292] J.C. Schense, J.A. Hubbell, Three-dimensional migration of neurites is mediated by adhesion site density and affinity, The Journal of biological chemistry 275(10) (2000) 6813-8.
[293] G.A. Silva, C. Czeisler, K.L. Niece, E. Beniash, D.A. Harrington, J.A. Kessler, S.I. Stupp, Selective differentiation of neural progenitor cells by high-epitope density nanofibers, Science 303(5662) (2004) 1352-5.
[294] S.P. Zustiak, S. Pubill, A. Ribeiro, J.B. Leach, Hydrolytically degradable poly(ethylene glycol) hydrogel scaffolds as a cell delivery vehicle: characterization of PC12 cell response, Biotechnology progress 29(5) (2013) 1255-64.
[295] E.J. Berns, S. Sur, L. Pan, J.E. Goldberger, S. Suresh, S. Zhang, J.A. Kessler, S.I. Stupp, Aligned neurite outgrowth and directed cell migration in self-assembled monodomain gels, Biomaterials 35(1) (2014) 185-95.

[296] J. Lam, S.T. Carmichael, W.E. Lowry, T. Segura, Design of experiments methodology to optimize hydrogel for iPSC-NPC culture, Advanced healthcare materials 4(4) (2015) 534-539.
[297] M. Yamada, K. Sekiguchi, Chapter Six - Molecular Basis of Laminin–Integrin Interactions, in: J.H. Miner (Ed.), Current topics in membranes, Academic Press2015, pp. 197-229.
[298] X. Li, X. Liu, B. Josey, C.J. Chou, Y. Tan, N. Zhang, X. Wen, Short Laminin Peptide for Improved Neural Stem Cell Growth, Stem Cells Translational Medicine 3(5) (2014) 662-670.
[299] S.P. Massia, S.S. Rao, J.A. Hubbell, Covalently immobilized laminin peptide Tyr-Ile-Gly-Ser-Arg (YIGSR) supports cell spreading and co-localization of the 67-kilodalton laminin receptor with α-actinin and vinculin, The Journal of biological chemistry 268(11) (1993) 8053-9.
[300] R. Bellamkonda, J.P. Ranieri, P. Aebischer, Laminin oligopeptide derivatized agarose gels allow three-dimensional neurite extension *in vitro*, Journal of neuroscience research 41(4) (1995) 501-9.
[301] J.W. Lee, K.Y. Lee, Dual peptide-presenting hydrogels for controlling the phenotype of PC12 cells, Colloids and surfaces. B, Biointerfaces 152 (2017) 36-41.
[302] T. Zhao, D.L. Sellers, Y. Cheng, P.J. Horner, S.H. Pun, Tunable, Injectable Hydrogels Based on Peptide-Cross-Linked, Cyclized Polymer Nanoparticles for Neural Progenitor Cell Delivery, Biomacromolecules 18(9) (2017) 2723-2731.
[303] M. Nomizu, Y. Kuratomi, S.-Y. Song, M.L. Ponce, M.P. Hoffman, S.K. Powell, K. Miyoshi, A. Otaka, H.K. Kleinman, Y. Yamada, Identification of Cell Binding Sequences in Mouse Laminin γ1 Chain by Systematic Peptide Screening, Journal of Biological Chemistry 272(51) (1997) 32198-32205.
[304] M. Hiraoka, K. Kato, T. Nakaji-Hirabayashi, H. Iwata, Enhanced survival of neural cells embedded in hydrogels composed of collagen and laminin-derived cell adhesive peptide, Bioconjugate chemistry 20(5) (2009) 976-83.
[305] M.D. Pierschbacher, E. Ruoslahti, Cell attachment activity of fibronectin can be duplicated by small synthetic fragments of the molecule, Nature 309 (1984) 30.
[306] R.O. Hynes, Integrins: bidirectional, allosteric signaling machines, Cell 110(6) (2002) 673-87.
[307] K. Saha, E.F. Irwin, J. Kozhukh, D.V. Schaffer, K.E. Healy, Biomimetic interfacial interpenetrating polymer networks control neural stem cell behavior, Journal of biomedical materials research. Part A 81(1) (2007) 240-9.

[308] W.D. Staatz, K.F. Fok, M.M. Zutter, S.P. Adams, B.A. Rodriguez, S.A. Santoro, Identification of a tetrapeptide recognition sequence for the α2β1 integrin in collagen, The Journal of biological chemistry 266(12) (1991) 7363-7.
[309] O.W. Blaschuk, R. Sullivan, S. David, Y. Pouliot, Identification of a cadherin cell adhesion recognition sequence, Developmental biology 139(1) (1990) 227-9.
[310] A. Nose, K. Tsuji, M. Takeichi, Localization of specificity determining sites in cadherin cell adhesion molecules, Cell 61(1) (1990) 147-55.
[311] E. Williams, G. Williams, B.J. Gour, O.W. Blaschuk, P. Doherty, A novel family of cyclic peptide antagonists suggests that N-cadherin specificity is determined by amino acids that flank the HAV motif, The Journal of biological chemistry 275(6) (2000) 4007-12.
[312] H.J. Lim, Z. Khan, T.S. Wilems, X. Lu, T.H. Perera, Y.E. Kurosu, K.T. Ravivarapu, M.C. Mosley, L.A. Smith Callahan, Human Induced Pluripotent Stem Cell Derived Neural Stem Cell Survival and Neural Differentiation on Polyethylene Glycol Dimethacrylate Hydrogels Containing a Continuous Concentration Gradient of N-Cadherin Derived Peptide His-Ala-Val-Asp-Ile, ACS Biomaterials Science & Engineering 3(5) (2017) 776-781.
[313] F. Gelain, D. Bottai, A. Vescovi, S. Zhang, Designer self-assembling peptide nanofiber scaffolds for adult mouse neural stem cell 3-dimensional cultures, PloS one 1 (2006) e119.
[314] S. Koutsopoulos, S. Zhang, Long-term three-dimensional neural tissue cultures in functionalized self-assembling peptide hydrogels, matrigel and collagen I, Acta Biomater 9(2) (2013) 5162-9.
[315] P.A. Janmey, J.P. Winer, J.W. Weisel, Fibrin gels and their clinical and bioengineering applications, J R Soc Interface 6(30) (2009) 1-10.
[316] Y. Li, H. Meng, Y. Liu, B.P. Lee, Fibrin Gel as an Injectable Biodegradable Scaffold and Cell Carrier for Tissue Engineering, The Scientific World Journal 2015 (2015) 685690.
[317] R.V. Shevchenko, S.L. James, S.E. James, A review of tissue-engineered skin bioconstructs available for skin reconstruction, Journal of the Royal Society Interface 7(43) (2010) 229-258.
[318] B. George, C. Matula, L. Kihlström, E. Ferrer, V. Tetens, Safety and Efficacy of TachoSil (Absorbable Fibrin Sealant Patch) Compared With Current Practice for the Prevention of Cerebrospinal Fluid Leaks in Patients Undergoing Skull Base Surgery: A Randomized Controlled Trial, Neurosurgery 80(6) (2017) 847-853.
[319] B. Wiman, D. Collen, Molecular mechanism of physiological fibrinolysis, Nature 272(5653) (1978) 549-50.

[320] J.C. Chapin, K.A. Hajjar, Fibrinolysis and the control of blood coagulation, Blood reviews 29(1) (2015) 17-24.
[321] T.A. Ahmed, M. Griffith, M. Hincke, Characterization and inhibition of fibrin hydrogel-degrading enzymes during development of tissue engineering scaffolds, Tissue Eng 13(7) (2007) 1469-77.
[322] A.H. Petter-Puchner, W. Froetscher, R. Krametter-Froetscher, D. Lorinson, H. Redl, M. van Griensven, The long-term neurocompatibility of human fibrin sealant and equine collagen as biomatrices in experimental spinal cord injury, Exp Toxicol Pathol 58(4) (2007) 237-245.
[323] J.W. Weisel, R.I. Litvinov, Mechanisms of fibrin polymerization and clinical implications, Blood 121(10) (2013) 1712-1719.
[324] A.C. Brown, T.H. Barker, Fibrin-based biomaterials: modulation of macroscopic properties through rational design at the molecular level, Acta Biomater 10(4) (2014) 1502-14.
[325] B. Blomback, N. Bark, Fibrinopeptides and fibrin gel structure, Biophys Chem 112(2-3) (2004) 147-51.
[326] K. Kubota, H. Kogure, Y. Masuda, Y. Toyama, R. Kita, A. Takahashi, M. Kaibara, Gelation dynamics and gel structure of fibrinogen, Colloids and surfaces. B, Biointerfaces 38(3-4) (2004) 103-9.
[327] J. Konings, J.W. Govers-Riemslag, H. Philippou, N.J. Mutch, J.I. Borissoff, P. Allan, S. Mohan, G. Tans, H. Ten Cate, R.A. Ariens, Factor XIIa regulates the structure of the fibrin clot independently of thrombin generation through direct interaction with fibrin, Blood 118(14) (2011) 3942-51.
[328] W. Ho, B. Tawil, J.C. Dunn, B.M. Wu, The behavior of human mesenchymal stem cells in 3D fibrin clots: dependence on fibrinogen concentration and clot structure, Tissue Eng 12(6) (2006) 1587-95.
[329] M.M. Martino, P.S. Briquez, A. Ranga, M.P. Lutolf, J.A. Hubbell, Heparin-binding domain of fibrin(ogen) binds growth factors and promotes tissue repair when incorporated within a synthetic matrix, Proceedings of the National Academy of Sciences of the United States of America 110(12) (2013) 4563-8.
[330] S.L.B. Oliveira, M.M. Pillat, A. Cheffer, C. Lameu, T.T. Schwindt, H. Ulrich, Functions of neurotrophins and growth factors in neurogenesis and brain repair, Cytometry Part A 83A(1) (2013) 76-89.
[331] E.F. Plow, T.A. Haas, L. Zhang, J. Loftus, J.W. Smith, Ligand binding to integrins, The Journal of biological chemistry 275(29) (2000) 21785-8.
[332] M.W. Mosesson, Fibrinogen and fibrin structure and functions, Journal of Thrombosis and Haemostasis 3(8) (2005) 1894-1904.

[333] A.M. Belkin, G. Tsurupa, E. Zemskov, Y. Veklich, J.W. Weisel, L. Medved, Transglutaminase-mediated oligomerization of the fibrin(ogen) αC domains promotes integrin-dependent cell adhesion and signaling, Blood 105(9) (2005) 3561-8.
[334] D.A. Cheresh, S.A. Berliner, V. Vicente, Z.M. Ruggeri, Recognition of distinct adhesive sites on fibrinogen by related integrins on platelets and endothelial cells, Cell 58(5) 945-953.
[335] S. Yakovlev, I. Mikhailenko, G. Tsurupa, A.M. Belkin, L. Medved, Polymerisation of fibrin αC-domains promotes endothelial cell migration and proliferation, Thromb Haemost 112(6) (2014) 1244-51.
[336] R. Pittier, F. Sauthier, J.A. Hubbell, H. Hall, Neurite extension and *in vitro* myelination within three-dimensional modified fibrin matrices, Journal of neurobiology 63(1) (2005) 1-14.
[337] Y.E. Ju, P.A. Janmey, M.E. McCormick, E.S. Sawyer, L.A. Flanagan, Enhanced neurite growth from mammalian neurons in three-dimensional salmon fibrin gels, Biomaterials 28(12) (2007) 2097-108.
[338] D. Stenzel, M. Wilsch-Brauninger, F.K. Wong, H. Heuer, W.B. Huttner, Integrin αvβ3 and thyroid hormones promote expansion of progenitors in embryonic neocortex, Development 141(4) (2014) 795-806.
[339] J.F. Marshall, D.C. Rutherford, A.C. McCartney, F. Mitjans, S.L. Goodman, I.R. Hart, αvβ1 is a receptor for vitronectin and fibrinogen, and acts with α5β1 to mediate spreading on fibronectin, Journal of cell science 108 (Pt 3) (1995) 1227-38.
[340] P.J. Johnson, S.R. Parker, S.E. Sakiyama-Elbert, Fibrin-based tissue engineering scaffolds enhance neural fiber sprouting and delay the accumulation of reactive astrocytes at the lesion in a subacute model of spinal cord injury, Journal of Biomedical Materials Research Part A 92(1) (2010) 152-63.
[341] D.A. McCreedy, T.S. Wilems, H. Xu, J.C. Butts, C.R. Brown, A.W. Smith, S.E. Sakiyama-Elbert, Survival, Differentiation, and Migration of High-Purity Mouse Embryonic Stem Cell-derived Progenitor Motor Neurons in Fibrin Scaffolds after Sub-Acute Spinal Cord Injury, Biomater Sci 2(11) (2014) 1672-1682.
[342] T.S. Wilems, J. Pardieck, N. Iyer, S.E. Sakiyama-Elbert, Combination therapy of stem cell derived neural progenitors and drug delivery of anti-inhibitory molecules for spinal cord injury, Acta Biomater 28 (2015) 23-32.
[343] J. Robinson, P. Lu, Optimization of trophic support for neural stem cell grafts in sites of spinal cord injury, Experimental neurology 291 (2017) 87-97.
[344] R. Pittier, F. Sauthier, J.A. Hubbell, H. Hall, Neurite extension and *in vitro* myelination within three-dimensional modified fibrin matrices, Journal of Neurobiology 63(1) (2005) 1-14.

[345] Y.E. Ju, P.A. Janmey, M. McCormick, E.S. Sawyer, L.A. Flanagan, Enhanced Neurite Growth from Mammalian Neurons in Three-Dimensional Salmon Fibrin Gels, Biomaterials 28(12) (2007) 2097-2108.
[346] W. Zhao, Q. Han, H. Lin, W. Sun, Y. Gao, Y. Zhao, B. Wang, X. Wang, B. Chen, Z. Xiao, J. Dai, Human basic fibroblast growth factor fused with Kringle4 peptide binds to a fibrin scaffold and enhances angiogenesis, Tissue engineering. Part A 15(5) (2009) 991-8.

CHAPTER II

Three-dimensional culture of single embryonic stem-derived neural/stem progenitor cells in fibrin hydrogels: neuronal network formation and matrix remodeling*

Ana R. Bento [1,2,3], Pedro Quelhas [1,2], Maria J. Oliveira [1,2,4], Ana P. Pêgo [1,2,3,5], Isabel F. Amaral [1,2,3]

[1] INEB - Instituto de Engenharia Biomédica, Universidade do Porto, Portugal; [2] i3S - Instituto de Investigação e Inovação em Saúde, Universidade do Porto, Portugal; [3] Faculdade de Engenharia, Universidade do Porto, Portugal; [4] Departamento de Patologia e Oncologia da Faculdade de Medicina da Universidade do Porto, Portugal; [5] Instituto de Ciências Biomédicas Abel Salazar, Universidade do Porto, Portugal.

Published in Journal of Tissue Engineering and Regenerative Medicine 2017, 11(12):3494–3507. DOI:10.1002/term.2262.

Abstract

In an attempt to improve the efficacy of neural stem/progenitor cell (NSPC) based therapies, fibrin hydrogels are being explored to provide a favorable microenvironment for cell survival and differentiation following transplantation. In this work, we explored the ability of fibrin to support the survival, proliferation, and neuronal differentiation of NSPCs derived from embryonic stem (ES) cells under monolayer culture. Single mouse ES-NSPCs were cultured within fibrin (fibrinogen concentration: 6 mg/mL) under neuronal differentiation conditions up to 14 days. ES-NSPCs retained high cell viability and proliferated within small-sized spheroids. Neuronal differentiation was evidenced through an increase in the levels of βIII-tubulin and NF200 over time. At D14, cell-matrix constructs were mainly comprised of NSPCs and neurons (46.5% βIII-tubulin^{+} cells). GABAergic and dopaminergic/noradrenergic neurons were also observed along with a network of synaptic proteins. ES-NSPCs expressed matriptase and secreted MMP-2/9, with MMP-2 activity increasing along time. Fibronectin, laminin and collagen type IV deposition was also detected. Fibrin gels prepared with higher fibrinogen concentrations (8/10 mg/mL) were less permissive to neurite extension and neuronal differentiation, possibly due to their smaller pore area and higher rigidity. Overall, we show that ES-NSPCs within fibrin are able to establish neuronal networks and to remodel fibrin through MMP secretion and extracellular matrix (ECM) deposition. This 3D culture system was also shown to support cell viability, neuronal differentiation and ECM deposition of human ES-NSPCs. The settled 3D platform is expected to constitute a valuable tool to develop fibrin-based hydrogels for ES-NSPC delivery into the injured central nervous system.

Keywords: three-dimensional culture; neural stem cells; neuronal maturation; fibrin hydrogel; extracellular matrix; fibronectin; laminin; matrix metalloproteinase activity.

Introduction

Nervous system disorders such as spinal cord injury (SCI), stroke, brain trauma, and neurodegenerative diseases, often result in life-long neurological deficits, with high burden to society and health systems. Regeneration of damaged central nervous system (CNS) tissue remains a challenging issue, as it comprises the regrowth of disrupted axons, the replacement of lost neural cells and the recovery of lost neural functions [1]. As in the adult CNS the intrinsic capacity of endogenous neural progenitors to replace lost cells is insufficient, transplantation of exogenous neural

stem/progenitor cells (NSPCs) has emerged as a possible therapy to compensate for injury-induced lost cells. Besides secreting cytokines with neurotrophic and immumodulatory effect, NSPCs are able to differentiate into neurons and glial cells, potentially contributing to the remyelinization of spared axons and to the establishment of relay neuronal circuitries. In preclinical models of SCI and ischemic stroke, transplanted NSPCs were shown to be capable of dividing, differentiate, and integrate into the injured tissue, partially overcoming functional deficits [1-3]. These findings led to the approval of clinical trials to assess the safety and preliminary efficacy of human fetal CNS-derived neural stem cell transplantation (https://clinicaltrials.gov).

Embryonic stem (ES) cells, due to their pluripotency and unlimited capacity for self-renewal have been explored as an alternative source of NSPCs [4, 5], particularly after the establishment of protocols to efficiently and reproducibly specify ES cells into pure populations of NSPCs [6, 7]. Moreover, ES-derived NSPCs (ES-NSPCs) retain a higher proliferative capacity and neuronal differentiation efficiency compared to somatic NSPCs [5], which can be of interest to counteract the high levels of cell death occurring following transplantation. Clinical trials involving ES-NSPC transplantation have also been approved (Geron, Inc.; Cell Cure Neurosciences Ltd; Ocata Therapeutics Inc.; CHABiotech CO., Ltd.), since ES-NSPCs were shown to survive, divide, differentiate and promote functional recovery in rodent models of SCI [4, 8].

Despite their functional benefits, NSPCs implanted as suspensions usually show poor cell survival, as well as limited differentiation along the neuronal lineage, as a result of the inhibitory milieu of the injured tissue [4]. Attempts are being made to improve NSPC transplantation efficacy, namely by combining NSPCs with biodegradable hydrogels [9]. Besides providing a structural support for axonal extension and allowing a homogenous distribution of transplanted cells, hydrogels contribute to sequester cell-secreted neurite-promoting factors and extracellular matrix (ECM) proteins, while supporting the exchange of nutrients within the surrounding tissue. Hydrogels may therefore contribute to the establishment of a more favorable microenvironment for NSPC survival and differentiation, as well as for regeneration [9, 10]. Fibrin is a FDA-approved hydrogel with widespread clinical use that emerged as a promising biomatrix for application in the CNS, either as an acellular graft [11] or as a vehicle for cell and drug delivery [3, 12]. Fibrin is a natural polymer formed during the blood coagulation cascade from its zymogen form, fibrinogen, with a central role in hemostasis. Due to its mechanical properties, inherent biocompatibility, and susceptibility to proteolytic degradation, fibrin constitutes a suitable matrix for cells normally residing in soft tissues

such as brain or spinal cord [13] and, in this sense has been successfully explored for the transplantation of NSPCs [3].

Commitment of ES cells into the neural fate is usually achieved by inducing embryoid body (EB) formation in suspension culture followed by treatment with retinoic acid [14]. Embryoid bodies containing neural progenitors have been shown to proliferate and differentiate following embedment in fibrin hydrogels [15]. Still, neural induction protocols relying on EB formation typically result in a heterogeneous cell population, due to the establishment of concentration gradients of morphogens existing from the outer edge of the multicellular aggregates to the core [16, 17]. This issue can be overcome using adherent monoculture systems to generate NSPCs from ES cells, which result in a more homogeneous population (>85% of cells expressing Sox1), due to the uniform exposure of cells to soluble factors [14, 17, 18].

In this sense, the aim of this work was to establish the conditions for the three-dimensional (3D) culture of NSPCs derived from ES cells under adherent monoculture in fibrin hydrogels, when seeded as single cell suspension. For this purpose, mouse ES derived-NSPCs (mES-NSPCs) were embedded within fibrin hydrogels as single cells and the seeding density leading to the highest cell viability, after 14 days of culture under differentiation conditions, was established. NSPC-fibrin constructs were then characterized in terms of cell morphology, proliferation, morphology, phenotype, distribution of cell-secreted ECM proteins, as well as in terms of matrix metalloproteinase (MMP) activity and matriptase expression. Moreover, the effect of fibrinogen concentration on NSPC viability, migration, proliferation, neuronal differentiation and MMP activity was assessed, as the density of bioactive domains and the structural and viscoelastic properties of hydrogels may impact the behavior of encapsulated cells [10]. Finally, to disclosure if this 3D culture system could be applied to human ES-derived NSCs (hES-NSCs), dissociated hES-NSCs were cultured within fibrin hydrogels for periods up to 21 days and cell viability, neuronal differentiation and ECM remodeling subsequently assessed.

Materials and Methods

Generation of neural stem/progenitor cells from mouse ES cells

The mouse embryonic stem (ES) cell line (46C) established at the Institute for Stem Cell Research (Edinburgh University, Scotland, UK) expressing green fluorescent

protein (GFP) under the promoter of the neural-specific *Sox1* gene, was used [19]. ES 46 cells were grown in KnockOut™ ESC/iPSC medium (Gibco) supplemented with 1% (v/v) penicillin/streptomycin (Pen/Strep), 2 μM glycogen synthase kinase-3 (GSK-3) inhibitor IX (Calbiochem), and 2 ng/mL recombinant murine leukemia inhibitory factor (LIF; produced in bacteria, a gift from Dr. Cláudia Lobato, Instituto Superior Técnico, Lisboa, Portugal), in 6-well tissue culture-grade plates coated with 0.1% (w/v) gelatin (Sigma-Aldrich). Cell culture medium was refreshed every day. To start the monolayer culture protocol, ES cells were cultured at high density (1×10^5 cells/cm^2) during 24 h with LIF [14]. To induce the neural phenotype, ES cells were cultured in monolayer in N2B27 medium, a 1:1 mixture of DMEM/F12 medium supplemented with modified N2 [7] with Neurobasal™ medium supplemented with B27 and L-glutamine (Neurobasal/B27), containing 1% (v/v) penicillin/streptomycin (all from Gibco). Cell culture medium was refreshed every other day. At day 5 of the monolayer culture differentiation protocol, Sox1-GFP expression was analyzed by fluorescence microscopy and flow cytometry, to assess the efficiency of neural conversion (Fig. S1A-B). For the latter, cells were dissociated using StemPro® Accutase® (Gibco), counted, suspended in FACS buffer [2% (v/v) fetal bovine serum (FBS) in PBS], and run on a flow cytometer (FACSCalibur™, BD Biosciences). Live cells were gated based on forward scatter (size) and side scatter (cell complexity) criteria, and fluorescence gates set using undifferentiated 46C ES cells as negative control. All analysis was performed using FlowJo™ software. The levels of Sox1-GFP expression of the ES-NSPCs used throughout this study are shown in Figure S1B, together with a representative fluorescence histogram. The phenotypic characterization of ES-NSPCs at day 5 of monolayer culture neural commitment is provided in Figure S1.

Culture of mES-NSPCs within fibrin gels

Fibrinogen solution was prepared dissolving plasminogen-free fibrinogen from pooled human plasma containing factor XIII (Sigma) in ultrapure water, followed by dialysis against tris-buffered saline (TBS, pH 7.4) for 24 h [20]. The resulting fibrinogen solution was then sterile-filtered and its concentration determined by UV spectroscopy. fibrinogen solution was then diluted to 12 mg/mL with sterile TBS. Fibrin gels (total volume: 50 μL) were obtained by mixing equal volumes of the fibrinogen solution and a thrombin solution in TBS containing $CaCl_2$ and aprotinin [final concentration of fibrin components: 6 mg/mL fibrinogen; 2 NIH U/mL thrombin from human plasma; 2.5 mM $CaCl_2$ (Merck); 25 μg/mL aprotinin (all Sigma-Aldrich except for $CaCl_2$)]. ES-NPSCs were dissociated into single cells and suspended in the fibrinogen solution prior to

transferring the polymerizing solution to the wells of 6-well plates. Different cell seeding densities were initially tested (1, 2 and 3×10^6 NSPCs/mL), for optimization the cell seeding density within fibrin gels. Fibrin gels were allowed to polymerize for 30 min at 37°C in a 5% CO_2 humidified incubator, before the addition of cell culture media (3 mL/well). The cell-matrix constructs were cultured for periods up to 14 days in the presence of 5 µg/mL of aprotinin to delay fibrin gel degradation, following a protocol for neuronal differentiation [21]. Cells were initially cultured in N2B27 supplemented with 10 ng/mL basic fibroblast growth factor (bFGF; PeproTech) and, at day 2 of culture, the medium was switched to the mix N2B27:Neurobasal/B27 (1:1) without growth factor. At day 8, half of the medium was replaced by the mix N2B27:Neurobasal/B27 (1:3) supplemented with 20 ng/mL brain-derived neurotrophic factor and 50 ng/mL nerve growth factor (BDNF and NGF; PeproTech). Half of the medium was changed every other day. To assess the effect of fibrinogen concentration on ES-NSPC behavior, fibrin gels with the following fibrinogen concentrations were prepared: 4, 6, 8 and 10 mg/mL. ES-NSPC were embedded within fibrin hydrogels and cultured as described above.

Culture of hES-NSCs within fibrin gels

H9-derived human ES-NSCs were purchased from Life Technologies and expanded according to the manufacturer's protocol (Gibco). For cell embedment in fibrin, hES-NPSCs were dissociated into single cells using StemPro® Accutase® and further suspended in fibrin gel (1×10^6 NSPCs/mL) as described for mES-NSPCs. The cell-matrix constructs were cultured for periods up to 21 days in the presence of 5 µg/mL of aprotinin. Human ES-NSCPs were initially cultured in StemPro® NSC serum-free media (SFM; Gibco) containing bFGF and epidermal growth factor (EGF) and, at day 2 of culture, the medium was switched to the mix StemPro® NSC SFM media:Neurobasal/B27 (1:1), without growth factors. At day 8, half of the medium was replaced by the mix StemPro® NSC SFM:Neurobasal/B27 (1:3) supplemented with 10 ng/mL of BDNF and 500 µM of dibutyryl cAMP (Sigma). Half of the medium was changed every other day.

Size of cellular spheroids formed within fibrin gels

The size of the cellular spheroids present within fibrin was assessed at day 14 of culture. Phase contrast images of the cell-fibrin constructs were acquired (Axiovert 200, Carl Zeiss), and the diameter size of each spheroid measured using AxioVision

software (Carl Zeiss). Spheroids smaller than 25 μm in diameter were not considered, as these were mainly correspondent to single or paired cells [22].

Immunocytometry

Immunocytometry analysis was performed in six-pooled fibrin drops, after cell isolation from the cell-fibrin constructs. Briefly, the constructs were washed twice with PBS, and sequentially incubated with 1.25 mg/mL of collagenase type II (Gibco; 1 h at 37°C) and 1× trypsin-EDTA (Gibco; 30 min at 37°C) under stirring (70 rpm). After trypsin inactivation with serum-containing media cells were gently dissociated, centrifuged, and suspended in cell culture medium. For staining of intracellular markers, cells were fixed with 1% (w/v) paraformaldehyde (PFA; 20 min at 4°C), and permeabilized with 0.2% (v/v) Triton X-100 (10 min at 4°C). Cells were then incubated in blocking buffer for 20 min and then incubated for 30 min with primary antibodies diluted in PBS buffer containing 1% (v/v) normal goat serum (NGS, Biosource) and 0.1% (w/v) saponin. Primary antibodies were detected by applying isotype-specific or species-specific secondary antibodies for 30 min. For immunolabeling of cell surface markers, the fixation and permeabilization steps were omitted, and the blocking/primary antibody solutions prepared without saponin. Cells were finally washed 3× and suspended in FACS buffer containing sodium azide, for flow cytometry analysis (BD FACSCalibur™). Primary and secondary antibodies are listed in Table S1. Unlabeled cells were used to set fluorescence gates. Cells stained with secondary antibody only or with the correspondent isotype control were used to assess the background fluorescence associated with non-specific binding of the secondary antibody. Representative fluorescence histograms are shown in Figure S3B.

Immunocytochemistry

Immunocytochemistry was performed in cell-fibrin constructs previously fixed in cell culture media containing 2% (v/v) PFA (30 min at 37°C). All subsequent steps were performed under stirring (50 rpm). When staining for intracellular markers cell-fibrin constructs were permeabilized for 45 min with 0.2% (v/v) Triton X-100. Cell-fibrin constructs were blocked for 1 h, incubated (overnight at 4°C) with the appropriate primary antibody, rinsed 3× with PBS, and incubated for 1 h with the appropriate secondary antibody. When necessary, nuclei were counterstained with DAPI (Gibco; 0.1 μg/mL). Samples were finally mounted in Fluoromount™ mounting media (Sigma-Aldrich) and observed under the confocal laser scanning microscope [CLSM; Leica

TCS SP5 II (Leica Microsystems, Germany)]. Primary and secondary antibodies are listed in Table S2.

Cell outward migration analysis

Neurite extension/cell outward migration from cellular spheroids was assessed at day 4 of ES-NSPC culture within fibrin. Cell-fibrin constructs were fixed and permeabilized as described for immunocytochemistry studies, incubated with PBS containing 1% (w/v) bovine serum albumin for 1 h under stirring, and then with Alexa Fluor® 594-conjugated phalloidin (Invitrogen; 1:40; 1 h under stirring), for visualization of filamentous actin (F-actin). After rinsing with PBS, nuclei were counterstained with DAPI and samples mounted in Fluoromount™. Fluorescence images were collected using the CLSM. Spheroid and F-actin positive regions were obtained using automatic segmentation of the 2D maximum intensity projections of DNA and F-actin CLSM image stacks, respectively. Given the segmented regions, the number of cell extensions protruding from the edge of each spheroid (sprouts), as well as the length of the longest sprout (maximal outgrowth), were analyzed [23]. For each condition, 10 randomly selected spheroids from 2 different fibrin gels were examined.

Microstructure analysis of fibrin gels

Fibrin gels microstructure was characterized using fluorescently-labeled fibrinogen. Fluorescent fibrin gels were prepared as described above, using a 1:100 ratio of Alexa Fluor® 488 human fibrinogen conjugate (Molecular Probes) to unlabeled fibrinogen. Acellular fibrin gels were allowed to polymerize (30 min at 37°C), and immediately observed under the CLSM, using a Plan-Apochromat 63x/1.4 NA oil objective (NA, numerical aperture). CLSM stacks of 10 optical sections covering a depth of 10 µm were acquired, and 2D projected. Pores were automatically segmented and their areas computed using MATLAB® software. Finally, the average pore area was determined. For each condition, 4 images from 2 different fibrin gels were analyzed.

Rheological analysis of fibrin gels

A Kinexus Pro Rheometer (Malvern) was used to examine the viscoelastic properties of acellular fibrin drops. fibrin polymerizing solution (50 µL) was pipetted into a plate-plate geometry (4 mm in diameter with sandblasted surfaces) previously set at 37°C, and allowed to polymerize *in situ* for 1 h under humidified atmosphere. A 10% compression

was then applied to the gel to avoid slippage. For each condition, the linear viscoelastic region (LVR) was first determined performing stress sweeps (strain: 1 to 100%; frequency: 0.1 Hz). Frequency sweeps (frequency: 0.01 to 10 Hz; strain: 5%) were then performed within the LVR. The storage modulus (G'), a measure of the elastic energy stored during the deformation imposed by one oscillation of the rheometer, was determined and used as a measure of fibrin drops stifness. The loss modulus (G''), which reflects the energy dissipated by fibrin drops during deformation was also recorded. Six fibrin gels were analyzed per condition.

Data analysis and statistics

Each independent experiment was established from mES-NSPCs obtained from different neural commitments. In each flow cytometry analysis, 1×10^4 events were captured inside the gate. Sample distribution was tested for normality using the Kolmogorov-Smirnov test, and data subsequently analyzed using the unpaired *t*-test. Unless mentioned otherwise, all data are presented as mean ± standard deviation (SD). The statistical significance level was set for p values < 0.05.

A detailed description of the methods used to culture mES-NSPCs on 2D substrates, as well as to assess cell viability and total cell number, proliferation, MMP activity, matriptase, βIII-tubulin and NF200 levels is provided in Supplementary Materials and Methods.

Results

Optimization of mES-NSPC cell seeding density within fibrin

To assess the optimal conditions to culture mES-NSPCs within fibrin, different cell seeding densities were initially explored (1, 2 and 3×10^6 cells/mL). Following entrapment within fibrin, single ES-NSPCs were found well dispersed within the fibrin gel, as shown by incubation of samples with calcein AM and Hoechst 33342 (Fig. S2A). The lowest cell seeding density (1×10^6 cells/mL) resulted in a lower number of dead cells and smaller-sized cellular spheroids after 14 days of culture, as shown by CLSM analysis of cell/fibrin constructs previously incubated with calcein AM/propidium iodide (PI; Fig. S2B). These qualitative results were further supported by flow cytometry analysis of cell viability, which showed for the lowest cell seeding density the lowest percentage of PI-labeled cells (Fig. S2C). As a result, this cell seeding density was

selected for use in subsequent studies. The cell culture medium was supplemented with aprotinin, a cell protease inhibitor, as the mere addition of aprotinin to the fibrin polymerizing solution was not sufficient to preserve cell/fibrin constructs integrity during the 14 days of culture (Fig. S2D). The addition of 5 μg/mL of aprotinin to the medium was effective in preventing the overall fibrin gel degradation, independently of the cell seeding density tested, while being permissive to fibrin degradation by migrating cells (data not shown).

Cell viability and proliferation of mES-NSPCs within fibrin gels

The distribution of live/dead cells within fibrin gels was assessed after 7 and 14 days of culture. Confocal analysis of cell/fibrin constructs, previously incubated with calcein AM/PI, showed for both time points the presence of live cells widely distributed throughout the fibrin gel, often growing as cellular spheroids. Formation of cellular spheroids was associated with proliferative capacities and not with aggregation at the initial cell embedment, since only single cells were detected within fibrin gels immediately after cell embedment (Fig. S2A). Neurite-like extensions were already observed at day 7, and at day 14 of culture, these formed a dense network of cellular processes (Fig. 1A). Propidium iodide (PI) uptake by cells was also observed at both time points analyzed. The quantitative analysis of live/dead cells within fibrin was assessed by flow cytometry, upon cell isolation from the fibrin gels. Cell viability within fibrin gels was found to be similar at both time points and at levels greater than 85%, in average, as demonstrated by the percentage of cells excluding PI (Fig. 1B). The percentage of cells remaining alive was found to be high for both time points considered, as shown by the percentage of cells retaining ability to hydrolyze calcein AM (99.9% and 94.3% for day 7 and day 14, respectively; Fig. S3A). ES-NSPCs within fibrin gels were able to proliferate, as evidenced by the five- and two-fold increase in cell number found over the first and second weeks of culture, respectively (Fig. 1C). At day 14 of culture, the presence of small-sized cellular spheroids inside cell/fibrin constructs, mostly frequently with diameters in the range of 50 to 75 μm (Fig. 1D), also suggests cell proliferation of ES-NSPCs within fibrin.

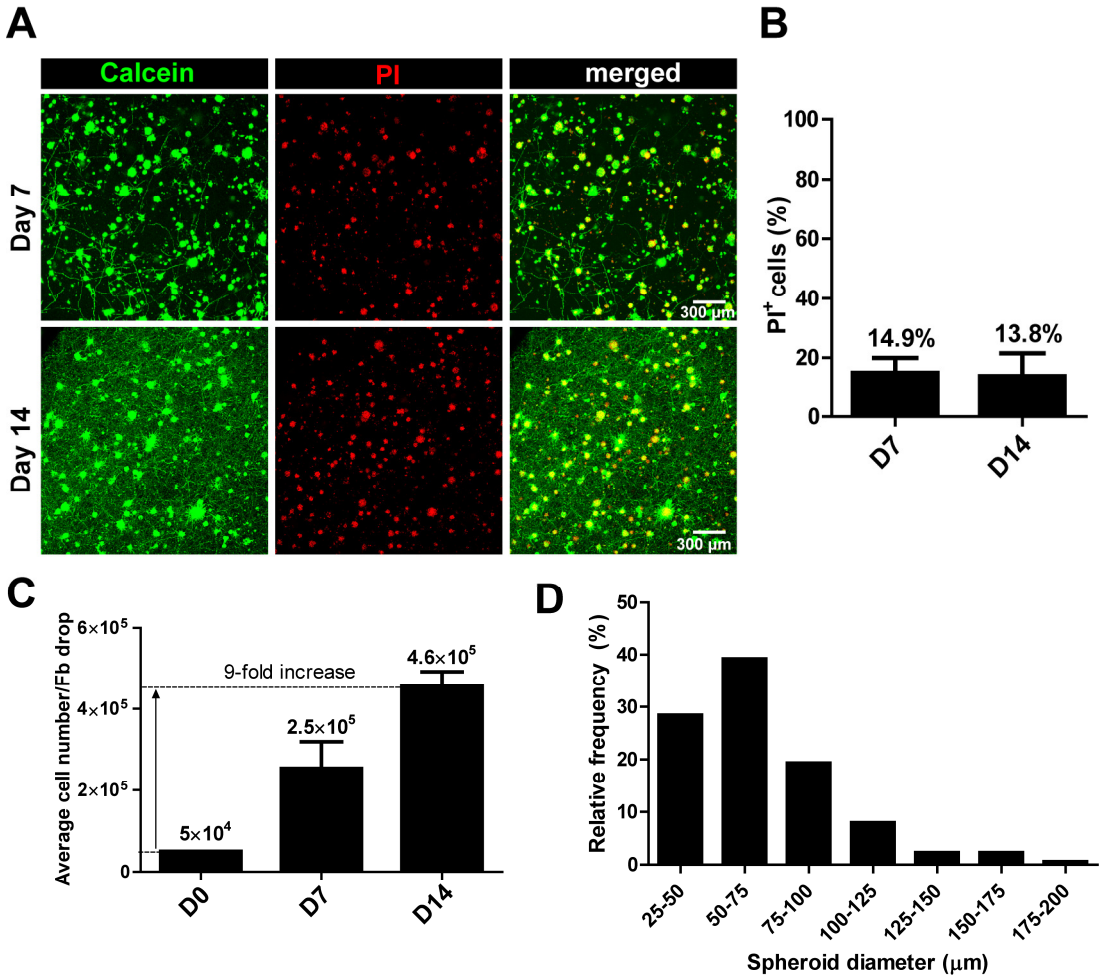

Figure 1. Cell viability, proliferation, and cellular spheroid diameter of mES-NSPCs within fibrin hydrogels. (A) Distribution of live and/or dead cells at day 7 and 14 of culture; cell-fibrin constructs were incubated with calcein AM and PI for detection of live and dead cells, respectively, and imaged by CLSM; representative 2D projections of CLSM stack images covering a depth of 300 µm are shown. **(B)** Quantitative analysis of cells incorporating PI (PI^+, non-viable cells) at day 7 and 14 of culture, as determined by flow cytometry (*n* = 3 independent experiments). **(C)** Total number of viable cells per fibrin drop at day 0 (upon cell embedment within fibrin), 7 and 14 of culture (*n* = 3 independent experiments). **(D)** Histogram of cellular spheroids (neurospheres) diameter distribution at day 14 of culture; analysis was performed in 4 fibrin drops from 2 independent experiments.

Phenotypic analysis of mES-NSPCs cultured within fibrin gels

Differentiation into the neuronal lineage over the cell culture period was initially followed by western blot of βIII-tubulin (developing and mature neurons) and NF200 (mature neurons). As expected, expression of βIII-tubulin and NF200 was not detected before ES-NSPC embedment in fibrin (data not shown). Throughout the culture period, the expression of these neuronal markers increased, attaining significantly higher levels at day 14, when compared to day 4, for both markers (Fig. 2A–B). For this

reason, a more detailed phenotypic analysis was performed at day 14 of cell culture by flow cytometry and immunocytochemistry (Fig. 2C). At this time point, a significant percentage of cells still expressed the NSPC marker nestin (53.1 ± 6.3%) and the neural stem cell (NSC) marker Sox1-GFP (37.7 ± 5.6%). The percentages found were always inferior to those of ES-NSPCs prior embedment within fibrin (87.7 ± 5.8% Sox1-GFP$^+$ cells and 86.5 ± 7.2 nestin$^+$ cells; Fig. S1C). Under these conditions, ES-NSPCs differentiated mainly into βIII-tubulin immunoreactive neurons, as shown by the higher percentage of βIII-tubulin$^+$ cells found (46.5 ± 12.5%) as compared to those of cells staining positive for GFAP or O4, astrocytic and oligodendrocytic markers, respectively. After 14 days of culture, the percentage of cells expressing SSEA-1, a marker for undifferentiated mouse ES cells, dropped from 57.3 ± 17.6% (Fig. S1C) to 20.6 ± 4.7%. CLSM analysis of samples processed for immunofluorescence at this same time point (day 14) supported the previous results. Images depict cell-matrix constructs composed by a heterogeneous cell population encompassing NSPCs (nestin$^+$ cells; Fig. 2E) and developing and mature neurons (βIII-tubulin$^+$ and NF200$^+$ cells; Fig. 2H–I). Neurites staining for βIII-tubulin were found mainly radially extending from cellular spheroids, forming a dense neuronal network throughout the whole fibrin gel (Fig. 2H). Astrocytes and oligodendrocytes were also detected but at lower amounts, and mostly located near the spheroids (Fig. 2F–G). A reminiscent population marking for SSEA-1 could be also observed at this time point (Fig. 2D). The presence of synaptic vesicles was assessed through synapsin immunodetection. Cell-fibrin constructs revealed an extensive network of synapsin (Fig. 2J), and the presence of dendritic spines along the axonal processes (arrowheads in Fig. 2J). Neuronal phenotype was further investigated. A ubiquitous expression of GAD67, a GABAergic phenotype marker, was observed throughout the cell/fibrin constructs (Fig. 2K). Furthermore, immunodetection of tyrosine hydroxylase (TH) revealed the presence of mature dopaminergic and/or noradrenergic neurons (Fig. 2L). TH-labeled neurons with long extensions are indicated by arrowheads.

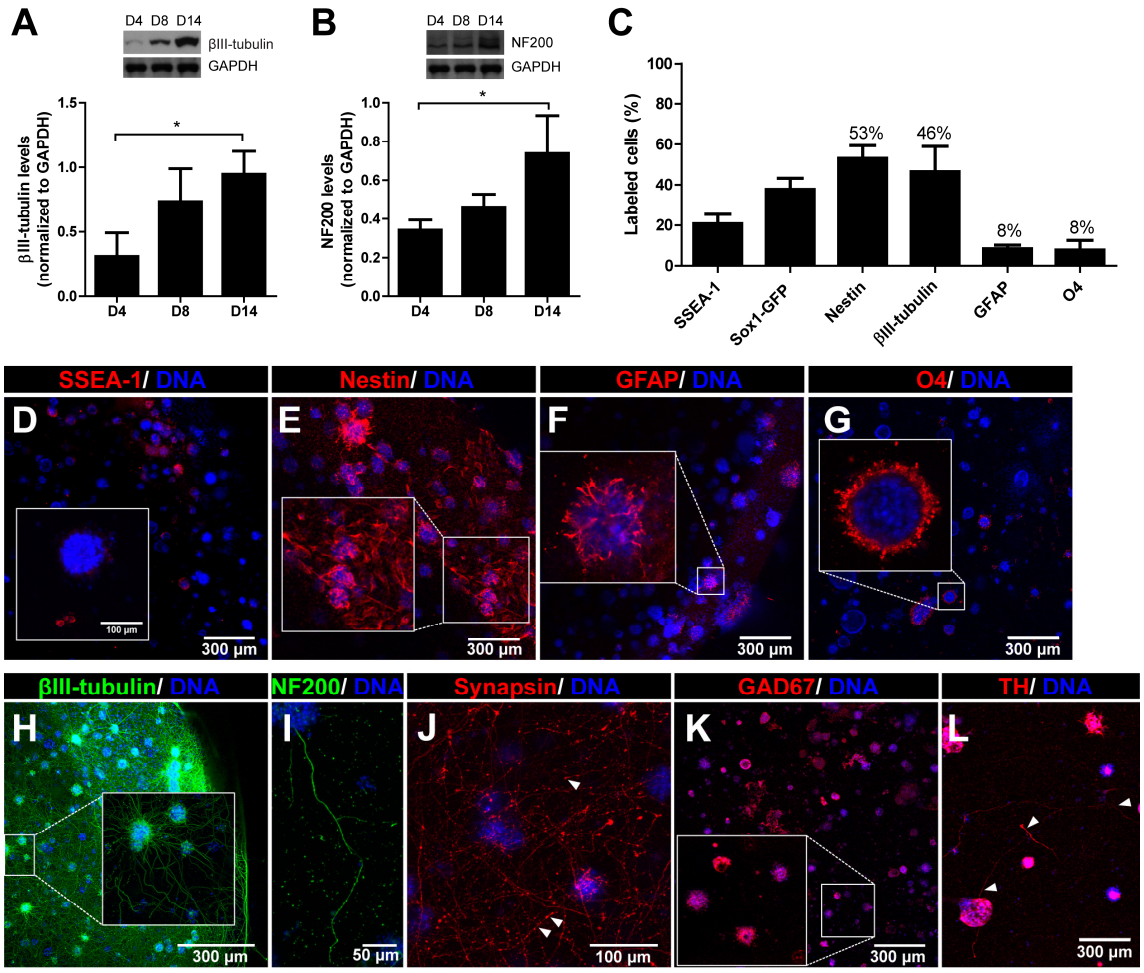

Figure 2. Phenotypic characterization of mES-NSPCs within fibrin hydrogels. Western blot analysis of **(A)** βIII-tubulin and **(B)** NF200 expression over the culture period (*n* = 3 independent experiments). **(C)** Quantitative expression of SSEA-1 (mouse embryonic stem cells), Sox1-GFP (early neuroectodermal marker), nestin (neural stem/progenitor cells), βIII-tubulin (developing and mature neurons), GFAP (astrocytes) and O4 (oligodendrocytes) at day 14 as determined by flow cytometry (*n* = 2 independent experiments). Representative 2D projections of CLSM stack images of cell/fibrin constructs at day 14 processed for immunofluorescence labeling of **(D)** SSEA-1, **(E)** nestin, **(F)** GFAP, **(G)** O4, **(H)** βIII-tubulin, **(I)** NF200 (mature neurons), **(J)** synapsin (synaptic vesicles), **(K)** GAD 67 (GABAergic phenotype) and **(L)** tyrosine hydroxylase (TH; dopaminergic and noradrenergic phenotype).

Distribution of cell-secreted ECM proteins, MMP activity and matriptase expression in 3D cultures of mES-NSPCs within fibrin gels

The distribution of cell-secreted ECM proteins was observed after 14 days of culture through immunodetection of fibronectin, laminin, and collagen IV. As fibronectin is a common contaminant in commercially available fibrinogen, acellular fibrin gels were also assessed for the presence of fibronectin, but no positive staining was detected in fibrin gels (data not shown). Cell-fibrin constructs revealed the presence of cell-secreted fibronectin fibrils following a similar deposition pattern of that described for

neurites, and often forming bundles near the cellular spheroids (Fig. 3A). This deposition pattern is in accordance with the role of fibronectin as a mediator of neuronal migration and outgrowth during development [24]. A network of laminin was also observed, mainly inside and near cellular aggregates (Fig. 3B). Collagen type IV was also detected at this time point, whether in the form of a tight network inside cell spheroids or as fibrils deposited within the fibrin gel, as depicted by arrowheads (Fig. 3C). In 2D cultures of ES-NSPCs on poly-D-lysine/laminin-coated glass coverslips carried out in parallel, the deposition of these three ECM proteins was also observed (Fig. 3D–F). The activity of MMPs was studied by performing gelatin zymography in conditioned media of ES-NSPC cultures within fibrin gel and by loading 20 μg of total conditioned media protein concentration. MMP activity was not detected in fibrin gels cultured without cells (data not shown). Zymograms showed that MMP-2 and MMP-9 were secreted by ES-NSPCs within fibrin, the latter being detected at a later period of culture (Fig. 3G). MMP-2 activity levels increased along the culture period, attaining levels significantly higher than those of day 4 of culture at day 14 (Fig. 3G). MMP-9 activity was only detected from day 8 of culture on, and no significant differences were found among the different time points analyzed (Fig. 3F). Matriptase expression of ES-NSPCs cultured within fibrin was subsequently investigated, since as ES-46C cells were reported to express this protease when cultured on a collagen-coated surface under neuronal differentiation conditions [25]. Western blot was performed for three independent experiments and matriptase levels normalized to GAPDH expression. As expected, matriptase expression was already detected in ES-NSPCs prior to embedment in fibrin (matriptase levels: 1.32, data not shown). Significant differences in matriptase expression were only found at day 14 of cell culture, for which 1.3-fold higher levels were found as compared to day 8 (Fig. 3H).

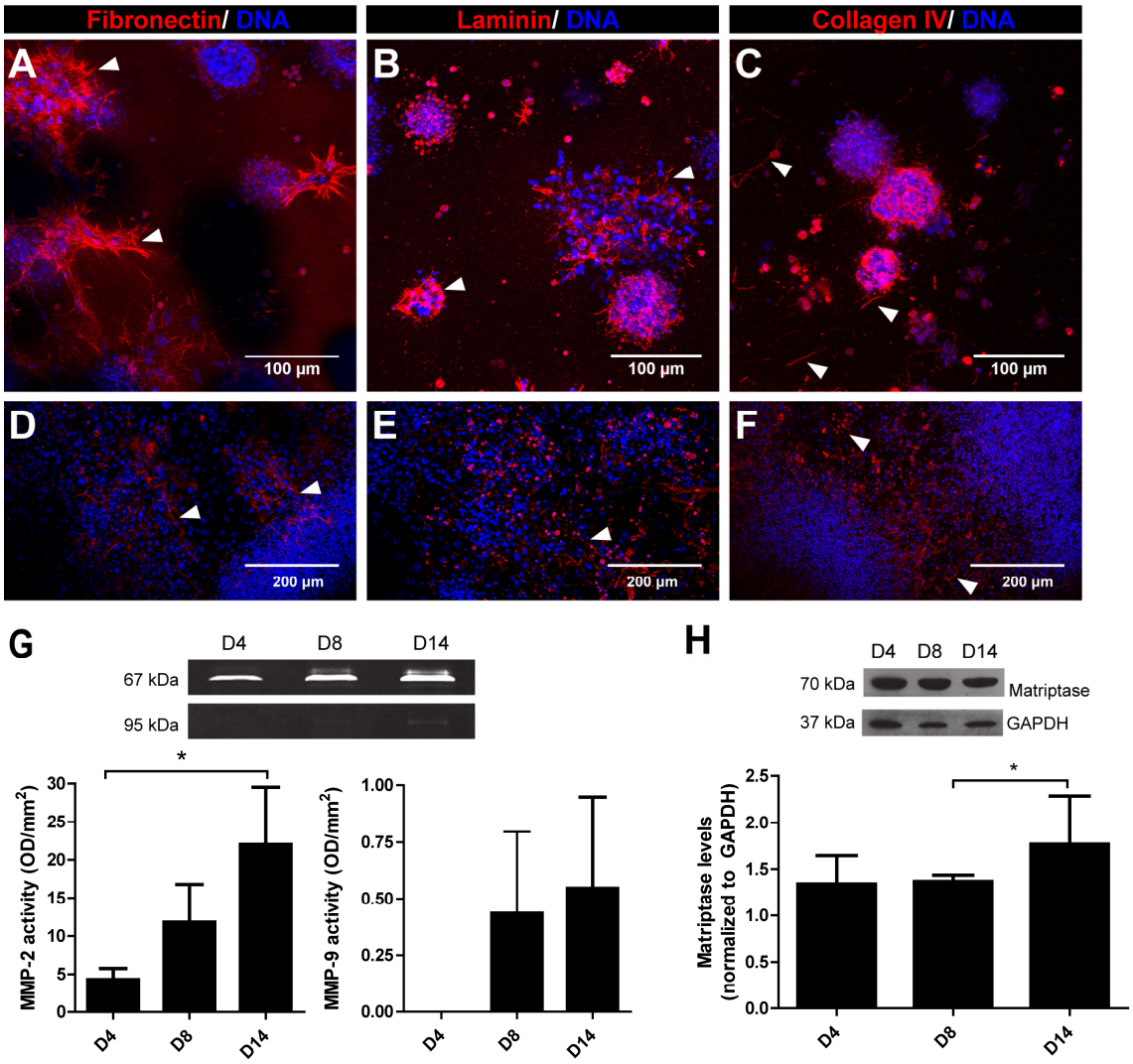

Figure 3. Characterization of mES-NSPC culture in terms of deposition of ECM proteins and proteolytic activity. Representative 2D projections of CLSM stack images of cell/fibrin constructs processed for immunofluorescence labeling of **(A)** fibronectin**, (B)** laminin and **(C)** collagen type IV, at day 14 of culture. Images **(D), (E)** and **(F)** correspond to immunofluorescent labeling of ES-NSPCs cultured on poly-D-lysine/laminin-coated glass coverslips, at the same time point. **(G)** Activity of secreted matrix metalloproteinases (MMPs) as determined by gelatin zymography (n = 3 independent experiments; * p < 0.05); ES-NSPCs embedded within fibrin secrete MMP-2 and MMP-9, MMP-9 being detected at a later stage of culture; MMP-2 activity increased at day 14 (n = 3 independent experiments; * p < 0.05). **(H)** Western blot analysis of matriptase expression over the culture period, showing that ES-NSPCs within fibrin endogenously express matriptase (n = 3 independent experiments; * p < 0.05).

Effect of fibrinogen concentration on mES-NSPC behavior within fibrin gels

To assess the effect of fibrinogen concentration on NSPC behavior within fibrin, fibrin gels were prepared with 4, 6, 8 or 10 mg/mL of fibrinogen and their structural and viscoelastic properties characterized. Fibrin gels prepared with 4 or 6 mg/mL of fibrinogen revealed a similar microstructure, while those prepared with higher

concentrations of fibrinogen (8 and 10 mg/mL) showed a denser network of fibrin fiber bundles and smaller pore size (Fig. 4A). Image analysis of 2D projected CLSM stack images further confirmed the qualitative results obtained, revealing a decrease of the average pore area with increasing fibrinogen concentration (0.71 ± 0.02, 0.65 ± 0.05, 0.53 ± 0.01 and 0.49 ± 0.02 μm^2 for fibrinogen concentrations of 4, 6, 8 and 10 mg/mL, respectively), statistically significant when comparing fibrin gels prepared with 8 or 10 mg/mL of fibrinogen with those prepared with 4 or 6 mg/mL of fibrinogen (Fig. 4B). Rheological analysis of fibrin gels consistently showed a significant increase of the storage (G') and loss modulus (G'') with increasing fibrinogen concentrations, with G' exceeding always G'' (Fig. 4C).

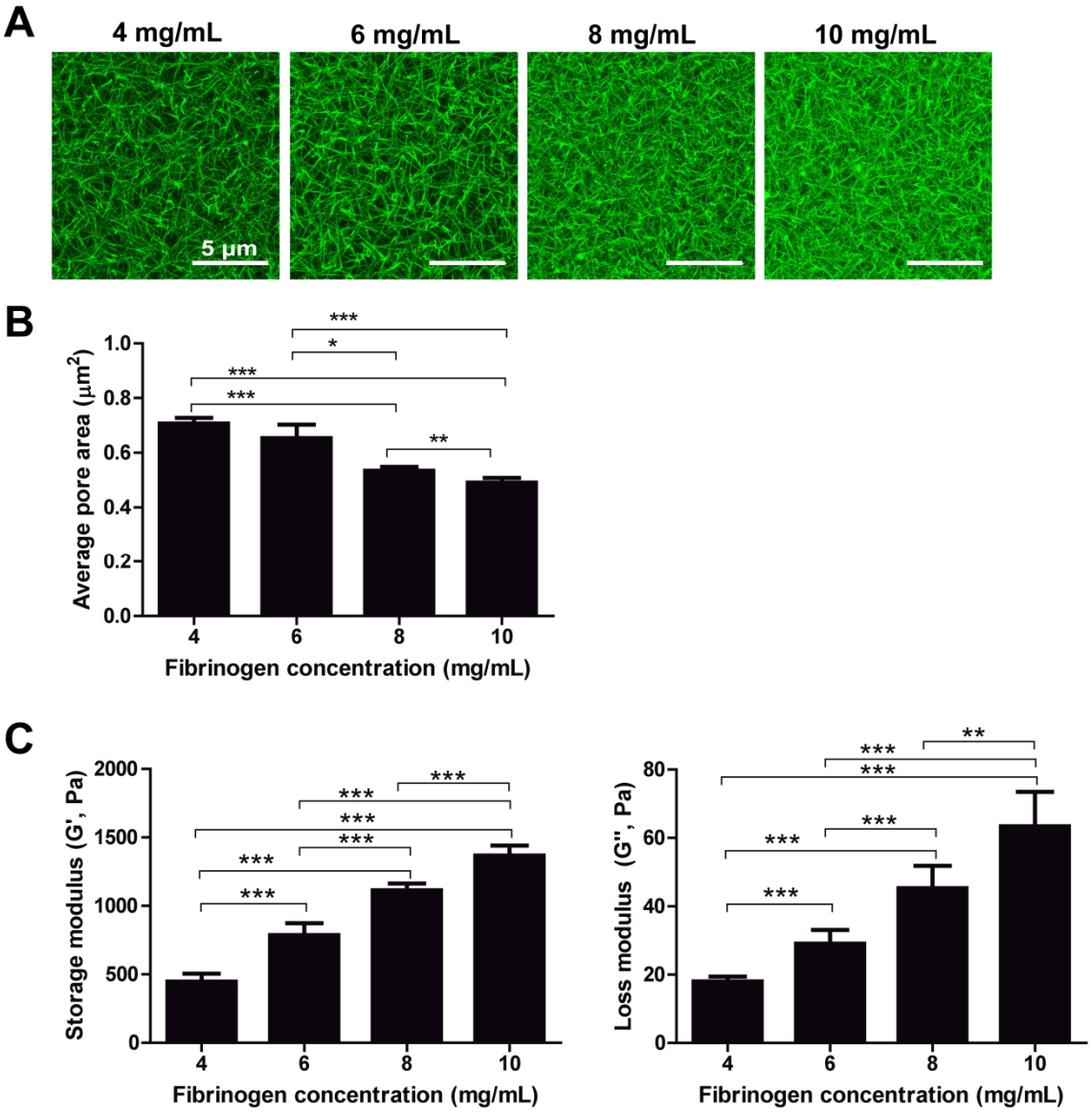

Figure 4. Effect of fibrinogen concentration on fibrin hydrogels microstructure and stiffness. (A) Microstructure of fibrin gels prepared with 4, 6, 8 or 10 mg/mL of fibrinogen spiked with Alexa Fluor® 488-labeled fibrinogen; representative 2D projections of CLSM stack images covering a depth of 10 µm are

shown. **(B)** Average pore area of fibrin hydrogels, as determined by image analysis of the 2D projected CLSM stacks (n = 4; * p < 0.05). **(C)** Storage modulus (G') and loss modulus (G'') of fibrin hydrogels, as assessed by rheological analysis (n = 6 independent experiments; * p < 0.05; ** p < 0.01; *** p < 0.005).

Neural stem/progenitor cells (ES-NSPCs) were then embedded within fibrin gels and cultured for periods up 14 days. The impact of fibrinogen concentration on neurite extension/cell outward migration was assessed at day 4 of culture. Fibrin gels prepared with 8 or 10 mg/mL of fibrinogen revealed to be less permissive to neurite extension/cell outward migration as compared to gels prepared with 4 and 6 mg/mL of fibrinogen, as shown by the significant decrease in the number of protruding cellular processes (sprouts) as well as in the maximal outgrowth from cellular spheroids found after image analysis (Fig. 5A). The effect of fibrinogen concentration on neuronal differentiation was investigated at day 14 of culture. As compared to fibrin gels with 4 or 6 mg/mL of fibrinogen, fibrin gels prepared with 8 or 10 mg/mL showed a less dense network of cellular processes labeled for βIII-tubulin, as shown by CLSM (Fig. 5B). After cell isolation from the constructs, flow cytometry analysis also revealed a lower percentage of βIII-tubulin immunoreactive cells within fibrin gels prepared with 8 or 10 mg/mL of fibrinogen, percentages significantly different from those found in fibrin gels prepared with 4 or 6 mg/mL of fibrinogen being achieved in fibrin gels with 10 mg/mL of fibrinogen (Fig. 5C). The analysis of the mean fluorescence intensity ratio of the histograms (mean fluorescence intensity of cells stained for βIII-tubulin normalized to that of cells incubated only with secondary antibody), also suggests lower expression of βIII-tubulin at the single level in fibrin gels prepared with 8 and 10 mg/mL of fibrinogen (Fig. 5D), further supporting immunocytochemistry data. In spite of hampering neuronal differentiation of ES-NSPCs within fibrin, fibrinogen concentration did not affect cell viability, regardless the fibrinogen concentration considered, as shown by trypan blue dye exclusion assay, performed at day 14 of culture (Fig. 5E). When analyzing the size of cellular spheroids present in cell-fibrin constructs at this same time point, large diameter-sized spheroids (diameter ≥ 125 μm) were found within fibrin gels prepared with 8 or 10 mg/mL of fibrinogen (Fig. S4A). These findings suggest that fibrin gels with fibrinogen concentrations ≥ 8 mg/mL possibly constitute less permissive microenvironments for neurite extension and cell migration, in line with the inhibitory effect on cell outward migration observed for fibrinogen concentrations of 8 and 10 mg/mL, at day 4 of culture (Fig. 5A). To assess the effect of fibrinogen concentration on cell proliferation, total cell number and the percentage of proliferative cells were determined at day 14 of culture, counting the average number of viable cells/fibrin drop and determining the fraction of cells incorporating 5-bromo-2'-deoxyuridine (BrdU), respectively. Results obtained showed no significant effect on

either the total cell number or the percentage of proliferative cells at this time point, when varying the fibrinogen concentration (Fig. S4B–C). Finally, the effect of fibrinogen concentration on MMP activity present in conditioned media of ES-NSPCs cultured for 14 days within fibrin was also investigated. Apart from an increase in MMP-2 activity levels found when increasing the fibrinogen concentration from 8 to 10 mg/mL, no significant differences were found among MMP-9 activity levels when varying the fibrinogen concentration (Fig. S4D).

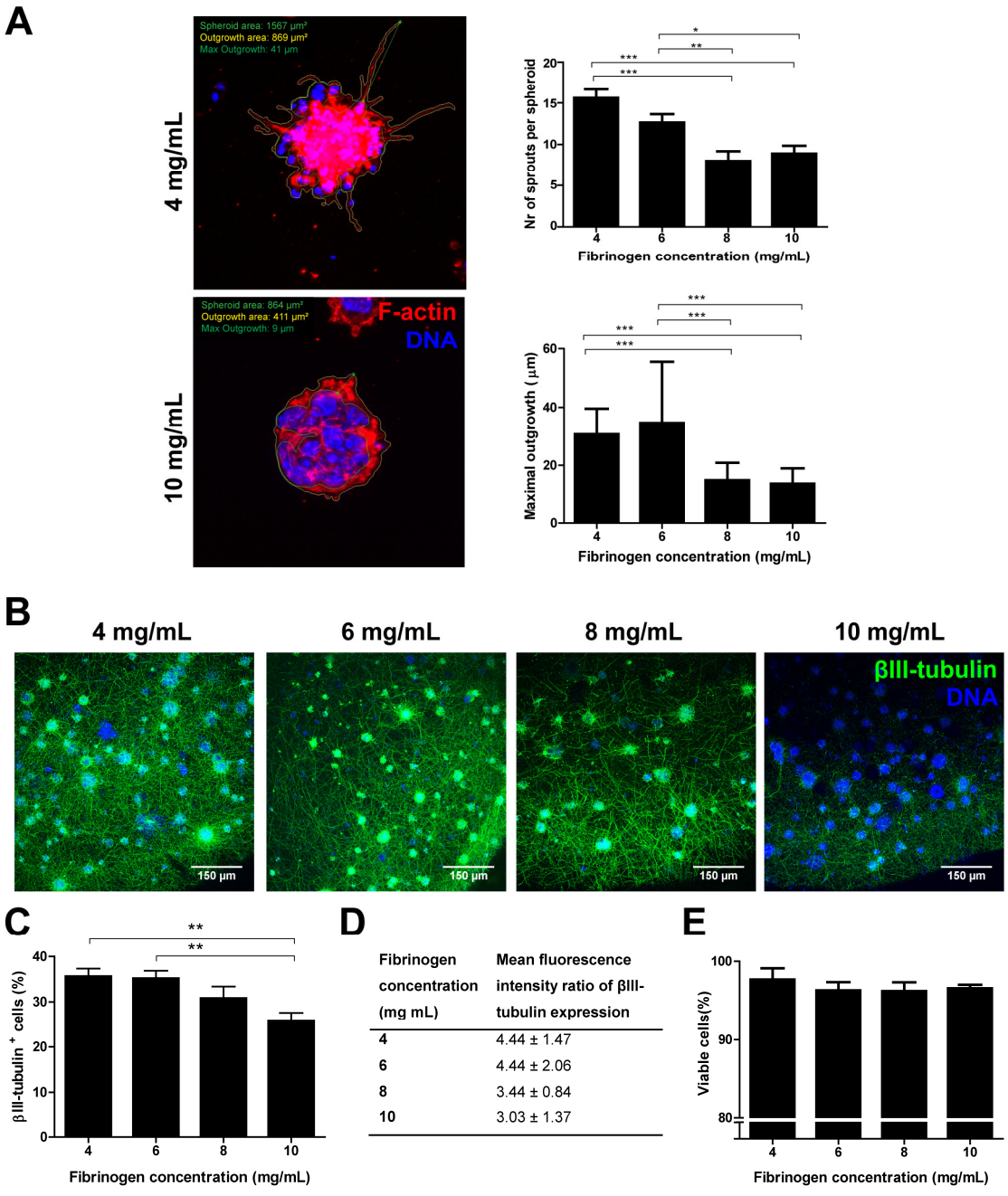

Figure 5. Effect of fibrinogen concentration on mES-NSPC outward migration, viability and neuronal differentiation within fibrin hydrogels. (A) Representative 2D projections of CLSM stack images of cell/fibrin constructs processed for F-actin/DNA staining at day 4 of culture; images

correspondent to fibrin hydrogels prepared with 4 or 10 mg/mL of fibrinogen are shown; neurite extension/outward migration from cellular spheroids was quantified by image analysis; bar graphs depict the number of sprouts (above) and the maximal outgrowth (below) per spheroid (n = 10 spheroids from 2 replicate cultures; * $p < 0.05$; ** $p < 0.01$; *** $p < 0.005$). **(B)** Neuronal network formed within fibrin hydrogels at day 14 of culture, as assessed by immunofluorescence labeling of βIII-tubulin; representative 2D projections of CLSM stack images of cell/fibrin constructs covering a depth of 100 μm are shown. **(C–D)** Flow cytometry analysis of βIII-tubulin expression at day 14 of culture. **(C)** Percentage of positive cells, showing a decrease in the percentage of βIII-tubulin$^+$ cells when increasing the fibrinogen concentration from 4 or 6 to 10 mg/mL (n = 4–6 independent experiments; ** $p < 0.01$); **(D)** the analysis of the mean fluorescence intensity ratio of the histograms also suggest a lower expression of βIII-tubulin in these fibrin gels. **(E)** Percentage of viable cells at day 14 of culture using Trypan Blue dye exclusion method (n = 4–6 independent experiments).

Culture of hES-NSCs within fibrin gels

We further investigated if this 3D culture model could support the neuronal differentiation of single hES-NSCs. Confocal analysis of cell-matrix constructs incubated with calcein AM/PI after 14 days of cell culture, showed the presence of live cells widely distributed throughout the fibrin gel growing as cellular spheroids, similarly to mouse ES-NSPCs in fibrin (Fig. 6A). At the same time point, the quantitative analysis of live/dead cells isolated from fibrin gels revealed a high percentage of viable cells (98.4%) and an average of 6.7% PI$^+$ cells (dead cells; Fig. 6B). Immunocytochemistry analysis showed the presence nestin$^+$ cells (Fig. 6C), as well as a population of differentiated neurons expressing βIII-tubulin and forming neurites radially extending from cellular spheroids (Fig. 6D). Synaptic proteins (synapsin) with a distribution pattern resembling that of neurites were also observed (Fig. 6E). Similarly to mES-NSPCs, hES-NSCs were found to deposit laminin and fibronectin (Fig. 6F–G). Fibronectin deposition was found to be closely associated with neurites expressing βIII-tubulin, as shown by double immunocytochemistry performed at day 21 (Fig. 6H).

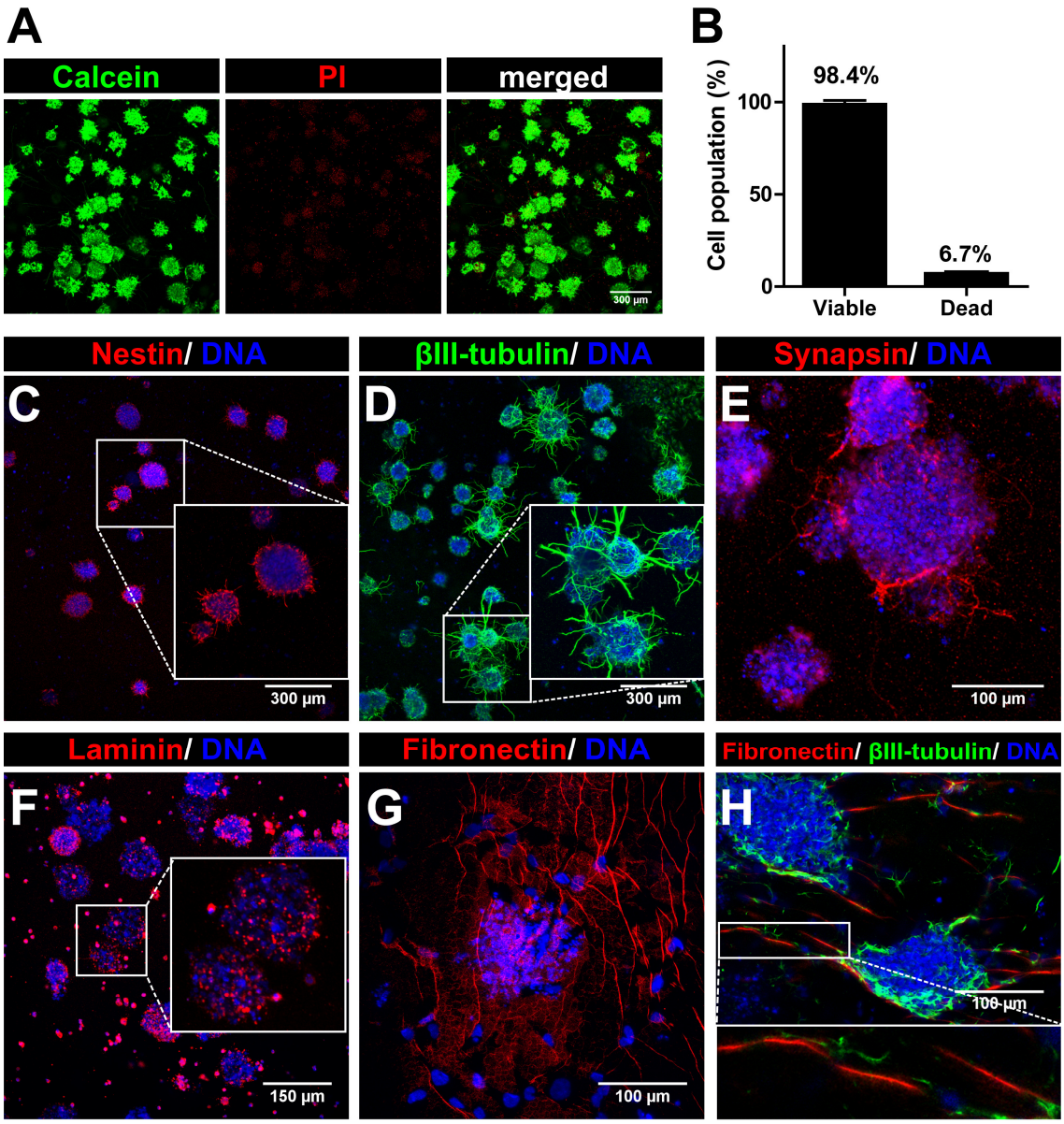

Figure 6. Cell viability, phenotype and ECM deposition of human ES-NSCs cultured within fibrin hydrogels. (A) Distribution of live and/or dead cells at day 14 of cell culture; cell-fibrin constructs were incubated with calcein AM and PI for detection of live and dead cells, respectively, and imaged by CLSM; representative 2D projections of CLSM stack images covering a depth of 150 µm are shown. **(B)** Quantitative analysis of live and dead cells at day 14, as determined by flow cytometry (*n* = 3 independent experiments). Representative 2D projections of CLSM stack images of cell/fibrin constructs processed for immunofluorescence labeling of **(C)** nestin, **(D)** βIII-tubulin, **(E)** synapsin (synaptic vesicles), **(F)** laminin, **(G)** fibronectin, and **(H)** fibronectin and βIII-tubulin; low panel shows a single confocal image (0.17 µm in depth) evidencing close association of fibronectin fibrils with neurites; images (C–G) correspond to day 14 of cell culture and image (H) to day 21.

Discussion

In this study, we established the 3D culture of neural stem/progenitor cells (NSPCs) derived from mouse embryonic stem cells under adherent monoculture, in fibrin hydrogels. Embryonic stem-derived NSPCs (ES-NSPCs) were seeded within fibrin in the form of single cells, and cultured under neuronal differentiation conditions. Cell viability, morphology, proliferation, phenotype, distribution of cell-secreted extracellular matrix (ECM) proteins, and proteolytic activity were subsequently characterized. Furthermore, we investigated the behavior of ES-NSPCs within fibrin in response to fibrinogen concentration.

The cell seeding density leading to the highest retention of cell viability in a fibrin gel with fixed composition (fibrinogen concentration in the polymerizing gel: 6 mg/mL) was initially established. When seeded at 1×10^6 cells/mL, ES-NSPCs were able to retain in average more than 85% of cell viability throughout the culture period and to proliferate, as shown by the 9-fold increase in total cell number observed at day 14 of culture (Fig. 1A–C). The high levels of cell viability observed may be associated with the presence of basic fibroblast growth factor (bFGF) during the first two days of culture, due to its mitogenic effect on $Sox1^+$ cells [7], as well as to the presence of brain-derived neurotrophic factor (BDNF) and nerve growth factor (NGF) during the last period of culture, two neurotrophins important for neuronal survival [26, 27] which, apart from being constitutively-secreted by NSPCs [28], were added to the media. Moreover, fibrin ability to sequester bFGF and BDNF through its heparin-binding domain [29] possibly contributed to their retention within fibrin and to prolong their bioavailability to cells. The addition of aprotinin to cell culture media, a serine protease inhibitor herein used to delay fibrin degradation, may have also contributed to cell viability, as aprotinin was shown to exert neuroprotective effects *in vitro* [30] and to increase cell viability of dissociated embryoid body-containing neural progenitors in fibrin [15]. ES-NSPCs entrapped within fibrin as single cells rapidly divided forming spherical-shaped clone-like multi-cellular clusters. The formation of large-sized cellular spheroids (diameter higher than 300 μm) is often a concern, since this can compromise the delivery of oxygen/nutrients/growth factors to the inner part of the spheroids, and ultimately lead to the formation of necrotic cores [31]. However, ES-NSPCs seeded at 1×10^6 cells/mL resulted in the formation of small-sized spheroids with diameters below values that could compromise cell viability in the core of the spheroids (Fig. 1D). Fibrin was able to sustain a pool of NSPCs, as shown by the high percentage of total cell population expressing the neural stem cell (NSC) marker Sox1-GFP and the NSPC marker nestin

at the end of culture, regardless of bFGF withdrawal from the cell culture medium at day 2 of culture (Fig. 2C and E). This is an important feature, as hydrogels for delivery of ES-NSPCs should provide an adequate microenvironment for the maintenance of a pool of NSPCs following transplantation, not only due to their potential to differentiate into mature neural cells but also because functional recovery is thought to be mainly mediated by neurotrophic factors secreted by NSPCs [7, 28]. Single ES-NSPCs seeded within fibrin gels efficiently generated neurons, giving rise to a dense neuronal network (46% of βIII-tubulin$^+$ cells; Fig. 2) and, to a lesser extent, to astrocytes and oligodendrocytes. The capacity of maturation of these neuronal cells was shown by the increase in NF200 expression (Fig. 2B), and detection of GABAergic (GAD67$^+$ cells) and dopaminergic/noradrenergic neurons (TH$^+$ cells), as well as by the presence of a network of synaptic vesicles and dendritic spines (Fig. 2J–L). Fibrin ability to support ES-NSPC differentiation into such neuronal populations, namely into GABAergic neurons, is most valuable, since several therapeutical strategies could profit in the transplantation of cells allowing a long-term supply of γ-aminobutyric acid (GABA) [32]. When differentiated on gelatin-coated surfaces, ES-NSPCs were found to express markers for glutamatergic, serotonergic and motor neuronal subtypes, besides GABAergic and dopaminergic markers [6]. Still, the ability of fibrin to sustain ES-NSPC differentiation into glutamatergic, serotonergic and motor neurons remains an issue to be addressed.

As fibrin acts as a provisional ECM that can be remodeled by invasive cells through cell-secreted proteases and cell-secreted ECM proteins, we further analyzed the ECM proteins distribution and the proteolytic activity in cell/fibrin constructs. Laminin and fibronectin expression by NSPCs was initially detected in floating aggregates of NSPCs (neurospheres) [33], and, more recently, collagen IV and vitronectin were also shown to be present in EB-containing neural progenitors [34]. We found that when cultured within fibrin, ES-NSPCs secrete endogenous ECM proteins, namely laminin, fibronectin and collagen type IV, contributing to fibrin remodeling (Fig. 3A–C). Comparing to laminin or collagen IV, fibronectin showed a wider distribution inside cell/fibrin constructs, which can be related to fibrin ability to sequester fibronectin through its fibronectin high affinity binding domains [35]. Matrix metalloproteinases (MMPs) are key players in ECM remodeling due to their ability to cleave ECM components such as collagen, laminin, and fibronectin [36], as well as to degrade fibrinogen and fibrin via proteolysis [37]. Increasing evidence is supporting MMP involvement in neurogenesis, neurite elongation and axonal growth, as well as in synaptogenesis along homeostasis and pathologic events [36, 38]. Interestingly, we observe that ES-NSPCs within fibrin

secrete MMPs (Fig. 3G) which, by locally contributing to ECM and fibrin degradation, possibly facilitated neurite extension and cell migration, leading to fibrin remodeling and to the formation of a more mature engineered tissue. In line with this hypothesis, Man *et al*. showed that neurite extension from dorsal root ganglia explants entrapped in fibrin is dependent on fibrinolysis and on MMPs and serine proteases secretion [39]. Interestingly, we found an increase of MMP-2 activity along the culture period, suggesting that this protease may play an important role in mediating ES-NSPC neurite extension and cell infiltration within fibrin. We detected MMP-9 activity at a later stage of ES-NSPC culture within fibrin, in accordance to the progress of neuronal differentiation and maturation observed [40]. The expression of matriptase, a type II transmembrane serine protease that acts upstream of MMP-2, which promotes ES-NSPC migration and neuronal differentiation [25], was also assessed. ES-NSPCs within fibrin retained the ability to express matriptase, showing an increase in matriptase expression during the second week of cell culture (Fig. 2H), in accordance to its role in neuronal differentiation. In this study we did not assess the expression of plasmin, one of the major fibrinolytic serine proteases, since ES-NSPCs were cultured within fibrin in the presence of aprotinin.

As the structural and viscoelastic properties of hydrogels affect stem cell behaviour and fate [39, 41], we assessed the effect of fibrinogen concentration on NSPC behaviour. In accordance to the literature, changes in fibrinogen concentration are expected to affect fibrin structural and viscoelastic properties at a greater degree, when compared to other fibrin components, such as thrombin and calcium [35]. Increasing the fibrinogen concentration resulted in increased fibrin stiffness and in a denser fibrin network with the presence of smaller pores (Fig. 4), in accordance to literature [35]. Still, significantly changes in average pore diameter were only observed when increasing fibrinogen concentration to 8 or 10 mg/mL. In this work, ES-NSPCs within fibrin were found to sense the changes in fibrin viscoelastic and structural properties, as shown by the decrease in both neurite extension/cell outgrowth migration and neuronal differentiation in fibrin gels with small-sized pores and stiffer matrices (Fig. 5A–C), correspondent to 8 or 10 mg/mL of fibrinogen. To sustain neuronal differentiation, neurite outgrowth, and cell infiltration, fibrin gel mechanical properties should ideally match those of native neural tissues while fibrin structural and biological properties should assure support to cells and provide an adequate density of bioactive domains for integrin/growth factor/ECM binding [39] The fibrinogen concentrations that induced a better performance of ES-NSPCs within fibrin (in terms of neurite extension, neuronal differentiation, and formation of smaller-size spheroids) were those of 4 and 6 mg/mL,

which resulted in fibrin gels with storage modulus comparable to that of neural tissue in the adult brain (400 to 1000 Pa) [42]. Our findings are in agreement with previous published studies reporting for adult NSCs cultured in alginate gels a decrease in βIII-tubulin expression levels when increasing the elastic modulus of these gels [41]. In contrast, we did not observe a decrease in cell proliferation when increasing the elastic modulus of fibrin hydrogels (Fig. S4C). This result may be related to the lower percentage of BrdU-incorporating cells found at this time point (< 5%), which may be too low to allow the detection of significant differences amongst the tested fibrinogen concentrations. Nevertheless, when considering an *in vivo* scenario, fibrin gels produced with fibrinogen concentrations of 8 and 10 mg/mL can also be of interest to reduce the polymerization time and the degradation rate [10, 35], as *in vitro* these fibrin hydrogels also supported neuronal differentiation.

Finally, we assessed if this 3D culture model could support human ES-NSC viability, neuronal differentiation and ECM remodeling. Although the culture of human fetal/adult NSPCs within hydrogels has been extensively explored (either seeded as single cells or as cellular aggregates), only a few studies report the 3D culture of dissociated NSPCs derived from human pluripotent stem cells within hydrogels [43, 44]. Similarly to mES-NSPCs, hES-NSCs within fibrin were found to retain cell viability and sustain a pool of NSPCs, while expressing neuronal and synaptic proteins. These results are in well agreement with the studies of Alessandri and colleagues [43], in which NSPCs derived from human induced pluripotent stem cells encapsulated as single cells within Matrigel® revealed high retention of cell viability (97.8% of viable cells), with expression of NSPC and neuronal markers. Additionally, our study evidenced that hES-NSCs cultured within a 3D fibrin hydrogel were able to remodel fibrin through cell-secreted fibronectin and laminin, two ECM proteins present in the embryonic neural stem cell niche [45].

Conclusions

In this work, we showed that mouse ES-NSPCs obtained in adherent monoculture, when seeded within a fibrin hydrogel as dissociated cells remain viable, while retaining the ability to proliferate, differentiate into mature neurons and establish neuronal networks. In this 3D system, ES-NSPCs were also able to secrete ECM proteins and MMPs, therefore contributing to fibrin remodeling and to the formation of a more mature engineered neural tissue. ES-NSPCs were found to respond to changes in fibrin viscoelastic and structural properties, neurite extension/cell outgrowth migration

and neuronal differentiation being hindered in fibrin gels with stiffer matrices and small-sized pores, herein correspondent to gels prepared with 8 or 10 mg/mL of fibrinogen. This 3D culture model was also shown to support cell viability, neuronal differentiation, expression of synaptic proteins and ECM deposition of human ES-derived neural stem cells seeded as single cells within fibrin. The settled 3D platform is expected to constitute a valuable tool for the development of fibrin-based hydrogels specifically designed for ES-NSPC delivery into the injured central nervous system. Moreover, it can be of interest for pharmacological screening and to unravel molecular mechanisms implicated in neurogenesis in an *in vitro* 3D microenvironment, which better mimics the *in vivo*.

Acknowledgements

The authors would like to acknowledge Prof. Domingos Henrique (Instituto de Medicina Molecular, Lisbon) for providing the ES 46C cell line. This work was supported by FEDER funds through the Programa Operacional Factores de Competitividade – COMPETE (FCOMP-01-0124-FEDER-021125) and by National funds FCT – Fundação para a Ciência e a Tecnologia (PTDC/SAU-BMA/118869/2010). A.R. Bento and M.J. Oliveira are supported by FCT (SFRH/BD/86200/2012; Investigator FCT).

References

[1] H. Okano, Neural stem cells and strategies for the regeneration of the central nervous system, P Jpn Acad B-Phys 86(4) (2010) 438-450.

[2] O. Lindvall, Z. Kokaia, Stem cells in human neurodegenerative disorders--time for clinical translation?, The Journal of clinical investigation 120(1) (2010) 29-40.

[3] P. Lu, Y. Wang, L. Graham, K. McHale, M. Gao, D. Wu, J. Brock, A. Blesch, E.S. Rosenzweig, L.A. Havton, B. Zheng, J.M. Conner, M. Marsala, M.H. Tuszynski, Long-distance growth and connectivity of neural stem cells after severe spinal cord injury, Cell 150(6) (2012) 1264-73.

[4] J.W. McDonald, D. Becker, T.F. Holekamp, M. Howard, S. Liu, A. Lu, J. Lu, M.M. Platik, Y. Qu, T. Stewart, S. Vadivelu, Repair of the injured spinal cord and the potential of embryonic stem cell transplantation, Journal of neurotrauma 21(4) (2004) 383-93.

[5] E. Colombo, S.G. Giannelli, R. Galli, E. Tagliafico, C. Foroni, E. Tenedini, S. Ferrari, S. Ferrari, G. Corte, A. Vescovi, G. Cossu, V. Broccoli, Embryonic stem-derived versus somatic neural stem cells: a comparative analysis of their developmental potential and molecular phenotype, Stem cells (Dayton, Ohio) 24(4) (2006) 825-34.

[6] T. Incitti, A. Messina, Y. Bozzi, S. Casarosa, Sorting of Sox1-GFP Mouse Embryonic Stem Cells Enhances Neuronal Identity Acquisition upon Factor-Free Monolayer Differentiation, BioResearch open access 3(3) (2014) 127-35.
[7] Q.L. Ying, M. Stavridis, D. Griffiths, M. Li, A. Smith, Conversion of embryonic stem cells into neuroectodermal precursors in adherent monoculture, Nature biotechnology 21(2) (2003) 183-6.
[8] S. Erceg, M. Ronaghi, M. Oria, M.G. Rosello, M.A. Arago, M.G. Lopez, I. Radojevic, V. Moreno-Manzano, F.J. Rodriguez-Jimenez, S.S. Bhattacharya, J. Cordoba, M. Stojkovic, Transplanted oligodendrocytes and motoneuron progenitors generated from human embryonic stem cells promote locomotor recovery after spinal cord transection, Stem cells (Dayton, Ohio) 28(9) (2010) 1541-9.
[9] A.P. Pêgo, S. Kubinova, D. Cizkova, I. Vanicky, F.M. Mar, M.M. Sousa, E. Sykova, Regenerative medicine for the treatment of spinal cord injury: more than just promises?, J Cell Mol Med 16(11) (2012) 2564-82.
[10] E.R. Aurand, K.J. Lampe, K.B. Bjugstad, Defining and designing polymers and hydrogels for neural tissue engineering, Neuroscience research 72(3) (2012) 199-213.
[11] A.H. Petter-Puchner, W. Froetscher, R. Krametter-Froetscher, D. Lorinson, H. Redl, M. van Griensven, The long-term neurocompatibility of human fibrin sealant and equine collagen as biomatrices in experimental spinal cord injury, Exp Toxicol Pathol 58(4) (2007) 237-245.
[12] I.F. Amaral, A.R. Ferreira, D. Veiga, F. Mar, D. Rocha, E. Abranches, E. Bekman, M. Sousa, D. Henrique, A.P. Pêgo, Evaluation of a fibrin gel for transplantation of embryonic stem-derived neuroprogenitors into the injured spinal cord., Histology and Histopathology - Cellular and Molecular Biology 26 (supplement 1) (2011) 291-292.
[13] P.A. Janmey, J.P. Winer, J.W. Weisel, Fibrin gels and their clinical and bioengineering applications, J R Soc Interface 6(30) (2009) 1-10.
[14] Q.L. Ying, A.G. Smith, Defined conditions for neural commitment and differentiation, Methods in enzymology 365 (2003) 327-41.
[15] S.M. Willerth, K.J. Arendas, D.I. Gottlieb, S.E. Sakiyama-Elbert, Optimization of fibrin scaffolds for differentiation of murine embryonic stem cells into neural lineage cells, Biomaterials 27(36) (2006) 5990-6003.
[16] J.L. Wilson, S. Suri, A. Singh, C.A. Rivet, H. Lu, T.C. McDevitt, Single-cell analysis of embryoid body heterogeneity using microfluidic trapping array, Biomedical microdevices 16(1) (2014) 79-90.
[17] S.K. Dhara, S.L. Stice, Neural differentiation of human embryonic stem cells, Journal of cellular biochemistry 105(3) (2008) 633-40.

[18] S.M. Chambers, C.A. Fasano, E.P. Papapetrou, M. Tomishima, M. Sadelain, L. Studer, Highly efficient neural conversion of human ES and iPS cells by dual inhibition of SMAD signaling, Nature biotechnology 27(3) (2009) 275-80.

[19] J. Aubert, M.P. Stavridis, S. Tweedie, M. O'Reilly, K. Vierlinger, M. Li, P. Ghazal, T. Pratt, J.O. Mason, D. Roy, A. Smith, Screening for mammalian neural genes via fluorescence-activated cell sorter purification of neural precursors from Sox1-gfp knock-in mice, Proceedings of the National Academy of Sciences of the United States of America 100 (2003) 11836-11841.

[20] J.C. Schense, J.A. Hubbell, Cross-linking exogenous bifunctional peptides into fibrin gels with factor XIIIa, Bioconjugate chemistry 10(1) (1999) 75-81.

[21] L. Conti, S.M. Pollard, T. Gorba, E. Reitano, M. Toselli, G. Biella, Y. Sun, S. Sanzone, Q.L. Ying, E. Cattaneo, A. Smith, Niche-independent symmetrical self-renewal of a mammalian tissue stem cell, PLoS biology 3(9) (2005) e283.

[22] H. Mori, K. Ninomiya, M. Kino-oka, T. Shofuda, M.O. Islam, M. Yamasaki, H. Kano, M. Taya, Y. Kanemura, Effect of neurosphere size on the growth rate of human neural stem/progenitor cells, Journal of neuroscience research 84(8) (2006) 1682-1691.

[23] S. Bessa, P. Quelhas, I. Amaral, Automatic Quantification of Cell Outgrowth from Neurospheres, in: J. Sanches, L. Micó, J. Cardoso (Eds.), Pattern Recognition and Image Analysis, Springer Berlin Heidelberg 2013, pp. 141-148.

[24] A.M. Sheppard, S.K. Hamilton, A.L. Pearlman, Changes in the distribution of extracellular matrix components accompany early morphogenetic events of mammalian cortical development, The Journal of neuroscience : the official journal of the Society for Neuroscience 11(12) (1991) 3928-42.

[25] J.D. Fang, H.C. Chou, H.H. Tung, P.Y. Huang, S.L. Lee, Endogenous Expression of Matriptase in Neural Progenitor Cells Promotes Cell Migration and Neuron Differentiation, Journal of Biological Chemistry 286(7) (2011) 5667-5679.

[26] A.K. Shetty, D.A. Turner, In vitro survival and differentiation of neurons derived from epidermal growth factor-responsive postnatal hippocampal stem cells: inducing effects of brain-derived neurotrophic factor, Journal of neurobiology 35(4) (1998) 395-425.

[27] R. Levi-Montalcini, P.U. Angeletti, Essential role of the nerve growth factor in the survival and maintenance of dissociated sensory and sympathetic embryonic nerve cells in vitro, Developmental biology 6 (1963) 653-9.

[28] P. Lu, L.L. Jones, E.Y. Snyder, M.H. Tuszynski, Neural stem cells constitutively secrete neurotrophic factors and promote extensive host axonal growth after spinal cord injury, Experimental neurology 181(2) (2003) 115-29.

[29] M.M. Martino, P.S. Briquez, A. Ranga, M.P. Lutolf, J.A. Hubbell, Heparin-binding domain of fibrin(ogen) binds growth factors and promotes tissue repair when incorporated within a synthetic matrix, Proceedings of the National Academy of Sciences of the United States of America 110(12) (2013) 4563-8.

[30] H. Davis, C. Gascho, J.A. Kiernan, Action of aprotinin on the survival of adult cerebellar neurons in organ culture, Acta neuropathologica 32(4) (1975) 359-62.

[31] A. Sen, M.S. Kallos, L.A. Behie, Effects of hydrodynamics on cultures of mammalian neural stem cell aggregates in suspension bioreactors, Ind Eng Chem Res 40(23) (2001) 5350-5357.

[32] D.S. Kim, S.J. Jung, T.S. Nam, Y.H. Jeon, D.R. Lee, J.S. Lee, J.W. Leem, D.W. Kim, Transplantation of GABAergic neurons from ESCs attenuates tactile hypersensitivity following spinal cord injury, Stem Cells 28(11) (2010) 2099-108.

[33] L.S. Campos, Neurospheres: insights into neural stem cell biology, Journal of neuroscience research 78(6) (2004) 761-9.

[34] S. Sart, T. Ma, Y. Li, Extracellular matrices decellularized from embryonic stem cells maintained their structure and signaling specificity, Tissue engineering. Part A 20(1-2) (2014) 54-66.

[35] A.C. Brown, T.H. Barker, Fibrin-based biomaterials: modulation of macroscopic properties through rational design at the molecular level, Acta Biomater 10(4) (2014) 1502-14.

[36] G.A. Tonti, F. Mannello, E. Cacci, S. Biagioni, Neural stem cells at the crossroads: MMPs may tell the way, The International journal of developmental biology 53(1) (2009) 1-17.

[37] T.A. Ahmed, M. Griffith, M. Hincke, Characterization and inhibition of fibrin hydrogel-degrading enzymes during development of tissue engineering scaffolds, Tissue Eng 13(7) (2007) 1469-77.

[38] H. Fujioka, Y. Dairyo, K. Yasunaga, K. Emoto, Neural functions of matrix metalloproteinases: plasticity, neurogenesis, and disease, Biochemistry research international 2012 (2012) 789083.

[39] A.J. Man, H.E. Davis, A. Itoh, J.K. Leach, P. Bannerman, Neurite outgrowth in fibrin gels is regulated by substrate stiffness, Tissue engineering. Part A 17(23-24) (2011) 2931-42.

[40] B.Z. Barkho, A.E. Munoz, X.K. Li, L. Li, L.A. Cunningham, X.Y. Zhao, Endogenous Matrix Metalloproteinase (MMP)-3 and MMP-9 Promote the Differentiation and Migration of Adult Neural Progenitor Cells in Response to Chemokines, Stem Cells 26(12) (2008) 3139-3149.

[41] A. Banerjee, M. Arha, S. Choudhary, R.S. Ashton, S.R. Bhatia, D.V. Schaffer, R.S. Kane, The influence of hydrogel modulus on the proliferation and differentiation of encapsulated neural stem cells, Biomaterials 30(27) (2009) 4695-9.
[42] B.S. Elkin, A.I. Ilankovan, B. Morrison, 3rd, A detailed viscoelastic characterization of the P17 and adult rat brain, Journal of neurotrauma 28(11) (2011) 2235-44.
[43] K. Alessandri, M. Feyeux, B. Gurchenkov, C. Delgado, A. Trushko, K.H. Krause, D. Vignjevic, P. Nassoy, A. Roux, A 3D printed microfluidic device for production of functionalized hydrogel microcapsules for culture and differentiation of human Neuronal Stem Cells (hNSC), Lab on a chip 16(9) (2016) 1593-604.
[44] W. Sun, T. Incitti, C. Migliaresi, A. Quattrone, S. Casarosa, A. Motta, Viability and neuronal differentiation of neural stem cells encapsulated in silk fibroin hydrogel functionalized with an IKVAV peptide, Journal of tissue engineering and regenerative medicine doi: 10.1002/term.2053 (2015).
[45] V. Solozobova, N. Wyvekens, J. Pruszak, Lessons from the Embryonic Neural Stem Cell Niche for Neural Lineage Differentiation of Pluripotent Stem Cells, Stem cell reviews 8(3) (2012) 813-829.

Supplementary Data

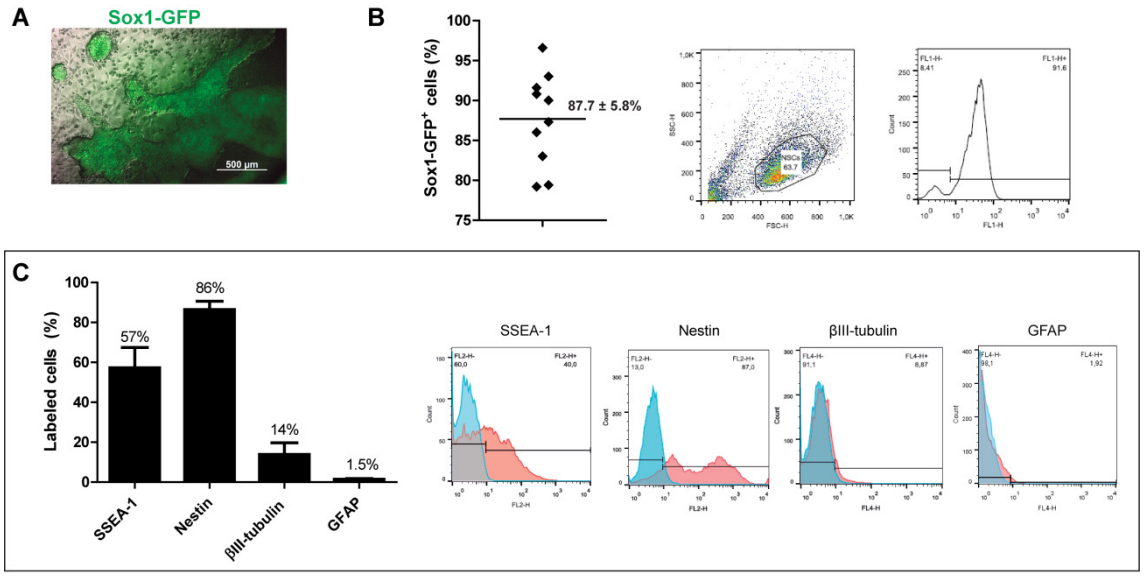

Figure S1. Phenotypic characterization of mES-NSPCs at day 5 of monolayer neural commitment. **(A)** Representative fluorescence image of the monolayer culture showing cells expressing Sox1-GFP (early neuroectodermal marker) after neural phenotypic induction. **(B)** Percentages of Sox1-GFP$^+$ cells attained in the different neural commitments performed as assessed by flow cytometry; live cells were gated using forward scatter (FSC, reflecting size) and side scatter (SSC, reflecting complexity) criteria, and fluorescence gates set using undifferentiated 46C ES cells; a representative dot plot and fluorescence intensity histogram is shown. **(C)** Immunocytometric analysis of SSEA-1 (mouse embryonic stem cells), nestin (neural stem/progenitor cells), βIII-tubulin (developing and mature neurons) and GFAP (astrocytes) expression (n = 3 independent experiments); fluorescence intensity histograms from a representative experiment are shown; the blue histogram represents the fluorescence of cells incubated only with the isotype-specific secondary antibody.

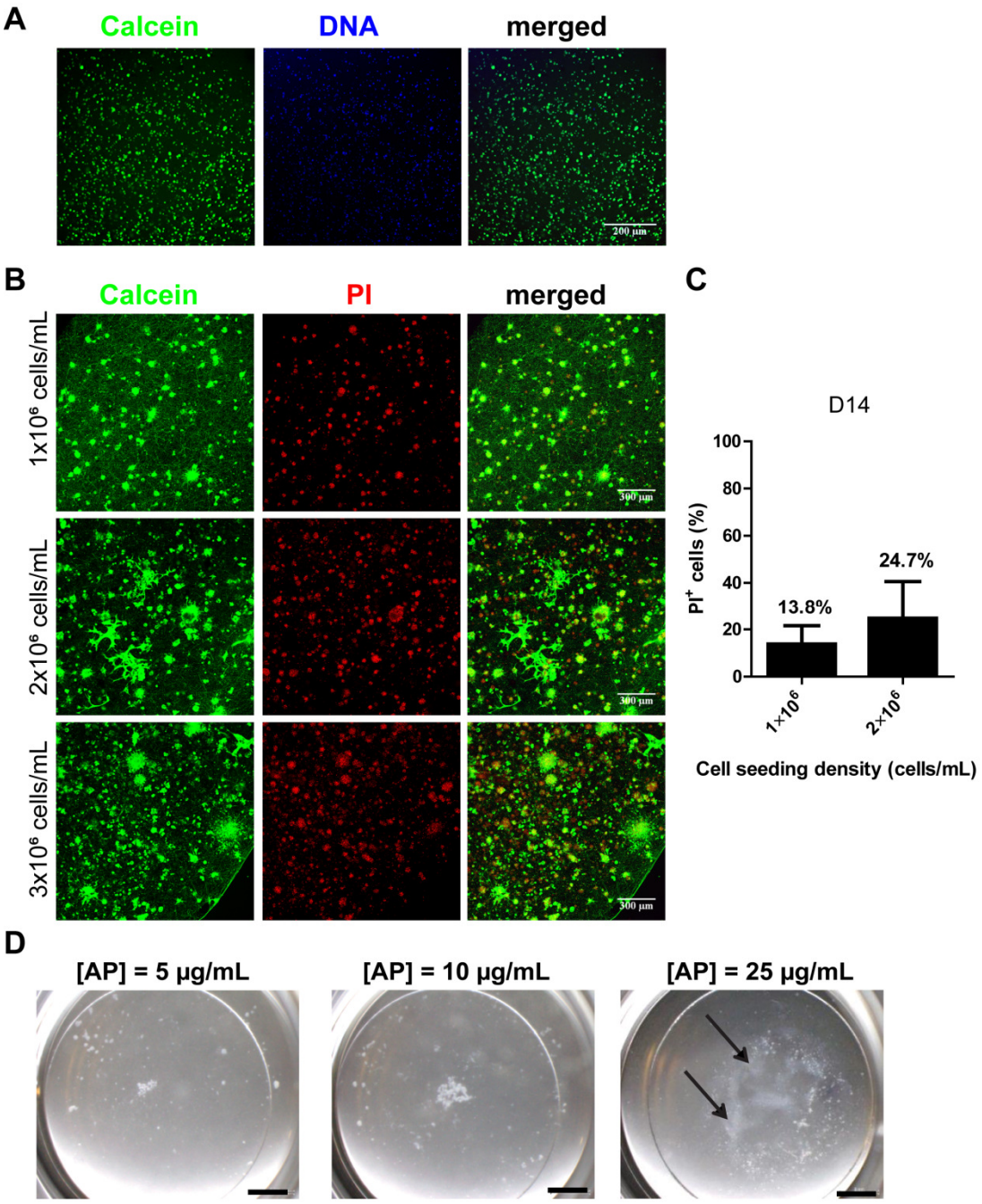

Figure S2. Distribution of viable cells within fibrin. (A) Distribution of viable cells following embedment in the hydrogel; fibrin gels containing mES-NSPCs (1×10^6 cells/mL of fibrin) were incubated with 4 µg/mL calcein AM for 30 min and 2.8 µg/mL Hoechst 33342 dye for 30 min at 37°C (both from Invitrogen), for detection of live cells (in green) and DNA (in blue), respectively, and immediately imaged by CLSM; representative 2D projections of CLSM stack images covering a depth of 140 µm are shown. **(B)** Distribution of live/dead cells at day 14 of culture, as a function of cell seeding density (1, 2 or 3×10^6 mES-NSPCs/mL of fibrin); cell-fibrin constructs were incubated with calcein AM and PI for detection of live and dead cells, respectively, and imaged by CLSM; representative 2D projections of CLSM stack images covering a depth of 200 µm are shown. **(C)** Quantitative analysis of cells incorporating PI (PI^+, dead cells) at day 14 of culture as determined by flow cytometry (n = 2–3 independent experiments). **(D)** Degradation of cell-fibrin constructs, as a function of aprotinin (AP) concentration within fibrin gel; mES-NSPCs were

embedded within fibrin gels prepared with 5, 10 and 25 µg/mL of AP, and cultured in medium without AP; representative images of whole cell-fibrin constructs acquired using a stereomicroscope (SFZ10, Olympus) at day 6 of culture are shown; the incorporation of AP in fibrin gel was not sufficient to delay the degradation of cell/fibrin constructs, independently of the concentration used. Fibrin gels prepared with 25 µg/mL of AP degraded at a lower rate, as suggested by the presence of residual fibrin gel at this time point (arrows); scale bars = 2 mm.

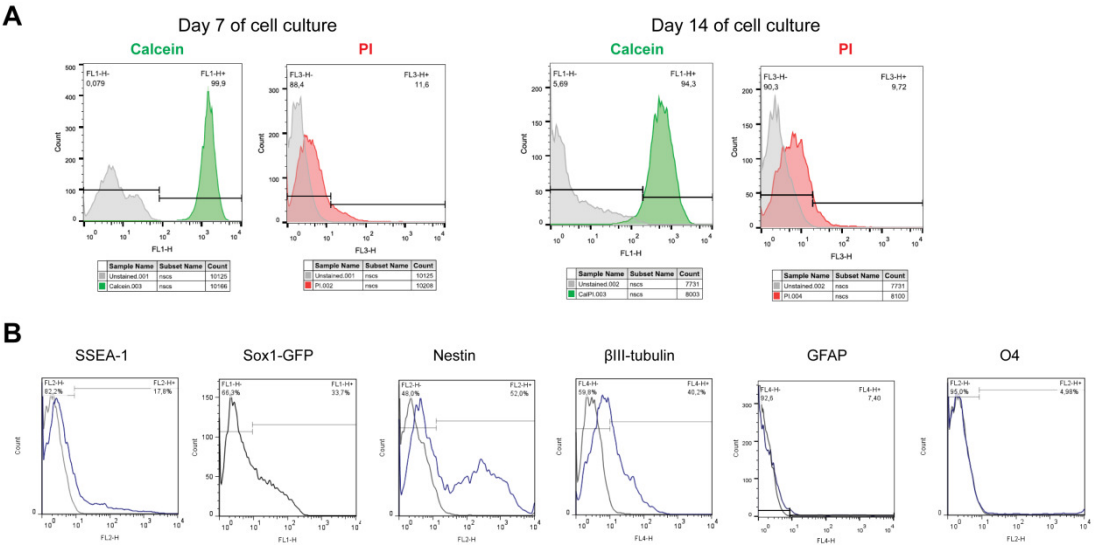

Figure S3. Representative flow cytometry fluorescence histograms correspondent to: (A) Live/dead assay performed at day 7 and 14 of mES-NSPC culture within fibrin; cells were isolated from the cell/fibrin constructs, incubated with calcein AM and PI (for detection of live and dead cells, respectively), and analyzed by flow cytometry. **(B)** Phenotypic characterization of mES-NSPCs cultured within fibrin for 14 days: SSEA-1 (mouse embryonic stem cells), Sox1-GFP (early neuroectodermal cells), nestin (neural stem/progenitor cells), βIII-tubulin (developing and mature neurons), GFAP (astrocytes), and O4 (olygodendrocytes); the grey line represents the fluorescence of cells incubated with secondary antibody only or with the correspondent isotype control.

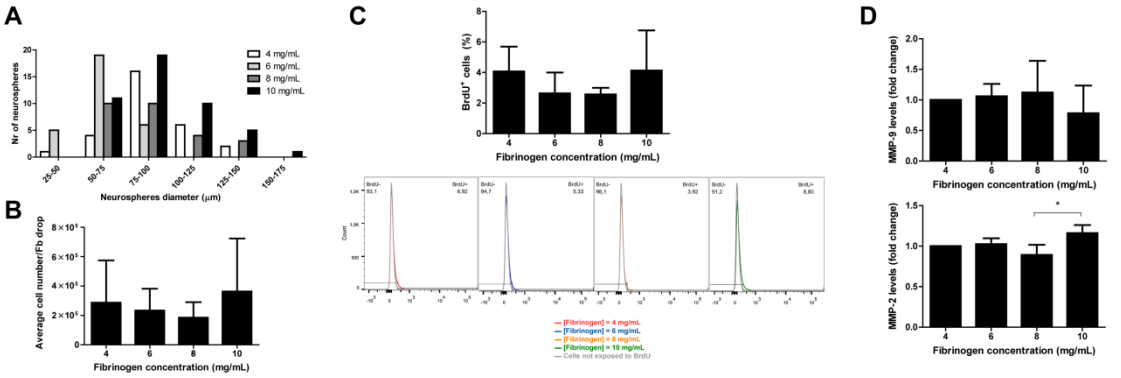

Figure S4. Effect of fibrinogen concentration on cellular spheroid diameter, total cell number, percentage of proliferative cells, and MMP activity, at day 14 of mES-NSPC culture within fibrin. (A) Histogram of cellular spheroids diameter distribution as a relative frequency (*n* = 252–373 spheroids); large cellular spheroids (diameter > 125 μm) were only observed in fibrin gels formed with the two highest fibrinogen concentrations tested (6 and 8 mg/mL). **(B)** Total cell number per fibrin drop, after cell isolation from cell/fibrin constructs (*n* = 3–6 independent experiments). **(C)** Percentage of proliferative cells assessed by BrdU incorporation and flow cytometry (*n* = 3–4 independent experiments); representative fluorescence histograms are shown; the fluorescence of cells not exposed to BrdU but processed in parallel for immunodetection of BrdU is also shown; varying the fibrinogen concentration did not significantly alter the total cell number per drop neither the percentage of proliferative cells ($BrdU^+$ cells) in the range of fibrinogen concentrations tested. **(D)** MMP-2 and MMP-9 activity present in cell culture conditioned media, as determined by gelatin zymography; MMP-activity levels were normalized to those of the lowest fibrinogen concentration tested (*n* = 3 independent experiments; * $p < 0.05$); apart from the difference found between MMP-2 activity levels obtained for fibrinogen concentrations of 8 and 10 mg/mL, no significant differences were among the fibrinogen concentrations tested, independently of the MMP considered.

Supplementary Materials and Methods

Culture of mES-NSPCs on laminin-coated glass coverslips under neuronal differentiation conditions

Glass coverslips previously coated with 10 µg/mL of poly-D-lysine (P7280, Sigma) were incubated overnight with 5 µg/mL of laminin (L2020, Sigma). After cell dissociation, cell suspension was transferred to poly-D-lysine/laminin-coated glass coverslips at 2×10^4 cells/cm^2. ES-NSPCs were cultured for 14 days under neuronal differentiation conditions, following the same protocol described for neuronal differentiation of ES-NSPCs within fibrin gels (for detailed description see section 2.2 of the manuscript).

Cell viability and total cell number

For qualitative cell viability analysis, cell-fibrin constructs were sequentially incubated with 4 µM calcein AM (Invitrogen; 30 min at 37°C) and 6 µM propidium iodide (PI; Sigma; 10 min at 37°C), for detection of live and dead cells, respectively. After incubation, samples were washed twice with PBS, transferred to cell culture media, and immediately observed under the confocal laser scanning microscope (CLSM; Leica TCS SP5II). Quantitative analysis of cell viability was performed in a pool of six fibrin drops after cell isolation from the cell-fibrin constructs, as described in Materials and Methods section. Cell number per drop was determined using a Neubauer chamber and the percentage of viable cells determined using trypan blue dye exclusion method or by flow cytometry. For flow cytometry analysis single cell suspensions were incubated with 67 nM calcein AM (20 min at 37°C) or with 6 µM PI (10 min at 37°C) to label live and dead cells, respectively. Cells were finally washed 3×, suspended in FACS buffer and analyzed by flow cytometry, unlabeled cells were used as negative control. Representative histograms are represented in Figure S3A. The average cell number per fibrin drop was determined dividing the total number of viable cells counted using the Neubauer chamber by the number of fibrin drops.

5-Bromo-2'-deoxyuridine assay

The percentage of proliferative cells was assessed by immunocytometry detection of BrdU incorporated into cells synthesizing DNA. 5-Bromo-2'-deoxyuridine (BrdU; Sigma) was added to the cell culture medium of six replicate fibrin drops at the final

concentration of 50 μM, and ES-NSPCs kept in culture for additional 18 h. Cells were isolated from the gels as described, fixed in 1% (w/v) paraformaldehyde (PFA; 20 min), permeabilized with 0.2% (v/v) Triton X-100 (10 min at 4°C) and further exposed to 2 M HCl for 20 min. Cells were subsequently incubated in blocking buffer [PBS buffer containing 5% normal goat serum (NGS, Biosource) and 0.1% (w/v) saponin] for 20 min followed by incubation with anti-BrdU (V450-conjugated anti-BrdU antibody, 560810, BD Horizon; 8 μg/mL) for 30 min. Cells were finally washed 3× and suspended in FACS buffer containing sodium azide for immunocytometry analysis (FACSCanto™ II, BD Biosciences). Samples not exposed to BrdU but processed in parallel for immunodetection of BrdU were used as negative control. Representative histograms are shown in Figure S4C.

Gelatin zymography

MMP activity in conditioned media of mES-NSPC cultures before and after embedment within fibrin was analyzed by gelatin zymography, as previously described [1]. For this purpose, media was collected at day 5 of the neural commitment protocol and after 4, 8, and 14 days of ES-NSPC culture within fibrin. Total protein was determined and 20 μg of total protein loaded per lane. MMP activity was analyzed using Quantity One software (BioRad). Data presented correspond to three independent experiments. MMP activity was analyzed using Quantity One software (BioRad), and interpreted based on the literature [2].

Western blot analysis

Western blot analysis was performed on protein extracts of mES-NSPCs, before and after cell embedment within fibrin. For this purpose, cold RIPA buffer was added to dissociated ES-NSCs at day 5 of neural commitment or added directly to a pool of six cell/fibrin constructs collected at day 4, 8, and 14 of culture. The constructs were sonicated, centrifuged at 13000 ×g (10 min at 4°C), and protein concentration in the supernatant fractions determined by the Dc protein assay (BioRad). Protein extracts (5 μg for matriptase expression, and 20 μg for βIII-tubulin and NF200 expression) were incubated at 95°C for 5 min and subjected to a 10% or 4-12% sodium dodecyl sulfate polyacrylamide gel electrophoresis (SDS-PAGE). After SDS-PAGE separation the proteins were transferred to a nitrocellulose membrane (GE Healthcare) and blocked in TBS-T buffer containing 5% (w/v) skim milk or 5% (w/v) bovine serum albumin for 1 h. The membranes were then incubated with rabbit polyclonal anti-matriptase (sc-48830,

Santa Cruz Technologies; 1:2000), rabbit monoclonal anti-βIII-tubulin (MRB-435P; Covance; 1:5000), rabbit polyclonal anti-NF200 (AB8135, Abcam; 1:2000), and mouse monoclonal anti-GAPDH (5G4-6C5, HyTest; 1:40000) overnight at 4°C. After rinsing with TBS-T buffer membranes were incubated for 1 h with horseradish peroxidase-conjugated secondary antibodies and the blots developed with horseradish peroxidase-reactive chemiluminescence reagents (GE Healthcare). After exposure to autoradiographic film, the relative density of the protein band was further analyzed with Quantity One software (BioRad).

Table S1 – Primary and secondary antibodies as well as isotype controls used for immunocytometry studies

Target	Blocking solution	Primary Antibody	Isotype control	Dilution	Origin and product number	Secondary Antibody	Dilution	Origin and product number
Mouse ES cells	5% (v/v) NGS in PBS	Mouse monoclonal anti-SSEA-1	-	1:100	SantaCruz Biotechnology sc-21702	Goat anti-mouse IgM-PE	1:100	Santa Cruz Biotechnology sc-3768
NSPCs	5% (v/v) NGS and 0.1% (w/v) saponin in PBS	Mouse monoclonal anti-nestin	-	1:100	Chemicon MAB353	Goat anti-mouse IgG1-PE	1:100	Santa Cruz Biotechnology sc-3764
Developing and mature neurons		Mouse monoclonal anti-βIII tubulin	-	1:500	Covance MMS-435P	Goat anti-mouse IgG-APC	1:100	Santa Cruz Biotechnology sc-3818
Astrocytes		Alexa Fluor® 647 mouse anti-GFAP	Alexa Fluor® 647 Mouse IgG2b	1:100	BD BioSciences 561470 (Ab) BD BioSciences 558713 (Isotype)	-	-	-
Oligodendrocytes	10% (v/v) NGS in PBS	Mouse monoclonal anti-O4	-	1:50	Chemicon MAB345	Goat anti-mouse IgM-PE	1:100	Santa Cruz Biotechnology sc-3768

Abbreviations: APC, allophycocyanin; ES, embryonic stem; GFAP, glial fibrillary acidic protein; IgG/G1/M, immunoglobulin G/G1/M; NGS, normal goat serum; NSPCs, neural stem/progenitor cells; PBS, phosphate buffer saline; PE, phycoerythrin; SSEA-1, stage-specific embryonic antigen 1; v/v, volume per volume percent; w/v, weight per volume percent.

Table S2 – Primary and secondary antibodies used for immunocytochemistry studies

Target	Blocking solution	Primary Antibody	Dilution	Origin and product number	Secondary Antibody	Dilution	Origin and product number
Cellular Markers							
Mouse ES cells	5% (v/v) NGS in PBS	Mouse monoclonal anti-SSEA-1	1:100	SantaCruz Biotechnology sc-21702	Alexa Fluor® 594 goat anti-mouse IgG	1:1000	Invitrogen A11020
NSPCs	5% (v/v) NGS in PBS containing 0.05% (v/v) Tween-20	Mouse monoclonal anti-nestin	1:100	Chemicon MAB353			
		Mouse monoclonal anti-nestin (human)	1:200	Chemicon AB22035			
Developing and mature neurons	5% (v/v) HS and 3% (v/v) BSA in PBS containing 0.05% (v/v) Tween-20	Rabbit monoclonal anti-βIII tubulin	1:500	Chemicon AB18207	Alexa Fluor® 647 donkey anti-rabbit IgG	1:1000	Invitrogen A11070
	5% (v/v) BSA in PBS	Mouse monoclonal anti-βIII tubulin	1:500	Covance MMS-435P	Alexa Fluor® 488 donkey anti-mouse IgG	1:1000	Invitrogen A21202
Astrocytes	5% (v/v) HS and 3% (v/v) BSA in PBS containing 0.05% (v/v) Tween-20	Rabbit polyclonal anti-GFAP	1:500	DAKO Z0334	Alexa Fluor® 647 donkey anti-rabbit IgG	1:1000	Invitrogen A11070
Oligodendrocytes	5% (v/v) NGS in PBS	Mouse monoclonal anti-O4	1:100	Chemicon MAB345	Alexa Fluor® 594 goat anti-mouse IgG	1:1000	Invitrogen A11020

Mature neurons	5% (v/v) NGS in PBS containing 0.05% (v/v) Tween-20	Rabbit polyclonal anti-NF200	1:1000	Chemicon AB8135	Alexa Fluor® 647 donkey anti-rabbit IgG	1:1000	Invitrogen A11070
Synapsin I, phosphoproteins associated to synaptic vesicles	10% (v/v) NGS in PBS	Rabbit polyclonal anti-synapsin I	1:1000	Chemicon AB1543P			
GABAergic neurons		Goat polyclonal anti-GAD67	1:200	Santa Cruz Biotechnology sc-7512	Alexa Fluor® 660 donkey anti-goat IgG	1:1000	Invitrogen A21983
Dopaminergic and noradrenergic neurons		Rabbit polyclonal anti-tyrosine hydroxylase	1:500	Chemicon AB152	Alexa Fluor® 647 donkey anti-rabbit IgG	1:1000	Invitrogen A11070
ECM markers							
Fibronectin	5% (v/v) BSA in PBS	Rabbit polyclonal anti-fibronectin	1:100	Sigma-Aldrich F3648	Alexa Fluor® 647 donkey anti-rabbit IgG	1:1000	Invitrogen A11070
Laminin	1% (v/v) BSA and 4% (v/v) FBS in PBS	Rabbit polyclonal anti-laminin	1:50	Sigma-Aldrich L9393			
Collagen IV	5% (v/v) BSA in PBS	Goat polyclonal anti-collagen IV	1:50	Chemicon AB769	Alexa Fluor® 660 donkey anti-goat IgG	1:1000	Invitrogen A21983

Abbreviations: BSA, bovine serum albumin; ECM, extracellular matrix; ES, embryonic stem; FBS, fetal bovine serum; GABA, γ-aminobutyric acid; GAD67, glutamic acid decarboxylase 67; GFAP, glial fibrillary acidic protein; HS, horse serum; IgG, immunoglobulin G; NF200, neurofilament 200; NGS, normal goat serum; NSPCs, neural stem/progenitor cells; PBS, phosphate buffer saline; PE, phycoerythrin; SSEA-1, stage-specific embryonic antigen 1; v/v, volume per volume percent.

Supplementary References

[1] A.P. Cardoso, M.L. Pinto, A.T. Pinto, M.I. Oliveira, M.T. Pinto, R. Goncalves, J.B. Relvas, C. Figueiredo, R. Seruca, A. Mantovani, M. Mareel, M.A. Barbosa, M.J. Oliveira, Macrophages stimulate gastric and colorectal cancer invasion through EGFR Y(1086), c-Src, Erk1/2 and Akt phosphorylation and smallGTPase activity, Oncogene 33(16) (2014) 2123-33.

[2] H. Frankowski, Y.H. Gu, J.H. Heo, R. Milner, G.J. Del Zoppo, Use of gel zymography to examine matrix metalloproteinase (gelatinase) expression in brain tissue or in primary glial cultures, Methods Mol Biol 814 (2012) 221-33.

CHAPTER III

Fibrin functionalization with synthetic adhesive ligands interacting with α6β1 integrin receptor enhance neurite outgrowth of embryonic stem cell-derived neural stem/progenitors*

Joana Silva [1,2§], Ana R. Bento [1,2,3§], Daniela Barros [1,2], Tiago L. Laundos [1,2], Susana R. Sousa [1,2,4], Pedro Quelhas [1,2], Mónica M. Sousa [2,5], Ana P. Pêgo [1,2,3,6], Isabel F. Amaral [1,2,3]

[§] These authors contributed equally to this work. [1] INEB - Instituto de Engenharia Biomédica, Universidade do Porto, Portugal; [2] i3S - Instituto de Investigação e Inovação em Saúde, Universidade do Porto, Portugal; [3] Faculdade de Engenharia, Universidade do Porto, Portugal;[4] ISEP - Instituto Superior de Engenharia do Porto, Instituto Politécnico do Porto, Portugal; [5] Nerve Regeneration Group, IBMC - Instituto de Biologia Molecular e Celular, Universidade do Porto, Portugal; [6] ICBAS - Instituto de Ciências Biomédicas Abel Salazar, Universidade do Porto, Portugal.

Published in Acta Biomaterialia 2017, 59:243–256. DOI: 10.1016/j.actbio.

Abstract

To enhance fibrin hydrogel affinity towards pluripotent stem cell-derived neural stem/progenitor cells (NSPCs) and its capacity to support NSPC migration and neurite extension, we explored the tethering of synthetic peptides engaging integrin α6β1, a cell receptor enriched in NSPCs. Six α6β1 integrin ligands were tested for their ability to support integrin α6β1-mediated adhesion of embryonic stem cell-derived NSPCs (ES-NSPCs) and sustain ES-NSPC viability, migration, and neuronal differentiation. Due to their better performance, peptides T1, HYD1, and A5G81 were immobilized into fibrin and functionalized gels characterized in terms of peptide binding efficiency, structure and viscoelastic properties. Tethering of T1 or HYD1 successfully enhanced cell outgrowth from ES-NSPC neurospheres (up to 2.4-fold increase), which exhibited a biphasic response to peptide concentration. Inhibition assays evidenced the involvement of α6β1 and α3β1 integrins in mediating radial outgrowth on T1-/HYD1-functionalized gels. Fibrin functionalization also promoted neurite extension of single ES-NSPCs in fibrin, without affecting cell proliferation and neuronal differentiation. Finally, HYD1-functionalized gels were found to provide a permissive environment for axonal regeneration, leading up to a 2.0-fold increase in neurite extension from rat dorsal root ganglia explants as compared to unmodified fibrin, and to significant improved locomotor function after spinal cord injury (complete transection), along with a trend toward a higher area positive for growth associated protein 43 (marker for axonal growth cone formation). Our results suggest that conjugation of α6β1 integrin-binding motifs is of interest to increase the biofunctionality of hydrogels used in 3D platforms for ES-NSPC culture and potentially, in matrix-assisted ES-NSPC transplantation.

Keywords: hydrogel; peptide immobilization; neural stem/progenitor cells; cell outgrowth; α6β1 integrin.

Introduction

Progress in the establishment of protocols for the efficient generation of neural stem/progenitor cells (NSPCs) from pluripotent stem cells has fostered their use in experimental regenerative therapies for central nervous system (CNS) disorders, particularly those involving the loss of multiple neural subtypes [1]. Still, despite their ability to survive, differentiate and integrate into the host neural circuitry, often leading to functional benefits [2, 3], neural progenitors injected as suspensions directly into the lesion site of chronic injuries show low survival and/or poor integration [4-6]. To overcome these limitations, NSPCs are being combined with injectable biodegradable hydrogels which, besides allowing a higher retention and homogenous distribution of transplanted cells at the lesion site, create a supportive niche for cell survival, anchorage and differentiation, as well as for axonal regeneration. Due to its important role in hemostasis and wound repair, fibrin has been successfully explored as a provisional matrix for cell delivery, including embryonic stem (ES)- and induced pluripotent stem (iPS)-derived NSPCs [3, 7]. In previous studies, we showed that ES-derived NSPCs embedded in a fibrin hydrogel as single cells and cultured under neuronal differentiation conditions proliferate forming small-sized spheroids and differentiate establishing neuronal networks [8]. In the present investigation, we aimed at increasing fibrin biospecificity towards ES-NSPCs through the incorporation of biophysical cues engaging cell receptors enriched in NSPCs involved in NSPC migration and neurite outgrowth.

The design of hydrogels targeted for the delivery of a particular cell type has to emulate the specific features of the cell microenvironment in native tissue [9]. In this sense, hydrogels should provide biophysical and/or biochemical cues present in the natural cell niche while presenting structural and mechanical properties matched to those of the native tissue [10]. On what concerns biophysical cues, while full length adhesive proteins provide hydrogels with multiple bioactive ligands for cell adhesion, ECM/growth factor binding, and self-assembly, short synthetic bioactive oligopeptides allow the incorporation of a higher density of bioactive domains and with higher control over their exposure [10]. Among the various cell surface adhesion receptors expressed by cells, integrins are interesting to target due to their linkage to the actomyosin cytoskeleton upon binding to ECM ligands. Integrin binding to ECM ligands is crucial for cell anchorage to the surrounding matrix, spreading, migration, and activation of intracellular signaling pathways [11]. Additionally it is central for cell response to local mechanical stimuli, through force-induced conformational changes of proteins within

focal adhesion complexes [12]. An attractive integrin candidate for NSPC targeting is integrin α6β1, an integrin highly expressed by human and mouse neural precursors that can potentially be used as a marker for human NSC isolation [13, 14]. Integrin α6β1 is mostly a receptor for laminins, which are present in the basement membrane of the embryonic neural tube [15] and in neurogenic niches [16]. Studies carried out with recombinant integrins showed that integrin α6β1 binds to several laminin (LN) isoforms, namely to LN 111, LN 332 and LN 511/521, the latter being its most preferred ligand [17]. Its role as a key mediator of NSPC migration was evidenced through antibody perturbation studies. Integrin α6β1 was found to be critical for chain migration of neural precursors *in vitro* [18], and *in vivo* namely along the adult mouse rostral migratory stream [19]. In addition, integrin α6β1 has been shown to mediate outward migration of human ES-derived neural progenitors, as well as adhesion and outward migration of embryonic mouse neural progenitors, on laminin substrates [20, 21]. We therefore hypothesized that the covalent binding of synthetic ligands engaging α6β1 integrin to a hydrogel could enhance its ability to support ES-NSPC migration and neurite outgrowth. As in fibrin, motifs interacting with α6β1 integrin receptors are absent [22], tethering of α6β1 integrin ligands to fibrin was expected to enhance its capacity to support neurite extension from ES-NSPC-derived neurons, ultimately contributing to the integration of transplanted ES-NSPCs and neuronal relay formation.

In this study we investigated six peptides with reported ability to support α6β1 integrin-mediated cell adhesion and spreading: three peptides derived from native proteins (T1 from the angiogenic inducer CCN1, and AG10 and A5G81 from the C-terminus globular domain of human LN α1 chain and mouse LN α5 chain, respectively [23-25]) and two peptides with no sequence homology to any of the LN chains or to known proteins (HYD1 and P3), identified through the use of random peptide display libraries [26-28]. The N4 sequence presenting homology with the domain IV of netrin-4 was also tested, since netrin-4 forms a complex with the LN λ1 chain which further binds to α6β1 integrin, leading to enhanced NSC migration and proliferation [29]. Peptides were initially examined for their ability to support ES-NSPC adhesion, viability, migration, and neuronal differentiation, when adsorbed to 2D surfaces. The peptides revealing the highest capability to promote NSPC adhesion mediated through α6β1 integrin were immobilized in fibrin, and the resulting functionalized gels characterized in terms of peptide binding efficiency and ability to promote ES-NSPC migration, using a radial outgrowth assay. We report that fibrin gels tethered with the synthetic peptide HYD1 are able to promote cell outgrowth from neurospheres and neurite extension of single ES-NSPCs. Moreover, we show that HYD1-functionalized fibrin provides a permissive

environment for axonal growth, leading to increased neurite extension from sensory neurons *in vitro* and to a trend for increased axonal growth along with improved functional recovery after spinal cord injury in adult rats, when compared to native fibrin.

Materials and Methods

Generation of Neural Stem/Progenitor Cells (NSPCs) from mouse ES cells

A modified mouse ES cell line (46C) established at the Institute for Stem Cell Research (Edinburgh University, Scotland, UK) expressing green fluorescent protein (GFP) under the promoter of the NSPC-specific *Sox1* gene was used. Neural commitment of ES cells was attained in adherent monoculture and N2B27 medium [30]. At day 5 of the neural commitment protocol, Sox1-GFP expression was analyzed by flow cytometry, to assess the efficiency of neural conversion (Fig. S1), and cells used whenever more than 75% expressed Sox1-GFP. To obtain floating aggregates (neurospheres), ES-NSPCs were plated at 2×10^5 Sox1-GFP$^+$ cells/mL into 35 mm non-tissue culture plastic Petri dishes (Easy-Grip), and cultured in N2B27 medium supplemented with 10 ng/mL of epidermal growth factor and basic fibroblast growth factor (EGF and bFGF; both PeproTech) for three days under dynamic conditions (55 rpm) on a rotary orbital shaker.

Analysis of α6 and β1 integrin expression in ES-NSPCs and floating aggregates of ES-NSPCs

The expression of α6 and β1 integrin subunits in ES-NSPCs was assessed by immunocytometry at day 5 of the neural commitment protocol, after gentle dissociation through incubation with StemPro® Accutase® (Gibco; 2–3 min; 37°C). For analysis of integrin expression in floating aggregates of ES-NSPCs, neurospheres were incubated with StemPro® Accutase® (10 min; 37°C) for cell dissociation, prior to be processed for immunocytometry. The distribution of α6 and β1 integrin subunits in neurospheres was detected by *en bloc* immunohistochemistry, in neurospheres allowed to adhere for 2 h on poly-D-lysine (PDL, Sigma)-coated (10 μg/mL; 1 h; RT) glass coverslips. At this time point the PDL-coated coverslips were inverted and the upper part of the neurospheres analyzed by confocal laser scanning microscopy (CLSM, Leica TCS SP2).

Evaluation of α6β1 synthetic ligands' ability to support ES-NSPC adhesion, viability, migration, and neuronal differentiation

Preparation of 2D substrates coated with α6β1 ligands

Peptides T1 (GTTSWSQCSKS), AG10 (NPWHSIYITRFG), HYD1 (KIKMVISWKG), P3 (VSWFSRHRYSPFAVS), N4 (CGLPYSSVC), and A5G81 (AGQWHRVSVRWG) with a C-terminal amide were synthesized by GenScript (purity > 95%). Peptides were dissolved at 1.292 mM in Milli-Q ultrapure water (Millipore) or in acetic acid solutions, filter-sterilized, aliquoted, freeze-dried, and stored at -20°C until further use. For adsorption onto 2D surfaces, peptides were diluted in Milli-Q ultrapure water and added to the wells of tissue-culture plates or to inserts in order to obtain peptide coating concentrations ranging from 5 to 100 nmoles/cm^2. Peptide adsorption was performed overnight at 37°C. Non-adsorbed peptides were removed by rinsing twice the wells with PBS, and peptide surface density quantified. Briefly, physisorbed peptides were extracted with 1% (v/v) Triton (25 min; 4°C; 200 rpm) and peptide concentration determined using the bicinchoninic acid method (Pierce BCA Protein Assay Kit; Thermo Scientific), according to the supplier instructions. Peptide concentration was extrapolated from a standard curve performed for each peptide, where absorbance was plotted against known concentrations of peptide.

ES-NSPC adhesion, viability, migration, and differentiation on 2D substrates coated with α6β1 ligands

Peptide-coated wells/inserts were incubated with 1% (w/v) heat-inactivated bovine serum albumin (BSA, Sigma) to block non-specific adhesion, and used for assessment of ES-NSPC adhesion, viability, migration, and differentiation (details are provided in Supporting Information). Wells incubated in parallel with 1% (w/v) heat-inactivated BSA were used as negative control, while wells incubated with 100 µg/mL of PDL, 20 µg/mL of laminin 111 from Engelbreth-Holm-Swarm murine sarcoma (LN 111, Sigma), or 20 µg/mL of human recombinant laminin 511 (LN 511, Biolamina), were used as positive controls. Glass coverslips previously coated with 10 µg/mL of PDL and then with 5 µg/mL of LN 111 (PDL-LN 111) were also prepared and used as an additional positive control in 24-h experiments or longer.

Preparation of functionalized fibrin hydrogels

For the formation of fibrin gels, a 6 mg/mL concentration of fibrinogen was selected, as this concentration was previously shown to yield gels permissive to ES-NSPC neurite extension and neuronal differentiation, and with storage modulus comparable to that of neural tissue in the adult brain [8, 31]. Synthetic α6β1 ligands were covalently bound to fibrin using the enzymatic cross-linking action of transglutaminase factor XIIIa [32]. For this purpose, bi-domain peptides containing the sequence of interest at the carboxyl terminus and a factor XIIIa substrate from the NH_2-terminal sequence of α2-plasmin inhibitor (residues NQEQVSPL) at the amino terminus were synthesized at GenScript with a C-terminal amide (purity > 95%). A bi-domain peptide containing an inactive scrambled sequence of HYD1 (HYDS - WIKSMKIVKG) [27] was also acquired for use in certain experiments. Peptides were dissolved at 1 mM in Milli-Q ultrapure water, filter-sterilized, aliquoted, and stored under nitrogen at -20°C for use within a month. fibrinogen solution was prepared dissolving plasminogen-free fibrinogen from pooled human plasma containing factor XIII (Sigma) in Milli-Q ultrapure water, followed by dialysis against tris-buffered saline (TBS, pH 7.4) for 24 h. The resulting fibrinogen solution was then sterile-filtered and its concentration determined spectrophotometrically at 280 nm, applying an extinction coefficient of 1.51 mL mg^{-1} cm^{-1} [33]. Fibrinogen solution was then diluted to 12 mg/mL with TBS. Functionalized fibrin gels were formed applying equal volumes of the fibrinogen solution and a thrombin solution in TBS containing $CaCl_2$, aprotinin, and the bi-domain peptides [final concentration of fibrin components: 6 mg/mL fibrinogen; 2 NIH U/mL thrombin from human plasma; 2.5 mM $CaCl_2$; 10 µg/mL aprotinin (all Sigma-Aldrich); 1 to 320 µM of bi-domain peptides] into the wells of a 6-well non-tissue culture plate (Becton Dickinson). Polymerizing gels were then incubated at 37°C for 30 min to allow cross-linking by factor XIIIa. Non-functionalized fibrin gels and fibrin gels containing 20 µg/mL LN 111 or LN 511 were also prepared and used as controls.

Characterization of functionalized fibrin gels: peptide incorporation, microstructure, and viscoelastic properties

The incorporation of bi-domain peptides into fibrin was determined using ^{125}I-labeled bi-domain peptides, as iodination of α2-plasmin inhibitor and that of peptides derived from its NH_2-terminus was previously shown not to alter their cross-linking to fibrin by factor XIIIa [32, 34]. Functionalized fibrin gels (50 µL) were prepared as described above using bi-domain peptides spiked with^{125}I-labeled peptides, in order to achieve a final

activity of ≅ 1.1×10^4 cpm/µg of bi-domain peptide. Fibrin gels containing ^{125}I-labeled soluble peptides or Na^{125}I (an amount leading to cpm values similar to those provided by ^{125}I-labeled bi-domains) were also prepared, and used as controls. Cross-linked fibrin gels were individually transferred to radioimmunoassay (RIA) tubes, and γ activity measured in a γ-counter (Wallac Wizard model 1470). The release of unbound bi-domain peptides from fibrin was followed over a 48-h period, incubating the gels with 125 µL of PBS buffer containing 2% (w/v) BSA. The buffer solution was transferred to new RIA tubes at 3, 6, 9, 12, 24, and 48 h for γ activity counting, and replaced by fresh buffer. Peptide cumulative release was calculated and expressed as a percentage of fibrin gel radioactivity prior to incubation in buffer, and the amount of bi-domain peptides incorporated into fibrin determined when peptide diffusion reached an equilibrium plateau.

Changes in the structure of fibrin network were detected using fluorescently-labeled fibrinogen. Functionalized fibrin gels (50 µL) were prepared as described above, using a 1:100 ratio of Alexa Fluor® 488 human fibrinogen conjugate (Molecular Probes) to unlabeled fibrinogen. Cross-linked fibrin gels were observed under CLSM using a Plan-Apochromat 63×/1.4 NA Oil objective, and stacks of 10 optical sections covering a depth of 10 µm acquired (NA, numerical aperture). Average pore area was determined in 2D projections of CLSM stacks, using MATLAB® software for automatic segmentation of pores and area computation. For each condition, 6 images from 2 different fibrin gels were examined.

The storage (G') and loss (G'') moduli of fibrin hydrogels were determined by rheometry using a Kinexus Pro Rheometer (Malvern Instruments), as previously described [8].

Cell outgrowth from ES-NSPC neurospheres on functionalized fibrin hydrogels

Embryonic stem-derived neural stem/progenitor cells (ES-NSPCs) migration on functionalized fibrin gels was assessed using floating aggregates of ES-NSPCs (neurospheres) and the radial outgrowth assay. Functionalized fibrin gels (10 µL) were formed as described above, in the lower wells of a 15-well µ-Slide angiogenesis plate (Ibidi). Neurospheres with diameter in the range of 200 to 250 µm were isolated under the stereoscopic magnifier and seeded on functionalized cross-linked fibrin gels (1 sphere per gel). Neurospheres were allowed to adhere for 2 h, and 40 µL of N2B27 medium supplemented with 10 ng/mL bFGF and 10 µg/mL aprotinin added to each well. Half of the medium was refreshed after 48 h of cell culture, and bFGF

concentration reduced to 5 ng/mL. To assess the contribution of specific integrins to radial outgrowth, function blocking monoclonal antibodies against α6 (clone NKI-GoH3, Serotec; 33.3 μg/mL), α3 (clone P1B5, Millipore; 10 μg/mL), or β1 (clone Ha2/5; BD Pharmigen; 10 μg/mL) integrin subunits, as well as isotype-matched controls for the α6 (rat IgG2a clone 2A3, Millipore; 33.3 μg/mL), α3 (mouse IgG1-k MOPC-21 clone, Millipore; 10 μg/mL), and β1 antibodies (hamster IgM λ1, Pharmigen; 10 μg/mL), were added to the culture medium. Radial outgrowth was determined in samples processed for F-actin/DNA staining at 72 h of cell culture and at 48 h for integrin blocking studies. Briefly, cells were fixed in 3.7% (w/v) paraformaldehyde (PFA) solution diluted 1:1 in culture media (30 min; 37°C), permeabilized with 0.2% (v/v) Triton X-100 in PBS (20 min; RT), and incubated with 1% (w/v) BSA for 1 h to minimize non-specific adsorption. F-actin was visualized incubating the samples with Alexa Fluor® 594-conjugated phalloidin (Molecular Probes; 1:100; 20 min; RT) while DNA was labeled with DAPI (Sigma; 0.1 μg/mL; 10 min; RT). Samples were finally mounted with Fluoromount™ (Sigma) and observed with the IN Cell Analyzer 2000 imaging system (GE Healthcare). Radial outgrowth was defined as the region comprised between the neurosphere edge and the migration front. Radial outgrowth was determined in the 3D image stacks, by segmenting the volume of the neurosphere and that correspondent to cells cytoskeleton, using DNA and F-actin fluorescence images, respectively. This process was guided by an initial 2D maximal projection of the data in Z. The outgrowth area was given by the 2D maximal projection in Z of F-actin stack images subtracting the neurosphere area, given by the 2D maximal projection of DNA fluorescence images. Outgrowth area was subsequently normalized to the neurosphere area at time point zero, determined in phase contrast images of the neurospheres immediately before the addition of culture media. Maximal outgrowth distance was computed analyzing the two segmented volumes, namely the distance from the neurosphere volume boundary to the boundary of the volume correspondent to cells cytoskeleton (Fig. S2).

Neuronal differentiation of ES-NSPCs within functionalized fibrin hydrogels

ES-NSPCs were embedded as single cells in functionalized fibrin gels (final cell seeding density: 1×10^6 cells/mL) and cultured for periods up to 14 days under neuronal differentiation conditions. At different time points, the cell-matrix constructs were processed for analysis of neurite outgrowth, distribution of viable/dead cells, total cell number, and expression of characteristic phenotypic markers: nestin (NSPC marker), βIII-tubulin (early neuronal marker), synapsin (synaptic vesicles marker), and glial fibrillary acidic protein (GFAP, astrocytic marker).

Neurite outgrowth from rat E18 dorsal root ganglia explants cultured within functionalized fibrin hydrogels

The effect of immobilized α6β1 ligands on neurite outgrowth from primary neurons was assessed using dorsal root ganglia (DRG) dissected from E18 Wistar rat embryos. Dorsal root ganglia explants were embedded in functionalized fibrin gels (10 μL) during fibrin polymerization (1 DRG per gel), and average neurite length quantified after 48 h of culture in samples processed for βIII-tubulin/DNA staining.

In vivo experiments

All procedures involving animals were approved by the local animal ethics committee and by the Portuguese official authority on animal welfare and experimentation (DGAV - Direção-Geral de Alimentação e Veterinária) in accordance with the EU Directive (2010/63/EU) and the Portuguese law (DL 113/2013). To assess the effect of functionalized fibrin gels on axonal regeneration, an *in vivo* model of spinal cord injury (SCI; total transection) was used. Chitosan tubular scaffolds were used to bridge the cavity formed upon spinal cord transection and provide mechanical support to the hydrogel (Fig. S3). Tubular scaffolds were prepared from squid pen chitosan (France Chitine; degree of acetylation 3.55) after purified (endotoxin levels < 0.1 EU/mL), as previously described [35]. For each experimental group, 10 female Wistar rats (10–13 weeks old) from Charles River Laboratories were used. Briefly, the spinal cord was transected by removing a 4 mm region encompassing T8, and chitosan tubular scaffolds (4-mm-long) prefilled with functionalized fibrin gel or unmodified fibrin (control) inserted into the defect, aligned along the longitudinal axis of the spinal cord. Animals were allowed to recover for 9 weeks and their locomotor function assessed once a week, using the Basso, Beattie and Bresnahan (BBB) score [36]. Ten weeks post-implantation, the animals were perfused and their spinal cords processed for cryostat sectioning. Longitudinal (coronal) cryostat sections (20 μm thickness) were serially collected and immunofluorescence labeled for detection of growth associated protein 43 (GAP43, marker for axonal growth cone formation), βIII-tubulin, GFAP, ionized calcium binding adaptor molecule 1 (Iba1, microglia and macrophage marker), nestin, and laminin. Sections were examined with the IN Cell Analyzer 2000 imaging system using a 20×/0.75 NA objective or using the CLSM (NA, numerical aperture). Axonal sprouting/regeneration in each animal was determined in 2D projections of the IN Cell Analyzer 3D stack images, analyzing the area of $GAP43^+$ axons in the lesion area, expressed as a percentage of the total lesion area. For each animal, four cryostat

sections were analyzed and GAP43$^+$ area averaged. A further detailed description of the methodologies and analysis used in the *in vivo* experiments is provided in Supplementary Data.

Statistical analysis

All *in vitro* and *ex vivo* experiments were performed at least three times and data treated using IBM® SPSS® Statistics Software (version 23). Statistically significant differences between two conditions were detected using the Student's *t*-test. To compare three or more conditions the one-way ANOVA was performed, followed by the Bonferroni correction for pairwise comparisons or the Dunnett's two-tailed test for comparisons with the control condition. Concerning the *in vivo* experiments, differences between BBB scores were assessed using a mixed model repeated measures ANOVA in which the *condition* tested was the between-subjects factor and *time* was the within-subjects factor (repeated measures), according to Scheff *et al.* [37]. A simple effect test and Bonferroni post-hoc tests were then performed to detect specific differences between groups. Results were considered significant for $p < 0.05$. A further detailed description of the methodologies followed in this study is provided in Supplementary Materials and Methods.

Results

Expression of α6 and β1 integrin subunits by ES-NSPCs and floating aggregates of ES-NSPCs

The expression of α6 and β1 integrin subunits in ES-NSPCs was examined by flow cytometry in neural progenitors from three different neural commitments. Representative fluorescence histograms are presented in Figure 1. NSPCs derived from the 46C mouse ES cell line showed α6 integrin expression in nearly all cells examined (95.7 ± 0.5%; Fig. 1A), which is a percentage of α6 positive cells higher than that reported for NSPCs derived from human ES cells through the differentiation of embryoid bodies (~46%) [20]. This fact may be associated to the more homogeneous access of cells to oxygen/nutrients/morphogens in adherent culture conditions than in suspension cultures of differentiating embryoid bodies. Almost all 46C-derived NSPCs expressed the β1 integrin subunit (91 ± 1.6%; Fig. 1A), similarly to human ES-NSPCs [20]. As in NSPCs α6 mostly dimerizes with β1 integrin subunit (the percentage of cells expressing β4, the other partner for α6, is either absent or lower than 15% [13, 20, 38]),

we assumed that α6β1 integrin was widely expressed by 46C-NSPCs. ES-NPCs subsequently expanded as floating aggregates retained the expression of β1 integrin (92.9 ± 2.6% β1 integrin$^+$ cells; Fig. 1B and D), but showed a small decrease in the percentage of α6 integrin positive cells (88.3 ± 0.5%; Fig. 1B and C). This reduction may be related to the presence of a small percentage of cells undergoing differentiation when grown as spheroids (13% of βIII-tubulin$^+$ cells, in average) [39], as NSC differentiation was reported to induce a decrease in α6 integrin expression without influencing that of β1 integrin subunit [29].

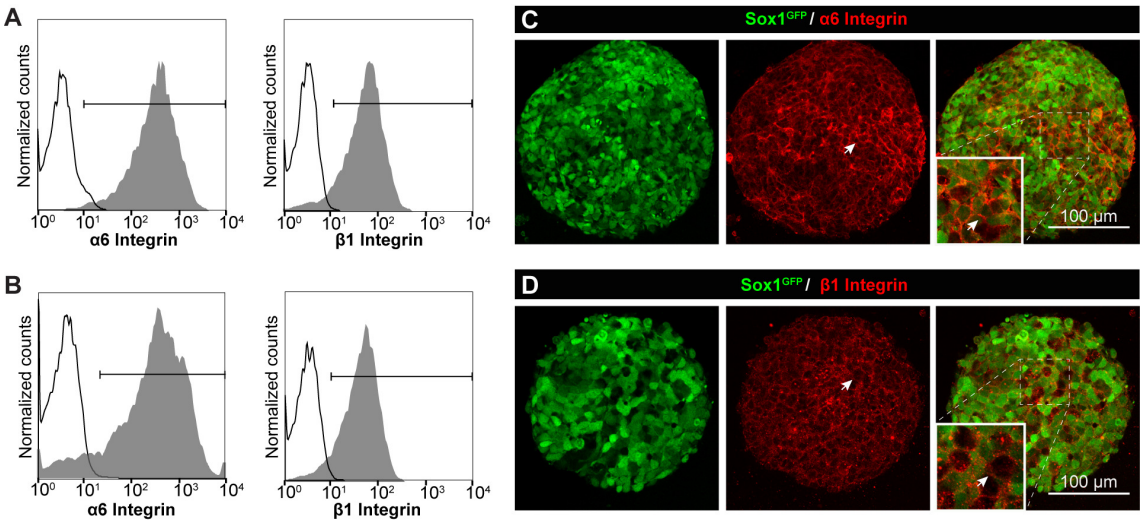

Figure 1. (A, B) Representative flow cytometry histograms obtained for the analysis of α6 and β1 integrin subunits expression in (A) ES-NSPCs and (B) floating aggregates of ES-NSPCs; cells incubated with the correspondent isotype control were used to determine the contribution of non-specific background staining (in black). **(C, D)** Expression of α6 and β1 integrin subunits in floating aggregates of ES-NSPCs, as shown by immunofluorescence labeling of (C) α6 or (D) β1integrin subunit in whole neurospheres; both subunits are highly expressed at cell-cell boundaries (arrows); images show 2D projections of CLSM 3D stack images covering a depth of 2 μm.

ES-NSPC adhesion, viability, migration, and differentiation on 2D substrates coated with α6β1 ligands

Six synthetic peptides with reported affinity to α6β1 integrin were evaluated in terms of ability to support ES-NSPC adhesion mediated through α6β1 integrin, viability, migration, and differentiation. For this purpose, ES-NSPCs were seeded on peptide-adsorbed wells and cultured for periods up to 6 days. Wells coated with PDL or LN 111, known to mediate nonspecific or integrin-dependent adhesion and migration of NSPCs, respectively [21, 38, 40], were used as positive controls. LN 511 coatings were used as an additional positive control, since LN 511 is described to be the most

preferred LN isoform ligand for integrin α6β1 [17]. Within the range of peptide coating concentrations initially tested (5 to 100 nanomoles/cm^2), that of 10 nanomoles/cm^2 was found to allow the attainment of a plateau of adherent cell numbers on all peptide-adsorbed surfaces (Fig. S4). As a result, this peptide coating concentration was used in these studies. ES-NSPC adhesion to the different peptides was initially investigated using a centrifugation adhesion assay [41]. The application of a centrifugal force after 2 h of cell culture revealed for HYD1 higher percentages of adherent cells as compared to P3 and N4 *(*$p = 0.017$ and $p < 0.001$, respectively), and corresponding to 84% of those observed on LN 111 (Fig. 2A). Cell adhesion quantified by the crystal violet colorimetric assay did not show statistical significant differences among peptides though a similar trend was found. Specifically, HYD1 revealed numbers of adherent cells of approximately 80% of LN 111 whilst on P3- and N4-adsorbed surfaces cell numbers did not exceed 60% of those observed on LN 111 (Fig. 2B). To assess if cell adhesion to the different surfaces was integrin-dependent, we incubated ES-NSPCs with EDTA, as divalent cations such as Mn^{2+} modulate integrin ligand-binding affinity [42]. Incubation with EDTA resulted in a decrease in the number of adherent cells on T1-, HYD1-, and A5G81-adsorbed surfaces of approx. 50% ($p \leq 0.013$, Fig. 2C), indicating that ES-NSPC adhesion to these peptides is divalent cation-dependent. Cell adhesion following ES-NSPC incubation with function-perturbing monoclonal antibodies against α6 and β1 integrin subunits was subsequently performed, to assess the contribution of α6β1 integrin to cell adhesion. Antibody concentrations optimized to efficiently inhibit ES-NSPC cell adhesion were used (details are provided in Supplementary Data). In the presence of a function-perturbing antibody against α6 integrin subunit, cell adhesion to T1-, HYD1-, and A5G81-adsorbed surfaces was inhibited namely in the range of 41 to 56% ($p \leq 0.002$ *vs.* the isotype-matched control antibody or untreated cells), evidencing that ES-NSPC adhesion to these peptides is partially mediated through α6β1 integrin (Fig. 2D). Incubation with a function-perturbing antibody against β1 integrin subunit led to similar or higher cell adhesion inhibition levels on these surfaces, further supporting this hypothesis ($p \leq 0.001$ *vs.* the isotype-matched control antibody or untreated cells). As expected, incubation with function-perturbing antibodies against α6 or β1 integrin subunits resulted in cell adhesion inhibition levels on PDL similar to those induced by the isotype-matched control antibodies (one-way ANOVA followed by Bonferroni's test), pointing that cell adhesion to PDL is not mediated through α6β1 integrin. The effect of physisorbed peptides on ES-NSPC viability was assessed after 24 h of cell culture, using a resazurin-based assay. Results revealed for HYD1-and A5G81-adsorbed wells numbers of viable cells

similar to LN 111, and higher cell numbers on HYD1-coated surfaces than on surfaces coated with T1, AG10, P3, or N4 ($p \leq 0.035$, Fig. 2E). Peptide effect on cell migration was evaluated plating ES-NSPCs into Transwell® inserts with peptide-coated membranes (8-μm pore). Amongst the tested peptides, HYD1 was the one supporting the highest cell migration ($p \leq 0.02$ *vs.* any other peptide, Fig. 2F). The reduced cell migration observed for peptide-coated membranes in comparison to Transwell® inserts coated with LN 111/511 is possibly associated to the lack of sequences sensitive to cell-secreted proteases such as those present in LN, which have a direct effect on cell invasion/migration. Finally we assessed the ability of physisorbed peptides to support ES-NSPC differentiation along the neuronal lineage. At the end of 6 days of culture under neuronal differentiation conditions, NSPCs showed immunoreactivity against the early neuronal marker βIII-tubulin on all peptide-adsorbed surfaces (60 to 84% of βIII-tubulin$^+$ cells, expressed as a function of LN 111), as well as long neuronal extensions which could not be observed on BSA-coated surfaces (Fig. S5). Importantly, none of the peptides induced astrocytic differentiation, as shown by the absence of GFAP$^+$ cells. As HYD1, T1, and A5G8 were found to support both divalent cation- and integrin α6β1-dependent NSPC cell adhesion, they were selected for immobilization in fibrin. An additional information provided by these studies was the higher ability of physisorbed LN 511 (herein used as positive control) to promote ES-NSPC adhesion, viability and migration, when compared to LN 111. Specifically, coating with LN 511 resulted in a 1.4-fold increase in the number of adherent cells ($p < 0.001$), 1.5-fold increase in the number of viable cells ($p < 0.001$), and to a 1.8-fold increase in the number of migrated cells ($p < 0.001$), as compared to LN 111, Fig. 2B, E–F).

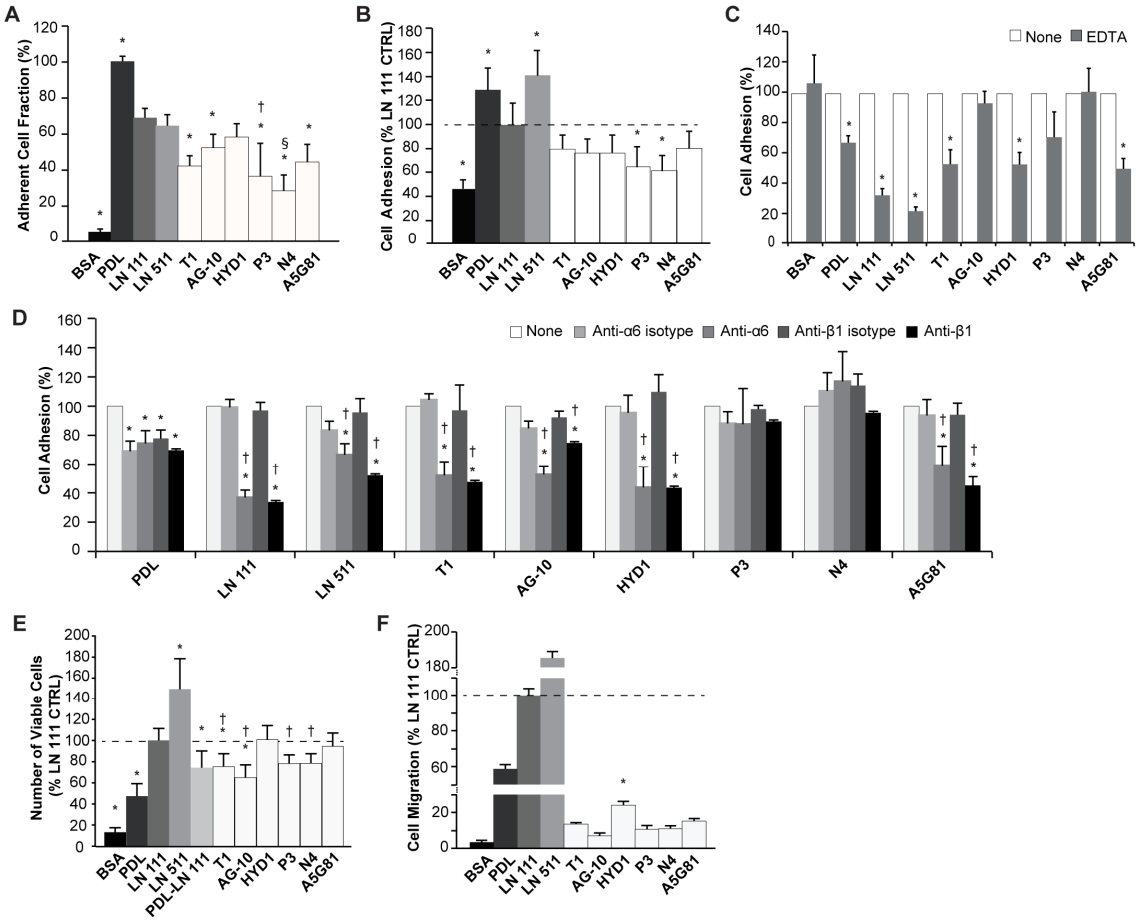

Figure 2. Evaluation of six synthetic peptides in terms of ability to support ES-NSPC adhesion, viability, and migration. ES-NSPCs were seeded on TCPS wells coated with physisorbed peptides or with BSA, PDL, LN 111, or LN 511 (controls). **(A)** Percentage of adherent cells after the application of a centrifugal force (mean ± SD, n = 5–6; * p < 0.05 *vs.* LN 111 one-way ANOVA followed by Dunnett's test, † p < 0.05 *vs.* HYD1, § p < 0.05 *vs.* AG10 and HYD1, one-way ANOVA followed by Bonferroni's test). **(B)** Number of adherent cells as a function of LN 111, determined using the crystal violet colorimetric assay (mean ± SD, n = 4; * p < 0.05 *vs.* LN 111, one-way ANOVA followed by Dunnett's test). **(C)** Number of adherent cells in the presence of EDTA, expressed as a percentage of untreated cells - None (mean ± SD, n = 4; * p < 0.05 *vs.* None, Student's *t*-test). **(D)** Number of adherent cells in the presence of function-perturbing antibodies against α6 and β1 integrin subunits, expressed as a percentage of untreated cells – None (mean ± SD, n = 4–5; * p < 0.05 *vs.* None; † p < 0.05 *vs.* None and the correspondent isotype control antibody, one-way ANOVA followed by Bonferroni's test). **(E)** Number of viable cells after 24 h of cell culture expressed as a function of LN 111, as determined using a resazurin-based assay (mean ± SD, n = 4–6; * p < 0.05 *vs.* LN 111, one-way ANOVA followed by Dunnett's test; † p < 0.05 HYD1 *vs.* T1, AG10, P3, and N4, one-way ANOVA followed by Bonferroni's test). **(F)** Cell migration through peptide-coated membrane inserts, as a function of LN 111 (mean ± SD, n = 4; * p < 0.05 HYD1 *vs*. any other peptide, one-way ANOVA followed by Bonferroni's test).

Peptide incorporation into fibrin hydrogels

The incorporation of bi-domain peptides into fibrin was determined using ^{125}I-labeled bi-domain peptides. The release of unbound peptides from fibrin gels formed using a 20 μM input concentration of bi-domain peptides in the polymerizing fibrin gel is shown in Figure 3A. The diffusion of unbound bi-domain peptides reached equilibrium after 12 h of incubation in PBS containing BSA, while free iodine (Na^{125}I) diffused during the first 6 hours. Peptide cumulative release determined after 24 h of incubation shows for all the peptides tested increased amounts of immobilized peptide with increasing input peptide concentrations. HYD1 and A5G81 bi-domain peptides revealed similar average binding efficiencies (20.0 ± 3.8% and 19.2 ± 3.7%, respectively), while T1 bi-domain peptide showed a higher average incorporation efficiency (31.9 ± 7.4%; $p < 0.001$, T1 *vs.* HYD1; $p < 0.001$, T1 *vs.* A5G81, one-way ANOVA; Fig. 3B). To get insight into the fraction of peptide incorporated into fibrin through non-covalent interactions (such as electrostatic interactions), fibrin gels containing 20 μM of soluble peptides (A5G81) were also prepared, and peptide diffusion compared to that of the correspondent bi-domain peptide. After 24 h of incubation, a reduced peptide retention was found for A5G81 as compared to the bi-domain peptide (8.2 ± 2.7% *vs.* 21.9 ± 3.6%; $p = 0.001$, Student's *t*-test), as expected from the covalent immobilization of the peptide through the activity of factor XIIIa (Fig. S6).

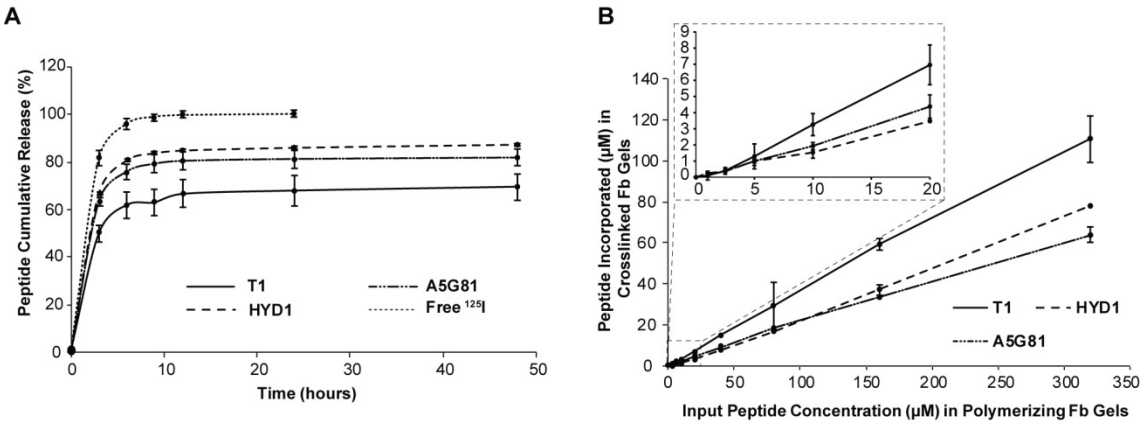

Figure 3. Peptide incorporation into fibrin gels, as determined using ^{125}I-labeled peptides. (A) Peptide release profile from fibrin (Fb) gels formed using a 20 μM input concentration of bi-domain peptides in the polymerizing fibrin gel (mean ± SD, $n = 4$); **(B)** Peptide incorporation into fibrin gels as a function of input peptide concentration (mean ± SD, $n = 4$).

Cell outgrowth from ES-NSPC neurospheres on functionalized fibrin hydrogels

To assess the effect of immobilized ligands on NSPC migration, floating aggregates of ES-NSPCs (neurospheres) were seeded on functionalized fibrin gels and radial outgrowth (outgrowth area and maximal outgrowth distance) determined after 72 h of cell culture using automatic image analysis. As the quantification of the outgrowth distance relying on 2D maximal projections of image stacks may collapse or even ignore cell outgrowth in the Z axis, the maximal outgrowth distance was computed analyzing the cell outgrowth volume. Results are presented in Figure 4A. The addition of soluble LN to fibrin polymerizing gel was not able to promote cell outgrowth from neurospheres, as shown by the decrease in the radial outgrowth area observed for the two LN isoforms used (p = 0.020, fibrin + LN 111 *vs.* unmodified fibrin; p = 0.008, fibrin + LN 511 *vs*. unmodified fibrin). The analysis of the maximal outgrowth distance revealed the same trend, depicting a significant reduction in the maximal outgrowth in gels containing soluble LN 511 (p = 0.008 *vs.* unmodified fibrin). Functionalization of fibrin with A5G81 was also not effective in promoting cell outgrowth, independently of the input concentration tested. Yet, covalent binding of T1 or HYD1 bi-domain peptides showed a biphasic effect on radial outgrowth. T1 immobilization resulted in enhanced cell outgrowth area when incorporated at 20 or 40 μM in the polymerizing fibrin gel, leading to a 1.9- and 2.2-fold increase relative to unmodified fibrin, respectively ($p <$ 0.001). In what concerns HYD1, input peptide concentrations of 10, 20, and 40 μM were efficient in promoting radial outgrowth ($p \leq 0.009$ *vs.* unmodified fibrin), maximal enhancement being observed for an input concentration of 20 μM, which a resulted in a 2.4-fold increase in the outgrowth area relative to native fibrin. Still, when comparing radial outgrowth enhancement induced by T1 or HYD1, no statistically significant differences were found among them. With increasing input peptide concentrations a trend for a reduction in the outgrowth area was observed. This effect was more pronounced in the case of HYD1, which, at the maximal input concentration, led to cell outgrowth inhibition (p = 0.006, 320 μM HYD1 *vs.* unmodified fibrin). Among the two peptides, HYD1 was the only peptide eliciting an increase in the maximal outgrowth distance besides leading to higher cell outgrowth areas. The maximal enhancement was observed for an input concentration of 20 μM, for which a 1.9-fold increase in the maximal outgrowth distance was observed ($p <$ 0.001 *vs.* unmodified fibrin). Maximal outgrowth distance revealed therefore a biphasic response to HYD1, and followed the same trend observed for the cell outgrowth area. We subsequently assessed if the addition of 20 μM of a bi-domain peptide containing a scrambled sequence of HYD1 (HYDS) was also able to induce an increase in radial outgrowth. As shown in Figure

4B, radial outgrowth on HYDS-functionalized fibrin gels was statistically similar to that of unmodified fibrin (Student's *t*-test), either considering the outgrowth area or the maximal outgrowth distance, evidencing the specificity of HYD1 to engage with ES-NSPCs. The T1-/HYD1-functionalized gels leading to maximal outgrowth area enhancement were then characterized in terms of ability to promote outward migration mediated through α6β1 integrin. The contribution of α3β1 integrin to radial outgrowth was also assessed, as HYD1, besides targeting the α6β1 heterodimer, also interacts with α3β1 integrin [27], an integrin which is also expressed by ES-NSPCs (Fig. S7). On unmodified fibrin gels, incubation with function-perturbing monoclonal antibodies against α6 and α3 integrin subunits barely affected the cell outgrowth, reducing the outgrowth area by 18% and 31%, respectively (p = 0.164 and 0.041 respectively, *vs*. the correspondent isotype control antibody; Fig. 4C). In contrast, on T1-/HYD1-functionalized gels, blocking α6 and α3 integrin subunits decreased the outgrowth area by 71 to 88% ($p \leq 0.002$ *vs.* isotype-matched control antibodies or untreated cells), indicating that promotion of cell outgrowth by immobilized T1 and HYD1 is mediated through α6β1 and α3β1 integrins. The addition of a function blocking antibody to β1 integrin subunit (which dimerizes with several α integrin subunits) completely inhibited cell outgrowth on both unmodified and T1-/HYD1-functionalized gels, reducing the outgrowth area by 94 to 96% ($p < 0.001$ *vs.* isotype-matched control antibodies or untreated cells). As the structural and viscoelastic properties of hydrogels can modulate cell behavior, we assessed whether the incorporation of T1 or HYD1 bi-domain peptides affected fibrin network structure, specifically the average pore diameter, and the storage and loss modulus. As shown in Figure 4D, for input peptide concentrations of 20 and 40 μM, T1 or HYD1 immobilization did not significantly impact the average pore area of fibrin network, neither the storage modulus of the hydrogels (ANOVA followed by Dunnett's test). Representative graphs of frequency sweep tests of unmodified and functionalized fibrin gels are provided in Figure S8.

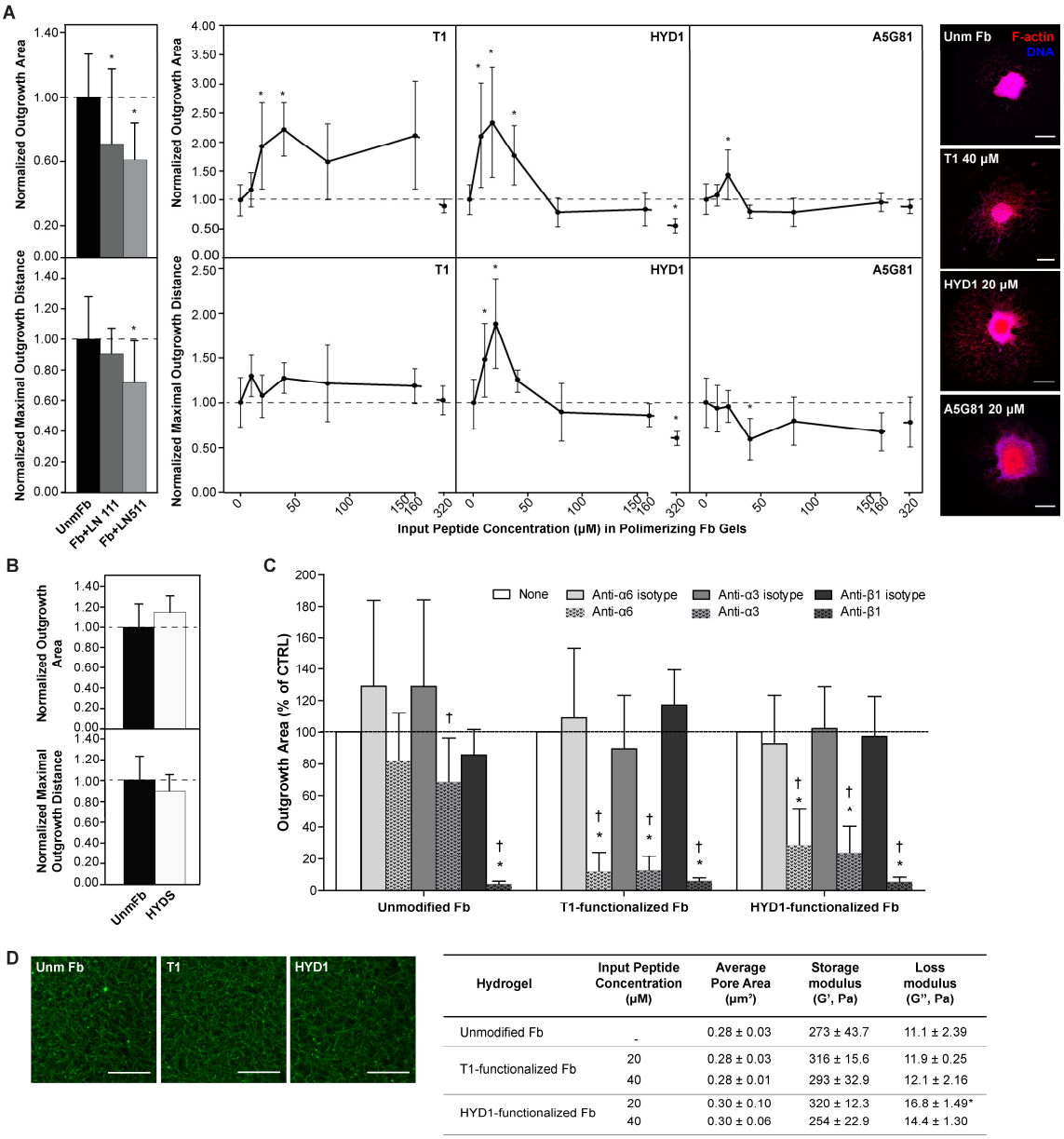

Hydrogel	Input Peptide Concentration (μM)	Average Pore Area (μm²)	Storage modulus (G', Pa)	Loss modulus (G'', Pa)
Unmodified Fb	-	0.28 ± 0.03	273 ± 43.7	11.1 ± 2.39
T1-functionalized Fb	20	0.28 ± 0.03	316 ± 15.6	11.9 ± 0.25
	40	0.28 ± 0.01	293 ± 32.9	12.1 ± 2.16
HYD1-functionalized Fb	20	0.30 ± 0.10	320 ± 12.3	16.8 ± 1.49*
	40	0.30 ± 0.06	254 ± 22.9	14.4 ± 1.30

Figure 4. ES-NSPC migration on T1-, HYD1-, and A5G81-functionalized fibrin hydrogels, as assessed using floating aggregates of ES-NSPCs and the radial outgrowth assay. (A) Outgrowth area and maximal outgrowth distance as a function of input peptide concentration; cell outgrowth was normalized to outgrowth on unmodified fibrin (Unm Fb), which corresponds to an input peptide concentration of 0 μM; the cell outgrowth on fibrin gels containing soluble LN (LN 111 or LN 511) is also shown in the bar charts at left (mean ± SD, *n* = 6; * $p < 0.05$ *vs.* Unm Fb, one-way ANOVA followed by Dunnett's test); binding of T1 or HYD1 bi-domain peptides promoted increase in cell outgrowth area, the highest enhancement being observed for fibrin gels functionalized with 20 μM of HYD1 or 40 μM of T1 (2.4-fold increase *vs.* native fibrin); representative 2D projections of CLSM stack images of neurospheres on fibrin hydrogels are shown at right, where radially migrating cells can be observed; scale bars = 300 μm. **(B)** The outgrowth area and the maximal outgrowth distance were not significantly altered when a scrambled sequence of HYD1 (HYDS, 20 μM) was used to functionalize fibrin (mean ± SD, *n* = 5). **(C)** Incubation with function blocking antibodies against α6 , α3, and β1 integrin subunits evidenced that promotion of cell outgrowth by immobilized T1 and HYD1 was mediated through α6β1 and α3β1 integrins

(mean ± SD, $n \geq 4$; * $p < 0.05$ *vs.* None; † $p < 0.05$ *vs*. the correspondent isotype control antibody, one-way ANOVA followed by Bonferroni's test). **(D)** Average pore size (mean ± SD, $n = 6$) and storage and loss moduli (G' and G'', mean ± SD, $n = 3$) of T1-/HYD1-functionalized gels, as determined using fluorescently-labeled fibrinogen and rheology, respectively; representative 2D projections of CLSM stack images of T1-/HYD1-functionalized gels are shown; scale bars = 20 μm.

3D culture of single ES-NSPCs in HYD1-functionalized fibrin gels: neurite extension, cell viability, proliferation, and neuronal differentiation

The impact of immobilized α6β1 integrin-binding ligands on ES-NSPCs when seeded as single cells in fibrin was subsequently assessed. For this study fibrin gels functionalized with 20 μM of HYD1 were used, due to their better performance in terms of ability to promote radial outgrowth from neurospheres (considering both the outgrowth area and the maximal outgrowth distance). Results are presented in Figure 5. ES-NSPCs entrapped within fibrin as single cells rapidly proliferated forming spheroidal clone-like multicellular clusters, as previously reported [8]. fibrin functionalization with HYD1 promoted neurite extension, as shown by the higher number of neuronal processes extending from cellular spheroids and higher length of the longest neurite found in HYD1-functionalized gels at day 6 of cell culture when compared to native fibrin (1.5- and 2.0-fold higher, respectively, Fig. 5A). ES-NSPCs cultured in HYD1-functionalized fibrin showed similar distribution of viable/dead cells at this time point of cell culture (Fig. 5B), and statistically similar cell numbers at days 7 and 14 of cell culture, as determined quantifying total DNA amount (Fig. 5C). Cell/fibrin constructs processed for immunofluorescence microscopy after 14 days of cell culture reveal for both conditions cells expressing nestin (NSPC marker) and a dense network of neurites staining for βIII-tubulin (early neuronal marker) with synaptic vesicles, radially sprouting from cellular spheroids and infiltrating the gel (Fig. 5D). Flow cytometry analysis of cells isolated from cell/fibrin constructs at this same time point and subsequently processed for immunolabeling of βIII-tubulin or GFAP (astrocytic marker), further suggests that immobilized HYD1 did not affect ES-NSPC differentiation in fibrin (Fig. 5E).

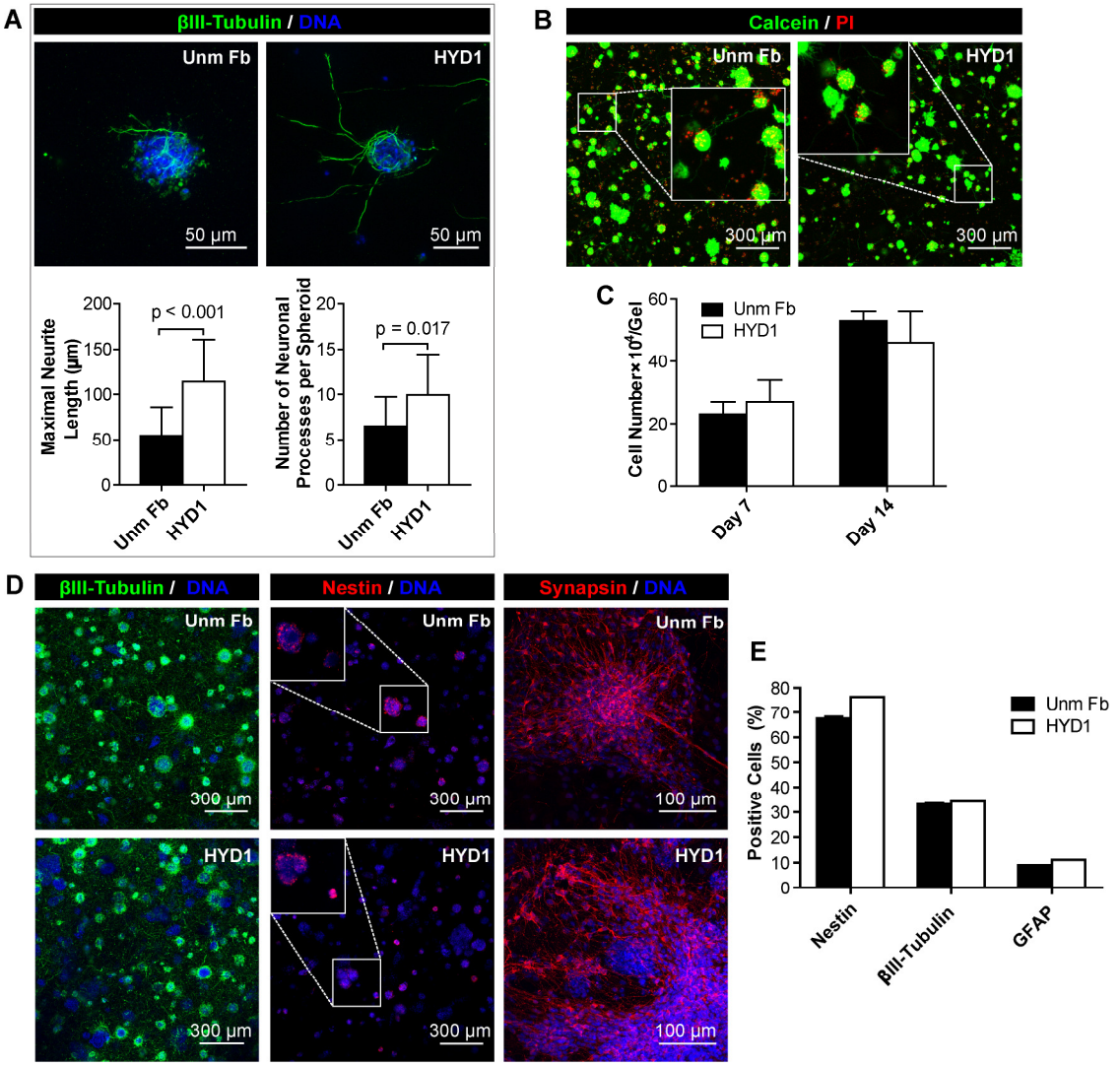

Figure 5. ES-NSPC behavior within fibrin hydrogels functionalized with 20 μM of HYD1 when seeded as single cells and cultured under neuronal differentiation conditions. At day 6 of cell culture, higher extension of neuronal processes from cellular spheroids was found in HYD1-functionalized gels (**A**; mean ± SD, *n* = 15–17 spheroids). When compared to unmodified fibrin (Unm Fb), HYD1-functionalized fibrin gels showed similar distribution of viable/dead cells at this time point of cell culture (**B**; viable cells are in green and dead cells in red), as well as similar cell numbers at both day 7 and 14 of cell culture (**C**; mean ± SD, *n* = 5 fibrin drop cultures). Immobilized HYD1 did not hinder ES-NSPC differentiation in fibrin, as suggested by immunofluorescence labeling of βIII-tubulin and synapsin in cell/constructs at day 14 of cell culture (**D**), and by flow cytometry analysis of βIII-tubulin and GFAP expression in cells isolated from cell/fibrin constructs at the same time point (**E**; mean ± SD, *n* = 2, each correspondent to a pool of 6 fibrin drop cultures); representative 2D projections of CLSM stack images are shown. Statistically significant differences were detected using Student's *t*-test.

Effect of HYD1-functionalized fibrin hydrogel on neurite outgrowth from rat E18 dorsal root ganglia

To get insight into the effect of immobilized ligands on axonal growth, HYD1-functionalized fibrin hydrogel was evaluated in terms of ability to support neurite outgrowth from rat E18 dorsal root ganglia (DRG) explants. The average neurite length of DRG explants cultured within fibrin gel functionalized with 10, 20, 100, or 250 µM of bi-domain peptide is presented in Figure 6.

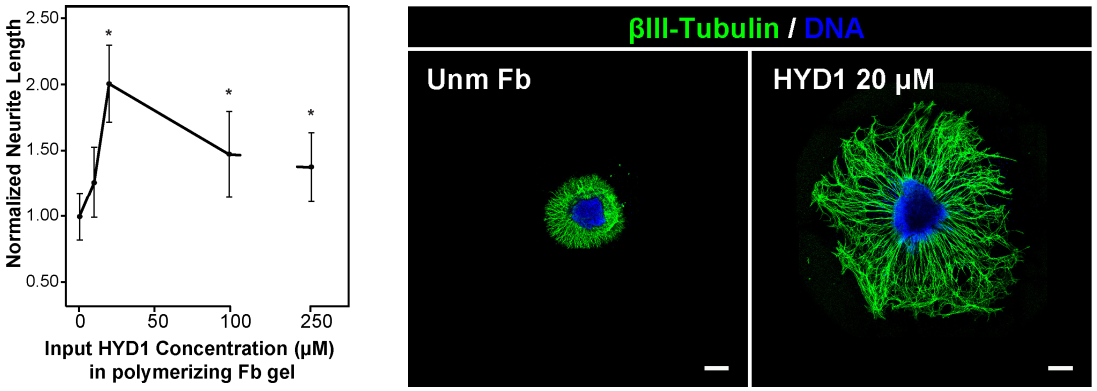

Figure 6. Neurite outgrowth from rat E18 DRG explants in HYD1-functionalized fibrin hydrogels, as a function of input peptide concentration. DRG explants were embedded in functionalized fibrin (Fb) gels and neurite outgrowth determined after 48 h of culture in samples processed for βIII-tubulin/DNA staining. Average neurite length was normalized to neurite extension in unmodified (Unm) Fb (mean ± SD, n = 6–9; * $p < 0.05$ *vs.* Unm Fb, one-way ANOVA followed by Dunnett's test). Representative 2D projections of CLSM stack images are shown; scale bars = 200 µm.

Tethering of HYD1 resulted in enhanced neurite outgrowth for input concentrations ≥ 20 µM, when compared to unmodified fibrin ($p \leq 0.022$), maximal enhancement being attained at an input concentration of 20 µM, for which a 2-fold increase in the average neurite length of DRG explants was observed when compared to unmodified fibrin ($p < 0.001$). Higher concentrations of bi-domain peptide resulted in lower enhancement in neurite outgrowth ($p < 0.01$, HYD1 20 µM *vs.* HYD1 100 and 250 µM). As T1- and A5G81-functionalized gels could also present ability to promote neurite extension of sensory neurons, these were subsequently evaluated. Similarly to HYD1-functionalized gels, neurite extension in both functionalized gels showed a biphasic response to peptide input concentration (Fig. S9), the highest increase in the average neurite length being observed in gels functionalized with 100 µM of T1 bi-domain peptide (1.9-fold increase; $p \leq 0.001$ *vs.* unmodified fibrin).

Effect of HYD1-functionalized fibrin hydrogels on axonal regeneration in a rat model of spinal cord injury

The effect of HYD1-functionalized fibrin on axonal regeneration in an animal model of SCI was also evaluated. Fibrin gels functionalized with 20 µM of HYD1 were selected for this purpose. Results from locomotor function assessment are presented in Figure 7A. Repeated measures ANOVA showed a significant main effect for condition (unmodified fibrin *versus* HYD1-functionalized fibrin; $F(1,16) = 5.03$, $p = 0.039$), a significant main effect for time ($F(3.5,56) = 21.27$, $p < 0.001$), and a significant condition × time interaction ($F(3.5,56) = 2.81$, $p = 0.040$), indicating that the effects observed on the BBB score over time differed depending on the condition. Simple effect tests further revealed significant differences between the two conditions ($p \leq 0.018$) from week 5 post-implantation until the end of the assay. Indeed, at the end of the experiment, 40% of the animals receiving HYD1-functionalized fibrin attained a BBB score higher or equal to 8 (sweeping with no weight support or plantar placement of the paw with no weight support), while in animals receiving unmodified fibrin, this score was only reached by 10% of the animals (Fig. S10A). After 10 weeks, spinal cords removed from operated animals showed the formation of a connective tissue bridge between the two stumps of the spinal cord (Fig. S10B). In both experimental groups, $GAP43^+$ fibers were present at the rostral and caudal site of the lesion and inside the tubular scaffold (Fig. 7B). Still, animals treated with HYD1-functionalized fibrin showed a trend to an increased area occupied by $GAP43^+$ fibers ($p = 0.08$ *vs.* unmodified fibrin; Fig. 7C). Both types of implants revealed infiltrating cells expressing βIII-tubulin often associated to laminin in the central region of the implant/lesion site (Fig. 7D), as expected from regenerating neurons [43]. The tissue bridges also contained cells expressing the neural progenitor marker nestin (Fig. 7E), precursor cells that may derive from ependymal cells of the central canal or from subpial astrocytes, which have been reported to differentiate into radial glia cells upon activation by injury [44]. In animals treated with HYD1-functionalized fibrin and similarly to the control group, cells expressing GFAP were mainly found at the borders of the lesion, whereas inside the tubular scaffolds the astrocytic cell population was minimal (Fig. 7F). Finally, Iba-1 immunolabeling showed for the two experimental groups similar distribution of activated microglia and macrophages, both at the implant/spinal cord interface as well as within the implant (Fig. S10C).

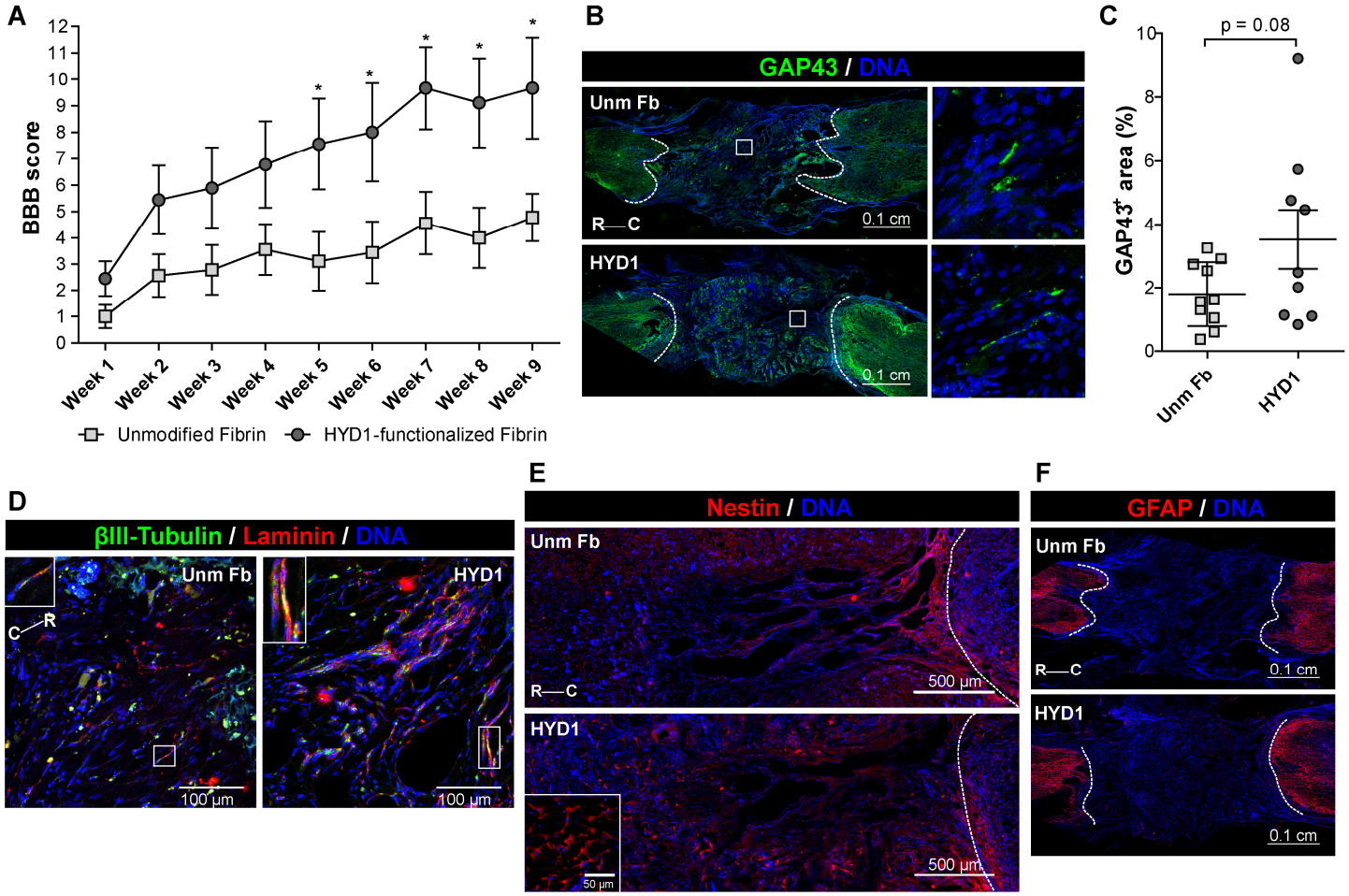
A
BBB score
Week 1
Week 2
Week 3
Week 4
Week 5
Week 6
Week 7
Week 8
Week 9
Unmodified Fibrin
HYD1-functionalized Fibrin
B
GAP43 / DNA
Unm Fb
HYD1
R—C
0.1 cm
C
p = 0.08
GAP43+ area (%)
Unm Fb
HYD1
D
βIII-Tubulin / Laminin / DNA
Unm Fb
HYD1
C—R
100 µm
E
Nestin / DNA
Unm Fb
HYD1
R—C
500 µm
50 µm
F
GFAP / DNA
Unm Fb
HYD1
R—C
0.1 cm

Figure 7. Evaluation of HYD1-functionalized fibrin gels in a rat model of SCI. Chitosan tubular porous scaffolds filled with fibrin gels functionalized with 20 μM of HYD1 were inserted into a 4-mm-long defect, aligned along the longitudinal axis of the spinal cord. **(A)** From week 5 post-implantation until the end of the experiment, animals treated with functionalized fibrin consistently exhibited a significantly higher locomotor capacity compared to control (Unm fibrin), as determined using the BBB locomotor rating scale (mean ± SEM, n = 9–10, * $p < 0.05$ *vs.* Unm fibrin, mixed repeated measures ANOVA followed by simple effect test). Ten weeks after implantation, histological analysis was performed in longitudinal (coronal) cryostat sections of the spinal cord. **(B)** Immunofluorescence labeling of GAP43 revealed the presence of growing axons inside the scaffold in both conditions; dashed lines delimit the lesion area. **(C)** Area fraction of fibers expressing GAP43; the dot plot depicts the values found for each animal, the mean, and the standard error of the mean (n = 9–10). Both types of implants revealed **(D)** infiltrating cells expressing βIII-tubulin often associated to laminin (arrows), **(E)** Nestin$^+$ cells inside the implanted scaffolds, and **(F)** GFAP$^+$ cells surrounding the lesion area (glial scar). R—C, rostral to caudal orientation of sections.

Discussion

In this study we assessed if the grafting of synthetic peptides engaging the laminin cell receptor integrin α6β1 could be used as a strategy to enhance the ability of a hydrogel to support ES-NSPC migration and neurite outgrowth. For this purpose we used NSPCs derived from mouse ES cells in chemically-defined medium and adherent monoculture, after being shown to express α6 and β1 integrin subunits.

Despite the attempts made to identify specific sequences mimicking the integrin binding activity of laminins, selection of the most effective α6β1 ligand is not straightforward. Conformation is important for ligand recognition and the optimal integrin α6β1 adhesive peptide might not necessarily correspond to an ECM sequence. For instance, studies by Ido and colleagues indicate that the binding site for integrin α6β1 in LN 511, located in the LG1 module of the globular domain of LN α chain, requires the tandem array of LG1-3 modules and the glutamic acid residue within the C-terminal region of LN γ chain for active conformation and full binding activity [45, 46]. For this study, we chose six synthetic peptides with reported ability to promote integrin α6β1-mediated cell adhesion or spreading. Peptide capability to support ES-NSPC adhesion and migration was first evaluated using adsorbed peptides. Regardless of P3 and N4 reported affinity to the α6β1 receptor, both physisorbed peptides failed to promote divalent cation- or integrin α6β1-dependent ES-NSPC adhesion. As these peptides have been used either conjugated with bovine serum albumin (P3) or in the soluble form (N4) [28, 29], these results suggest that peptides underwent conformational changes following physisorption which prevented ligand recognition. The other four peptides (T1, AG10, HYD1, and A5G81) showed ability to support

integrin α6β1-mediated ES-NSPC adhesion, while sustaining neuronal differentiation of ES-NSPCs. Of note, among all, HYD1 was the peptide eliciting the highest cell migration while leading to percentages of adherent cells and numbers of viable cells similar to those present on LN 111. All peptides were selected for immobilization into fibrin except AG-10, since on AG10-adsorbed surfaces ES-NSPCs showed a tendency for reduced cell viability and migration. The fact that cell binding to AG10 was not affected by EDTA suggests that AG10 interaction with α6β1 integrin occurred distant from metal-ion-dependent adhesion sites, in which divalent cations such as Mn^{2+} modulate integrin ligand-binding affinity by inducing conformational changes [42, 47].

Peptides T1, HYD1, and A5G81, carrying a substrate for activated factor XIII from the α2-plasmin inhibitor at the *N*-terminus, were bound to fibrin through the enzymatic cross-linking action of factor XIIIa. This strategy allows the covalent incorporation of peptides into fibrin to sites in the fibrin(ogen) α chain not used for intermolecular fibrinogen cross-linking [48], with retention of biological activity [49]. In the range of input peptide concentrations tested, a saturation plateau for covalent incorporation of the bi-domain peptides was not observed for any of the peptides. Peptides were incorporated at levels up to 6.27 ± 0.65 mol/mol fibrinogen (observed for a concentration of 320 μM of T1 bi-domain peptide in the polymerizing fibrin solution), which is far below the saturating levels reported for peptide incorporation into fibrin using this approach, namely of 17 moles of peptide per each of the two α chains of the fibrinogen molecule, attained when a large molar excess of peptide over fibrinogen is used [32]. The average peptide binding efficiencies found (19% through 32%), apparently low, are in fact slightly superior to the maximum cross-linking efficiency reported for factor XIIIa-catalyzed incorporation of bi-domain peptides containing the same factor XIIIa substrate (~14%) [49], a fact that may be associated with the different peptide labeling techniques used for peptide incorporation quantification.

To disclose the effect of immobilized T1, HYD1, and A5G81 on NSPC migration, the radial outgrowth assay was performed and fibrin gels containing soluble LN 111/511 used as controls. Cell migration is a process requiring a sustained balance between adhesion and tractile forces governed by a signaling axis involving integrin-ligand interactions, RhoA signaling, and actomyosin contractility forces, ultimately dependent on matrix properties, soluble factors and proteolytic activity [50, 51]. Integrin-ligand interactions are key in this process, and depend on integrin expression levels, ligand levels, and integrin-ligand binding affinity [52, 53]. Studies have shown that the higher the integrin-ligand binding affinity, the lower the ligand concentration required to induce

maximal cell migration or neurite extension [52, 53]. Tethering of T1 or HYD1 bi-domain peptides resulted in enhanced cell outgrowth area when incorporated at 20 or 40 μM in the polymerizing fibrin gel, and, in the case of HYD1, also in enhanced maximal outgrowth distance. The ability of HYD1 to induce radial outgrowth enhancement similar to that elicited by T1, but at lower levels of immobilized peptide in cross-linked gels relative to T1 (p = 0.001, HYD1 20 μM *vs.* T1 20 μM; $p < 0.001$, HYD1 40 μM *vs.* T1 40 μM), suggests that HYD1 has a higher affinity for receptor binding than T1. Studies have evidenced that cell migration and neurite extension in 2D and in 3D microenvironments exhibit a biphasic dependence on ligand concentration, the fastest migration occurring at an intermediate level of receptor occupancy, behind which further increasing the cell-matrix adhesiveness results in reduced cell migration [52, 53]. The biphasic effect of immobilized T1 and HYD1 on radial outgrowth is consistent to these observations. Particularly the trend for cell migration inhibition observed in gels formed at input concentrations of HYD1 higher than 40 μM, suggests that over this input concentration of HYD1 fibrin gels became too adhesive. The use of functional blocking antibodies evidenced that the migratory behavior elicited by T1 and HYD1 immobilized peptides was mediated by α6β1 and α3β1 integrins. In agreement to our results, the D-amino acid sequence of HYD1 is described to interact with both α6β1 and α3β1 integrins and to support cell adhesion when immobilized [27]. T1 peptide from the angiogenic inducer CCN1 is described to support α6β1-mediated cell adhesion, also in line with our findings, but, at the best of our knowledge, its interaction with α3β1 integrin has not been previously described [23]. Tethering of T1 or HYD1 at input peptide concentrations of 20 or 40 μM did not induce significant changes in the average pore diameter of fibrin network or in fibrin storage modulus. These results are in accordance with previous findings reporting minor disruption of fibrin structure or alterations in fibrin rheological properties due to peptide incorporation [49, 54]. Our results therefore indicate that the cell outgrowth enhancement observed in these gels was not associated to changes in fibrin network structure or viscoelastic properties.

In our study, the incorporation of soluble LN 111/511 did not promote cell migration, despite of their multiple bioactive domains, resulting in partial inhibition of cell outgrowth, more evident in the case of LN 511. These findings may be related to the absence in fibrin of binding motifs for LN and to the competition for receptor binding of exogenous soluble LN with cell-secreted LN, which is detected in 3D cultures of ES-NSPCs in fibrin mostly near cellular aggregates [8]. As expected, blocking of α6 and α3 integrin subunits showed a minor impact on radial outgrowth on unmodified fibrin, due to the absence in fibrin of motifs interacting with these integrins [22]. The small levels of

outgrowth inhibition registered may be related to the presence of cell-secreted LN, which, by being prevented to bind to α6β1 and α3β1 integrins was unable to provide adhesive cues for NSPC migration. In contrast, blocking of β1 integrin subunit resulted in a high cell outgrowth inhibition on unmodified fibrin (~96%, $p < 0.001$). Fibrin contains two endogenous RGD sequences that provide adhesiveness cues for neurite outgrowth [53]. Therefore, this result suggests that β1 integrin subunit may be involved in ES-NSPC binding to fibrin RGD domains, most possibly combined with α_V integrin subunit [55]. Fibronectin, present as a contaminant in commercially-available fibrinogen and secreted by ES-NSPCs during fibrin remodeling [8], may have also contributed to this effect. Fibronectin ability to support cell migration of neural progenitors is primarily mediated by α5β1 integrin [21] and, in contrast to LN, fibronectin is sequestered by fibrin through high affinity binding domains [22]. Finally, the inability of A5G81 bi-domain peptide to promote radial outgrowth suggests that A5G81 may require a free N-terminus for its bioactivity.

The effect of immobilized α6β1 integrin-binding ligands on the behavior of ES-NSPCs when seeded as single cells in fibrin was then assessed using fibrin gels functionalized with HYD1 (20 μM in the polymerizing gel). HYD1-functionalized gels led to significantly higher neurite extension from ES-NSPCs in a 3D environment, further supporting the pro-migratory activity of immobilized HYD1. Alterations in ES-NSPC proliferation or in the percentage of cells undergoing neuronal differentiation were not detected. The lack of an effect of immobilized HYD1 on cell proliferation is not surprising given that α6β1 integrin is not involved in LN-induced NSPC proliferation, unlike in LN-induced NSPC migration [18]. Moreover, although ES-NSPC neuronal differentiation is induced on LN substrates [20], α6β1 integrin involvement in this process still remains to be examined.

Finally, as α6 integrin mRNA was reported to be upregulated in regenerating DRG neurons and spinal motor neurons in adult rats after axonal injury [56, 57], HYD1-functionalized fibrin gel was evaluated in terms of ability to promote neurite extension in an *ex vivo* model of axonal growth. Immobilized HYD1 revealed to be effective in promoting neurite extension of rat E18 DRG neurons inducing a biphasic response similar to that observed for ES-NSPC neurospheres. However, cell response of DRG neurons to α6β1 ligands was observed over a broader range of input peptide concentrations. This finding may be explained by the ability of sensory neurons to post-translationally alter the amount of α6β1 integrin receptors expressed at the surface as a function of ligand availability, to maintain neurite outgrowth and neuronal growth-cone motility over a wide range of ligand densities [58]. Therefore, these results prompted us

to assess the effect of HYD1-functionalized gel on axonal regeneration *in vivo.* To examine axonal regeneration we used a rodent model of SCI in which the spinal cord is completely transected. A 4-mm-long segment of the spinal cord was further removed to assure the absence of spared axons between the nerve stumps [43]. Even though being the most reliable model to study axonal regeneration, complete transections are extremely disabling to animals, and the BBB scores attained by untreated animals at 9 weeks post-surgery typically range from 2 to 3 [7, 59]. Previous studies report that polymeric conduits filled with fibrin hydrogel lead to increased axonal regeneration as compared to unfilled conduits, when implanted in a completely transected spinal cord [60]. As the objective was to compare HYD1-functionalized fibrin with unmodified fibrin, and the presence of the chitosan porous conduit was transversal to the two conditions, animals receiving empty chitosan conduits were not included as a control group. We observed that rats treated with HYD1-functionalized fibrin attained BBB scores higher than those observed for unmodified fibrin, and notably, comparable to those reported for rats with complete spinal cord transection treated with much complex combinatorial therapies [59]. Furthermore, the presence of $GAP43^{+}$ fibers both in the central, rostral and caudal sites of the implantation/lesion area in both experimental groups indicates that the tethering of HYD1 to fibrin did not affect fibrin ability to support axonal growth. While in partial spinal cord lesions, axonal growth may arise either from regeneration of transected axons or sprouting of neighboring intact axons, in complete transection lesions axonal growth can only be associated with regeneration, particularly if a spinal cord segment is also removed. As such, our results provide evidence that HYD1-functionalized fibrin constitutes a permissive environment for axonal regeneration, either from axotomized neurons or from endogenous progenitors. Noteworthy, the trend for increased $GAP43^{+}$ area in animals receiving HYD1-functionalized fibrin as compared to those treated with unmodified fibrin, correlated well with the improved locomotor function observed in this experimental group. Nevertheless, to further impact axonal regeneration HYD1 concentration might need to be adjusted, since previous investigations have shown an upregulation of α6 and β1 integrin subunits after axonal injury in the adult rat [56]. Moreover, our results revealed that HYD1-functionalized fibrin supports the deposition of laminin, a well-known axonal-growth-permissive molecule [61].

Taken together, these studies provide insight into the benefits of decorating hydrogels with synthetic adhesive ligands interacting with integrin α6β1, when envisaging their use in *in vitro* 3D platforms involving ES-NSPCs and in regenerative therapies of the injured CNS. Future *in vivo* studies are required to determine how HYD1-functionalized

fibrin gel will perform when used as vehicle for ES-NSPCs in an *in vivo* scenario of chronic CNS injury, namely in terms of ability to promote donor cell survival, migration and neurite outgrowth, as well as infiltration of resident neural progenitors.

Conclusions

In this study we have shown that functionalization of fibrin hydrogels with the α6β1 integrin-binding peptides T1 and HYD1 provides adhesive cues promoting radial migration of ES-NSPC neurospheres on fibrin. We found that this process is mediated by α6β1 and α3β1 integrin receptors and that ES-NSPC migration exhibits a biphasic response to immobilized T1 and HYD1 peptides, with maximum enhancement being attained at input peptide concentrations of 20 or 40 μM. HYD1-functionalized fibrin was also shown to support neuronal regeneration, leading to enhanced neurite extension of sensory neurons *in vitro* when compared to native fibrin, and to a trend for increased axonal growth along with improved functional recovery after complete spinal cord transection. Our results point to the potential of HYD1-functionalized fibrin for the 3D culture of ES-NSPCs and for application in regenerative approaches for the treatment of CNS injuries.

Acknowledgements

The authors would like to acknowledge Prof. Domingos Henrique (Instituto de Medicina Molecular, Lisbon) for providing the ES 46C cell line. This work was supported by FEDER funds through the Programa Operacional Factores de Competitividade – COMPETE (FCOMP-01-0124-FEDER-021125) and by National Funds through FCT – Fundação para a Ciência e a Tecnologia (PTDC/SAU-BMA/118869/2010). A.R.B. and D.B. are supported by FCT (SFRH/BD/86200/2012; PD/BD/105953/2014).

References

[1] L.H. Thompson, A. Bjorklund, Reconstruction of brain circuitry by neural transplants generated from pluripotent stem cells, Neurobiology of disease 79 (2015) 28-40.
[2] O. Lindvall, Z. Kokaia, Stem cells in human neurodegenerative disorders - time for clinical translation?, Journal of Clinical Investigation 120(1) (2010) 29-40.
[3] P. Lu, G. Woodruff, Y. Wang, L. Graham, M. Hunt, D. Wu, E. Boehle, R. Ahmad, G. Poplawski, J. Brock, L.S.B. Goldstein, M.H. Tuszynski, Long-Distance Axonal Growth

from Human Induced Pluripotent Stem Cells after Spinal Cord Injury, Neuron 83(4) (2014) 789-796.

[4] H.S. Keirstead, G. Nistor, G. Bernal, M. Totoiu, F. Cloutier, K. Sharp, O. Steward, Human embryonic stem cell-derived oligodendrocyte progenitor cell transplants remyelinate and restore locomotion after spinal cord injury, Journal of Neuroscience 25(19) (2005) 4694-4705.

[5] S. Karimi-Abdolrezaee, E. Eftekharpour, J. Wang, C.M. Morshead, M.G. Fehlings, Delayed transplantation of adult neural precursor cells promotes remyelination and functional neurological recovery after spinal cord injury, Journal of Neuroscience 26(13) (2006) 3377-3389.

[6] A.P. Pêgo, S. Kubinova, D. Cizkova, I. Vanicky, F.M. Mar, M.M. Sousa, E. Sykova, Regenerative medicine for the treatment of spinal cord injury: more than just promises? , Journal of cellular and molecular medicine 16(11) (2012) 2564-2582.

[7] P. Lu, Y. Wang, L. Graham, K. McHale, M. Gao, D. Wu, J. Brock, A. Blesch, E.S. Rosenzweig, L.A. Havton, B. Zheng, J.M. Conner, M. Marsala, M.H. Tuszynski, Long-distance growth and connectivity of neural stem cells after severe spinal cord injury, Cell 150(6) (2012) 1264-73.

[8] A.R. Bento, P. Quelhas, M.J. Oliveira, A.P. Pêgo, I.F. Amaral, Three-dimensional culture of single embryonic stem-derived neural/stem progenitor cells in fibrin hydrogels: neuronal network formation and matrix remodeling, Journal of tissue engineering and regenerative medicine 11(12) (2017) 3494-3507.

[9] P.M. Kharkar, K.L. Kiick, A.M. Kloxin, Designing degradable hydrogels for orthogonal control of cell microenvironments, Chemical Society reviews 42(17) (2013) 7335-7372.

[10] K. Saha, J.F. Pollock, D.V. Schaffer, K.E. Healy, Designing synthetic materials to control stem cell phenotype, Current Opinion in Chemical Biology 11(4) (2007) 381-387.

[11] J.T. Parsons, A.R. Horwitz, M.A. Schwartz, Cell adhesion: integrating cytoskeletal dynamics and cellular tension, Nat Rev Mol Cell Bio 11(9) (2010) 633-643.

[12] C.C. DuFort, M.J. Paszek, V.M. Weaver, Balancing forces: architectural control of mechanotransduction, Nat Rev Mol Cell Bio 12(5) (2011) 308-319.

[13] P.E. Hall, J.D. Lathia, N.G.A. Miller, M.A. Caldwell, C. Ffrench-Constant, Integrins are markers of human neural stem cells, Stem Cells 24(9) (2006) 2078-2084.

[14] J.D. Lathia, B. Patton, D.M. Eckley, T. Magnus, M.R. Mughal, T. Sasaki, M.A. Caldwell, M.S. Rao, M.P. Mattson, C. Ffrench-Constant, Patterns of laminins and integrins in the embryonic ventricular zone of the CNS, J. Comp. Neurol. 505(6) (2007) 630-643.

[15] A.J. Copp, R. Carvalho, A. Wallace, L. Sorokin, T. Sasaki, N.D.E. Greene, P. Ybot-Gonzalez, Regional differences in the expression of laminin isoforms during mouse neural tube development, Matrix Biology 30(4) (2011) 301-309.
[16] L.S. Campos, D.P. Leone, J.B. Relvas, C. Brakebusch, R. Fassler, U. Suter, C. ffrench-Constant, b1 integrins activate a MAPK signalling pathway in neural stem cells that contributes to their maintenance, Development 131(14) (2004) 3433-3444.
[17] R. Nishiuchi, J. Takagi, M. Hayashi, H. Ido, Y. Yagi, N. Sanzen, T. Tsuji, M. Yamada, K. Sekiguchi, Ligand-binding specificities of laminin-binding integrins: A comprehensive survey of laminin-integrin interactions using recombinant α 3 β 1, α 6 β 1, α 7 β 1 and α 6 β 4 integrins, Matrix Biology 25(3) (2006) 189-197.
[18] T.S. Jacques, J.B. Relvas, S. Nishimura, R. Pytela, G.M. Edwards, C.H. Streuli, C. ffrench-Constant, Neural precursor cell chain migration and division are regulated through different β 1 integrins, Development 125(16) (1998) 3167-3177.
[19] J.G. Emsley, T. Hagg, α 6 β 1 integrin directs migration of neuronal precursors in adult mouse forebrain, Experimental Neurology 183(2) (2003) 273-285.
[20] W. Ma, T. Tavakoli, E. Derby, Y. Serebryakova, M.S. Rao, M.P. Mattson, Cell-extracellular matrix interactions regulate neural differentiation of human embryonic stem cells, Bmc Dev Biol, 2008.
[21] M.C. Tate, A.J. Garcia, B.G. Keselowsky, M.A. Schumm, D.R. Archer, M.C. LaPlaca, Specific β(1) integrins mediate adhesion, migration, and differentiation of neural progenitors derived from the embryonic striatum, Molecular and Cellular Neuroscience 27(1) (2004) 22-31.
[22] A.C. Brown, T.H. Barker, Fibrin-based biomaterials: Modulation of macroscopic properties through rational design at the molecular level, Acta Biomaterialia 10(4) (2014) 1502-1514.
[23] S.J. Leu, Y. Liu, N.Y. Chen, C.C. Chen, S.C.T. Lam, L.F. Lau, Identification of a novel integrin α(6)β(1) binding site in the angiogenic inducer CCN1 (CYR61), Journal of Biological Chemistry 278(36) (2003) 33801-33808.
[24] M. Nomizu, W.H. Kim, K. Yamamura, A. Utani, S.Y. Song, A. Otaka, P.P. Roller, H.K. Kleinman, Y. Yamada, Identification of Cell-Binding Sites in the Laminin α-1 Chain Carboxyl-terminal Globular Domain by Systematic Screening of Synthetic Peptides, Journal of Biological Chemistry 270(35) (1995) 20583-20590.
[25] F. Katagiri, M. Ishikawa, Y. Yamada, K. Hozumi, Y. Kikkawa, M. Nomizu, Screening of integrin-binding peptides from the laminin α 4 and α 5 chain G domain peptide library, Archives of Biochemistry and Biophysics 521(1-2) (2012) 32-42.

[26] I.B. DeRoock, M.E. Pennington, T.C. Sroka, R.S. Lam, G.T. Bowden, E.L. Bair, A.E. Cress, Synthetic peptides inhibit adhesion of human tumor cells to extracellular matrix proteins, Cancer research 61(8) (2001) 3308-3313.
[27] T.C. Sroka, M.E. Pennington, A.E. Cress, Synthetic D-amino acid peptide inhibits tumor cell motility on laminin-5, Carcinogenesis 27(9) (2006) 1748-57.
[28] O. Murayama, H. Nishida, K. Sekiguchi, Novel peptide ligands for integrin α6β1 selected from a phage display library, Journal of biochemistry 120(2) (1996) 445-451.
[29] F.I. Staquicini, E. Dias-Neto, J.X. Li, E.Y. Snyder, R.L. Sidman, R. Pasqualini, W. Arap, Discovery of a functional protein complex of netrin-4, laminin γ1 chain, and integrin α6β1 in mouse neural stem cells, Proceedings of the National Academy of Sciences of the United States of America 106(8) (2009) 2903-2908.
[30] Q.L. Ying, M. Stavridis, D. Griffiths, M. Li, A. Smith, Conversion of embryonic stem cells into neuroectodermal precursors in adherent monoculture, Nature Biotechnology 21(2) (2003) 183-186.
[31] P.C. Georges, W.J. Miller, D.F. Meaney, E.S. Sawyer, P.A. Janmey, Matrices with compliance comparable to that of brain tissue select neuronal over glial growth in mixed cortical cultures, Biophys J 90(8) (2006) 3012-3018.
[32] A. Ichinose, T. Tamaki, N. Aoki, Factor-XIII-Mediated Cross-Linking of NH_2-Terminal Peptide of α2-Plasmin Inhibitor to Fibrin, FEBS letters 153(2) (1983) 369-371.
[33] E. Mihalyi, Physicochemical studies of bovine fibrinogen. 4. Ultraviolet adsorption and its relation to structure of molecule, Biochemistry 7(1) (1968) 208-223.
[34] N. Aoki, T. Tamaki, A. Ichinose, Cross-linking of α2-plasmin inhibitor to fibrin catalized by activated fibrin-stabilizing factor, Thrombosis and Haemostasis 50(1) (1983) 169-169.
[35] I.F. Amaral, I. Neiva, F.F. da Silva, S.R. Sousa, A.M. Piloto, C.D.F. Lopes, M.A. Barbosa, C.J. Kirkpatrick, A.P. Pêgo, Endothelialization of chitosan porous conduits via immobilization of a recombinant fibronectin fragment ($rhFNIII_{7-10}$), Acta Biomaterialia 9(3) (2013) 5643-5652.
[36] D.M. Basso, M.S. Beattie, J.C. Bresnahan, Graded histological and locomotor outcomes after spinal cord contusion using the NYU weight-drop device versus transection, Experimental neurology 139(2) (1996) 244-256.
[37] S.W. Scheff, D.A. Saucier, M.E. Cain, A statistical method for analyzing rating scale data: the BBB locomotor score, Journal of neurotrauma 19(10) (2002) 1251-60.
[38] L.A. Flanagan, L.M. Rebaza, S. Derzic, P.H. Schwartz, E.S. Monuki, Regulation of human neural precursor cells by laminin and integrins, Journal of neuroscience research 83(5) (2006) 845-856.

[39] T.L. Laundos, J. Silva, M. Assunção, P. Quelhas, C. Monteiro , M.J. Oliveira, A.P. Pêgo, I.F. Amaral, Rotary orbital suspension culture of embryonic stem cell-derived neural stem/progenitor cells: impact of hydrodynamic culture on aggregate yield, morphology and cell phenotype, Journal of tissue engineering and regenerative medicine 11(8) (2017) 2227-2240.

[40] S.S. Rao, J.O. Winter, Adhesion Molecule-Modified Biomaterials for Neural Tissue Engineering, Frontiers in neuroengineering, 2009.

[41] C.D. Reyes, A.J. Garcia, A centrifugation cell adhesion assay for high-throughput screening of biomaterial surfaces, Journal of Biomedical Materials Research Part A 67A(1) (2003) 328-333.

[42] B.H. Luo, C.V. Carman, T.A. Springer, Structural basis of integrin regulation and signaling, Annual Review of Immunology (2007), pp. 619-647.

[43] M.H. Tuszynski, O. Steward, Concepts and Methods for the Study of Axonal Regeneration in the CNS, Neuron 74(5) (2012) 777-791.

[44] S. Shibuya, O. Miyamoto, T. Itano, S. Mori, H. Norimatsu, Temporal progressive antigen expression in radial glia after contusive spinal cord injury in adult rats, Glia 42(2) (2003) 172-183.

[45] H. Ido, K. Harada, Y. Yagi, K. Sekiguchi, Probing the integrin-binding site within the globular domain of laminin-511 with the function-blocking monoclonal antibody 4C7, Matrix Biology 25(2) (2006) 112-117.

[46] H. Ido, A. Nakamura, R. Kobayashi, S. Ito, S. Li, S. Futaki, K. Sekiguchi, The requirement of the glutamic acid residue at the third position from the carboxyl termini of the laminin γ chains in integrin binding by laminins, Journal of Biological Chemistry 282(15) (2007) 11144-11154.

[47] P.H. Weinreb, W.J. Yang, S.M. Violette, M. Couture, K. Kimball, R.B. Pepinsky, R.R. Lobb, S. Josiah, A cell-free electrochemiluminescence assay for measuring β1-integrin-ligand interactions, Analytical biochemistry 306(2) (2002) 305-313.

[48] S. Kimura, N. Aoki, Cross-Linking site in Fibrinogen for A-2-Plasmin Inhibitor, Journal of Biological Chemistry 261(33) (1986) 5591-5595.

[49] J.C. Schense, J.A. Hubbell, Cross-linking exogenous bifunctional peptides into fibrin gels with factor XIIIa, Bioconjugate Chemistry 10(1) (1999) 75-81.

[50] M.H. Zaman, L.M. Trapani, A. Siemeski, D. MacKellar, H. Gong, R.D. Kamm, A. Wells, D.A. Lauffenburger, P. Matsudaira, Migration of tumor cells in 3D matrices is governed by matrix stiffness along with cell-matrix adhesion and proteolysis, Proceedings of the National Academy of Sciences of the United States of America 103(29) (2006) 10889-10894.

[51] R.J. Petrie, K.M. Yamada, At the leading edge of three-dimensional cell migration, Journal of cell science 125(24) (2012) 5917-5926.
[52] S.P. Palecek, J.C. Loftus, M.H. Ginsberg, D.A. Lauffenburger, A.F. Horwitz, Integrin-ligand binding properties govern cell migration speed through cell-substratum adhesiveness, Nature 385(6616) (1997) 537-540.
[53] J.C. Schense, J.A. Hubbell, Three-dimensional migration of neurites is mediated by adhesion site density and affinity, Journal of Biological Chemistry 275(10) (2000) 6813-6818.
[54] K. Nam, J.P. Jones, P. Lei, S.T. Andreadis, O.J. Baker, Laminin-111 Peptides Conjugated to Fibrin Hydrogels Promote Formation of Lumen Containing Parotid Gland Cell Clusters, Biomacromolecules 17(6) (2016) 2293-2301.
[55] J. Arulmoli, H.J. Wright, D.T.T. Phan, U. Sheth, R.A. Que, G.A. Botten, M. Keating, E.L. Botvinick, M.M. Pathak, T.I. Zarembinski, D.S. Yanni, O.V. Razorenova, C.C.W. Hughes, L.A. Flanagan, Combination scaffolds of salmon fibrin, hyaluronic acid, and laminin for human neural stem cell and vascular tissue engineering, Acta Biomaterialia 43 (2016) 122-138.
[56] H. Hammarberg, W. Wallquist, F. Piehl, M. Risling, S. Cullheim, Regulation of laminin-associated integrin subunit mRNAs in rat spinal motoneurons during postnatal development and after axonal injury, Journal of Comparative Neurology 428(2) (2000) 294-304.
[57] W. Wallquist, J. Zelano, S. Plantman, S.J. Kaufman, S. Cullheim, H. Hammarberg, Dorsal root ganglion neurons upregulate the expression of laminin-associated integrins after peripheral but not central axotomy, Journal of Comparative Neurology 480(2) (2004) 162-169.
[58] M.L. Condic, P.C. Letourneau, Ligand-induced changes in integrin expression regulate neuronal adhesion and neurite outgrowth, Nature 389(6653) (1997) 852-856.
[59] K. Fouad, L. Schnell, M.B. Bunge, M.E. Schwab, T. Liebscher, D.D. Pearse, Combining Schwann cell bridges and olfactory-ensheathing glia grafts with chondroitinase promotes locomotor recovery after complete transection of the spinal cord, The Journal of neuroscience : the official journal of the Society for Neuroscience 25(5) (2005) 1169-78.
[60] E.C. Tsai, P.D. Dalton, M.S. Shoichet, C.H. Tator, Matrix inclusion within synthetic hydrogel guidance channels improves specific supraspinal and local axonal regeneration after complete spinal cord transection, Biomaterials 27(3) (2006) 519-33.
[61] M.A. Anderson, J.E. Burda, Y.L. Ren, Y. Ao, T.M. O'Shea, R. Kawaguchi, G. Coppola, B.S. Khakh, T.J. Deming, M.V. Sofroniew, Astrocyte scar formation aids central nervous system axon regeneration, Nature 532(7598) (2016) 195-200.

Supplementary Data

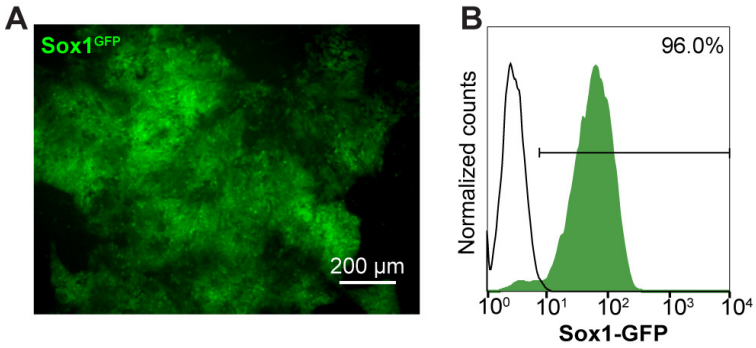

Figure S1. Analysis of Sox1^{GFP} (neural progenitor marker) expression in ES-derived NSPCs at day 5 of monolayer neural commitment. **(A)** Representative fluorescence microscopy image, showing the presence of neural progenitors (Sox1-GFP^{+} cells), often radially-distributed into rosette-like structures reminiscent of the structure of the developing neural tube. **(B)** Representative flow cytometry profile of undifferentiated 46C ES cells (in black) and Sox1-GFP^{+} cells (in green).

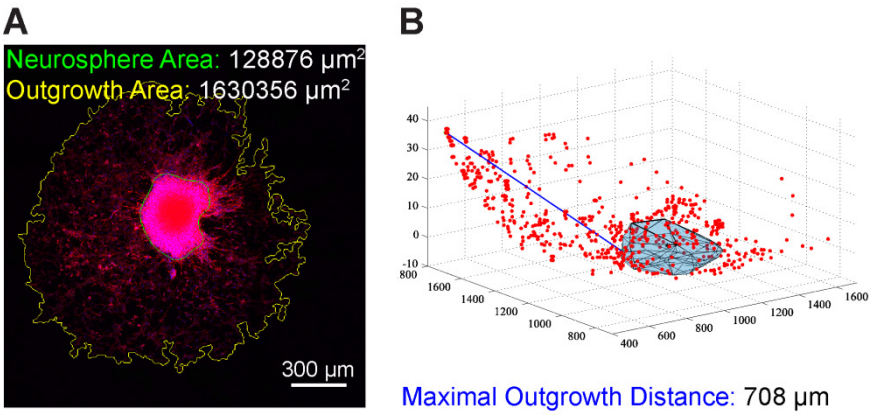

Figure S2. Quantitative image analysis methodology developed for the automatic quantification of the radial outgrowth area and the maximal outgrowth distance of ES-derived NSPCs neurospheres cultured on unmodified/functionalized fibrin gels. Radial outgrowth was defined as the region comprised between the neurosphere edge and the migration front. Radial outgrowth was determined in the 3D image stacks, by segmenting the volume of the neurosphere and that correspondent to cells cytoskeleton, using DNA and F-actin fluorescence images, respectively. This process was guided by an initial 2D maximal projection of the data in Z. The outgrowth area was given by the 2D maximal projection in Z of F-actin stack images subtracting the neurosphere area, given by the 2D maximal projection of DNA fluorescence images **(A)**. Maximal outgrowth distance was computed analyzing the two segmented volumes, namely the distance from the neurosphere volume boundary to the boundary of the volume correspondent to cells cytoskeleton **(B)**.

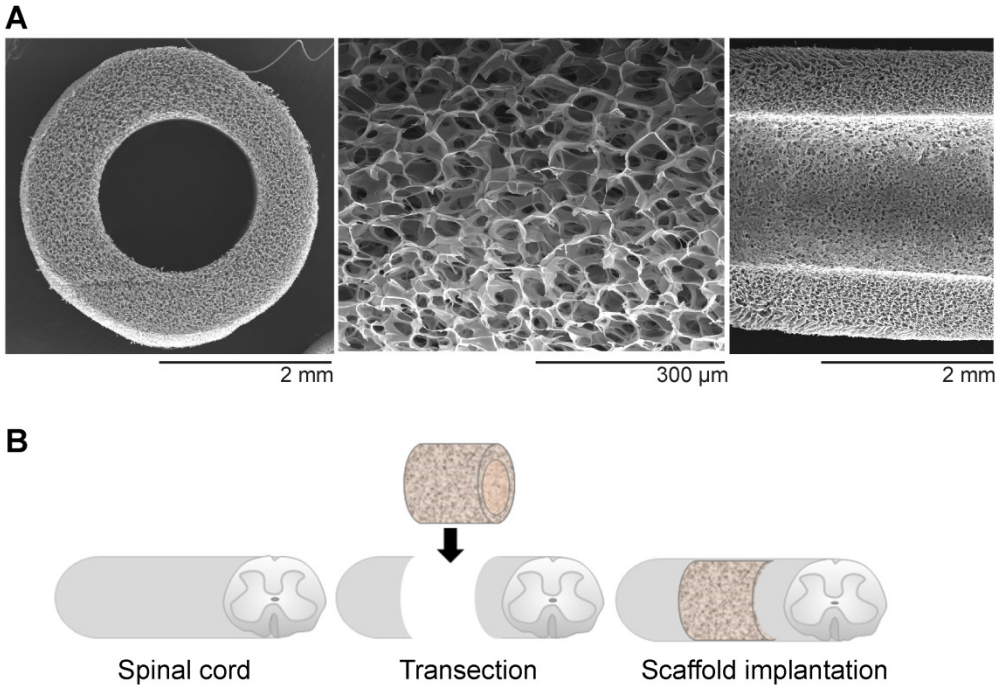

Figure S3. (A) Scanning electron micrographs of the chitosan tubular scaffolds used to bridge the cavity formed upon spinal cord transection; transversal (image left) and longitudinal (image right) cross-sections of dehydrated scaffolds are shown; the tubular scaffolds present outer and luminal surfaces with open porosity; high magnification images of the cross sections (image center) reveal an interconnected porous structure with average pore diameter of 56 ± 10 µm (Amaral *et al.,* 2013). **(B)** Schematic illustrating the implantation of the tubular scaffolds; the spinal cord was transected by removing a 4 mm region encompassing T8 and the porous conduit filled with unmodified or fibrin gel functionalized with 20 µM of HYD1 inserted into the defect, aligned along the longitudinal axis of the spinal cord.

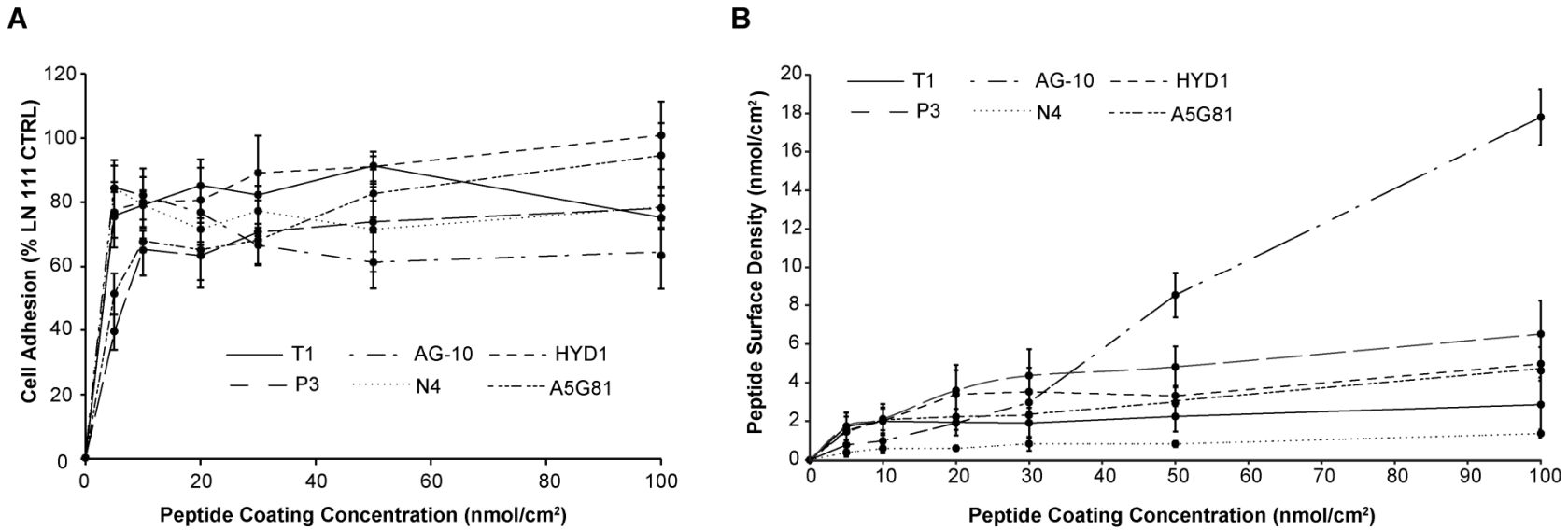

Figure S4. (A) Number of adherent ES-NSPCs on TCPS wells coated with synthetic peptides, as a function of the initial peptide coating concentration; ES-NSPCs were seeded on peptide-coated surfaces at 2×10^4 cells/cm^2, and the number of adherent cells quantified after 24 h of cell culture using a resazurin-based assay; cell numbers are expressed as a percentage of the LN 111 positive control (mean ± SD, *n* = 4–6). **(B)** Peptide adsorption as a function of peptide coating concentration assessed using the BCA method (mean ± SD, *n* = 6); the increase in AG10 adsorption observed with increasing peptide coating concentration may be due to AG10 net positive charge at pH 7.0 (+1.1) associated to its hydrophobic character [average hydrophilicity*: (-0.8)], as hydrophobic residues increase the tendency of peptide aggregation in the presence of polar solvents such as water. *Average hydrophilicity values calculated according to the Hopp-Woods hydrophilicity scale of amino acids.

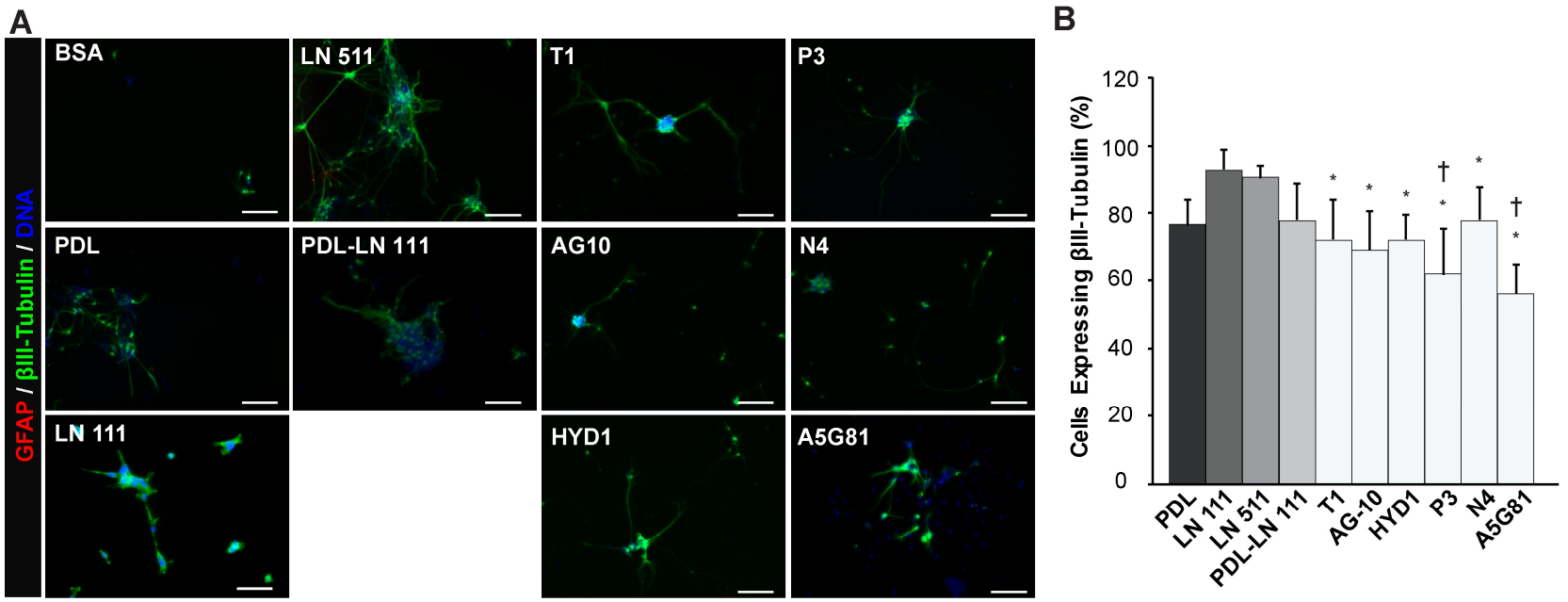

Figure S5. Evaluation of the ability of six synthetic peptides to support ES-NSPC neuronal differentiation. ES-NSPCs were seeded on TCPS wells coated with physisorbed peptides or with controls (BSA, PDL, LN 111, LN 511, or PDL-LN 111) and cultured for 6 days under neuronal differentiation conditions. **(A)** Double immunofluorescence staining of βIII-tubulin (early neuronal marker) and GFAP (astrocytic marker), showing cells expressing βIII-tubulin on all peptide-adsorbed surfaces; scale bars = 100 µm. **(B)** Percentages of βIII-tubulin$^+$ cells on peptide-adsorbed surfaces, as determined by image analysis (mean ± SD, n = 20 fields analyzed from 3 replicate cultures, * $p < 0.05$ *vs.* LN 111, one-way ANOVA followed by Dunnett's test); the percentage of βIII-tubulin$^+$ cells on BSA-treated surfaces is not depicted as the number of adhered cells was too low to proceed with quantification; among the different peptide-coated surfaces, P3- and A5G81-adsorbed surfaces showed the lowest number of βIII-tubulin$^+$ cells († $p < 0.05$ *vs.* T1, HYD1 and N4, one-way ANOVA followed by Bonferroni post-hoc test).

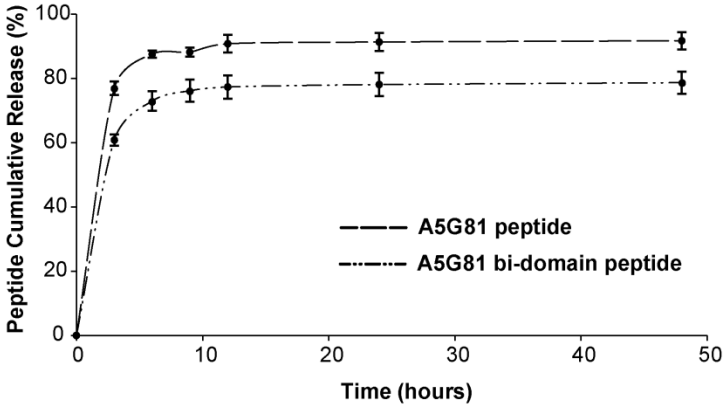

Figure S6. Release profile of soluble A5G81 *versus* bi-domain A5G81 from Fb gels, as determined using ^{125}I-labeled peptides. Fb gels were formed using a 20 μM input concentration of A5G81 (soluble) or A5G81 bi-domain peptide in the polymerizing gel. Results are the mean ± SD (n = 4). Peptide cumulative release after 24 h of incubation shows for gels containing the bi-domain peptide, higher peptide retention than those with the soluble peptide (21.9 ± 3.6% *vs.* 8.2 ± 2.7%; p = 0.001, Student's t-test), as expected from the covalent immobilization of the peptide through the activity of factor XIIIa.

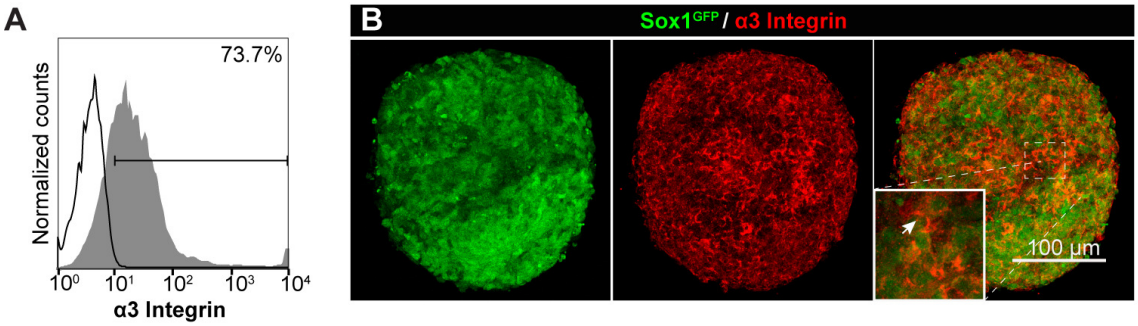

Figure S7. Analysis of α3 integrin expression in (**A**) ES-NSPCs, and in (**B**) floating aggregates of ES-NSPCs (neurospheres). **(A)** Flow cytometry analysis of cells stained with a monoclonal antibody against α3 integrin subunit (in gray) shows a percentage of cells expressing α3 integrin of 73.7%, after subtracting the percentage of positive events detected in cells incubated with the correspondent isotype control (in black); a representative fluorescence histogram is shown. **(B)** Integrin α3 subunit is highly expressed at cell-cell boundaries (arrow), as shown by immunofluorescence labeling of α3 integrin in whole neurospheres; images show 2D projections of CLSM 3D stack images covering a depth of 13 μm, from the surface to the core of the neurospheres.

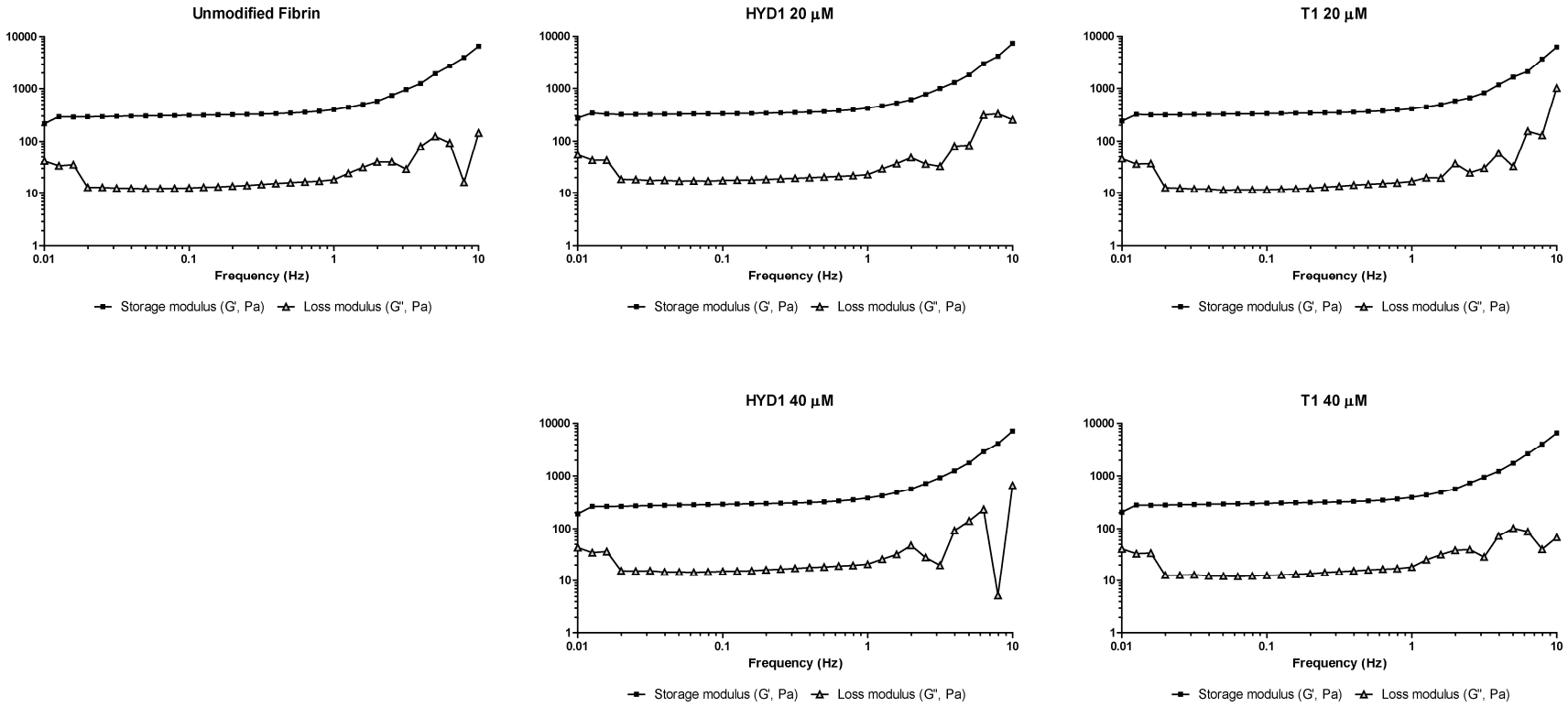

Figure S8. Representative graphs of frequency sweep tests carried out between 0.01 and 10 Hz at a fixed strain of 5% at 37°C for unmodified, HYD1- and T1-functionalized fibrin hydrogels.

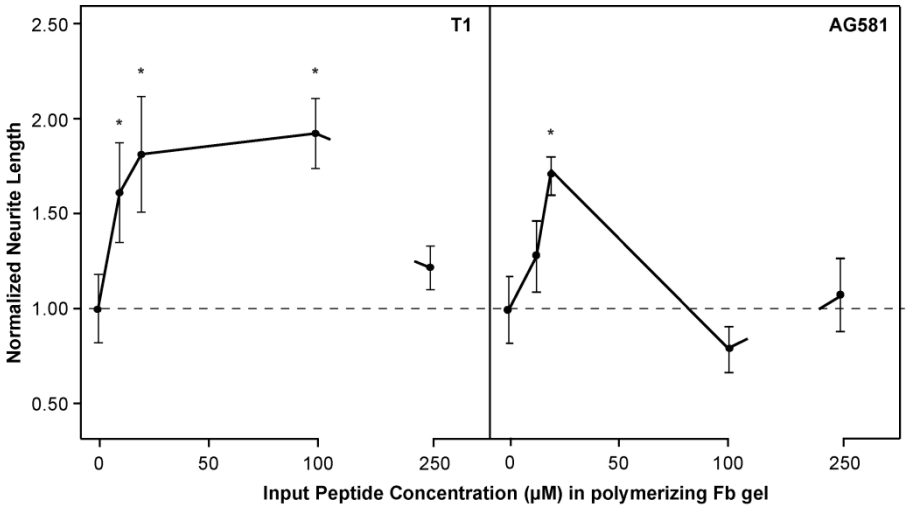

Figure S9. Neurite outgrowth from rat E18 dorsal root ganglia explants in T1- or A5G81-functionalized fibrin hydrogels, as a function of input peptide concentration. Dorsal root ganglia were embedded in functionalized fibrin gels and neurite outgrowth determined after 48 h of culture in samples processed for βIII-tubulin/DNA staining. Average neurite length was normalized to neurite extension in unmodified fibrin (mean ± SD, n = 6–9; * $p < 0.05$ vs. unmodified fibrin, ANOVA followed by Dunnett's test).

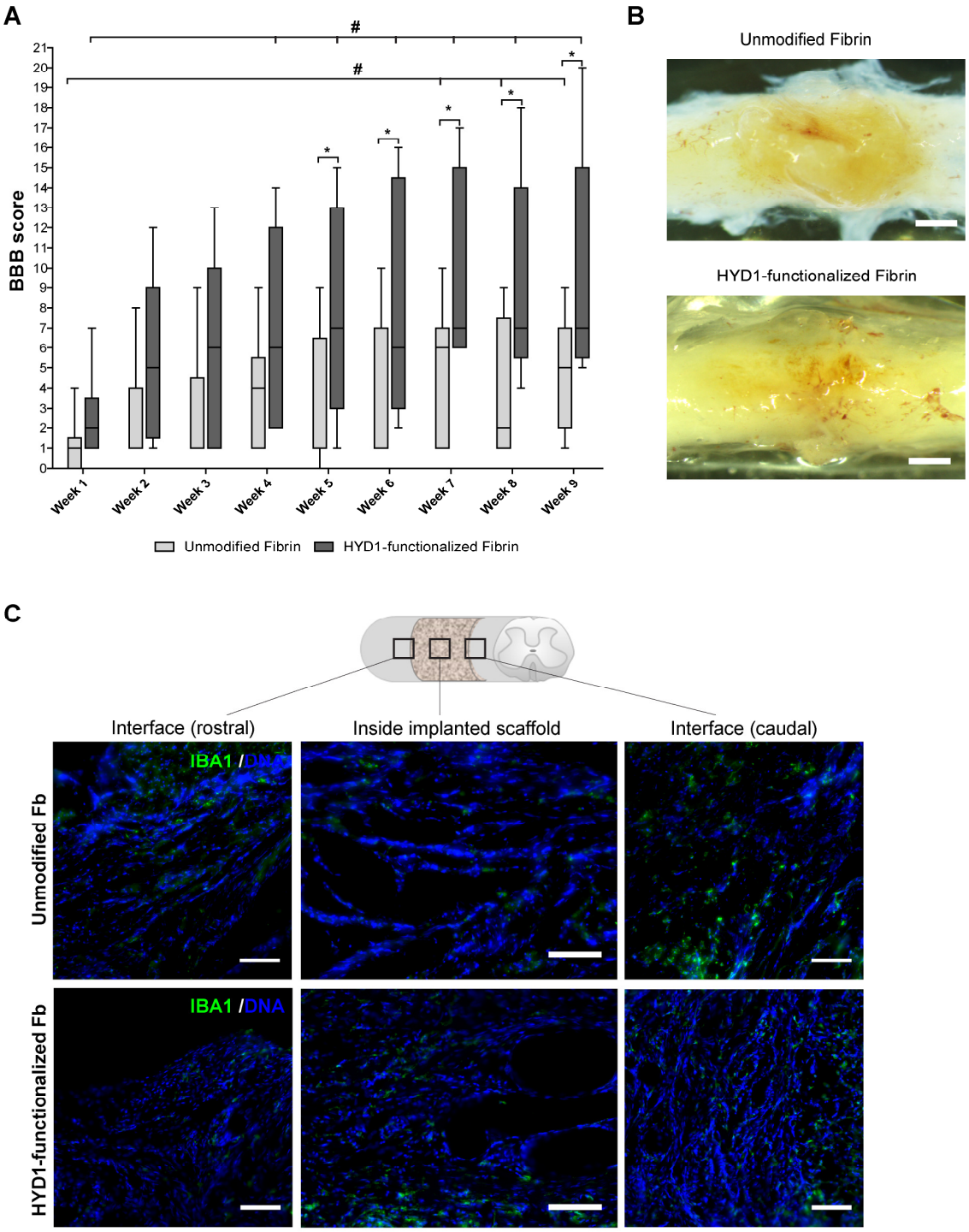

Figure S10. (A) BBB locomotor scores of the two experimental groups; the box plot chart depicts the minimum, the 25th percentile, the median, the 75th percentile, and the maximum (n = 9–10; * $p < 0.05$ *vs.* unmodified fibrin mixed repeated measures ANOVA followed by simple effect test; # $p < 0.05$ *vs.* week 1, one-way repeated measures ANOVA followed by Bonferroni post-hoc test). **(B)** Ten weeks after implantation of the chitosan tubular porous scaffolds, gross observation of the lesion site (dorsal view) shows the presence of a connective tissue bridge between the stumps of the spinal cord in both experimental groups; scale bars = 1 mm. **(C)** Immunofluorescence labeling of Iba1 in longitudinal (coronal) cryostat sections of the spinal cord revealed the presence of activated microglia and macrophages

predominantly at the implant-tissue interface as well as inside the scaffold in both conditions; scale bars = 100 µm. Fb, fibrin.

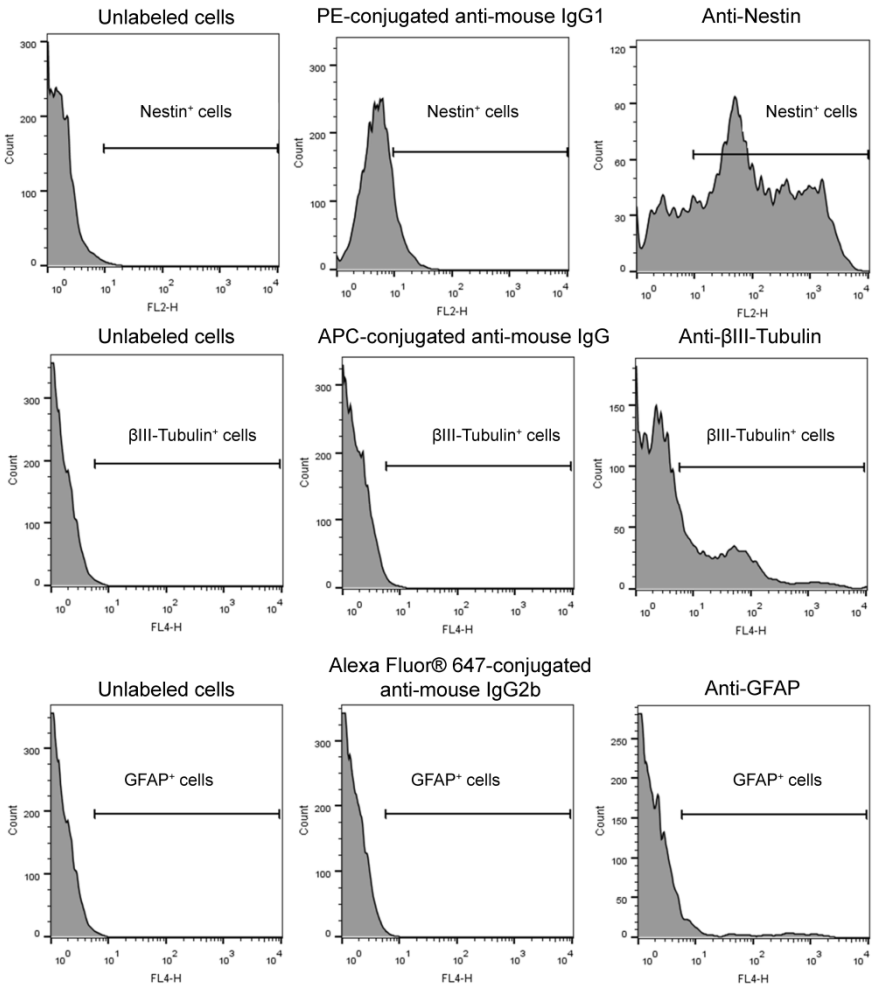

Figure S11. Representative flow cytometry histograms obtained for the phenotypic analysis of ES-NSPCs cultured under neuronal differentiation conditions within unmodified fibrin. At day 14 of cell culture cells were isolated from the fibrin matrices and processed for flow cytometry analysis. Cell debris was excluded by gating on forward and side scatter and unlabeled cells (fixed and permeabilized) processed in parallel used to set fluorescence gates. Cells incubated with secondary antibody only or with the correspondent isotype control were used to eliminate nonspecific background secondary antibody staining.

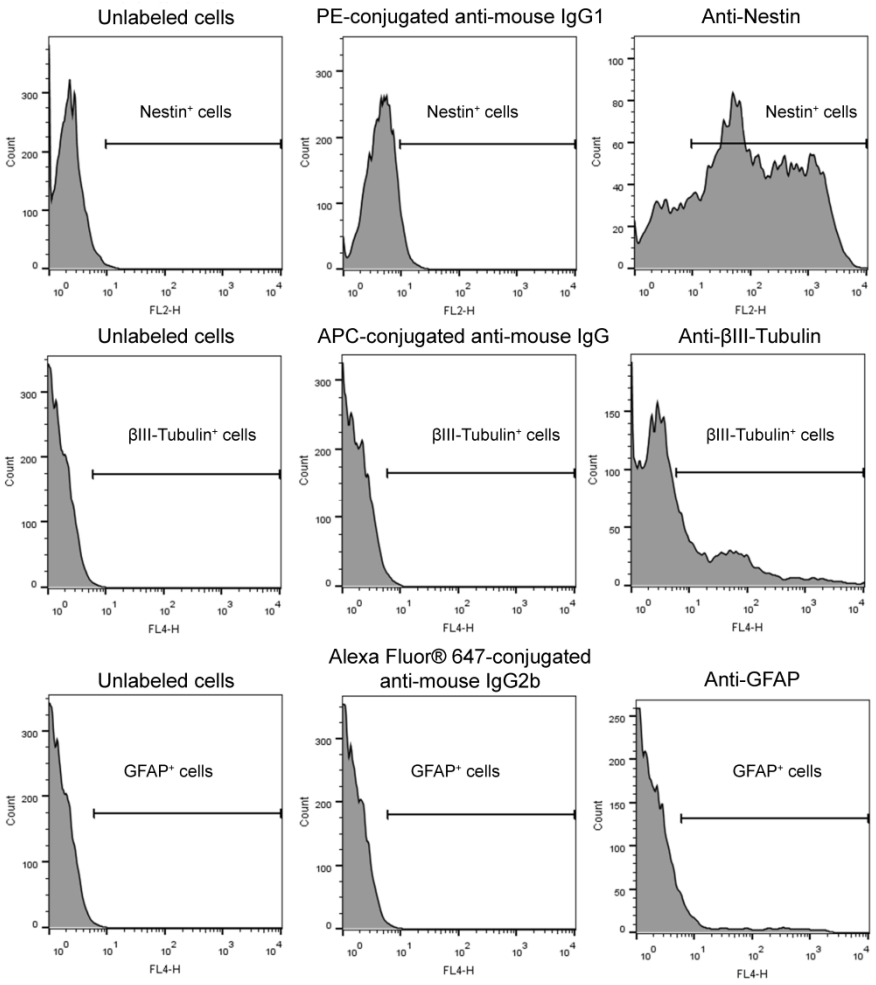

Figure S12. Representative flow cytometry histograms obtained for the phenotypic analysis of ES-NSPCs cultured under neuronal differentiation conditions within fibrin hydrogels functionalized with 20 μM of HYD1. At day 14 of cell culture cells were isolated from the fibrin matrices and processed for flow cytometry analysis. Cell debris was excluded by gating on forward and side scatter and unlabeled cells (fixed and permeabilized) processed in parallel used to set fluorescence gates. Cells incubated with secondary antibody only or with the correspondent isotype control were used to eliminate nonspecific background secondary antibody staining.

Supplementary Materials and Methods

Embryonic stem cell culture

A mouse embryonic stem (ES) cell line (46C) established at the Institute for Stem Cell Research (Edinburgh University, Scotland, UK) expressing green fluorescent protein (GFP) under the promoter of the neural-specific *Sox1* gene was used. Embryonic stem cells were propagated in KnockOut™ ESC/iPSC medium (Gibco) supplemented with 1% (v/v) penicillin/streptomycin (Pen/Strep; Gibco), 2 μM GSK-3 inhibitor IX (Calbiochem), and 1000 U/mL leukemia inhibitory factor (Chemicon) in 6-well tissue culture plates pre-adsorbed with 0.1% (w/v) gelatin (Sigma).

Neural commitment of embryonic stem cells

Neural commitment of ES cells was attained in chemically-defined medium and adherent monoculture on gelatin-coated wells [1]. Prior to initiating neural commitment, cells were cultured at a high cell seeding density (1×10^5 cells/cm^2) during 24 h. To start monolayer differentiation, cells were dissociated with StemPro® Accutase® (Gibco), resuspended in N2B27 medium, and plated onto gelatin-coated wells at 2×10^4 cells/cm^2, the medium being renewed every 2 days. N2B27 is a 1:1 mixture of DMEM/F12 medium without phenol red, supplemented with 1% (v/v) modified N2 [1] and Neurobasal™ medium (supplemented with 2% (v/v) B27 and 1% (v/v) L-glutamine) supplemented with 1% (v/v) Pen/Strep (all Gibco). At day 5 of the monolayer differentiation protocol, Sox1-GFP expression was analyzed by flow cytometry, to assess the efficiency of neural conversion. For this purpose, cells were dissociated, resuspended in PBS buffer containing 2% (v/v) fetal bovine serum, and run on a flow cytometer (FACSCalibur™ Becton Dickinson). Live cells were gated based on forward scatter (size) and side scatter (cell complexity) criteria, and fluorescence gates set using undifferentiated 46C ES cells as negative control. A minimum of 1×10^4 events was captured inside the gate, and data analyzed using FlowJo™ software. A representative fluorescence histogram is shown in Figure S1.

Immunohistochemistry

Samples were washed twice with PBS, fixed in 3.7% (w/v) paraformaldehyde (PFA) solution diluted 1:1 in culture media (30 min; 37°C), and, when staining for intracellular markers, permeabilized with 0.2% (v/v) Triton X-100 in PBS (45 min; RT). Samples

were then incubated with blocking buffer (60 min) and then with primary antibodies (overnight; 4°C). To detect primary antibodies, samples were incubated with the appropriate species-specific Alexa Fluor® conjugated secondary antibodies (Molecular Probes; 1:500) for 4 h. When necessary, nuclei were counterstained with DAPI (Sigma; 0.1 µg/mL) for 10 min. Samples were finally mounted with Fluoromount™ (Sigma) and observed under confocal laser scanning microscopy (CLSM; Leica TCS SP5II). All primary antibodies and solutions are listed in Table S1.

Immunocytometry

Cells were fixed in 1% (w/v) PFA in PBS buffer (20 min; 4°C) and, when staining for intracellular markers, permeabilized with 0.2% (v/v) Triton X-100 in PBS (10 min; 4°C). Cells were subsequently incubated in blocking buffer (20 min; 4°C) and then with primary antibodies or with isotype controls (30 min; RT). Primary antibodies were detected by applying isotype-specific or species-specific secondary antibodies (30 min; RT). Cells were finally washed trice with FACS buffer [2% (v/v) fetal bovine serum and 0.1% sodium azide (w/v) in PBS], and analyzed by flow cytometry. Cell debris and dead cells were excluded from the analysis based on electronic gates using forward scatter and side scatter criteria and unlabeled cells used to set fluorescence gates. Cells stained with secondary antibody only or with the correspondent isotype control were used to eliminate nonspecific background secondary antibody staining. All antibodies and solutions are listed in Table S2.

Evaluation of α6β1 synthetic ligands' ability to support ES-NSPC adhesion, viability, migration, and differentiation

Peptides were physisorbed to the wells of tissue-culture plates or to inserts (overnight; 37°C) as described in methods, rinsed twice with PBS, and incubated with 1% (w/v) heat-inactivated BSA (1 h; 4°C) to block non-specific adhesion.

Cell adhesion centrifugation assay: to compare cell adhesion of embryonic stem-derived neural stem/progenitor cells (ES-NSPCs) to the various physisorbed peptides, a centrifugation cell adhesion assay that applies uniform detachment forces was used [2]. ES-NSPCs were fluorescently-labeled with 2 µM of calcein AM (Molecular Probes; 10 min; 37°C), resuspended in N2B27 medium, and transferred to peptide-adsorbed surfaces at 3×10^5 cells/cm^2. Cells were allowed to adhere for 2 h, and before subjecting the cells to centrifugation, pre-spin fluorescence readings were measured using a

microwell plate reader (BioTek's Synergy™ Mx). After overfilling the wells with PBS until a positive meniscus was observed, the plates sealed with transparent tape, inverted, and spun at 100 RCF (relative centrifugal force) for 5 min. Following cell detachment, the media was gently aspirated from the wells, and the wells refilled with medium for measurement of post-spin fluorescence readings. For each well, the adherent cell fraction was determined as the ratio of post-spin to pre-spin fluorescence readings (λ_{ex} = 485 nm; λ_{em} = 535 nm).

Cell adhesion inhibition assay: the contribution of divalent cations and α6/β1 integrin subunits to cell adhesion was assessed quantifying cell adhesion in the absence or presence of EDTA or function-blocking antibodies, respectively. Due to the high number of experimental conditions involved, the crystal violet method was used as an alternative to the cell adhesion centrifugation assay, to avoid delay in centrifugation and, as a result, different incubation periods between multi-well plates. For this purpose, ES-NSPCs were incubated for 15 min at 37°C in N2B27 medium in the absence or presence of 5 mM EDTA or monoclonal antibodies against α6 (clone NKI-GoH3, Serotec; 20 μg/mL) or β1 (clone Ha2/5, BD Pharmigen; 10 μg/mL) integrin subunits. To evaluate the contribution of non-specific antibody interactions to cell adhesion inhibition, incubation with isotype-matched controls for α6 (rat IgG2a, Millipore; 20 μg/mL) and β1 antibodies (hamster IgM λ1, Pharmigen; 10 μg/mL) was also performed. Preliminary experiments were performed to optimize the concentration of both monoclonal antibodies in terms of cell adhesion inhibition. Concentrations of 20 and 10 μg/mL were selected for incubation with α6 and β1 monoclonal antibodies, respectively, since the use of higher concentrations did not result in statistical significant higher cell adhesion inhibition levels (data not shown). Cell suspension was then transferred to peptide-adsorbed surfaces at 3×10^5 cells/cm^2, and cells were allowed to adhere for 2 h in the absence or presence of inhibitors. At the end of this period, the wells were washed twice in order to remove non-adherent cells, fixed in 3.7% (w/v) PFA solution diluted 1:1 in culture media (30 min; 37°C), and stained with 0.1% (w/v) crystal violet in 20% methanol for 30 min. Excess dye was washed off with distilled water and the plate was left to dry overnight. For crystal violet extraction, the cells were incubated with 10% (v/v) CH_3COOH, and adherent cells quantified by measuring the optical density at 570 nm (BioTek's Synergy™ Mx microwell plate reader).

Cell viability: ES-NSPCs were resuspended in N2B27 medium supplemented with 10 ng/mL of basic fibroblast growth factor (bFGF), and plated on peptide-adsorbed

surfaces at 2×10^4 cells/cm^2. After 24 h of cell culture, the number of viable cells was quantified using a resazurin-based assay [3]. Briefly, the cell layers were incubated with culture medium containing resazurin (Sigma) at a final concentration of 10 µg/mL (4 h at 37°C). At the end of this period, 100 µL of the culture medium was transferred to a black-walled 96-well plate, fluorescence measured (λ_{ex} = 530 nm; λ_{em} = 590 nm), and the fluorescence values correspondent to unseeded wells subtracted. Cell numbers were extrapolated from a standard curve where fluorescence was plotted against known number of cells seeded on poly-D-lysine/laminin 111-coated coverslips in parallel.

Cell migration: the migratory capacity of ES-NSPCs was evaluated using a Transwell® system with 8-µm pore membrane (Falcon®) and vascular endothelial growth factor (VEGF) as chemoattractant. Both sides of the Transwell® membrane were coated (overnight; 37°C). Peptide-adsorbed membranes were rinsed and blocked as described for the preparation of peptide-adsorbed wells, and the inserts placed in culture wells of companion plates containing 700 µL of N2B27 medium supplemented with 50 ng/mL of VEGF. ES-NSPCs were resuspended in N2B27 at 10×10^5 cells/mL and 200 µL of cell suspension added to the upper chamber. Cells were allowed to migrate towards VEGF during 4 h (37°C; 5% CO_2). After incubation, cells were fixed in 3.7% (w/v) PFA solution diluted 1:1 in culture media (30 min; 37°C), and the cells remaining in the upper side of the insert removed by cotton swabs. The membrane was incubated with 0.1 µg/mL DAPI for DNA labeling, and the nuclei of migrated cells counted under an inverted optical fluorescence microscope (Axiovert 200, Carl Zeiss) in 10 randomly selected fields/membrane using a 20× magnification objective.

Neuronal differentiation: to assess the ability of physisorbed peptides to support ES-NSPC differentiation along the neuronal lineage, ES-NSPCs were resuspended in N2B27 and plated on peptide-adsorbed surfaces at 2×10^4 cells/cm^2. Cells were cultured for 6 days following a protocol for neuronal differentiation [4]. Initially, cells were cultured in N2B27 supplemented with 10 ng/mL bFGF and, at day 2 of culture, the medium was switched to the mix N2B27:Neurobasal/B27 (1:1) without growth factor, half of the medium being changed every other day. At day 6 of cell culture, the samples were processed for double immunofluorescence staining of βIII-tubulin (early neuronal marker) and glial fibrillary acid protein (GFAP, astrocytic marker), and incubated with DAPI for DNA labeling. Samples were finally observed under fluorescence microscopy and the percentage of βIII-tubulin$^+$ cells quantified using an automatic image analysis tool developed using MATLAB®. The image analysis

approach comprised the application of a low pass filter, applied to both nuclei and βIII-tubulin image channels followed by an Otsu automatic segmentation to obtain binary images. Subsequently the βIII-tubulin image was compared with the nuclei image. The nuclei overlapping the βIII-tubulin objects were quantified, and expressed as a percentage of the total number of nuclei. For each condition, 20 randomly selected fields from two replicate cultures were analyzed, corresponding to a minimum of 2×10^3 cells on peptide-adsorbed surfaces.

^{125}I-labeling of bi-domain peptides

To facilitate radioiodination, bi-domain peptides lacking a tyrosine residue (such as T1, HYD1, and A5G81 bi-domain peptides) were reacted with sulfosuccinimidyl-3-(4-hydroxyphenyl)propionate (Sulfo-SHPP, Pierce-Thermo Scientific™), to conjugate a tyrosine-like residue to the N-terminal amine. Briefly, bi-domain peptides (2 mg) were dissolved in 100 mM borate buffer and modified with Sulfo-SHPP according to the supplier at a lower pH (8.5), to increase selectivity towards the N-terminal amine. Bi-domain peptides were separated from non-reacted Sulfo-SHPP by gel filtration (PD MidiTrap G-10 columns, GE Healthcare) using PBS as elution buffer, and further detected by UV-vis spectrophotometry at 280 nm. Peptide concentration was determined by the bicinchoninic acid method (Pierce® BCA Protein Assay, Thermo Scientific™), using standard curves prepared from known amounts of the target peptides, freshly resuspended. Bi-domain peptides (5 µg) were subsequently labeled with 0.5 mCi of $Na^{125}I$ (Perkin Elmer) using the Iodogen method [5], and further purified using a PD MidiTrap G-10 column, to remove free ^{125}I ions. Labeled peptides were stored at -20°C and used the following day.

Neuronal differentiation of ES-NSPCs cultured within functionalized fibrin hydrogels

ES-NSPCs were dissociated with StemPro® Accutase® into single cells and embedded in functionalized fibrin gels [6]. Briefly, ES-NSPCs were resuspended in fibrinogen solution, and functionalized Fb gels (50 µL) formed in the wells of a 6-well non-tissue culture plate (6 gels per well) as described in methods (final cell seeding density: 1×10^6 cells/mL). Polymerizing gels were incubated at 37°C for 30 min before the addition of 3 mL of culture medium. Cells were cultured within the gels for periods up to 14 days following a protocol for neuronal differentiation [4]. Initially cells were cultured in N2B27 supplemented with 10 ng/mL bFGF and, at day 2 of culture, the medium was switched to the mix N2B27:Neurobasal/B27 (1:1) without growth factor. At day 8, half of the

medium was replaced by the mix N2B27:Neurobasal/B27 (1:3) supplemented with 20 ng/mL brain-derived neurotrophic factor and 50 ng/mL nerve growth factor (BDNF and NGF; PeproTech), half of the medium being changed every other day. To delay fibrin degradation, 5 µg/mL of aprotinin were added to the culture medium.

Neurite outgrowth: neurite outgrowth from cellular spheroids was quantified at day 6 of cell culture in samples processed for βIII-tubulin/DNA staining. This time point was selected to avoid overlapping of cell processes extending between neighboring spheroids (which could compromise image analysis of neurite outgrowth). Processed samples were analyzed by CLSM. Spheroid- and neurite-containing regions were obtained by automatic segmentation of 2D maximum intensity projections of DNA and βIII-tubulin CLSM image stacks, respectively. Given the segmented regions, the number of neuronal processes protruding from the edge of cellular spheroids was manually annotated, and the length of the longest neurite automatically computed using MATLAB® software.

Distribution of viable/dead cells: the cell/matrix constructs were processed for analysis of cell viability at day 6 of cell culture. Samples were rinsed with warm PBS, and sequentially incubated with 4 µM calcein AM (30 min; 37°C) and 6 µM propidium iodide (Sigma; 10 min; 37°C) for detection of viable and dead cells, respectively. After incubation, samples were washed twice with PBS, transferred to culture media, and immediately observed under CLSM.

Total cell number: total cell number was estimated by quantifying total DNA amount in each gel at days 7 and 14 of cell culture, after cell isolation from the cell-matrix constructs. Briefly, at the end of each culture period the constructs were washed twice with warm PBS, and sequentially incubated with 1.25 mg/mL of collagenase type II (Gibco; 1 h; 37°C) and 1× trypsin-EDTA (Gibco; 20 min; 37°C) in the orbital shaker (70 rpm). After trypsin inactivation with serum-containing media cells were gently dissociated, centrifuged, and incubated with 1% (v/v) Triton X-100 (60 min; 4°C) in the orbital shaker (200 rpm) for cell lysis. The resultant cell lysate was centrifuged (10 000×g; 10 min) to remove cell debris and total DNA quantified using the Quant-iT™PicoGreen® dsDNA assay kit (Invitrogen), according to the manufacturer's instructions. Cell numbers were inferred from the mean DNA content of a known number of ES-NSPCs (n = 3) frozen at the beginning of the experiment.

Expression of characteristic phenotypic markers: after 14 days of cell culture, cell phenotype was analyzed by immunohistochemistry and by flow cytometry.

Immunohistochemistry analysis was performed in whole-mount cultures as described above, using antibodies against nestin (NSPC marker), βIII-tubulin (early neuronal marker), synapsin (synaptic vesicles marker), and glial fibrillary acidic protein (GFAP, astrocytic marker). For flow cytometry analysis, cells from six-pooled gels were isolated as described above, and the resultant single cell suspensions processed for immunocytometry (see above), using antibodies against nestin, βIII-tubulin, and GFAP. Representative fluorescence histograms are shown in Figures S11 and S12.

Neurite extension from rat E18 dorsal root ganglia cultured within functionalized fibrin hydrogels

Dorsal root ganglia (DRG) were dissected from E18 Wistar rat embryos. Functionalized fibrin gels (10 µL) were formed in the lower wells of a 15-well µ-Slide Angiogenesis plate from Ibidi as described for the radial outgrowth assay, and DRG explants transferred to the center of polymerizing fibrin gels (1 DRG/well) with the help of Dumont forceps. After incubation at 37°C for 30 min, 40 µL of DMEM/F12 medium supplemented with 2% (v/v) B27, 30 ng/mL nerve growth factor (NGF; Calbiochem), 1% (v/v) P/S, 1.25 µg/mL amphotericin B (Gibco), and 10 µg/mL aprotinin were added to each well. Neurite outgrowth was quantified after 48 h of cell culture. Samples were processed for βIII-tubulin/DNA staining, and average neurite length quantified in images acquired by inverted optical fluorescence microscopy (Axiovert 200, Carl Zeiss). Average neurite length was computed as the width of an annulus of area equal to the area of the neurite zone: $L = (1/\pi)^{1/2} [(A_{inner} + A_{outer})^{1/2} - (A_{inner})^{1/2}]$, where A_{inner} represents the area covered by the cell bodies and A_{outer} corresponds to the area between the cell bodies and the neurites ends [7].

In vivo experiments

To assess the effect of functionalized fibrin gels on axonal regeneration, an *in vivo* model of spinal cord injury (SCI; total transection) was used. Chitosan tubular scaffolds prefilled with functionalized fibrin gel or unmodified fibrin (control) were used to bridge the cavity formed upon spinal cord transection.

Preparation of chitosan porous conduits filled with functionalized fibrin gel: chitosan cylindrical hollowed porous scaffolds (4 mm long and inner diameter of 1.8 mm; Fig. S3A) were prepared as previously described [8], from squid pen chitosan (France Chitine; degree of acetylation 3.55), after purified (endotoxin levels < 0.1 EU/mL). The

scaffolds were sterilized in 70% (v/v) ethanol, equilibrated in sterile PBS (2×; 10 min), and 30 µL of HYD1-functionalized polymerizing fibrin gel (6 mg/mL fibrinogen; 2 NIH U/mL thrombin; 2.5 mM $CaCl_2$; 25 µg/mL aprotinin; 20 µM of HYD1 bi-domain peptide) were added to the inner channel of the porous conduits, under the stereoscopic magnifier. The fibrin-filled scaffolds were incubated at 37°C for 30 min to allow cross-linking, and then placed in 500 µL of N2B27 medium containing 5 µg/mL of aprotinin. Chitosan porous conduits filled with unmodified fibrin were prepared in parallel to be used as controls.

Animal surgery, implantation of fibrin-filled porous conduits, and post-operative care: a total of 20 female Wistar rats (Charles River Laboratories) 10–13 weeks old and weighting 210–240 g were used. Animals were given proper bedding material (corn cob) and shredded paper and cardboard rolls as nesting material. Food and water were provided *ad libitum*. Animals were randomized into 2 experimental groups, to be implanted with either HYD1-functionalized fibrin or unmodified fibrin control. Surgeries were done in parallel over multiple days. Prior to surgery, buprenorphine (0.04 mg/kg) and glycosylated serum were administered subcutaneously. Animals were anesthetized through intraperitoneal administration of a saline solution containing ketamine (37.5 mg/kg) and medetomidine (0.25 mg/kg). Surgical procedures started when deep anesthesia was observed (loss of postural, caudal, pedal and palpebral reflexes). The animal fur was removed right above the T10 vertebrae, and the surgical area disinfected with 70% (v/v) ethanol and povidone-iodide solution (3×). During surgery, the animals were kept on a heating pad kept at 37°C, a saline solution was applied to the animal's eyes every 5 min, and deep anesthesia maintained through a continuous supply of 1% isoflurane mixed with oxygen. The spinal cord was exposed by laminectomy made at the T7–T9 level and the cord was fully transected by removing a 4 mm region encompassing T8 using a straight spring scissor (Fine Science Tools). The porous conduit filled with HYD1-functionalized fibrin/unmodified fibrin was then inserted into the defect, aligned along the longitudinal axis of the spinal cord (Fig. S10B), assuring that the severed ends of the cord fit tightly. Tisseel Lyo® (Baxter; 100 µL/animal) was applied to the top of the lesion to hold the tubular scaffold in place. After suturing the muscle and the skin layers, atipamezole (1 mg/kg) was administered subcutaneously to reverse medetomidine-induced anesthesia. After surgery, the animal was placed in a box containing humid food and an electric heating blanket to maintain the animal body temperature. During the first 3 days post-surgery, animals received buprenorphine (0.04 mg/kg) twice a day, as well as Duphalyte® (injectable solution with vitamins and amino acids), subcutaneously, to relief pain and prevent animal

dehydration, respectively. To prevent urinary infections Bactrim™ was added to the water (4.4 mL/500 mL of water) during the first week post-surgery. Throughout all the post-operative period, the bladders were manually voided twice a day. Animals were monitored every day and weighted weekly.

Locomotor recovery and histological analysis: locomotor function was assessed during training (pre-injury) and post-injury, weekly during 9 weeks, using the Basso, Beattie, and Bresnahan (BBB) open-field locomotion rating scale [9]. Before surgery, all the animals were healthy with a maximum BBB score, and animals were evenly distributed among both groups. The test was conducted in a blinded manner by two independent operators. Ten weeks post-implantation, the animals were anesthetized with ketamine (75 mg/kg) and medetominide (0.5 mg/kg) and transcardially perfused with 150 mL of ice-cold sodium phosphate buffer 0.2 M (pH = 7.4) followed by 4% (w/v) PFA in sodium phosphate buffer. The spinal cord was carefully dissected, post-fixed in 4% (w/v) PFA (overnight at 4°C), washed with PBS (3×), and transferred to 30% (w/v) sucrose in PBS at 4°C for 24 h, for cryoprotection. Spinal cords were then transferred to fresh 30% sucrose solution in PBS and stored at -20°C until use. For tissue sectioning, spinal cords were embedded in Richard-Allan Scientific™ Neg-50™ Frozen Section Medium (Thermo Scientific). Longitudinal (coronal) cryostat sections were cut at 20 µm increments and serially collected in SuperFrost® slides for immunohistochemical staining, with every 10th section mounted on the same slide. Sections were rinsed in PBS, blocked with 5% donkey serum or normal goat serum in 0.3% (v/v) Triton-X 100 in PBS (1 h; RT), and incubated with the following primary antibodies in blocking buffer (overnight; 4°C): rabbit anti-GAP43 (AB5220, Millipore; 1:500), rabbit anti-GFAP (Z0334, Dako; 1:400), mouse anti-βIII-tubulin (801201, Biolegend; 1:500), mouse anti-nestin (MAB353, Chemicon; 1:200), rabbit anti-laminin (L9393, Sigma; 1:100) and rabbit anti-Iba1 (019-19741, Wako; 1:500). Sections were washed with PBS and then incubated with Alexa-fluorophore-conjugated donkey or goat secondary antibodies (Molecular Probes) in blocking buffer (1:1000; 1 h; RT). Following incubation, the samples were rinsed with PBS and nuclei stained using Hoechst 33342 (Invitrogen; 1 µg/mL; 10 min; RT). The sections were finally mounted in Fluoromount™ and examined with the IN Cell Analyzer 2000 imaging system (GE Healthcare) using a 20×/0.75 NA objective or using the CLSM. Axonal sprouting/regeneration in each animal was determined in 2D projections of the IN Cell Analyzer 3D stack images, analyzing the area occupied by $GAP43^+$ axons in the lesion area, expressed as a percentage of the total lesion area (see dashed lines; Fig. 7B). Similar and sequential sections were stained for GFAP to help to identify the lesion margins, and matched to

lesion margins defined in the GAP43 stained sections. Sections processed in parallel in the absence of primary antibodies were used to establish the threshold pixel intensity. For each animal, four sections from two different slides were analyzed, and the $GAP43^{+}$ area averaged. All analyses were conducted in a blinded manner.

Table S1 – Solutions and primary antibodies used in immunohistochemistry.

Marker	**Permeabilization**	**Blocking buffer**	**Primary antibody**			
			Name	**Reference**	**Company**	**Dilution**
α3 integrin subunit	-	5% (v/v) NGS in PBS	Anti-integrin α3 (clone P1B5)	MAB1952P	Millipore	1:50
α6 integrin subunit			Rat anti-human CD49f (clone NKI-GoH3)	MCA699GA	Serotec	1:50
β1 integrin subunit			Anti-mouse CD29 (clone KMI6)	14-0292-82	eBiosciences	1:20
Nestin	0.2% (v/v) Triton X-100 in PBS	5% (v/v) NGS in PBS containing 0.05% (v/v) Tween-20	Mouse anti-nestin (clone rat-401)	MAB353	Chemicon	1:100
βIII-tubulin			Rabbit anti-βIII-tubulin	ab18207	Abcam	1:500
Synapsin		5% (v/v) NGS + 5% (v/v) FBS in PBS	Rabbit anti-synapsin	ab1543P	Abcam	1:1000
GFAP		M.O.M.™ mouse IgG blocking reagent (Vector)	Purified mouse anti-GFAP	556327	BD Pharmingen	1:500

Abbreviations: FBS, fetal bovine serum; GFAP, glial fibrillary acidic protein; NGS, normal goat serum; PBS, phosphate buffer saline.

Table S2 – Solutions and antibodies used in immunocytometry.

Marker	Permeabilization	Blocking buffer	Primary antibody				Secondary antibody			
			Name	Reference	Company	Dilution	Name	Reference	Company	Dilution
α3 integrin subunit	-	5% (v/v) NGS in PBS	Anti-integrin α3 (clone P1B5)	MAB1952P	Millipore	1:50	APC-conjugated goat anti-mouse IgG F(ab')2	sc-3818	Santa Cruz Biotech	1:100
			Mouse IgG1 negative control	CBL610	Millipore	1:50				
α6 integrin subunit			Rat anti-human CD49f (clone NKI-GoH3)	MCA699GA	Serotec	1:50	APC-conjugated goat anti-rat IgG F(ab')2	sc-3832		
			Rat IgG2a negative control	MCA1124R	Serotec	1:4				
β1 integrin subunit			Anti-mouse CD29 (clone KMI6)	14-0292-82	eBiosciences	1:20				
			Rat IgG2a negative control	MCA1124R	Serotec	1:4				
Nestin	0.2% (v/v) Triton X-100 in PBS	5% (v/v) NGS in PBS containing 0.1% (w/v) Saponin	Mouse anti-nestin (clone rat-401)	MAB353	Chemicon	1:100	PE-conjugated goat anti-mouse IgG1	sc-3764		
βIII-tubulin			Mouse anti-βIII-tubulin	MMS-435P	Covance	1:500	APC-conjugated goat anti-mouse IgG F(ab')2	sc-3818		
GFAP			Alexa Fluor® 647 mouse anti-GFAP	561470	BD Pharmigen	1:100	-			
			Alexa Fluor® 647 mouse IgG2b isotype control	558713						

Abbreviations: GFAP, glial fibrillary acidic protein; NGS, normal goat serum; PBS, phosphate buffer saline.

Supplementary References

[1] Q.L. Ying, M. Stavridis, D. Griffiths, M. Li, A. Smith, Conversion of embryonic stem cells into neuroectodermal precursors in adherent monoculture, Nature Biotechnology 21(2) (2003) 183-186.

[2] C.D. Reyes, A.J. Garcia, A centrifugation cell adhesion assay for high-throughput screening of biomaterial surfaces, Journal of Biomedical Materials Research Part A 67A(1) (2003) 328-333.

[3] J. O'Brien, I. Wilson, T. Orton, F. Pognan, Investigation of the Alamar Blue (resazurin) fluorescent dye for the assessment of mammalian cell cytotoxicity. , European Journal of Biochemistry 267 (2000) 5421-5426.

[4] L. Conti, S.M. Pollard, T. Gorba, E. Reitano, M. Toselli, G. Biella, Y.R. Sun, S. Sanzone, Q.L. Ying, E. Cattaneo, A. Smith, Niche-independent symmetrical self-renewal of a mammalian tissue stem cell, Plos Biology, 2005.

[5] Iodine-^{125}, a guide to radioiodination techniques, in: A.L. Sciences (Ed.) Amersham International, Little Chalfont, Buckinghamshire, UK, 1993, p. p. 64.

[6] A.R. Bento, P. Quelhas, M.J. Oliveira, A.P. Pêgo, I.F. Amaral, Three-dimensional culture of single embryonic stem-derived neural/stem progenitor cells in fibrin hydrogels: neuronal network formation and matrix remodeling, Journal of tissue engineering and regenerative medicine 11(12) (2017) 3494-3507.

[7] C.B. Herbert, C. Nagaswami, G.D. Bittner, J.A. Hubbell, J.W. Weisel, Effects of fibrin micromorphology on neurite growth from dorsal root ganglia cultured in three-dimensional fibrin gels, Journal Biomedical Materials Research 40 (1998) 551-559.

[8] I.F. Amaral, I. Neiva, F.F. da Silva, S.R. Sousa, A.M. Piloto, C.D.F. Lopes, M.A. Barbosa, C.J. Kirkpatrick, A.P. Pêgo, Endothelialization of chitosan porous conduits via immobilization of a recombinant fibronectin fragment (rhFNIII$_{7-10}$), Acta Biomaterialia 9(3) (2013) 5643-5652.

[9] D.M. Basso, M.S. Beattie, J.C. Bresnahan, Graded histological and locomotor outcomes after spinal cord contusion using the NYU weight-drop device versus transection, Experimental Neurology 139(2) (1996) 244-256.

CHAPTER IV

Controlling the density of α6β1 integrin- or syndecan-binding motifs tethered to fibrin improve the outgrowth of hES-derived neural stem cells

Ana R. Bento [1,2,3], Ana P. Pêgo [1,2,3,4], Isabel F. Amaral [1,2,3]

[1] INEB - Instituto de Engenharia Biomédica, Universidade do Porto, Portugal; [2] i3S - Instituto de Investigação e Inovação em Saúde, Universidade do Porto, Portugal; [3] Faculdade de Engenharia, Universidade do Porto, Portugal;[4] ICBAS - Instituto de Ciências Biomédicas Abel Salazar, Universidade do Porto, Portugal.

Abstract

The transplantation of neural stem/progenitor cells (NSPCs) derived from pluripotent stem cells holds much promise for the treatment of central nervous system (CNS) disorders. In an effort to provide a more permissive environment for cell survival and engraftment following transplantation the combination of NSPCs with biodegradable hydrogels such as fibrin is being explored. Besides preventing cell dispersion following injection these vehicles provide a physical support for NSPC anchorage, migration and differentiation, ultimately contributing to their integration and to the formation of functional neuronal relay circuits. Recently, we reported that fibrin functionalization with synthetic adhesive peptides engaging the laminin receptor integrin α6β1 results in enhanced neurite outgrowth both from murine embryonic stem (ES)-derived NSPCs and rat dorsal root ganglia explants. Envisaging the translation of the developed hydrogels into the clinic, we assessed if the tethering of integrin α6β1-binding peptides HYD1 (KIKMVISWKG) or T1 (GTTSWSQCSKS) could enhance fibrin capacity to support the outgrowth of human ES-derived neural stem cells (hES-NSCs). Furthermore, to improve fibrin bioactivity towards hES-NSCs, we explored the immobilization of a syndecan-binding peptide with neurite outgrowth promoting activity, namely the AG73 peptide sequence from the globular domain of laminin α1 chain (RKRLQVQLSIRT). Due to the modulatory role of syndecans on integrin signaling, the combination of HYD1 or T1 with AG73 is expected to synergistically increase outward migration of hES-NSCs. In line with our previous results, fibrin functionalization with HYD1 was effective in enhancing cell outgrowth of hES-NSCs in fibrin when incorporated at 20 μM (1.2-fold increase *vs.* unmodified fibrin), although the improvement was smaller when compared to that obtained with murine ES-NSPCs. The tethering of AG73 peptide to fibrin also promoted the outgrowth of hES-NSCs, namely when incorporated at 60 μM in the polymerizing gels (up to 1.3-fold increase *vs.* unmodified fibrin). Altogether, our results demonstrate that the conjugation of α6β1 integrin- or syndecan-binding motifs can be of interest to increase the bioactivity of hydrogels used in the 3D culture of hES-NSCs and potentially, in matrix-assisted NSPC transplantation for the treatment of the injured CNS, foreseeing a better efficacy of these therapeutic approaches.

Keywords: human embryonic stem-derived neural stem cells, α6β1 integrin, fibrin, cell outgrowth, syndecan, laminin, peptide immobilization.

Introduction

Transplantation of neural stem cells (NSCs) is a promising therapeutic approach to restore neurological function of patients suffering from central nervous system (CNS) disorders. Through the release of soluble factors, including neurotrophic factors, growth factors and cytokines, transplanted NSCs can protect existing neural cells against damage *in situ* [1], while promoting the regrowth of disrupted neuronal axons [2]. Furthermore, the transplantation of NSCs offers the possibility of replacing lost neurons and supporting cells, particularly the oligodendrocytes that form myelin sheaths around axons. In fact, transplanted NSCs have been reported to contribute for the recovery the lost neural function in experimental models of several CNS diseases, such as spinal cord injury, stroke and neurodegenerative diseases [1, 3]. Despite being already tested in clinical trials, the bolus injection of a suspension of neural stem/progenitor cells (NSPCs) into the lesion site often leads to limited neuroprotection/tissue repair, due to low cell survival and/or poor integration [4, 5]. To overcome this, biodegradable hydrogels have been explored for *in situ* delivery of single NSCs or aggregates of NSCs (neurospheres). Besides allowing a homogenous NSC distribution at the site of injury, hydrogels contribute to sequester neurite-promoting factors, providing a supportive niche for cell survival, differentiation and axonal regeneration [6, 7]

In order to efficiently deliver NSCs into the damaged CNS, hydrogels should provide biophysical and/or biochemical cues present in the natural cell niche while presenting structural and mechanical properties matched to those of the native tissue [8]. The incorporation of biophysical cues in hydrogels, like full length extracellular matrix (ECM) proteins or short synthetic bioactive oligopeptides, can be used to recreate biological processes such as enabling enzyme-mediated degradation [9], specific binding of soluble biomolecules such as growth factors, or directing cell adhesion, migration, proliferation and differentiation [10, 11].

In an effort to enhance fibrin bioactivity for use as a NSC vehicle, namely in terms of its capacity to sustain NSC neurite outgrowth and migration, we have recently explored its functionalization with synthetic adhesive peptides interacting with integrin α6β1, a laminin receptor that recognizes the LG1–3 module of laminin α chains [12]. This cell adhesion receptor is highly enriched in human NSCs [13] and plays a crucial role in NSC migration [14]. Specifically, integrin α6β1 was shown to mediate the migration of neural precursors *in vivo* [15] and of human ES-derived neural progenitors on laminin substrates [16]. As in fibrin, motifs interacting with α6β1 integrin receptors are absent [17], we hypothesized that the tethering of α6β1 integrin ligands could enhance its

capacity to support neurite outgrowth of embryonic stem (ES)-NSC-derived neurons, ultimately contributing to the integration of transplanted ES-NSCs into the host tissue. We reported that the functionalization of fibrin with the integrin α6β1-binding motifs HYD1 or T1 peptides enhanced the radial outgrowth of murine ES-NSPCs (mES-NSPCs), and that this process is mediated by α6β1 and α3β1 integrins. Moreover, HYD1-functionalized fibrin hydrogels were also shown to promote neurite extension of sensory neurons, and to improve the recovery of locomotor function in a spinal cord injury experimental model [18].

The use of cell adhesive binding motifs interacting with syndecans can also be of interest to enhance the biofunctionality of fibrin hydrogels towards NSPCs, due to their role in modulating integrin-dependent processes such as cytoskeletal organization, cell adhesion, migration, proliferation, and differentiation, including neurogenesis and synaptogenesis [19-21]. Syndecans are a small family of four transmembrane proteoglycans in mammals: syndecan-1, -2, -3 and -4. These cell adhesion receptors are comprised of an extracellular domain, a single transmembrane domain and a short cytoplasmic domain (Figure 1).

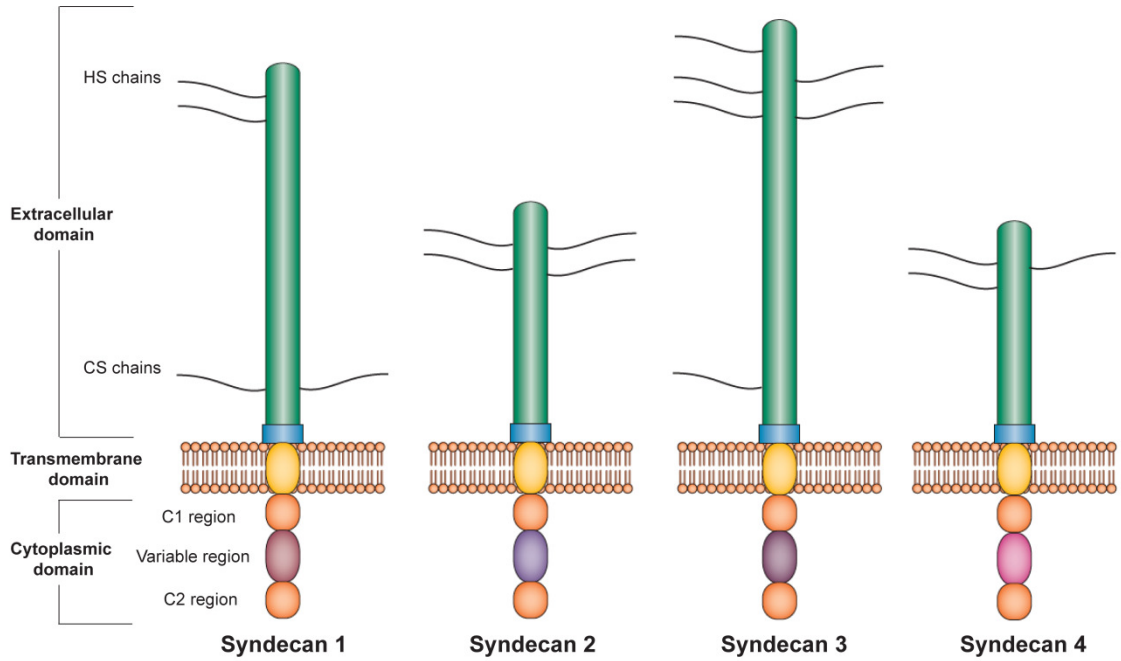

Figure 1. Schematic of syndecans structure. HS, heparan sulfate. CS, chondroitin sulfate. Image adapted from Pap and Bertrand [22], Copyright© 2012, with permission from Springer Nature.

The extracellular domain of syndecans contains heparan sulfate (HS) and/or chondroitin sulfate (CS) chains that bind to growth factors [e.g. basic fibroblast growth factor (bFGF) and epidermal growth factor (EGF)], and to extracellular matrix (ECM)

molecules, namely to laminin and fibronectin [23]. Moreover, both syndecan-1 and -4 have been described to interact directly or indirectly with several integrin heterodimers, leading to the activation of downstream signaling pathways that control cellular behavior [24, 25]. In particular, the cooperation of syndecan-4 with α5β1 integrin was shown to be required for focal adhesion formation and cell migration [26].

Syndecans bind to laminin through the LG4–5 (laminin G-like) region of laminin α chains [27, 28]. Syndecan-1 also interacts with the *N*-terminal laminin EGF-like (LE) domains of the laminin γ2 chain to regulate cell adhesion and motility [29]. Given that LG domains of the laminin α chains are capable of binding to syndecan and integrin α6β1, it is likely that both receptors associate to act synergistically. Despite that mechanisms are not completely understood, it has been proposed that syndecans make the initial contacts with the ECM, but are then moved laterally by localized actin polymerization to allow integrin engagement [30, 31]. The cross-talk between integrins and syndecans is known to be complex, and possibly regulated by innumerous mechanisms, that can each regulate a subset of functions depending on cellular context and the dynamic regulation of interactions with ECM, growth factors, chemokines, directional cues and receptor tyrosine kinases/phosphatases [20].

Interestingly, several investigations address the key role of the syndecan family in the biology and function of NSCs. Syndecan-1 is required for mouse NSPC maintenance and proliferation [32], and syndecan-4 is known to regulate neural induction [33]. Amongst the four proteins of the syndecan family, syndecan-1, -2 and -3 demonstrated high expression in basal human NSCs derived from the H9 ES cells, with extended culture upregulating syndecan-2 and -3 expression [34]. Syndecan-4 expression was found to be upregulated following neuronal differentiation [34].

The tethering of syndecan-binding peptides to hydrogel matrices to promote neurite outgrowth is not new [35]. Specifically, the modification of alginate- [36] and collagen-based hydrogels [21] with the RKRLQVQLSIRT sequence (AG73 peptide) from the LG4 module of laminin α1 chain, interacting with syndecan-1 and -4 [37, 38], was reported to promote neurite outgrowth of PC12 neuronal cells.

In the present study, and foreseeing the translation of the developed hydrogels into a clinical setting, we assessed if fibrin functionalization with HYD1 or T1 integrin α6β1-binding peptides could also be effective in enhancing neurite extension of hES-NSCs. Furthermore, we explored if covalent immobilization of the syndecan-binding peptide AG73 could enhance fibrin ability to support hES-NSC outgrowth. Since little is known

concerning the expression profile of integrins and syndecans in hES-NSCs [39], we started by assessing the expression of integrin α6, α3 and β1 subunits, and also of syndecan-1 and -4, in hES-NSCs, when cultured under basal conditions. We have previously reported the capacity of unmodified fibrin hydrogels to support cell viability, and neuronal differentiation of hES-NSCs seeded within fibrin in the form of single cells [40]. Therefore, dissociated hES-NSCs were cultured within HYD1-/T1-/AG73-functionalized fibrin gels, and cell outward migration quantified as a function of input peptide concentration [18]. Moreover, the ability of functionalized fibrin hydrogels to support hES-NSC neuronal differentiation was also evaluated.

Materials and Methods

Culture of hES-NSC within functionalized fibrin gels

Human neural stem cells derived from H9 ES cells (hES-NSC) were purchased from Life Technologies and expanded in poly-L-ornithine/laminin 111-coated tissue culture polystyrene (TCPS) plates, according to the manufacturer's protocol (Gibco). Passage 15 was set as the longest time in culture [41]. Fibrin hydrogels functionalized with peptides HYD1 (KIKMVISWKG), T1 (GTTSWSQCSKS) and AG73 (RKRLQVQLSIRT) were prepared as previously described [18], using the enzymatic cross-linking action of the transglutaminase factor XIIIa for peptide immobilization into fibrin [42]. For this purpose, bi-domain peptides containing the sequence of interest at the carboxyl terminus and a factor XIIIa substrate from the NH_2-terminal sequence of α2-plasmin inhibitor (residues NQEQVSPL) at the amino terminus were synthesized at GenScript with a C-terminal amide (purity > 95%). Functionalized fibrin gels were formed by mixing equal volumes of a fibrinogen solution and a thrombin solution in TBS containing $CaCl_2$, aprotinin, and the bi-domain peptides [final concentration of Fb components: 6 mg/mL plasminogen-free fibrinogen from pooled human plasma containing factor XIII; 2 NIH U/mL thrombin from human plasma; 2.5 mM $CaCl_2$; 25 μg/mL aprotinin (all Sigma-Aldrich); 2.5 to 160 μM of bi-domain peptides]. Human ES-NSCs were dissociated into single cells using StemPro® Accutase® [Gibco, 4 min at room temperature (RT)] and further suspended in the fibrinogen solution before transferring the polymerizing fibrin solution (50 μL gels; 1×10^6 hES-NSCs/mL) to 13 mm tissue culture coverslips (Sarstedt). Polymerizing gels were then incubated at 37°C for 30 min to allow cross-linking by factor XIIIa. The cell-matrix constructs were cultured under neuronal differentiation conditions in presence of 10 μg/mL of aprotinin (Sigma-Aldrich) as previously described [40], for periods up to 14 days. In brief, hES-NSCs

within fibrin were initially cultured in StemPro® NSC serum free media (SFM) containing basic fibroblast growth factor (bFGF) and epidermal growth factor (EGF) and, at day 2 of culture, the medium was switched to the mix StemPro® NSC SFM media:Neurobasal/B27 (1:1), without growth factors (all from Gibco). At day 8, half of the medium was replaced by the mix StemPro® NSC SFM:Neurobasal/B27 (1:3) supplemented with 10 ng/mL of recombinant human brain-derived growth factor (BDNF, Peprotech) and 500 µM of dibutyryl cyclic adenosine monophosphate (Sigma-Aldrich). Half of the medium was changed every other day. Unmodified fibrin (Unm Fb) gels were used as controls in every experiment performed.

Immunocytometry

Immunocytometry analysis was performed after gentle cell dissociation using StemPro Accutase. Briefly, hES-NSCs were washed once with PBS, and sequentially incubated with StemPro® Accutase® (4 min at RT). Cells were gently dissociated, diluted in Glasgow's MEM (BHK-21; Gibco) containing 10% inactivated fetal bovine serum (1:3, FBS; Sigma), centrifuged, and suspended in cell culture medium. For staining of intracellular markers, cells were fixed with 1% (w/v) paraformaldehyde (PFA; 20 min at 4°C), and permeabilized with 0.2% (v/v) Triton X-100 (10 min at 4°C). Cells were then incubated in blocking buffer for 20 min and then incubated for 30 min with primary antibodies diluted in PBS buffer containing 1% (v/v) normal goat serum (NGS, Biosource) and 0.1% (w/v) saponin. Primary antibodies were detected by applying isotype-specific or species-specific secondary antibodies for 30 min. For immunolabeling of cell surface markers, the fixation and permeabilization steps were omitted, and the blocking/primary antibody solutions prepared without saponin. Cells were finally washed 3× and suspended in FACS buffer containing sodium azide, for flow cytometry analysis (BD FACSCalibur™). The following primary antibodies were used: anti-integrin α3 (1:50; clone P1B5; MAB1952P, Millipore), rat anti-human CD49f (1:50; clone NKI-GoH3; MCA699GA, Serotec), anti-αvβ3 (1:50; clone LM609, MAB1976; Chemicon), anti-CD29 (1:25; clone MEM-101A; 21270293, Immunotools), anti-syndecan-1 (1:50; clone B-A38; ab34164, Sigma) and anti-syndecan-4 (1:40; clone 5G9; sc-12766, Santa Cruz). Cell debris was excluded from the analysis based on electronic gates using forward scatter and side scatter criteria, and unlabeled cells processed in parallel were used to set fluorescence gates. Cells stained with secondary antibody only or with the correspondent isotype control were used to assess the background fluorescence associated with non-specific binding of the secondary antibody. In each flow cytometry analysis, 10 000 events were captured inside the

gate. In each flow cytometry analysis, 1×10^4 events were captured inside the gate. Representative fluorescence dot plots are shown in Figure S1.

Immunocytochemistry

Immunocytochemistry was performed in cell-fibrin constructs previously fixed in cell culture media containing 2% (v/v) PFA (30 min at 37°C). All subsequent steps were performed under stirring (50 rpm). Cell-fibrin constructs were permeabilized for 45 min with 0.2% (v/v) Triton X-100, blocked for 1 h, incubated (overnight at 4°C) with mouse anti-βIII-tubulin (1:500; Biolegend 801201), rinsed 3× with PBS, and incubated for 1 h with the Alexa Fluor® 488 donkey anti-mouse IgG (1:1000; Invitrogen 21202). Nuclei were counterstained with DAPI (Gibco; 0.1 µg/mL). Samples were finally mounted in Fluoromount™ mounting media (Sigma-Aldrich) and observed under the confocal laser scanning microscope [CLSM; Leica TCS SP5 II (Leica Microsystems, Germany)].

Cell outward migration analysis

Neurite extension/cell outward migration from cellular spheroids was assessed at day 6 of hES-NSC culture within fibrin. Cell-fibrin constructs were fixed and permeabilized as described for immunocytochemistry studies, incubated with PBS containing 1% (w/v) bovine serum albumin for 1 h under stirring, and then with Alexa Fluor® 594-conjugated phalloidin (Invitrogen; 1:100; 1 h under stirring) for visualization of filamentous actin (F-actin). After rinsing with PBS, nuclei were counterstained with DAPI and samples mounted in Fluoromount™. Fluorescence images were collected using a Plan-Apochromat 40×/1.30 NA oil objective of the CLSM (NA, numerical aperture). Cell outgrowth was determined in the 3D image stacks, by segmenting the volume of the spheroid and that correspondent to cells cytoskeleton, using DNA and F-actin fluorescence images, respectively. The area occupied by cell extensions protruding from the edge of each spheroid (outgrowth area), as well as the length of the longest sprout (maximal outgrowth distance) were given by the 2D maximal projection in Z of F-actin stack images subtracting the spheroid area. Maximal outgrowth distance in 3D was computed analyzing the two segmented volumes, namely the distance from the spheroid volume boundary to the boundary of the volume correspondent to cells cytoskeleton [18]. For each condition, 10 images of 10 randomly selected spheroids per cell-fibrin construct replicate were examined, and up to 4 independent experiments were performed.

Statistical analysis

Experimental data was treated using IBM® SPSS® Statistics Software (version 23). Statistically significant differences between three or more conditions were detected using the one-way ANOVA, followed by the Dunnett's two-tailed test for comparisons with unmodified fibrin (the control condition). Results were considered significant for $p < 0.05$.

Results

Expression profile of integrins and syndecans in hES-NSCs

The expression profile of α6, α3 and β1 integrin subunits, integrin αvβ3 and syndecans-1 and -4 was examined by flow cytometry in hES-NSCs expanded in poly-L-ornithine/laminin-coated TCPS plates (passage 9). Results are presented in Table I and representative fluorescence dot plots are shown in Figure S1 (Supplementary Data). Integrin α6 subunit was found to be expressed by 88.8% of the hES-NSCs analyzed, whereas the percentage of cells expressing the α3 subunit was of 14.7%. Integrin β1 subunit was expressed by 91.5% of hES-NSCs analyzed. We also evaluated the expression of integrin αvβ3, a cell adhesion receptor recognizing the RGD sequence of several plasma and ECM proteins, including that of fibrinogen [43]. This integrin receptor was found to be expressed by 68% of the cells. Finally, we assessed the expression of syndecan-1 and -4, since these were the cell receptors capable of interacting with AG73 [37, 38]. High levels of syndecan-1 were found to be expressed by the majority of cells (98.6%), whereas syndecan-4 was expressed by only 2.62% of cells, as expected for undifferentiated hES-NSCs [34]. Furthermore, 93% of hES-NSCs expressing syndecan-1 were found to co-express integrin α6 subunit.

Table I – Expression profile of integrins and syndecans in hES-NSCs, as determined by flow cytometry

Cell receptor/ receptor subunit	***Expressing cells (%)***
Integrin α6 subunit	88.8%
Integrin α3 subunit	14.7%
Integrin β1 subunit	91.5%
Integrin αvβ3	68.0%
Syndecan-1	98.6%
Syndecan-4	2.62%
Syndecan-1 and integrin α6 subunit	93.0%

Effect of fibrin functionalization on the outgrowth of hES-NSCs

To unravel the effect of immobilized ligands on cell outward migration of hES-NSCs, H9-derived NSCs were cultured for 6 days within fibrin gels prepared with different input peptide concentrations of HYD1, T1 or AG73, namely 2.5, 5, 10, 20, 40, 60, 80, 120 and 160 μM. At day 6, cell/fibrin constructs were processed for F-actin/DNA staining and fluorescence images were collected using the CLSM. The cell outgrowth was quantified through automatic image analysis using three parameters: 3D maximal outgrowth distance, maximal outgrowth distance (from Z-projections of CLSM stacks) and outgrowth area. Results are presented in Figure 2. Representative Z-projections of CLSM stacks correspondent to 3D cultures for which a significant increase in cell outgrowth was detected are depicted in Figure 3. Since the qualitative analysis of CLSM images correspondent to fibrin gels functionalized with AG73 at input peptide concentrations ≥ 120 μM clearly showed a negative impact on cell outgrowth (images not shown) quantitative analysis was not performed in these gels.

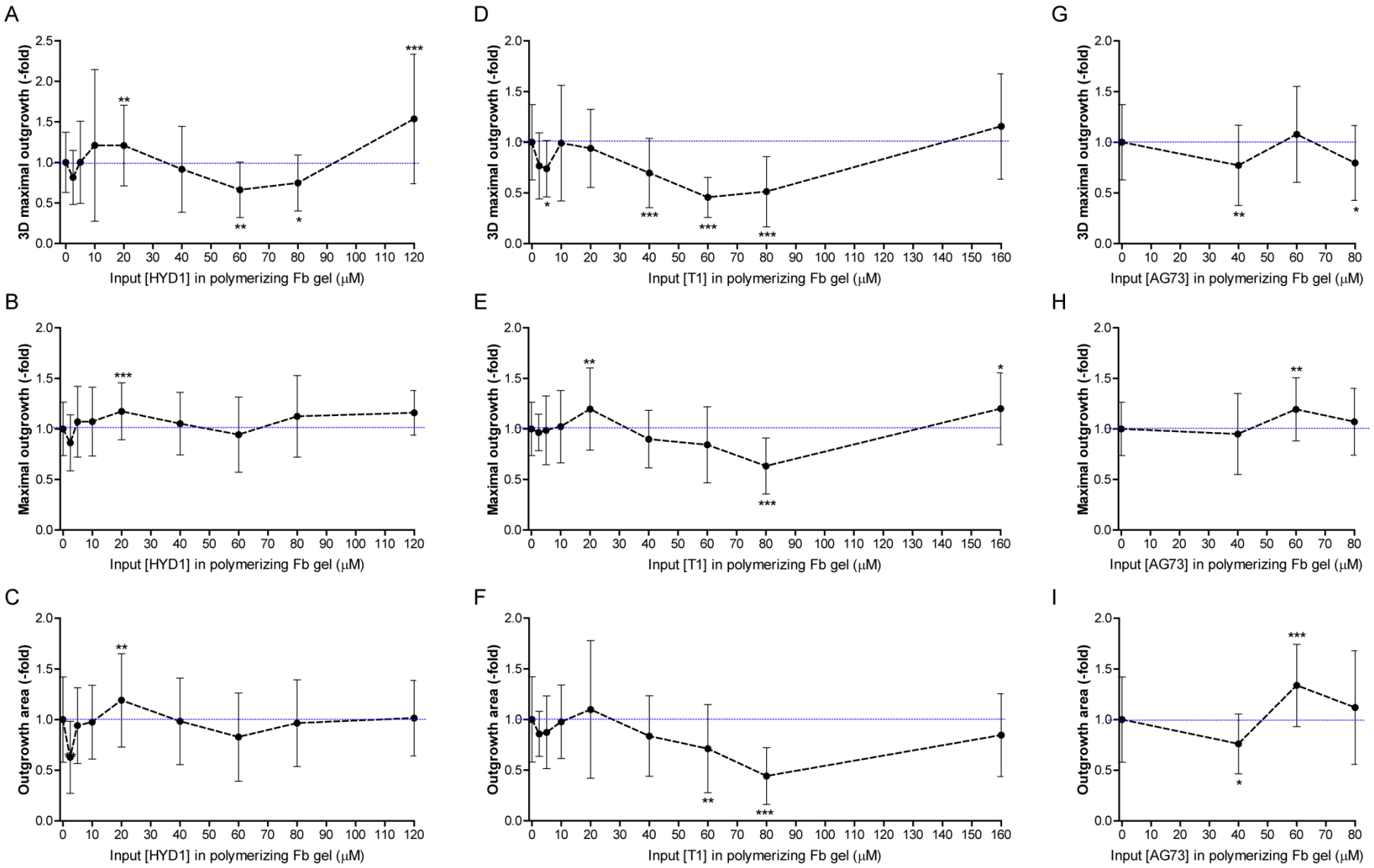
A
3D maximal outgrowth (-fold)
Input [HYD1] in polymerizing Fb gel (μM)
B
Maximal outgrowth (-fold)
Input [HYD1] in polymerizing Fb gel (μM)
C
Outgrowth area (-fold)
Input [HYD1] in polymerizing Fb gel (μM)
D
3D maximal outgrowth (-fold)
Input [T1] in polymerizing Fb gel (μM)
E
Maximal outgrowth (-fold)
Input [T1] in polymerizing Fb gel (μM)
F
Outgrowth area (-fold)
Input [T1] in polymerizing Fb gel (μM)
G
3D maximal outgrowth (-fold)
Input [AG73] in polymerizing Fb gel (μM)
H
Maximal outgrowth (-fold)
Input [AG73] in polymerizing Fb gel (μM)
I
Outgrowth area (-fold)
Input [AG73] in polymerizing Fb gel (μM)

Figure 2. Maximal outgrowth distance and outgrowth area of hES-NSCs within **(A–C)** HYD1-, **(D–F)** T1- or **(G–I)** AG73-functionalized fibrin (Fb) gels (day 6 of cell culture), as a function of input peptide concentration. The maximal outgrowth distance was computed analyzing the 3D stack of CLSM stack images (3D maximal outgrowth distance) as well as the correspondent Z projection (maximal outgrowth distance). Cell outgrowth was normalized to outgrowth in unmodified fibrin, which corresponds to an input peptide concentration of 0 μM. Mean ± SD, n ≥ 20 neurospheres, * $p < 0.05$, ** $p < 0.01$, *** $p < 0.005$ *vs.* unmodified fibrin, one-way ANOVA followed by Dunnett's test.

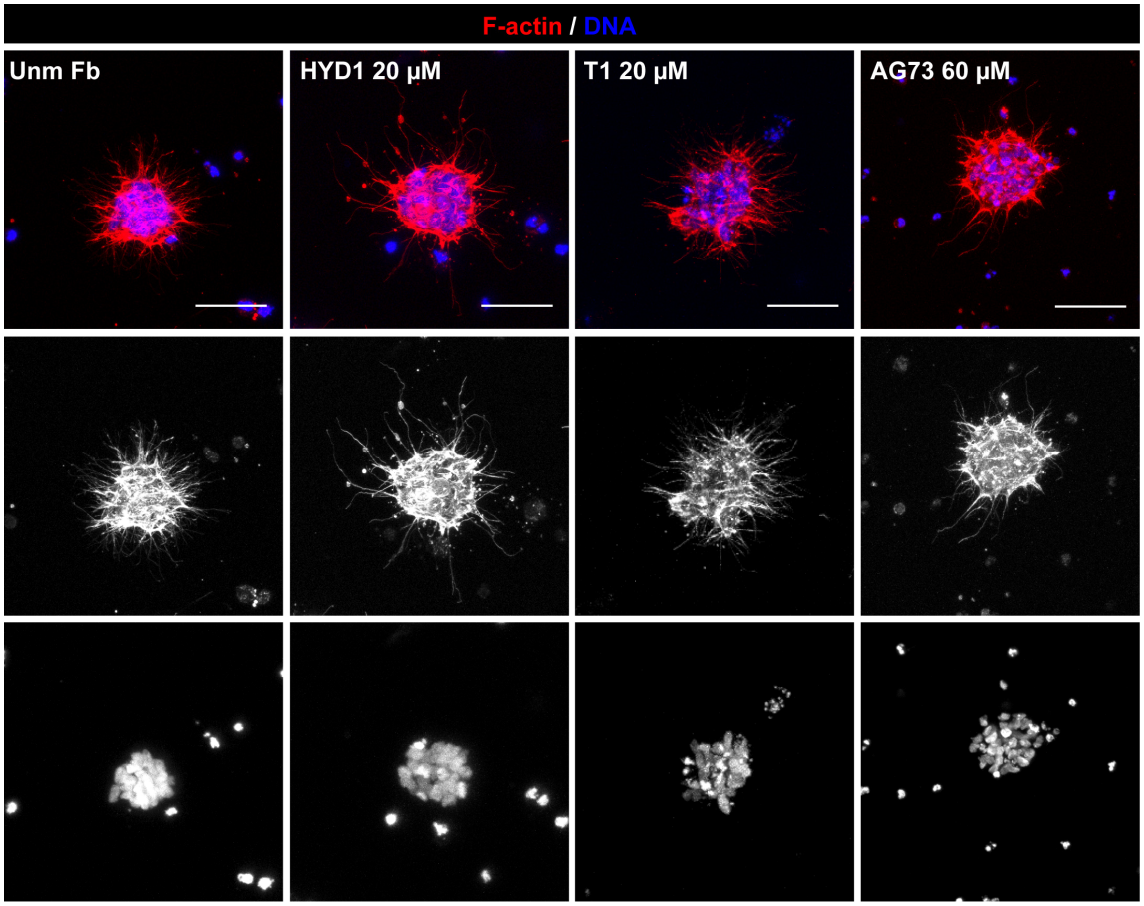

Figure 3. Representative Z-projections of CLSM stack images of hES-NSCs cultured within unmodified fibrin (Unm Fb), HYD1-, T1- or AG73-functionalized fibrin gels (day 6 of cell culture). Images shown correspond to fibrin hydrogels prepared with 20 μM of HYD1, 20 μM of T1, and 60 μM of AG73. Scale bars, 50 μm.

Cell outgrowth of hES-NSCs revealed a biphasic response to covalently-bound HYD1 noticeable in the three outgrowth parameters quantified up to an input peptide concentration of 60 μM (Fig. 2A–C). In this range of concentrations, maximal enhancement was observed for an input concentration of 20 μM, which led to a 1.2-fold increase in cell outgrowth when compared to unmodified fibrin ($p < 0.01$), considering the three outgrowth parameters evaluated. An input HYD1 concentration of 120 μM also led to increased values of 3D maximal outgrowth *vs.* unmodified fibrin, which could

be associated with changes in the structural and viscoelastic properties of the gels resulting from the incorporation of such an amount of exogenous peptides. Still, this effect was not detected in the two other cell outgrowth parameters assessed.

Similarly to HYD1, immobilized T1 elicited a biphasic effect on hES-NSC outgrowth detectable in the three outgrowth parameters up to an input peptide concentration of 80 μM (Fig. 2D–F). Within this range of concentrations, fibrin gels functionalized with 20 μM of T1 were those accomplishing the best results, leading to a 1.2-fold increase in the maximal outgrowth distance, when comparing to unmodified fibrin (p = 0.0022), although the 3D maximal outgrowth and the outgrowth area were not significantly altered. When increasing the input peptide concentration from 80 to 160 μM, a trend for an increase in cell outgrowth was observed, particularly in the case of the maximal outgrowth distance, which attained significant higher values when compared to unmodified fibrin (p = 0.0119). This effect suggests that the incorporation of this amount of peptides may have compromised fibrin polymerization and, as such, altered the structural or mechanical properties of the gels.

Covalent binding of AG73 also induced a biphasic effect on hES-NSC outgrowth, following the same trend observed for HYD1- and T1-functionalized gels (Fig. 2G–I). In this case, a significant increase in the cell outgrowth relative to unmodified fibrin was observed for the input peptide concentration of 60 μM, although the 3D maximal outgrowth was not significantly altered. In these AG73-functionalized gels the maximal outgrowth distance registered a 1.2-fold increase (p = 0.0032) while that correspondent to the outgrowth area showed a 1.3-fold increase (p = 0.0003).

In parallel, a preliminary test was performed to evaluate if the combination of HYD1 with AG73 could exert an additive or synergistic effect on hES-NSC outgrowth in fibrin. For this purpose, hES-NSCs were cultured within fibrin functionalized with 10 μM HYD1 and 10 μM AG73. The qualitative analysis of CLSM images correspondent to this condition revealed no impact of fibrin functionalization on cell outgrowth when comparing to unmodified fibrin gels.

Neuronal differentiation of hES-NSCs within HYD1-/T1-functionalized fibrin

Since fibrin gels functionalized with 20 μM of HYD1 or T1 peptides showed a higher capacity of promoting cell outward migration of hES-NSCs, we assessed if these gels also supported the neuronal differentiation of hES-NSCs. For this purpose, hES-NSCs were cultured under neuronal differentiation conditions within fibrin gels functionalized

with 20 μM of HYD1 or T1 peptides. The distribution of neurons was detected through immunodetection of βIII-tubulin (neuronal marker) in cell-fibrin constructs. Representative fluorescence images are shown in Figure 4.

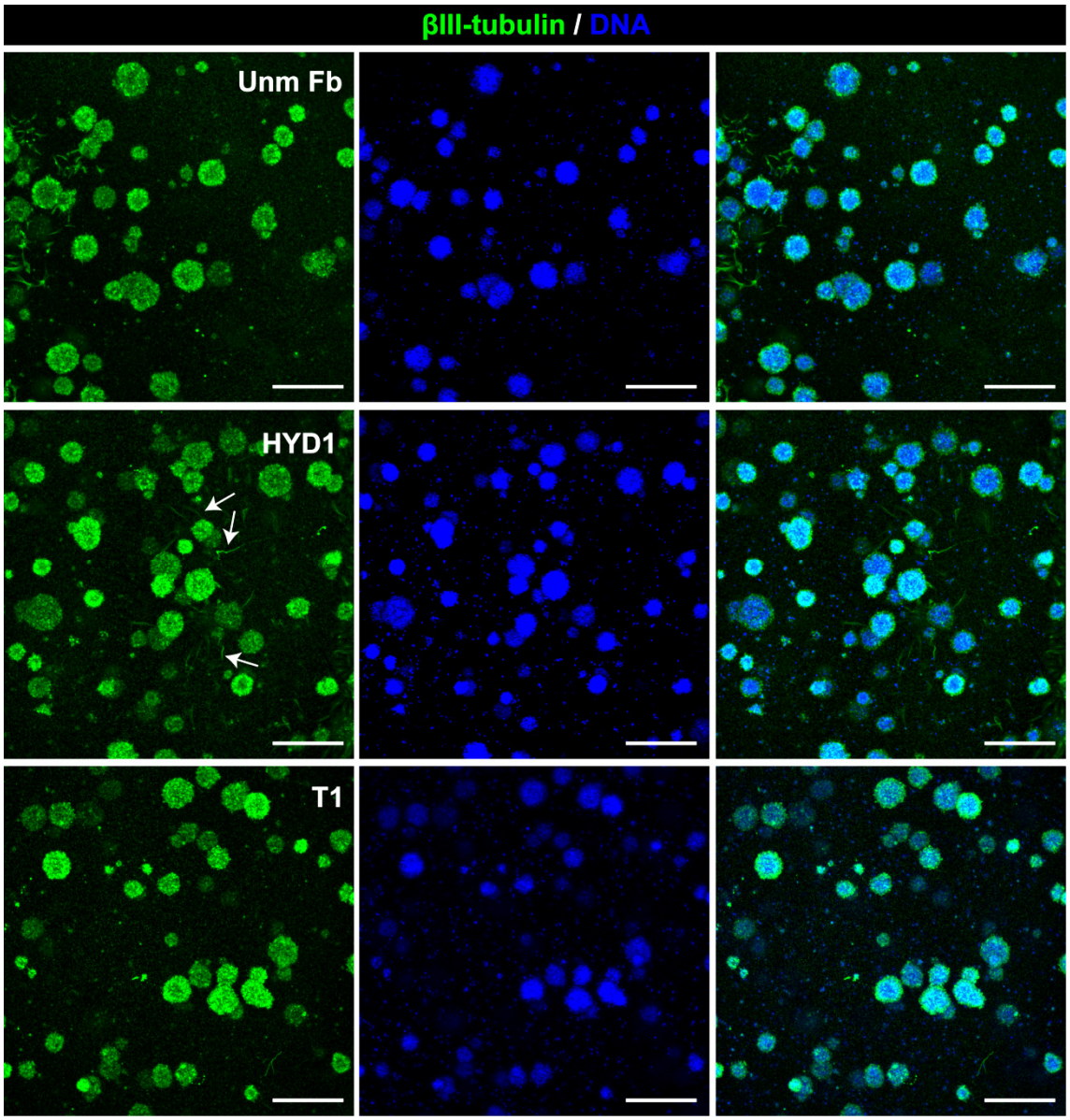

Figure 4. H9-derived hES-NSCs cultured within unmodified (Unm Fb) and HYD1-/T1-functionalized fibrin gels differentiate into neurons expressing βIII-tubulin (20 μM for both peptides; 14 days *in vitro*). Arrows depict neurites expressing βIII-tubulin protruding from neurospheres. Images show 2D projections of CLSM 3D stack images covering a depth of 150 μm. Scale bars, 300 μm.

Confocal analysis of cell/fibrin constructs showed for HYD1-/T1-functionalized fibrin a homogeneous distribution of neuronal cells expressing βIII-tubulin, similarly to unmodified fibrin (Figure 4), although a neuronal network could not be observed for any condition at this time point.

Discussion

This work aimed to unravel if fibrin functionalization with α6β1 integrin-binding motifs could be effective in promoting the outgrowth of hES-NSCs, as we reported for mES-NSPCs [18]. Specifically, we assessed if the covalent binding of the synthetic cell adhesive peptides HYD1 and T1 engaging integrin α6β1 could be used to improve the outgrowth of hES-NSCs in fibrin hydrogels. Furthermore, we explored if covalent immobilization of the syndecan-binding peptide AG73 could enhance fibrin ability to support hES-NSC outgrowth.

We started to assess the expression profile of integrins and syndecans in hES-NSCs, when cultured under expansion conditions. We found that hES-NSCs widely express both α6 and β1 integrin, similar to that reported for human fetal NSPCs. In fact, the same study by Hall *et al.* also showed that all hNSPCs $\alpha6^+$ expressed integrin β1 subunit, indicating that integrin α6β1 is expressed by hNSPCs [44]. Accordingly, since in NSPCs α6 generally dimerizes with integrin β1 subunit (the percentage of cells expressing β4, the further partner for α6, is either absent or lower than 15% [16, 44, 45]), these results suggest that integrin α6β1 is likely expressed by hES-NSCs. As in previous studies we showed that the pro-migratory effect of immobilized HYD1/T1 peptides on mES-NSPCs was mediated by integrins α6β1 and α3β1 [18], we subsequently evaluated the expression of integrin α3 subunit in hES-NSCs. We found that 14.7% of hES-NSCs analyzed expressed α3 integrin. Our results match these of recent studies, reporting that hES-derived neural progenitors express very low amounts of integrin α3 subunit [46]. Concerning the expression of syndecan receptors, syndecan-1 was found to be highly expressed by hES-NSCs, whereas syndecan-4 expression was minimal, as expected from ES-NSCs in an undifferentiated state [34].

Since integrin αvβ3 is likely involved in the modulation of neurite extension within fibrin matrices via interaction with fibrinogen RGD domains [47, 48], we also assessed the expression of this integrin in hES-NSCs. We found that hES-NSCs significantly express integrin αvβ3 (68%), one of the major cell adhesion receptors expressed by neural progenitors [49, 50]. Moreover, this receptor may also mediate the interactions of hES-NSCs with fibronectin [51], an ECM protein secreted by hES-NSCs cultured within fibrin matrices [40] with reported high affinity to fibrin [52], also involved in neuronal migration and outgrowth [53]. Future studies are needed to disclose if integrin αvβ3 mediates neurite extension of hES-NSCs cultured within fibrin gels, due to its ability to interact with fibrinogen and fibronectin [43, 50].

The covalent binding of HYD1, T1 or AG73 bi-domain peptides to fibrin showed a biphasic effect on the outgrowth of hES-NSCs, similar to that resultant from the incorporation of RGD peptides [54]. Specifically, 2D and 3D studies have demonstrated that improved cell migration occurs at an intermediate level of receptor occupancy and so, for higher ligand concentrations the cell migration is decreased, due to excessive cell-matrix adhesiveness [55, 56]. In line with our previous results, an input peptide concentration of 20 μM of HYD1 was effective in enhancing cell outgrowth of hES-NSCs in fibrin, although leading to a lesser increase when compared to that obtained with mES-NSPCs (2.4-fold increase in the outgrowth area relative to unmodified fibrin) [18]. Also in the case of T1-functionalized fibrin gels cell response of hES-NSCs to ligand concentration differed from that previously observed for mES-NSPCs. For instance, while an input peptide concentration of 60 μM was found to be inhibitory to the outgrowth of hES-NSCs, the same exerted no effect on the radial outgrowth of mES-NSPCs. As the pro-migratory effect of HYD1 and T1 peptides was found to be mediated by α6β1 and α3β1 integrins [18], these differences may be related to the integrin expression profile of the two cell types. In fact, the reduced cell response of hES-NSCs to immobilized HYD1/T1 peptides when compared to mES-NSPCs may be partially explained by the lower percentage of cells expressing integrin α3 subunit in hES-NSCs in comparison to mES-NSPCs (14.7% *vs.* 73.7%, respectively).

The increase in the maximal outgrowth of hES-NSCs registered in HYD1- and T1-functionalized gels prepared using the highest input concentration tested (120 and 160 μM, respectively), may be explained by alterations in the viscoelastic or structural properties of fibrin resultant from the incorporation of synthetic peptides. Even though we did not observed changes in the viscoelastic or structural properties of fibrin gels modified up to 40 μM of HYD1 and T1 [18], we cannot disregard this possibility when using such relatively high input peptide concentrations (120–160 μM). To address this issue, the rheological characterization and structural analysis of these functionalized gels is required. Interestingly, we did not observe this effect with mES-NSPCs neurospheres cultured on top of fibrin gels functionalized with 160 μM of HYD1 or T1 [18]. In fact, in a 3D environment processes involving cell migration or extension of neurites depend not only on the presence of cell adhesion domains, but also on the cells capacity to degrade the surrounding matrix. Thus, cells cultured within a 3D environment, as in the present study, are more challenged to migrate and also more sensitive to alterations in the biophysical properties of the matrix, when compared to cells cultured on 2D substrates, as we showed in the previous study.

The second main objective of this work was to address if fibrin functionalization with the syndecan-binding peptide AG73 could promote the outgrowth of hES-NSCs. We found that fibrin functionalization with 60 μM of AG73 was effective in promoting hES-NSC outgrowth in 3D fibrin hydrogels (up to 1.3-fold increase *vs.* unmodified fibrin). The biphasic response observed in AG73-functionalized fibrin was unexpectedly short, wherein input AG73 concentrations higher than 60 μM either exerted no effect or inhibited the outgrowth of hES-NSCs. Syndecans are expected to bind with high affinity to fibrin due to the presence of heparin-binding domains in the *N*-terminus of each Bβ chain of fibrinogen [17, 57]. As a result, the conjugation of syndecan-binding peptides at high input peptide concentrations may result in an overstated adhesiveness of fibrin, ultimately leading to an inhibition of cell outgrowth and migration. For instance, unpublished results from our group have showed that AG73-functionalized poly(ethylene glycol) (PEG) hydrogels increase the outgrowth of hES-ESCs when compared to unmodified PEG, which, in opposite to fibrin, do not contain heparin-binding motifs or RGD domains. Actually, these results indicate that the use of syndecan-binding adhesive peptides can be a good strategy to enhance neurite outgrowth and outward migration of hES-ESCs in 3D hydrogel matrices.

The incorporation of AG73 peptide in combination with α6β1 integrin-binding ligands is expected to exert an additive or a synergistic effect on neurite outgrowth of hES-NSCs within fibrin. In an attempt to develop a biomaterial with the biological activities of multifunctional laminin chains, Nomizu and colleagues have explored the mixed conjugation of AG73 and laminin-derived integrin-binding peptides to the surface of chitosan membranes [58]. The combination of AG73 with an integrin α6β1 ligand from mouse laminin α2 chain (A2G10) was found to synergistically enhance the cell attachment of fibroblasts on chitosan membranes [58], supporting our hypothesis. Although we did not observe an additive effect on hES-NSC outgrowth upon fibrin functionalization with 10 μM of AG73 and HYD1, the co-expression of syndecan-1 and integrin α6 subunit in more than 90% of hES-NSCs suggests that syndecan-1 may cooperate with α6β1 integrin in the presence of both types of ligands, leading to a synergistic effect of hES-NSC neurite outgrowth in fibrin. As such, based on the effect elicited by HYD1 and AG73 when incorporated alone into fibrin, future studies should explore if the combined incorporation of 60 μM of AG73 with 20 μM of HYD1 induces an additive or synergistic effect on hES-NSC outward migration, when compared to that exerted by single peptides. In order to verify if syndecan-1 acts as a co-receptor of α6β1 integrin in hES-NSCs, immunoprecipitation and/or functional blocking experiments should be performed.

Finally, fibrin gels functionalized with HYD1 or T1 were also shown to support neuronal differentiation for input peptide concentrations of 20 μM, as evidenced by the presence of neurons inside the neurospheres. In future, the quantitative analysis of the percentage of cells expressing neuronal markers (βIII-tubulin, NeuN) will be fundamental to detect if the tethering of HYD1/AG73 peptides also has an effect on hES-NSC neuronal differentiation within 3D fibrin gels, besides impacting cell outward migration. Moreover, since the expression of syndecan-4 is expected to increase after neuronal differentiation [34], it would be interesting to analyze the expression of these receptors after long-term culture of hES-NSCs within functionalized fibrin. Additionally, given that substrates containing the laminin α5 chain were recently found to promote *in vitro* functional development of hES-derived neurons [59], the bioactivity of synthetic peptides derived from mouse laminin α5 chains homologous to AG73 should be tested.

Altogether, this study constitutes a proof-of-concept that decorating hydrogels with synthetic adhesive ligands interacting with integrin α6β1 or syndecans can be advantageous for the development of 3D hydrogel platforms for the culture of human pluripotent-derived NSCs. This strategy could also allow the improvement of more efficient hydrogel vehicles for the transplantation of NSPCs to treat the damaged CNS.

Conclusions

This work revealed that the outward migration of hES-NSCs in fibrin can be maximized by controlling the type and the density of α6β1 integrin- or syndecan-binding peptides. Furthermore, we proved that hES-NSCs are capable of differentiating into neurons when cultured within fibrin gels functionalized within 20 μM of HYD1 or T1 peptides. The proposed strategy constitutes an advantage to develop biomimetic matrices that can be used as reproducible 3D platforms for *in vitro* culture of hES-NSCs and as vehicles for the transplantation of NSCs envisaging the treatment of the damaged CNS.

Acknowledgements

The authors would like to acknowledge Prof. Celso Reis and Dr. Ana Magalhães for providing the antibodies for syndecan-1 and -4. This work was supported by FEDER funds through the Programa Operacional Factores de Competitividade – COMPETE (FCOMP-01-0124-FEDER-021125), by National Funds through FCT – Fundação para a Ciência e a Tecnologia (PTDC/SAU-BMA/118869/2010) and by the project NORTE-

01-0145-FEDER-000012, financed by Norte Portugal Regional Operational Programme (NORTE 2020), under the PORTUGAL 2020 Partnership Agreement, through the European Regional Development Fund (ERDF). A.R.B. was supported by FCT (SFRH/BD/86200/2012).

References

[1] Y. Tang, P. Yu, L. Cheng, Current progress in the derivation and therapeutic application of neural stem cells, Cell Death Dis 8(10) (2017) e3108.

[2] P. Lu, L.L. Jones, E.Y. Snyder, M.H. Tuszynski, Neural stem cells constitutively secrete neurotrophic factors and promote extensive host axonal growth after spinal cord injury, Experimental neurology 181(2) (2003) 115-29.

[3] K. Reekmans, J. Praet, J. Daans, V. Reumers, P. Pauwels, A. Van der Linden, Z.N. Berneman, P. Ponsaerts, Current challenges for the advancement of neural stem cell biology and transplantation research, Stem cell reviews 8(1) (2012) 262-78.

[4] J.W. McDonald, D. Becker, T.F. Holekamp, M. Howard, S. Liu, A. Lu, J. Lu, M.M. Platik, Y. Qu, T. Stewart, S. Vadivelu, Repair of the injured spinal cord and the potential of embryonic stem cell transplantation, Journal of neurotrauma 21(4) (2004) 383-93.

[5] M.H. Amer, F.R.A.J. Rose, K.M. Shakesheff, M. Modo, L.J. White, Translational considerations in injectable cell-based therapeutics for neurological applications: concepts, progress and challenges, npj Regenerative Medicine 2(1) (2017) 23.

[6] Z.Z. Khaing, R.C. Thomas, S.A. Geissler, C.E. Schmidt, Advanced biomaterials for repairing the nervous system: what can hydrogels do for the brain?, Materials Today 17(7) (2014) 332-340.

[7] R.Y. Tam, T. Fuehrmann, N. Mitrousis, M.S. Shoichet, Regenerative therapies for central nervous system diseases: a biomaterials approach, Neuropsychopharmacology : official publication of the American College of Neuropsychopharmacology 39(1) (2014) 169-88.

[8] K. Saha, J.F. Pollock, D.V. Schaffer, K.E. Healy, Designing synthetic materials to control stem cell phenotype, Current Opinion in Chemical Biology 11(4) (2007) 381-387.

[9] H.W. Jun, V. Yuwono, S.E. Paramonov, J.D. Hartgerink, Enzyme-Mediated Degradation of Peptide-Amphiphile Nanofiber Networks, Adv Mater 17(21) (2005) 2612-2617.

[10] R. Derda, S. Musah, B.P. Orner, J.R. Klim, L.Y. Li, L.L. Kiessling, High-Throughput Discovery of Synthetic Surfaces That Support Proliferation of Pluripotent Cells, Journal of the American Chemical Society 132(4) (2010) 1289-1295.

[11] D. Stroumpoulis, H.N. Zhang, L. Rubalcava, J. Gliem, M. Tirrell, Cell adhesion and growth to peptide-patterned supported lipid membranes, Langmuir : the ACS journal of surfaces and colloids 23(7) (2007) 3849-3856.
[12] R. Timpl, D. Tisi, J.F. Talts, Z. Andac, T. Sasaki, E. Hohenester, Structure and function of laminin LG modules, Matrix Biology 19(4) (2000) 309-317.
[13] P.E. Hall, J.D. Lathia, N.G.A. Miller, M.A. Caldwell, C. Ffrench-Constant, Integrins Are Markers of Human Neural Stem Cells, STEM CELLS 24(9) (2006) 2078-2084.
[14] L.A. Flanagan, L.M. Rebaza, S. Derzic, P.H. Schwartz, E.S. Monuki, Regulation of human neural precursor cells by laminin and integrins, Journal of Neuroscience Research 83(5) (2006) 845-856.
[15] J.G. Emsley, T. Hagg, α6β1 integrin directs migration of neuronal precursors in adult mouse forebrain, Experimental neurology 183(2) (2003) 273-85.
[16] W. Ma, T. Tavakoli, E. Derby, Y. Serebryakova, M.S. Rao, M.P. Mattson, Cell-extracellular matrix interactions regulate neural differentiation of human embryonic stem cells, Bmc Dev Biol 8 (2008) 90.
[17] A.C. Brown, T.H. Barker, Fibrin-based biomaterials: modulation of macroscopic properties through rational design at the molecular level, Acta Biomater 10(4) (2014) 1502-14.
[18] J. Silva, A.R. Bento, D. Barros, T.L. Laundos, S.R. Sousa, P. Quelhas, M.M. Sousa, A.P. Pêgo, I.F. Amaral, Fibrin functionalization with synthetic adhesive ligands interacting with α6β1 integrin receptor enhance neurite outgrowth of embryonic stem cell-derived neural stem/progenitors, Acta Biomater 59 (2017) 243-256.
[19] Y. Yamaguchi, Heparan sulfate proteoglycans in the nervous system: their diverse roles in neurogenesis, axon guidance, and synaptogenesis, Seminars in cell & developmental biology 12(2) (2001) 99-106.
[20] M.R. Morgan, M.J. Humphries, M.D. Bass, Synergistic control of cell adhesion by integrins and syndecans, Nature reviews. Molecular cell biology 8(12) (2007) 957-969.
[21] Y. Yamada, F. Katagiri, K. Hozumi, Y. Kikkawa, M. Nomizu, Cell behavior on protein matrices containing laminin α1 peptide AG73, Biomaterials 32(19) (2011) 4327-35.
[22] T. Pap, J. Bertrand, Syndecans in cartilage breakdown and synovial inflammation, Nature Reviews Rheumatology 9 (2012) 43.
[23] H. Chung, H.A.B. Multhaupt, E.S. Oh, J.R. Couchman, Minireview: Syndecans and their crucial roles during tissue regeneration, FEBS letters 590(15) (2016) 2408-2417.
[24] J.A. Roper, R.C. Williamson, M.D. Bass, Syndecan and integrin interactomes: large complexes in small spaces, Curr Opin Struct Biol 22(5) (2012) 583-90.

[25] M.R. Morgan, M.J. Humphries, M.D. Bass, Synergistic control of cell adhesion by integrins and syndecans, Nature reviews. Molecular cell biology 8(12) (2007) 957-69.
[26] Z. Mostafavi-Pour, J.A. Askari, S.J. Parkinson, P.J. Parker, T.T.C. Ng, M.J. Humphries, Integrin-specific signaling pathways controlling focal adhesion formation and cell migration, The Journal of cell biology 161(1) (2003) 155-167.
[27] O. Okamoto, S. Bachy, U. Odenthal, J. Bernaud, D. Rigal, H. Lortat-Jacob, N. Smyth, P. Rousselle, Normal human keratinocytes bind to the α3 LG4/5 domain of unprocessed laminin-5 through the receptor syndecan-1, The Journal of biological chemistry 278(45) (2003) 44168-77.
[28] A. Utani, M. Nomizu, H. Matsuura, K. Kato, T. Kobayashi, U. Takeda, S. Aota, P.K. Nielsen, H. Shinkai, A unique sequence of the laminin α3 G domain binds to heparin and promotes cell adhesion through syndecan-2 and -4, The Journal of biological chemistry 276(31) (2001) 28779-88.
[29] T. Ogawa, Y. Tsubota, J. Hashimoto, Y. Kariya, K. Miyazaki, The short arm of laminin γ2 chain of laminin-5 (laminin-332) binds syndecan-1 and regulates cellular adhesion and migration by suppressing phosphorylation of integrin β4 chain, Molecular biology of the cell 18(5) (2007) 1621-33.
[30] E. Atilgan, B. Ovryn, Nucleation and Growth of Integrin Adhesions, Biophysical journal 96(9) (2009) 3555-3572.
[31] J.A. Roper, R.C. Williamson, M.D. Bass, Syndecan and integrin interactomes: large complexes in small spaces, Current Opinion in Structural Biology 22(5) (2012) 583-590.
[32] Q. Wang, L. Yang, C. Alexander, S. Temple, The niche factor syndecan-1 regulates the maintenance and proliferation of neural progenitor cells during mammalian cortical development, PloS one 7(8) (2012) e42883.
[33] S. Kuriyama, R. Mayor, A role for Syndecan-4 in neural induction involving ERK- and PKC-dependent pathways, Development 136(4) (2009) 575-84.
[34] L.E. Oikari, R.K. Okolicsanyi, A. Qin, C. Yu, L.R. Griffiths, L.M. Haupt, Cell surface heparan sulfate proteoglycans as novel markers of human neural stem cell fate determination, Stem Cell Res 16(1) (2016) 92-104.
[35] F. Katagiri, K. Takeyama, Y. Ohga, K. Hozumi, Y. Kikkawa, Y. Kadoya, M. Nomizu, Amino acid sequence requirements of laminin β1 chain peptide B133 (DISTKYFQMSLE) for amyloid-like fibril formation, syndecan binding, and neurite outgrowth promotion, Biochemistry 49(28) (2010) 5909-18.
[36] Y. Yamada, K. Hozumi, F. Katagiri, Y. Kikkawa, M. Nomizu, Biological activity of laminin peptide-conjugated alginate and chitosan matrices, Biopolymers 94(6) (2010) 711-20.

[37] M.P. Hoffman, M. Nomizu, E. Roque, S. Lee, D.W. Jung, Y. Yamada, H.K. Kleinman, Laminin-1 and laminin-2 G-domain synthetic peptides bind syndecan-1 and are involved in acinar formation of a human submandibular gland cell line, The Journal of biological chemistry 273(44) (1998) 28633-41.

[38] M. Mochizuki, D. Philp, K. Hozumi, N. Suzuki, Y. Yamada, H.K. Kleinman, M. Nomizu, Angiogenic activity of syndecan-binding laminin peptide AG73 (RKRLQVQLSIRT), Arch Biochem Biophys 459(2) (2007) 249-55.

[39] J. Pruszak, W. Ludwig, A. Blak, K. Alavian, O. Isacson, CD15, CD24, and CD29 define a surface biomarker code for neural lineage differentiation of stem cells, Stem Cells 27(12) (2009) 2928-40.

[40] A.R. Bento, P. Quelhas, M.J. Oliveira, A.P. Pêgo, I.F. Amaral, Three-dimensional culture of single embryonic stem-derived neural/stem progenitor cells in fibrin hydrogels: neuronal network formation and matrix remodelling, Journal of tissue engineering and regenerative medicine 11(12) (2017) 3494-3507.

[41] H. Darr, Y. Mayshar, N. Benvenisty, Overexpression of NANOG in human ES cells enables feeder-free growth while inducing primitive ectoderm features, Development 133(6) (2006) 1193-201.

[42] A. Ichinose, T. Tamaki, N. Aoki, Factor XIII-mediated cross-linking of NH_2-terminal peptide of α2-plasmin inhibitor to fibrin, FEBS letters 153(2) (1983) 369-371.

[43] A.B.J. Prowse, F. Chong, P.P. Gray, T.P. Munro, Stem cell integrins: Implications for *ex-vivo* culture and cellular therapies, Stem Cell Research 6(1) (2011) 1-12.

[44] P.E. Hall, J.D. Lathia, N.G. Miller, M.A. Caldwell, C. ffrench-Constant, Integrins are markers of human neural stem cells, Stem Cells 24(9) (2006) 2078-84.

[45] L.A. Flanagan, L.M. Rebaza, S. Derzic, P.H. Schwartz, E.S. Monuki, Regulation of human neural precursor cells by laminin and integrins, Journal of neuroscience research 83(5) (2006) 845-56.

[46] D. Varun, G.R. Srinivasan, Y.H. Tsai, H.J. Kim, J. Cutts, F. Petty, R. Merkley, N. Stephanopoulos, D. Dolezalova, M. Marsala, D.A. Brafman, A robust vitronectin-derived peptide for the scalable long-term expansion and neuronal differentiation of human pluripotent stem cell (hPSC)-derived neural progenitor cells (hNPCs), Acta Biomaterialia 48(Supplement C) (2017) 120-130.

[47] R. Pittier, F. Sauthier, J.A. Hubbell, H. Hall, Neurite extension and in vitro myelination within three-dimensional modified fibrin matrices, Journal of Neurobiology 63(1) (2005) 1-14.

[48] Y.E. Ju, P.A. Janmey, M. McCormick, E.S. Sawyer, L.A. Flanagan, Enhanced Neurite Growth from Mammalian Neurons in Three-Dimensional Salmon Fibrin Gels, Biomaterials 28(12) (2007) 2097-2108.

[49] D. Stenzel, M. Wilsch-Bräuninger, F.K. Wong, H. Heuer, W.B. Huttner, Integrin αvβ3 and thyroid hormones promote expansion of progenitors in embryonic neocortex, Development 141(4) (2014) 795-806.
[50] X. Wu, D.S. Reddy, Integrins as Receptor Targets for Neurological Disorders, Pharmacology & therapeutics 134(1) (2012) 68-81.
[51] E.F. Plow, T.A. Haas, L. Zhang, J. Loftus, J.W. Smith, Ligand Binding to Integrins, Journal of Biological Chemistry 275(29) (2000) 21785-21788.
[52] E. Makogonenko, G. Tsurupa, K. Ingham, L. Medved, Interaction of fibrin(ogen) with fibronectin: further characterization and localization of the fibronectin-binding site, Biochemistry 41(25) (2002) 7907-13.
[53] A.M. Sheppard, S.K. Hamilton, A.L. Pearlman, Changes in the distribution of extracellular matrix components accompany early morphogenetic events of mammalian cortical development, The Journal of neuroscience : the official journal of the Society for Neuroscience 11(12) (1991) 3928-42.
[54] J.C. Schense, J. Bloch, P. Aebischer, J.A. Hubbell, Enzymatic incorporation of bioactive peptides into fibrin matrices enhances neurite extension, Nature biotechnology 18(4) (2000) 415-9.
[55] S.P. Palecek, J.C. Loftus, M.H. Ginsberg, D.A. Lauffenburger, A.F. Horwitz, Integrin-ligand binding properties govern cell migration speed through cell-substratum adhesiveness, Nature 385(6616) (1997) 537-540.
[56] J.C. Schense, J.A. Hubbell, Three-dimensional migration of neurites is mediated by adhesion site density and affinity, Journal of Biological Chemistry 275(10) (2000) 6813-6818.
[57] M.M. Martino, P.S. Briquez, A. Ranga, M.P. Lutolf, J.A. Hubbell, Heparin-binding domain of fibrin(ogen) binds growth factors and promotes tissue repair when incorporated within a synthetic matrix, Proceedings of the National Academy of Sciences of the United States of America 110(12) (2013) 4563-8.
[58] D. Otagiri, Y. Yamada, K. Hozumi, F. Katagiri, Y. Kikkawa, M. Nomizu, Cell attachment and spreading activity of mixed laminin peptide-chitosan membranes, Biopolymers 100(6) (2013) 751-9.
[59] A. Hyysalo, M. Ristola, M.E.L. Mäkinen, S. Häyrynen, M. Nykter, S. Narkilahti, Laminin α5 substrates promote survival, network formation and functional development of human pluripotent stem cell-derived neurons *in vitro*, Stem Cell Research 24(Supplement C) (2017) 118-127.

Supplementary Data

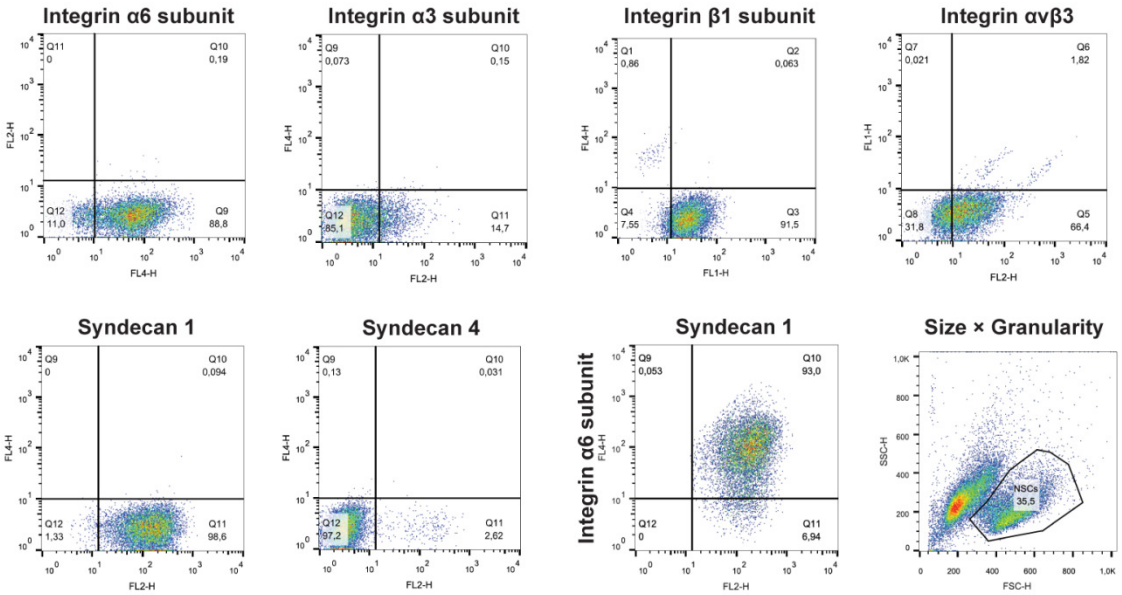

Figure S1. Representative flow cytometry dot plot charts obtained for the integrin and syndecan expression profiling of hES-NSCs, expanded in poly-L-ornithine/laminin-coated tissue culture polystyrene plates (passage 9). Cell debris was excluded by gating on forward and side scatter, and unlabeled cells processed in parallel were used to set fluorescence gates (fixed and permeabilized). Cells incubated with secondary antibody only or with the correspondent isotype control were used to eliminate non-specific background secondary antibody staining.

CHAPTER V

Concluding Remarks

The central nervous system (CNS) has a limited capacity to spontaneously regenerate and, due to insufficient regenerative strategies available, a small number of treatment options are provided for patients with CNS injuries or diseases [1]. With recent advances in stem cell biology and technology, the transplantation of neural stem/progenitor cells (NSPCs) has raised expectations as potential therapeutic approach to restore neurological function in these patients. Still, despite their functional benefits, NSPC transplantation has been hampered by low cell survival and/or poor integration into the host tissue [2].

This work aimed at creating an engineering approach to increase the ability of 3D hydrogel matrices to sustain NSPC neurite outgrowth and migration by mimicking cell receptor-extracellular matrix (ECM) interactions occurring in neurogenic niches, enhancing the efficacy of NSPC-based regenerative therapies of the damaged CNS. To pursue this objective, we hypothesized that the functionalization of hydrogel matrices with cell adhesive sequences interacting with integrin α6β1 or syndecans could enhance their ability to support NSPC migration and neurite outgrowth, and ultimately contribute to the integration of transplanted cells into the damaged CNS and neuronal relay formation. Fibrin gel was selected to test this hypothesis, due to the absence of α6β1 integrin binding domains in its structure, along with its tunable properties and innate bioactivity.

Given this, we first established a fibrin-based 3D system to culture dissociated NSPCs derived from murine embryonic stem cells (mES-NSPCs), capable of sustaining cell survival, allowing ES-NSPCs to proliferate, differentiate into mature neurons and establish neuronal networks. In this 3D culture system, ES-NSPCs are able to deposit ECM proteins, such as laminin, fibronectin and collagen IV, as well as to secrete matrix metalloproteinases, features important for matrix remodeling. Since the viscoelastic and structural properties of biomaterials can alter cell function [3], we assessed the effect of fibrinogen concentration in NSPC behavior. We observed that the outgrowth and neuronal differentiation of ES-NSPCs was hindered in fibrin gels with stiffer matrices and small-sized pores, herein correspondent to gels prepared with 8 or 10 mg/mL of fibrinogen. Furthermore, we showed that this 3D culture system also supports the survival, neuronal differentiation, expression of synaptic proteins and ECM deposition of human ES-derived neural stem cells (NSCs). Using the developed fibrin platform, we subsequently assessed the response of ES-NSPCs to immobilized cell adhesive motifs interacting with integrin α6β1, a laminin receptor highly expressed by

NSCs in neurogenic niches [4] which also mediates laminin-dependent NSPC migration [5].

As follows, six integrin α6β1 ligands were tested for their capacity to support integrin α6β1-mediated ES-NSPC adhesion. The ligands revealing a better performance were further immobilized in fibrin using the cross-linking action of factor XIIIa, including HYD1 (KIKMVISWKG) [6], T1 (GTTSWSQCSKS) [7] and A5G81 (AGQWHRVSVRWG) [8] peptides. After characterizing the resultant gels in terms of peptide binding efficiency, functionalized gels were evaluated in terms of ability to promote NSPC outward migration using the radial outgrowth assay and floating aggregates of ES-NSPCs (neurospheres). We have showed that the tethering of HYD1 or T1 peptides to fibrin provides adhesive cues promoting ES-NSPC outgrowth, while that of A5G81 barely affected radial outgrowth indicating that for full retention of bioactivity after immobilization A5G81 may require a free *N*-terminus [9]. Noteworthy, this study was pioneer in exploring the adhesive and pro-migratory properties of HYD1 to confer bioactivity to a hydrogel matrix. Cell outgrowth exhibited a biphasic response to immobilized T1 and HYD1 peptides with maximum enhancement being attained at input concentrations of 20 or 40 μM. The biphasic effect of T1 and HYD1 concentration on radial outgrowth is in agreement with other studies in which cell migration and neurite extension in both 2D and in 3D microenvironments was found to exhibit a biphasic dependence on ligand concentration [10, 11]. In fact, in accordance to S. Palecek *et al*., maximal migration occurs at an optimal, intermediate level of receptor occupancy, behind which further increasing the cell-matrix adhesiveness results in reduced cell migration [10]. The radial outgrowth enhancement induced by HYD1 was similar to that elicited by T1, but at lower levels of immobilized peptide, which suggests that HYD1 has a higher affinity for receptor binding than T1. Indeed, according to Leu *et al.* different integrin α6β1 ligands may interact with distinct coordination sites to trigger different signaling pathways and elicit distinct biological activities [7]. Moreover, the effect of HYD1 and T1 peptides on radial outgrowth was found to be mediated by α6β1 and α3β1 integrin receptors. In line with our results, the D-amino acid sequence of HYD1 is described to interact with both α6β1 and α3β1 integrins and to support cell adhesion when immobilized [6]. Future studies should address the immobilization of the D-amino acid analog of HYD1 in fibrin and its bioactivity since, unlike L-amino acids used in this work, D-amino acids rarely act as substrates for endogenous proteases which greatly increases the peptide stability towards proteolysis [12]. Furthermore, our findings also corroborate the ability of T1 peptide to support integrin α6β1-mediated cell adhesion described for fibroblasts and endothelial cells, but at the best of our

knowledge, its interaction with α3β1 integrin has not been previously reported [7]. Of note, the blocking of α6 and α3 integrins functional activity in ES-NSPCs cultured in unmodified fibrin elicited a minor impact on radial outgrowth, consistent with the absence of fibrin(ogen) domains interacting with α6 and α3 integrins [13]. In contrast, blocking of β1 integrin subunit resulted in a significant inhibition of ES-NSPC outgrowth on unmodified fibrin (~96%), which suggests the involvement of αvβ1, expressed by NSPCs [14], in mediating the migration of these cells in fibrin [15, 16]. Also, we showed that the cell outgrowth enhancement observed in HYD1-/T1-functionalized fibrin gels was not associated to changes in fibrin network structure or viscoelastic properties. Importantly, the stiffness of HYD1-/T1-functionalized fibrin gels (~300 Pa) was found to be within the optimal range for supporting neurite branching [17] and NSPC differentiation [3, 18, 19], also matching the compliance of human brain tissue (~100–1000 Pa) [20-22].

The impact of immobilized α6β1 integrin-binding motifs on ES-NSPC behavior when seeded as single cells in fibrin was subsequently assessed. For this purpose, fibrin gels functionalized with 20 μM of HYD1 were used, due to their better performance in terms of ability to promote radial outgrowth from neurospheres (up to 2.4-fold increase *vs.* unmodified fibrin). HYD1-functionalized fibrin gels led to significantly higher neurite extension from ES-NSPCs, further supporting the pro-migratory activity of immobilized HYD1. Moreover, immobilization of HYD1 in fibrin did not alter ES-NSPC proliferation, since α6β1 integrin is not involved in laminin-induced NSPC proliferation [23]. Still, the role of laminin/α6β1 integrin signaling in directing neuronal differentiation of ES-NCPCs remains to be studied.

Since the α6 integrin mRNA is upregulated in regenerating dorsal root ganglia (DRG) neurons and spinal motor neurons in adult rats after axonal injury [24, 25], we subsequently evaluated the ability of HYD1-functionalized fibrin gel to promote neurite extension in an *ex vivo* model of axonal growth. We report that the incorporation of 20 μM of HYD1 into fibrin promoted neurite extension of rat E18 DRG neurons, inducing a biphasic response similar to that observed for ES-NSPC neurospheres. As a result, the capability of HYD1-functionalized fibrin gels to sustain axonal regeneration was tested using a spinal cord experimental model (complete transection). The presence of fibers expressing the growth associated protein 43 (GAP43) was observed both in the central, rostral and caudal sites of the implantation/lesion area in HYD1-operated animals, as well as in control group (unmodified fibrin). Our results provided evidence that HYD1-functionalized fibrin constitutes a permissive environment for axonal

regeneration, either from axotomized neurons or from endogenous progenitors. Noteworthy, we observed a trend for increased $GAP43^+$ area in animals receiving HYD1-functionalized fibrin *vs*. control, which correlates well with the improved recovery in locomotor function of HYD1-operated animals *vs.* control. Notably, HYD1-operated animals achieved an enhancement of functional recovery comparable to that reported for rats with complete spinal cord transection treated with much complex combinatorial therapies [26]. Overall, the results presented here suggest that conjugation of α6β1 integrin-binding motifs, in particular of HYD1 peptide, is of interest to increase the biofunctionality of hydrogels used in 3D platforms for ES-NSPC culture and potentially, in matrix-assisted ES-NSPC transplantation for the treatment of CNS injuries.

Envisaging a possible clinical application, we tested if fibrin functionalization with HYD1 or T1 integrin α6β1-binding ligands could also be effective in promoting the outgrowth of human ES-NSCs. In line with our previous results, an input peptide concentrations of 20 μM of HYD1 was effective in enhancing cell outgrowth of hES-NSCs in fibrin (1.2-fold increase *vs*. unmodified fibrin), although leading to a smaller increase when compared to that obtained with mES-NSPCs. As we found that the pro-migratory effect of HYD1 is mediated both by α6β1 and α3β1 integrins, we attributed this difference to the lower expression of integrin α3 subunit in hES-NSCs in comparison to mES-NSPCs (14.7% *vs.* 73.7%, respectively). The slighter impact of T1 immobilization on hES-NSC cell outgrowth as compared to that observed for mES-NSPCs may also result from differences in α3 integrin expression levels, as T1 besides targeting the α6β1 heterodimer also interacts with α3β1 integrin. Lastly, we also found that T1-/HYD1-functionalized fibrin hydrogels are capable of sustaining neuronal differentiation from hES-NSCs.

In order to improve fibrin bioactivity towards hES-NSCs, we explored the tethering of a syndecan-binding peptide with neurite outgrowth promoting activity, namely the AG73 peptide sequence from the laminin α1 chain, alone or in combination with integrin α6β1-binding ligands. Due to the modulatory role of syndecans on integrin signaling the combination of AG73 with T1 or HYD1 was expected to synergistically increase hES-NSC outgrowth. Similarly to that observed for HYD1- and T1-functionalized gels covalent binding of AG73 induced a biphasic effect on hES-NSC outgrowth, leading to enhanced outgrowth when incorporated at 60 μM in fibrin (up to 1.3-fold increase *vs.* unmodified fibrin). Importantly, the outgrowth of hES-NSC exhibited a biphasic response to immobilized AG73, similar to that observed for mES-NSPCs. Even though we did not detect an additive effect on hES-NSCs outgrowth upon fibrin

functionalization with 10 μM of AG73 and HYD1, the co-expression of syndecan-1 and integrin α6 subunit in more than 90% of hES-NSCs suggests that syndecan-1 might cooperate with α6β1 integrin in the presence of both types of ligands, leading to a synergistic enhancement of neurite outgrowth in fibrin. Based on the effect elicited by HYD1 and AG73 when incorporated alone into fibrin, future studies should address if the conjugation of 60 μM of AG73 with 20 μM of HYD1 induces an additive or synergistic increase in hES-NSC outward migration, when compared to that exerted by single peptides. Altogether, our findings constitute a proof-of-concept that decorating hydrogels with synthetic adhesive ligands interacting with integrin α6β1 or syndecans can be advantageous for the development of 3D hydrogel platforms for the culture of human pluripotent stem-derived NSCs.

In conclusion, this study describes a novel approach to promote neurite outgrowth of NSPCs in 3D hydrogel matrices. Specifically, it reports that the tethering of HYD1 peptide to fibrin enhances the neurite outgrowth of mES-NSPCs and hES-NSCs, while allowing a permissive microenvironment for axonal regeneration and functional recovery in a spinal cord injury experimental model. Therefore, future studies should evaluate the efficacy of HYD1-functionalized hydrogels for delivery of hES-NSCs into the injured CNS in a pre-clinical scenario.

Overall, this thesis significantly impacts the development of engineered matrices for use as 3D platforms for *in vitro* culture of human pluripotent-derived NSCs and as vehicles for NSPC transplantation envisaging the treatment of the damaged CNS. Indeed, the incorporation of integrin α6β1- or syndecan-binding adhesive motifs can also be of interest to confer bioactivity to synthetic hydrogels designed to deliver ES-NSPCs into the injured CNS, such as poly(ethylene glycol)-based hydrogels. Finally, the developed fibrin platform can also be useful for pharmacological screening and to study the molecular mechanisms implicated in neurogenesis in a 3D microenvironment which better mimics the *in vivo* conditions. Summing up, our findings open new avenues in the design of more efficient hydrogel matrices for application in NSPC-based regenerative approaches for the treatment of traumatic CNS disorders or neurodegenerative diseases.

References

[1] R.Y. Tam, T. Fuehrmann, N. Mitrousis, M.S. Shoichet, Regenerative therapies for central nervous system diseases: a biomaterials approach, Neuropsychopharmacology

: official publication of the American College of Neuropsychopharmacology 39(1) (2014) 169-88.
[2] J.W. McDonald, D. Becker, T.F. Holekamp, M. Howard, S. Liu, A. Lu, J. Lu, M.M. Platik, Y. Qu, T. Stewart, S. Vadivelu, Repair of the injured spinal cord and the potential of embryonic stem cell transplantation, Journal of neurotrauma 21(4) (2004) 383-93.
[3] K. Saha, A.J. Keung, E.F. Irwin, Y. Li, L. Little, D.V. Schaffer, K.E. Healy, Substrate modulus directs neural stem cell behavior, Biophysical journal 95(9) (2008) 4426-38.
[4] Q. Shen, Y. Wang, E. Kokovay, G. Lin, S.-M. Chuang, S.K. Goderie, B. Roysam, S. Temple, Adult SVZ stem cells lie in a vascular niche: A quantitative analysis of niche cell-cell interactions, Cell stem cell 3(3) (2008) 289-300.
[5] W. Ma, T. Tavakoli, E. Derby, Y. Serebryakova, M.S. Rao, M.P. Mattson, Cell-extracellular matrix interactions regulate neural differentiation of human embryonic stem cells, Bmc Dev Biol, 2008.
[6] T.C. Sroka, M.E. Pennington, A.E. Cress, Synthetic D-amino acid peptide inhibits tumor cell motility on laminin-5, Carcinogenesis 27(9) (2006) 1748-57.
[7] S.J. Leu, Y. Liu, N. Chen, C.C. Chen, S.C. Lam, L.F. Lau, Identification of a novel integrin α6β1 binding site in the angiogenic inducer CCN1 (CYR61), J Biol Chem 278(36) (2003) 33801-8.
[8] F. Katagiri, M. Ishikawa, Y. Yamada, K. Hozumi, Y. Kikkawa, M. Nomizu, Screening of integrin-binding peptides from the laminin α4 and α5 chain G domain peptide library, Archives of biochemistry and biophysics 521(1-2) (2012) 32-42.
[9] M.K. Nguyen, E. Alsberg, Bioactive factor delivery strategies from engineered polymer hydrogels for therapeutic medicine, Progress in polymer science 39(7) (2014) 1236-1265.
[10] S.P. Palecek, J.C. Loftus, M.H. Ginsberg, D.A. Lauffenburger, A.F. Horwitz, Integrin-ligand binding properties govern cell migration speed through cell-substratum adhesiveness, Nature 385(6616) (1997) 537-40.
[11] J.C. Schense, J.A. Hubbell, Three-dimensional migration of neurites is mediated by adhesion site density and affinity, Journal of Biological Chemistry 275(10) (2000) 6813-6818.
[12] M. Melchionna, K.E. Styan, S. Marchesan, The Unexpected Advantages of Using D-Amino Acids for Peptide Self-Assembly into Nanostructured Hydrogels for Medicine, Curr Top Med Chem 16(18) (2016) 2009-18.
[13] A.C. Brown, T.H. Barker, Fibrin-based biomaterials: Modulation of macroscopic properties through rational design at the molecular level, Acta Biomaterialia 10(4) (2014) 1502-1514.

[14] R. Milner, I.L. Campbell, The integrin family of cell adhesion molecules has multiple functions within the CNS, Journal of Neuroscience Research 69(3) (2002) 286-291.
[15] J.F. Marshall, D.C. Rutherford, A.C. McCartney, F. Mitjans, S.L. Goodman, I.R. Hart, αvβ1 is a receptor for vitronectin and fibrinogen, and acts with α5β1 to mediate spreading on fibronectin, Journal of cell science 108 (Pt 3) (1995) 1227-38.
[16] J. Arulmoli, H.J. Wright, D.T.T. Phan, U. Sheth, R.A. Que, G.A. Botten, M. Keating, E.L. Botvinick, M.M. Pathak, T.I. Zarembinski, D.S. Yanni, O.V. Razorenova, C.C.W. Hughes, L.A. Flanagan, Combination scaffolds of salmon fibrin, hyaluronic acid, and laminin for human neural stem cell and vascular tissue engineering, Acta Biomater 43 (2016) 122-138.
[17] P. Georges, M. McCormick, L. Flanagan, Y.E. Ju, E. Sawyer, P. Janmey, Tuning the Elasticity of Biopolymer Gels for Optimal Wound Healing, MRS Proceedings 897 (2011).
[18] N.D. Leipzig, M.S. Shoichet, The effect of substrate stiffness on adult neural stem cell behavior, Biomaterials 30(36) (2009) 6867-78.
[19] A.J. Keung, E.M. de Juan-Pardo, D.V. Schaffer, S. Kumar, Rho GTPases mediate the mechanosensitive lineage commitment of neural stem cells, Stem Cells 29(11) (2011) 1886-97.
[20] W.J. Tyler, The mechanobiology of brain function, Nature Reviews Neuroscience 13 (2012) 867.
[21] R. Uibo, I. Laidmae, E.S. Sawyer, L.A. Flanagan, P.C. Georges, J.P. Winer, P.A. Janmey, Soft materials to treat central nervous system injuries: evaluation of the suitability of non-mammalian fibrin gels, Biochimica et biophysica acta 1793(5) (2009) 924-30.
[22] I. Levental, P.C. Georges, P.A. Janmey, Soft biological materials and their impact on cell function, Soft matter 3(3) (2007) 299-306.
[23] T.S. Jacques, J.B. Relvas, S. Nishimura, R. Pytela, G.M. Edwards, C.H. Streuli, C. ffrench-Constant, Neural precursor cell chain migration and division are regulated through different β1 integrins, Development 125(16) (1998) 3167-3177.
[24] H. Hammarberg, W. Wallquist, F. Piehl, M. Risling, S. Cullheim, Regulation of laminin-associated integrin subunit mRNAs in rat spinal motoneurons during postnatal development and after axonal injury, The Journal of comparative neurology 428(2) (2000) 294-304.
[25] W. Wallquist, J. Zelano, S. Plantman, S.J. Kaufman, S. Cullheim, H. Hammarberg, Dorsal root ganglion neurons up-regulate the expression of laminin-associated

integrins after peripheral but not central axotomy, The Journal of comparative neurology 480(2) (2004) 162-9.
[26] K. Fouad, L. Schnell, M.B. Bunge, M.E. Schwab, T. Liebscher, D.D. Pearse, Combining Schwann cell bridges and olfactory-ensheathing glia grafts with chondroitinase promotes locomotor recovery after complete transection of the spinal cord, The Journal of neuroscience : the official journal of the Society for Neuroscience 25(5) (2005) 1169-78.